OPERANDO INVESTIGATIONS OF MECHANICAL CHANGES IN LITHIUM-ION BATTERIES

BY

KIMBERLY LUNDBERG BASSETT

DISSERTATION

Submitted in partial fulfillment of the requirements
for the degree of Doctor of Philosophy in Chemistry
in the Graduate College of the
University of Illinois at Urbana-Champaign, 2019

Urbana, Illinois

Doctoral Committee:

Professor Andrew A. Gewirth, Chair
Professor Ralph G. Nuzzo
Professor Nancy R. Sottos
Assistant Professor Renske M. van der Veen

Abstract

Li-ion batteries are increasingly present in modern life. They principally power compact, handheld devices and electric vehicles. Mechanical changes are always occurring within batteries due to expansion and contraction of the active materials during lithiation and delithiation, degradation of the electrodes, decomposition of the electrolyte, and external cell pressure. The work presented here seeks to describe and understand the interplay between electrochemical cycling and mechanical changes within Li-ion cathodes.

Stress, Strain, and Electrochemical Stiffness in Lithium Manganese Oxide Cathodes. In-situ strain and stress measurements are performed on composite electrodes to monitor potential-dependent stiffness changes in lithium manganese oxide ($LiMn_2O_4$). Lithium insertion and removal results in asynchronous strain and stress generation in the electrode. Electrochemical stiffness changes are calculated by combining coordinated stress and strain measurements. The electrode experiences dramatic changes in electrochemical stiffness due to potential-dependent Li^+ intercalation mechanisms. The development of stress in the early stages of delithiation (at ca. 3.95 V) due to a kinetic barrier at the electrode surface gives rise to stiffness changes in the electrode. Strain generation due to phase transformations reduces stiffness in the electrode at 4.17 V during delithiation and at 4.11 V during lithiation. During lithiation, stress generation due to Coulombic repulsions between occupied and incoming Li^+ leads to stiffening of the electrode at 3.96 V. The electrode also experiences greater changes in stiffness during delithiation compared to lithiation. These changes in electrochemical stiffness provide insight into the interplay between mechanical and electrochemical properties which control electrode response to lithiation and delithiation.

Stress and Strain in Lithium Iron Phosphate Cathodes. We wondered whether in the asynchronous stress and strain behavior see in in $LiMn_2O_4$ would present in other common Li-ion cathodes. In this study, we employ in-situ stress and strain measurements to investigate potential-dependent mechanical changes in lithium iron phosphate ($LiFePO_4$) cathodes during cyclic voltammetry in $LiPF_6$ and $LiClO_4$-containing electrolytes. Analysis of the stress and strain derivatives in $LiClO_4$–containing electrolytes both exhibit single peaks during lithiation and delithiation that coincide with $LiFePO_4$ phase transformations. An additional feature in the stress

and strain derivatives is observed in $LiPF_6$–containing electrolytes at the onset of the delithiation process. The current peak splitting in $LiPF_6$ are larger than in $LiClO_4$, and electrochemical impedance spectroscopy measurements show higher impedances in $LiPF_6$ versus $LiClO_4$-containing electrolytes in lithiated $LiFePO_4$. The larger current peak splitting and higher impedance in $LiPF_6$ electrolytes suggest the potential-dependent growth of a thick and resistive cathode/electrolyte interface (CEI) layer on $LiFePO_4$ cathodes. We hypothesize that kinetic limitations in Li^+ transport through the CEI leads to additional stress and strain development at the electrode surface.

Operando Observations and First Principles Calculations of Reduced Lithium Insertion in Au-Coated $LiMn_2O_4$. The deposition of protective coatings on the spinel LMO lithium-ion battery cathode is effective in reducing Mn dissolution from the electrode surface. Although protective coatings positively affect LMO cycle life, much remains to be understood regarding the interface formed between these coatings and LMO. Using operando powder X-ray diffraction with Rietveld refinement, we show that, in comparison to bare LMO, the lattice parameter of a model Au-coated LMO is significantly reduced upon re-lithiation. Less charge passes through Au-coated LMO in comparison to bare LMO, suggesting that the reduced lattice parameter is associated with decreased Li^+ solubility in the Au-coated LMO. Density functional theory (DFT) calculations show that a more Li^+-deficient near-surface is thermodynamically favorable in the presence of the Au coating, which may further stabilize these cathodes through suppressing formation of the Jahn-Teller distorted $Li_2Mn_2O_4$ phase at the surface. Electronic structure and chemical bonding analyses show enhanced hybridization between Au and LMO for delithiated surfaces leading to partial oxidation of Au upon delithiation. This study suggests that, in addition to transition metal dissolution from electrode surfaces, protective coating design must also balance potential energy effects induced by charge transfer at the electrode-coating interface.

Acknowledgements

While this is my thesis, I think it's fair and obvious to say that many people contributed to my success as a graduate student. Without these people, graduate school would have simply been impossible.

To my husband, Will Bassett: Did you know you're my favorite? Thanks for being infinitely supportive and for talking through all the tough research times with me. Without you, I probably would have become a shell of a person during graduate school. I'm beyond privileged to call you my husband.

To my PI, Prof. Andrew Gewirth: I now know to call you Andy, but that only took a couple of years to figure out. Boundless thanks to you for letting me try new science and new techniques that our group hadn't performed before. Thank you for being kind, supportive, and cognizant of when I needed a push in the right direction. I consider myself extremely lucky to have worked for you.

To my committee (Ralph Nuzzo, Nancy Sottos, and Renske van der Veen), thank you for your guidance and suggestions in my research.

To my main collaborator at Argonne National Laboratory, Dr. Tim Fister: I think you taught me the coolest stuff during graduate school. Thanks for being patient with this chemist who is still trying to learn physics. The time and care you took in teaching me and including me in your research efforts still astounds me. Thanks for never letting me belittle my accomplishments and trusting me with performing and communicating your research. Your vote of confidence means so much to me. Thank you for remaining upbeat and excited during beamtime and the accompanying sleep deprivation. You're an amazing scientist, and I can't wait to see what you do in the coming years.

To my undergraduate PIs and lab mates at Texas Tech: Prof. Louisa Hope-Weeks and Prof. Dom Casadonte, thank you for welcoming me into your labs and giving me the tools to succeed in graduate school. To Dr. Geneva Peterson and Dr. Fernando Hung Low, thank you for training me with care and patience. To Donald Ramirez and Roya Baghi, thank you for being my friends and showing me what dedicated, hard-working graduate students look like.

To my main collaborators at UIUC, Dr. Ö. Özgür Çapraz and Prof. Nancy Sottos: Thank you for always being enthusiastic and curious about our work. I'm proud of the work we've

produced together and the communication we've accomplished in translating chemistry into engineering and engineering into chemistry.

To Robert Warburton and Prof. Jeff Greeley: I couldn't have asked for better theory collaborators. Robert, I'll always be thankful for our productive Skype meetings in which we talked slowly and used small words to explain our science to one another. We had *a lot* to teach each other and you made it fun. I really love the paper we wrote together.

To the members of the CEES EFRC, especially Dr. Paul Fenter: Thank you for creating an environment in which Robert and I could casually set up a Skype meeting to talk shop and walk away with an idea for a great paper. Thank you for inspiring a collegial atmosphere in which to talk about science and learn from each other.

To all the beam line scientists at the Advanced Photon Source, including but not limited to the following. To Alan Kastengren and Katie Matusik at 7BM, y'all were crazy fun to work and talk with. You helped me every time I asked a question, which was often. A girl could only be so lucky to have you two as her beamline scientists. To Wenqian Xu at 17BM, thank you for answering my many questions about diffraction data workup. Thank you for keeping one of the most organized and well-stocked beamlines I've ever been to. To Kamila Wiaderek, thank you for letting me borrow your cell, showing me how to use it weeks ahead of beamtime, and being available for planning meetings.

To Scottie McCormack, thank you for teaching me to use GSAS. My progress would have been glacial without your help.

To the Gewirth group students and post-docs, what the heck would I have done without you? Y'all are the best group ever, and I wish I could take many of you with me when I leave. To Jen Esbenshade, thank you for training me and riding bikes, crocheting/knitting, and going to beamtime (too many memories to transcribe here) with me. And thanks for always keeping me humble. To Yeyoung Ha, thank you for teaching me to be stressed. Thank you for being lab champion for fun and frivolity. I wish I could channel even a quarter of your energy. To Bruno Nicolau, thanks for the many rambling discussions in lab during the late afternoon. You were my favorite person to bounce ideas off of when I was in a rut. To Lingzi Sang, thank you so much for being a magical ray of sunshine. Your optimism, unending smiles, and stash of Choco Pies kept me sane through many beam times. You're the nicest person I know. To Kim Ta, thank you for the painful high-fives, hallway dances (a professor still hasn't caught us), and endless sanity during

beam time. To Ken Madsen, thanks for being my workout buddy and constant source of dark whimsy during my last two years in grad school. I am so happy you're to one taking over my tomography project. I trust you with my baby. You would say I'm foolish, but I know otherwise.

To my best friends in graduate school, my year mates: To Elena Montoto, you are the sanest person I know. You also like wine and riding bikes, and you are kind to everyone. Is it a wonder that you helped me through some difficult times? To Sarah Perlmutter, my best hobby buddy, I'm going to miss you and your constant kindness, cupcakes, and bike riding enthusiasm. Is there anything better than playing hooky to ride bikes on a Friday afternoon? To Ryan Rooney, my best guy friend and lab mate, I'm going to miss constantly talking to you about everything and nothing. To Kali Miller, thank you for being one of the most unabashedly goofy and affectionate people I know. You and Carrie helped crack me out of my shell. To Michael Drummond, may we both stay cute forever. To Carrie Levinn, I don't know how you continued to care for all of us when your life wasn't optimal. Thank you for being so giving and lovely.

To my Women Chemists Committee co-chairs and members: I am honored and thrilled to have worked with so many talented people. I will always be proud of our accomplishments. To Ellen Althaus, thank you for encouraging me to be involved and giving me every opportunity to do good in the department. To Patricia Simpson, you stepped in when we needed you. You did a fantastic job and were an unending joy to work with. To Lloyd Munjanja, you arrived and were charged with many difficult tasks. Keep up the good work and the enthusiasm! I am so glad you're here for the graduate students. To the board I chaired (Corryn Neumann, Tabitha Miller, Marina Philip, Kim Ta, Cecilia Gentle, Courtney Ford, Michaela Carlson), y'all enabled us to try so many new things and kept me from getting us into anything too crazy. I think you all deserve massive awards for your good work. I'm convinced you spoiled me completely by being proactive and engaged in every board meeting. I doubt I'll ever meet another board as efficient, enthusiastic, and inspired as y'all.

To the SCS machine shop, especially Hodge: I'll miss shooting the breeze with you. Your technical expertise and that of the entire shop coupled with fast turnaround times saved my rear end so many times. Thank you for making me high quality parts and never complaining when I changed designs on you.

To the IMP office staff (Beth Myler, Theresa Struss, Karen Watson, Stacy Dudzinski, and Katie Trabaris): you were my moms away from mom and my pillars of sanity, love, and chocolate

on which to lean. I don't know if you ladies know how much good you do for the graduate students in our department, but it's immeasurable. I love you all.

To my family: thank you for loving me through the stress and my inability to travel home as often as we all would have liked. I mourn not getting to watch all the kiddos grow up and having to miss important birthdays and events. You are the rock on which I have built myself. To my dad, who I can really talk shop with, thanks for understanding the Ph.D. process and always being supportive. To my mom, thank you for being my biggest fan. To my sister and soul mate, thanks for talking nonsense and having big, important chats with me. To my brother, who has never let me settle for less.

To My Husband, Who Grounds Me

Table of Contents

Chapter 1: Introduction

1.1 Motivation

Modern consumer society maintains two key demands concerning energy sources: (1) decreased emissions and (2) ease of portability.

The 2018 Inventory of U.S. Greenhouse Emissions and Sinks released by the U.S. Environmental Protection Agency (EPA) documents changes in greenhouse gases between 1990–2016. This report clearly shows that CO_2 remains the U.S.'s highest released greenhouse gas by a factor of 8 above the next contender (methane). The transportation sector ranks second in CO_2 emissions and is tied in first for largest contributor to overall greenhouse emissions.[1]

One way to alleviate the amount of emissions released is to use more efficient or petroleum free vehicles. The EPA reports that the CO_2 emissions from gasoline are 8,887 grams of CO_2/gallon of fuel burned.[2] Therefore, driving a gasoline-powered vehicle with better fuel efficiency can already make large gains towards decreased emissions. The marriage of batteries with traditional fuel-combustion engines to create hybrid electric vehicles (HEV) and plug-in hybrid electric vehicles (PHEV) has created automobiles that are more fuel efficient that their gasoline-driven competitors by almost a factor of two.[3] Even so, technologies that release no emissions are now available to consumers. All electric vehicles (EV) release no tailpipe emissions and fuel cell vehicles (FCV) release only water vapor.[2]

From the previous paragraph, it's enticing to assume that EV and FCV are a panacea for the transportation sector's emissions. Unfortunately both of these technologies require input from the energy grid to charge a battery (in EV) or generate H_2 fuel (in FCV). The method with which electricity is generated also greatly affects the amount of emissions released per mile driven. Indeed, the production of electrical power outputs more CO_2 than the transportation (1.81 gigatons vs 1.78 gigatons), also due to fossil fuel combustion.[1] Therefore in order for EV, PHEV, and PCV vehicles to become truly lower emission than HEV and fossil fuel vehicles, the upstream fuel source for electricity generation must also be evaluated.

Nevertheless, HEVs decrease the gallons of gas consumed per mile driven and EV and PHEV vehicles can be charged using electricity generated by renewable energy sources. The remaining obstacles for consumer vehicles is vehicle range and weight. For these criteria, I'll only examine EVs since they depend solely on a battery without the added complication added by a

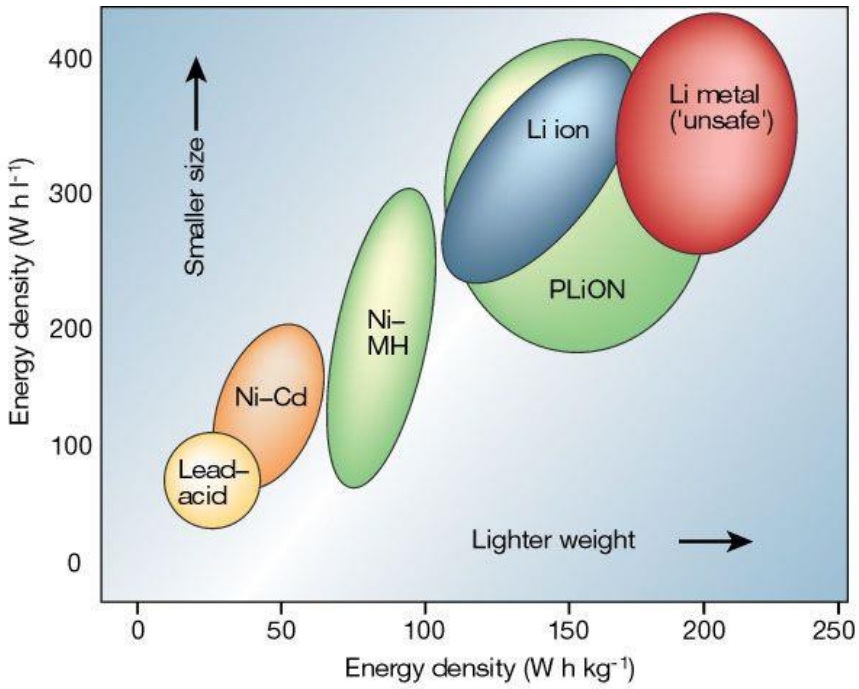

Figure 1.1. Comparison of volumetric and gravimetric energy densities in different battery technologies.[4]

coupled internal combustion engine. In 2019, top-of-the-line EVs have ranges from 57-315 miles with optional fast (30 minutes) and slow (3-12 hours) charging times.[3] Increasing weight in an EV negatively affects the range, and therefore adding a larger number heavy batteries is not an ideal solution to increasing the range. The overall goal is to increase the capacity (or number of electrons stored) of the battery without increasing the weight of the battery.

In addition to greener vehicles, there is a strong consumer demand for smaller and longer lasting handheld electronics. To achieve this goal, companies must manufacture batteries with higher volumetric energy densities.

Among widely commercialized battery technologies, Li-ion batteries offer the highest volumetric and gravimetric energy densities (Figure 1.1) over lead-acid, nickel-cadmium, and nickel-metal hydride batteries, and so it is here that we will continue our discussion.[4]

Engineering advances to Li-ion battery construction have facilitated most gains in gravimetric and volumetric energy density since Sony first introduced the $LiCoO_2$/graphite Li-ion battery in 1991.[5,6] The scientific community is actively pursuing creating batteries with increased energy density and lifetime by improving current materials or designing new state-of-the-art materials.

1.2 Introduction to Li-ion Batteries

A battery is an electrochemical cell consisting of an anode, cathode, electrolyte, and external circuit (Figure 1.2).[7] In a typical Li-ion battery during discharge, Li^+ leave (deintercalate from) the anode and Li^+ infiltrates (or intercalates) into the cathode material. Electrons pass through the external circuit, from anode to cathode, to maintain charge balance. A liquid electrolyte shuttles Li^+ between the anode and cathode while remaining electronically insulating. The external circuit may either charge the battery or discharge the battery by drawing energy from the battery to power a device.[8]

The theoretical energy of a battery is the maximum amount of energy that the battery could deliver. To manufacture batteries that can last longer on a single charge, this number must be maximized. The energy of a battery can also be reported with respect to unit mass (gravimetric energy density) or volume (volumetric energy density). The theoretical energy is the mathematical product of the cell voltage and capacity, so the goal is to further maximize these two values. The anode and cathode materials in a battery dictate the cell voltage. For example, the difference in standard reduction potential between a Li anode (-3.01 V vs standard hydrogen electrode (SHE)) and a $LiMn_2O_4$ cathode (1.2 V vs SHE) is ca. 4.2 V. The capacity expresses the total number of electrons involved in charging or discharging a battery. The capacity of a battery depends upon

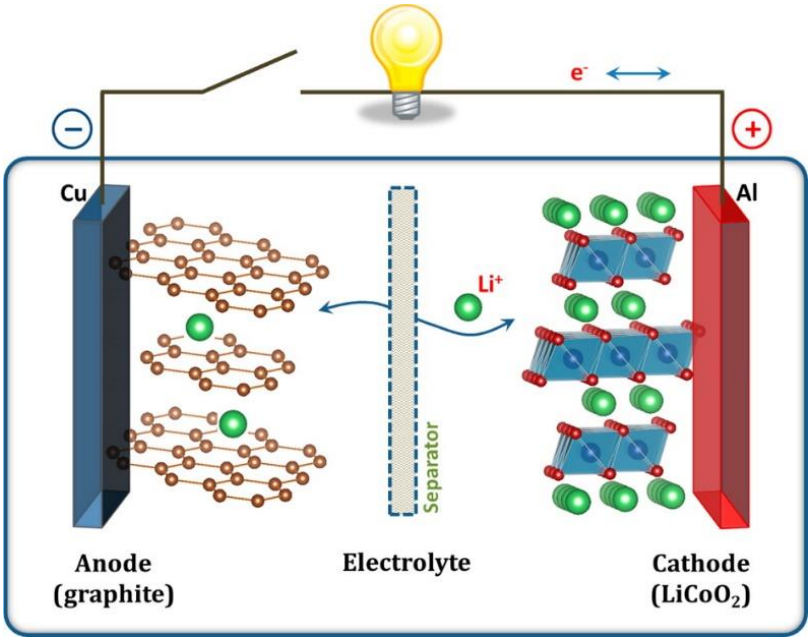

Figure 1.2. Schematic of the main Li-ion battery components with a graphite anode, liquid electrolyte, and $LiCoO_2$ cathode.[7]

the amount of active anode and cathode material present and the quantity of lithium stored per unit mass.

Li metal is a logical goal for battery anodes because it is not only exhibits the lowest reduction potential (-3.04 V vs standard hydrogen electrode) out of all metals but is also the lightest (M = 6.94 g/mol, ρ = 0.53 g/cm^3).[4] The low reduction potential allows for higher energy batteries, and the low molar mass of the metal allows for battery construction with high gravimetric energy density. The downfall to using Li metal as an anode in batteries is the dendritic plating of Li in liquid electrolytes.[9,10] Dendritic growth can lead to shorting in the battery and increased risk of fires. For this reason, the first commercialized battery instead used graphite (ca. -2.8 V vs SHE) as an anode in which Li^+ are stored between the graphite sheets instead of plated as a metal.

The most common type of Li-ion cathodes are intercalation materials in which Li^+ enter the host material, travel through channels or between layers in the structure, and then reside within the structure as charged ions.[11] Ideally, the Li^+ can be inserted and extracted repeatedly for thousands of cycles. Metal oxides are often used because of their high oxidation potentials (typically >3.7 V vs Li/Li^+), but metal phosphates (~3.5 V vs Li/Li^+) are also implemented for their superior lithiation/delithiation rate capabilities.[8]

Liquid electrolytes are comprised of one or more solvents and a lithium salt. The solvent must be organic in nature because the electrochemical stability for water is 1.2 V.[12] Li salts are selected based on anion stability at anodic and cathodic potentials, ionic conductivity, and safety, among other considerations.[13,14] Most electrolytes contain $LiPF_6$ because of its high ionic conductivity (10^{-2} S/cm) although there are serious safety concerns involving $LiPF_6$ reacting with water to HF. Most electrolyte solvents consist of cyclic ethylene carbonate (EC) mixed with one or more linear carbonates (such as dimethyl carbonate and ethyl methyl carbonate).

Paradoxically, almost no organic solvents are stable at the extremely oxidizing and reducing electrode potentials (near 0 and 4.5 V vs Li/Li^+) within Li-ion batteries.[15–20] During cycling the electrolyte salt and solvent react at the anode and cathode and form a passivation film called the solid electrolyte interphase (SEI). An ideal SEI is both ionically conducting and electronically resistive. Such a film prevents further electrolyte decomposition at the electrodes and allows for the anode and cathode to operate as previously described. A non-ideal SEI is often too insulating–resulting in increased impedance in the cell– and decreases the available capacity in the cell by consuming Li^+ during its formation.

Recently, interest in solid electrolytes (SE) has grown in hopes that they will be less flammable than liquid electrolytes and allow Li metal anodes to be utilized.[21–24] Calculations predict that high shear modulus materials (like many SE) should block dendritic Li growth.[25,26] Still, many papers report shorting and crack formation in SE during cycling.[27–29] Many open questions remain concerning the connection between mechanical stability, ionic conductivity, and interfacial reactivity in SE.

1.3. Techniques to Measure Mechanical Changes in Li-ion Batteries

1.3.1 Electrochemical Stress Measurements

Surface stress provides a handle to study atomistic changes at a surface and their effect on macroscopic properties without needing an initial detailed description of the surface.[30] Simply, surface stress occurs when surface bond lengths at equilibrium are not equal to those in the bulk. In order to achieve the surface equilibrium bond lengths, surface atoms must exert a force upon the underlying bulk atom.

One prominent method for measuring stress uses the bending cantilever technique.[30,31] In general, the bending cantilever technique indirectly measures surface stress by monitoring the elastic deformation of a thin substrate by changes in stress at the surface. The force exerted by the surface onto the bulk bends the cantilever substrate and a laser deflection system is used to measure the extent of this deformation.

In order for the experiment to proceed, several key assumptions must be made and followed.[30,31] One, the curvature change of the cantilever must remain small such that the coordinate system imposed is still operable. Two, the thickness of the film (h_f in Figure 1.3) must be much smaller than the thickness of the cantilever (h_s), which must be much smaller than the width (w) of the cantilever, which must be much smaller than the length (L) of the cantilever.

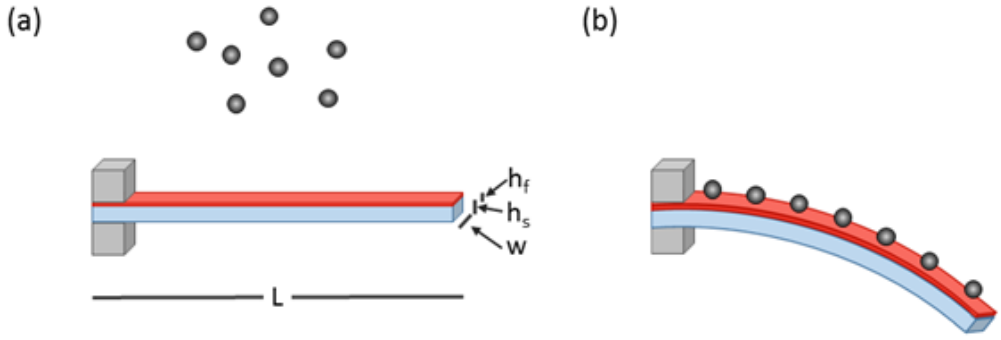

Figure 1.3. A film on a cantilever both (a) undeformed and (b) deformed by adsorbates.

These vague suggestions on dimensions are unsatisfying for practical use, but there is some guidance when designing a sample found in Thin Film Materials by Freund and Suresh, Chapter 2.[31] Three, the underlying substrate must only deform elastically. Four, stress is acting in-plane only and along the longest cantilever dimension. Five, only one side of the cantilever is experiencing changes in stress that are driving cantilever deformation. There are additional constraints that can be found elsewhere.

Consider Figure 1.3 in which a clean cantilever remains undeformed since any interactions at one surface are counteracted by those on the opposite side. Whenever adsorbates interact with the film surface, such that the bond lengths of the substrate on one side of the cantilever and the force they exert on the bulk are no longer equal to the opposite side, then the cantilever bends in response to the newly exerted force. Stoney was the first to develop a mathematical model for measuring the surface stress based on substrate curvature changes in 1909.[32] Stoney deposited Ni films onto steel substrates and calculated the amount of surface stress by additionally measuring the film thickness and elastic modulus of the steel cantilever. Stoney's equation,

$$\sigma = {Yh_s^2 d\kappa}\Big/{6t(1-\nu_s)} \tag{1.1}$$

is exceedingly convenient for an experimentalists' use because it only depends upon the mechanical properties of the substrate. Here, $d\kappa$ is the cantilever curvature; h_s, Y, and ν_s are the thickness, Young's modulus, and Poisson's ratio of the cantilever substrate, respectively; and σ is the integrated stress through t, the film thickness. Whenever the cantilever becomes concave (contracts on the film side), there is a tensile mismatch stress at the surface and a positive stress magnitude is measured. Conversely, the cantilever becomes convex upon a compressive mismatch in stress and the stress magnitude is negative.

The bending cantilever system used herein was based on a system by Cahill and coworkers.[33,34] As seen in Figure 1.4, an oscillating mirror manipulates a He-Ne laser to an amplitude of 1.32° and a frequency of 133 Hz. The oscillating mirror introduces a frequency that the lock-in amplifier can match, making the apparatus largely insensitive to environmental noise. The oscillating mirror optics direct the beam to the cantilever within a liquid cell. The beam is reflected and focused onto a position-sensitive detector. Any changes in cantilever curvature will change the focus of the beam on the position-sensitive detector and allow for detection. A lock-in amplifier measures the signal and the output is proportional to the curvature, such that

$$d\kappa = \sqrt{2}F^2V \Big/ f^2 nLF\beta \tag{1.2}$$

where F and f are focal lengths in the system, V is the rms output of the lock-in amplifier, n is the refractive index of the liquid in the cell, L is the beam width at the sample, and β is the calibration constant of the position-sensitive detector.

A vast majority of previous studies on stress at substrate/electrolyte interfaces studied metallic surfaces in aqueous electrolytes. Early studies included direct measurements of stress in polycrystalline Au and Pt in an electrolyte, formation of silicon oxide in etchants, and various studies performed during electrochemical control.[35–39] More recently, battery anode and cathode thin films, such as Sn, $LiMn_2O_4$, and $LiCoO_2$, have been interrogated in organic electrolytes during galvanostatic or potentiostatic cycling.[40–45] Our group has expanded this work to include electrodes cast from conventional slurries as opposed to applied with a vacuum deposition technique.[46]

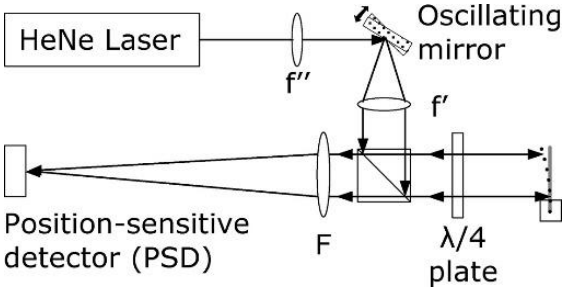

Figure 1.4. Diagram of the stress experimental setup. The mirror oscillates at 133 Hz. The focal lengths of F, f', and f'' are 500 mm, 50 mm, and 150 mm.[33]

1.3.2 Operando X-ray Tomography

X-ray tomography provides a three-dimensional view of internal changes in a material, and the added use of brilliant and high energy synchrotron X-rays allows for tomography to be collected during the operation of a device or when a system undergoes chemical changes.[47–49] Figure 1.5 shows other methods for imaging internal structures are limited to ex-situ analysis paired with intensive sample preparation involving serial sectioning or polishing and analysis under vacuum or within non-ideal cell geometries made for these environments.[47] Tomography can resolve features down to the micron scale, while electron microscope techniques can image features on the length scale of tens of nanometers.[47] Tomography is performed under ambient pressures, while synchrotron radiation adds the flexibility of using custom cells for air sensitive samples, samples under flow or pressure, etc.

X-ray tomography is performed illuminating a sample with X-ray radiation.[47] The X-ray energy is usually selected far away from any relevant absorption edges and such that the sample thickness is close to one absorption length at the chosen energy. The sample attenuates the X-rays such that

$$I/I_0 = \exp(-\mu z) \tag{1.3}$$

in which I_0 is the intensity of the incident radiation, I is the radiation intensity after passing through a sample of thickness z with absorption coefficient μ.[50] The absorption coefficient varies approximately by Z^4 such that higher Z materials more effectively attenuate radiation. The radiation that escapes the sample interacts with a scintillation screen to convert the X-rays into visible light and is recorded with a CCD camera. A sample stage rotates the sample over 180° or 360° and images are collected at least as many angles as pixel columns on the detector. Reconstruction software then takes these many rotated views, overlaps them, and returns a horizontal view of the sample for every vertical pixel position. Further processing of these reconstructed slices can yield important information on the sample such as morphology, pore size, pore volume, and possibly material identification.

When a monochromatic X-ray energy and the Z contrast between a material before and after a chemical transformation is large, it is possible to estimate the percentage of different phases

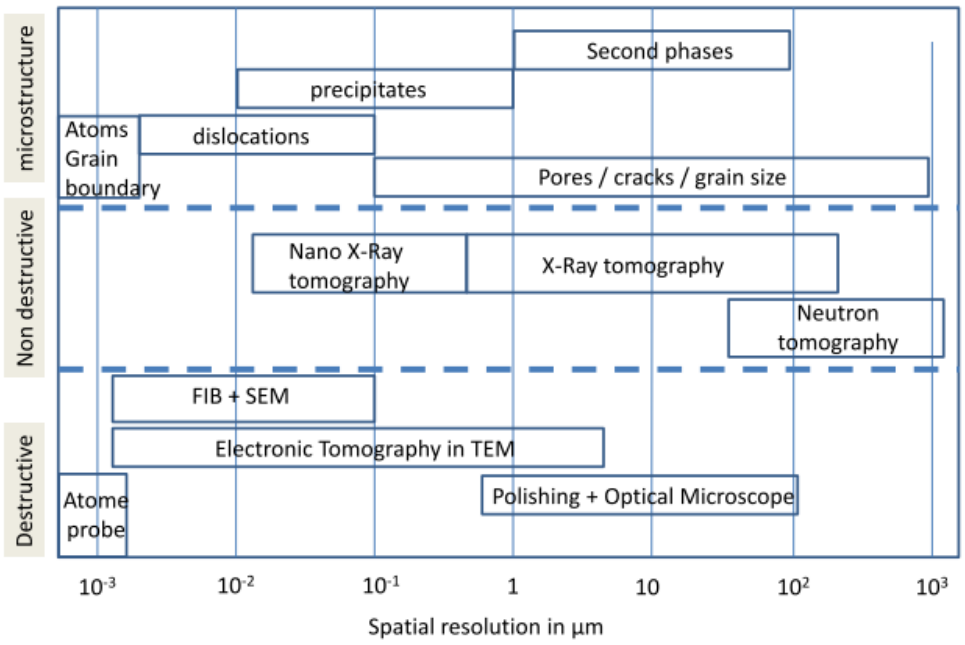

Figure 1.5. Comparison of different imaging techniques based on resolvable features and destructiveness.[47]

present. Ebner et al. performed operando tomography on SnO anode materials and were able to track the transformation from SnO to Li_2O and Sn nanoparticles.[51] Other studies use a polychromatic beam (also referred to as a white or pink beam) to interrogate high Z or high density materials, such as stainless steel.[52]

In this work, I utilize X-ray tomography to describe the mechanical changes, especially crack formation, in solid electrolytes during electrochemical cycling between Li metal electrodes. X-ray tomography performed at a synchrotron provides the needed flux and energy to probe batteries within sealed, air and moisture-free cells during cycling. Monochromatic X-rays enable us to examine solid electrolytes made of low Z elements, such as Li, S, and P.

1.4 References

(1) United States Environmental Protection Agency. *Inventory of U.S. Greenhouse Gas Emissions and Sinks: 1990-2016*; Washington D.C., 2018.

(2) United States Environmental Protection Agency Office of Transportation and Air Quality; Quality, A.; Division, C. *Greenhouse Gas Emissions from a Typical Passenger Vehicle*; Washington D.C., 2018.

(3) United States Department of Energy Office of Energy Efficiency and Renewable Energy; United States Environmental Protection Agency. *Fuel Economy Guide - Model Year 2019*; 2019.

(4) Tarascon, J.-M.; Armand, M. *Nature* **2001**, *414*, 359.

(5) Li, J.; Du, Z.; Ruther, R. E.; AN, S. J.; David, L. A.; Hays, K.; Wood, M.; Phillip, N. D.; Sheng, Y.; Mao, C.; Kalnaus, S.; Daniel, C.; Wood, D. L. *JOM* **2017**, *69*, 1484.

(6) Manthiram, A. *ACS Cent. Sci.* **2017**, *3*, 1063.

(7) Goodenough, J. B.; Park, K.-S. *J. Am. Chem. Soc.* **2013**, *135*, 1167.

(8) Reddy, T. B. *Linden's Handbook of Batteries*; 4th Ed.; McGraw-Hill, 2011.

(9) Orsini, F.; du Pasquier, A.; Beaudouin, B.; Tarascon, J. M.; Trentin, M.; Langenhuizen, N.; de Beer, E.; Notten, P. *J. Power Sources* **1999**, *81–82*, 918.

(10) Harry, K. J.; Hallinan, D. T.; Parkinson, D. Y.; MacDowell, A. A.; Balsara, N. P. *Nat.*

Mater. **2014**, *13*, 69.

(11) Whittingham, M. S. *Chem. Rev.* **2004**, *104*, 4271.

(12) Bard, A. J.; Faulkner, L. R. *Electrochemical Methods*; Harris, D.; Swain, E.; Bobey, C.; Aiello, E., Eds.; 2nd ed.; John Wiley & Sons, Inc.: Hoboken, New Jersey, 2001.

(13) Etacheri, V.; Marom, R.; Elazari, R.; Salitra, G.; Aurbach, D. *Energy Environ. Sci.* **2011**, *4*, 3243.

(14) Marcinek, M.; Syzdek, J.; Marczewski, M.; Piszcz, M.; Niedzicki, L.; Kalita, M.; Plewa-Marczewska, A.; Bitner, A.; Wieczorek, P.; Trzeciak, T.; Kasprzyk, M.; P.Łężak; Zukowska, Z.; Zalewska, A.; Wieczorek, W. *Solid State Ionics* **2015**, *276*, 107.

(15) An, S. J.; Li, J.; Daniel, C.; Mohanty, D.; Nagpure, S.; Wood, D. L. *Carbon N. Y.* **2016**, *105*, 52.

(16) Bülter, H.; Peters, F.; Schwenzel, J.; Wittstock, G. *Angew. Chemie Int. Ed.* **2014**, *53*, 10531.

(17) Lu, P.; Li, C.; Schneider, E. W.; Harris, S. J. *J. Phys. Chem. C* **2014**, *118*, 896.

(18) Cheng, X.-B.; Zhang, R.; Zhao, C.-Z.; Wei, F.; Zhang, J.-G.; Zhang, Q. *Adv. Sci.* **2016**, *3*, 1500213.

(19) Verma, P.; Maire, P.; Novák, P. *Electrochim. Acta* **2010**, *55*, 6332.

(20) Edström, K.; Gustafsson, T.; Thomas, J. O. *Electrochim. Acta* **2004**, *50*, 397.

(21) Kim, J. G.; Son, B.; Mukherjee, S.; Schuppert, N.; Bates, A.; Kwon, O.; Choi, M. J.; Chung, H. Y.; Park, S. *J. Power Sources* **2015**, *282*, 299.

(22) Richards, W. D.; Miara, L. J.; Wang, Y.; Kim, J. C.; Ceder, G. *Chem. Mater.* **2016**, *28*, 266.

(23) Takada, K. *Acta Mater.* **2013**, *61*, 759.

(24) Li, J.; Ma, C.; Chi, M.; Liang, C.; Dudney, N. J. *Adv. Energy Mater.* **2015**, *5*, 1401408.

(25) Monroe, C.; Newman, J. *J. Electrochem. Soc.* **2004**, *151*, A880.

(26) Monroe, C.; Newman, J. *J. Electrochem. Soc.* **2005**, *152*, A396.

(27) Porz, L.; Swamy, T.; Sheldon, B. W.; Rettenwander, D.; Frömling, T.; Thaman, H. L.; Berendts, S.; Uecker, R.; Carter, W. C.; Chiang, Y.-M. *Adv. Energy Mater.* **2017**, *7*, 1701003.

(28) Ren, Y.; Shen, Y.; Lin, Y.; Nan, C.-W. *Electrochem. commun.* **2015**, *57*, 27.

(29) Cheng, E. J.; Sharafi, A.; Sakamoto, J. *Electrochim. Acta* **2017**, *223*, 85.

(30) Haiss, W. *Reports Prog. Phys.* **2001**, *64*, 591.

(31) Freund, L. B.; Suresh, S. *Thin Film Materials*; First.; Cambridge University Press: Cambridge, UK, 2003.

(32) Stoney, G. G. *Proc. R. Soc. A Math. Phys. Eng. Sci.* **1909**, *82*, 172.

(33) Langer, J. L.; Economy, J.; Cahill, D. G. *Macromolecules* **2012**, *45*, 3205.

(34) Zhang, X.; Cahill, D. G. *Langmuir* **2006**, *22*, 9062.

(35) Ibach, H.; Bach, C. E.; Giesen, M.; Grossmann, A. *Surf. Sci.* **1997**, *375*, 107.

(36) Haiss, W.; Sass, J. K. *J. Electroanal. Chem.* **1996**, *410*, 119.

(37) Cattarin, S.; Pantano, E.; Decker, F. *Electrochem. commun.* **1999**, *1*, 483.

(38) Fredlein, R. A.; Damjanovic, A.; Bockris, J. O. *Surf. Sci.* **1971**, *25*, 261.

(39) Gokhshtein, A. Y. *Electrochim. Acta* **1970**, *15*, 219.

(40) Mukhopadhyay, A.; Kali, R.; Badjate, S.; Tokranov, A.; Sheldon, B. W. *Scr. Mater.* **2014**, *92*, 47.

(41) Sheth, J.; Karan, N. K.; Abraham, D. P.; Nguyen, C. C.; Lucht, B. L.; Sheldon, B. W.; Guduru, P. R. *J. Electrochem. Soc.* **2016**, *163*, A2524.

(42) Mukaibo, H.; Momma, T.; Shacham-Diamand, Y.; Osaka, T.; Kodaira, M. *Electrochem. Solid-State Lett.* **2007**, *10*, A70.

(43) Fakkao, M.; Kimura, Y.; Funayama, K.; Nakamura, T.; Kuwata, N.; Kawamura, J.; Kawada, T.; Amezawa, K. *Solid State Ionics* **2017**, *299*, 8.

(44) Mukhopadhyay, A.; Sheldon, B. W. *Prog. Mater. Sci.* **2014**, *63*, 58.

(45) Tavassol, H.; Cason, M. W.; Nuzzo, R. G.; Gewirth, A. A. *Adv. Energy Mater.* **2015**, *5*, 1400317.

(46) Tavassol, H.; Jones, E. M. C.; Sottos, N. R.; Gewirth, A. A. *Nat. Mater.* **2016**, *15*, 1182.

(47) Salvo, L.; Suéry, M.; Marmottant, A.; Limodin, N.; Bernard, D. *Comptes Rendus Phys.* **2010**, *11*, 641.

(48) Buffiere, J.-Y.; Maire, E.; Adrien, J.; Masse, J.-P.; Boller, E. *Exp. Mech.* **2010**, *50*, 289.

(49) Cnudde, V.; Boone, M. N. *Earth-Science Rev.* **2013**, *123*, 1.

(50) Willmott, P. *An Introduction to Synchrotron Radiation*; 1st ed.; John Wiley & Sons, Ltd: West Sussex, UK, 2011.

(51) Ebner, M.; Marone, F.; Stampanoni, M.; Wood, V. *Science (80-.).* **2013**, *342*, 716.

(52) Matusik, K. E.; Duke, D. J.; Kastengren, A. L.; Sovis, N.; Swantek, A. B.; Powell, C. F. *Int. J. Engine Res.* **2018**, *19*, 963.

Chapter 2: Electrochemical Stiffness Changes in Lithium Manganese Oxide Electrodes

Reproduced with permission from Çapraz, Ö. Ö.; Bassett, K. L.; Gewirth, A. A.; Sottos, N. R. Electrochemical Stiffness Changes in Lithium Manganese Oxide Electrodes. Adv. Energy Mater. 2016, 1601778. Copyright 2016 Advanced Energy Materials.

2.1 Introduction

Rechargeable Li-ion batteries have a desirable combination of high energy and power density, making them prime candidates for powering portable electronics and electric vehicles.[1] One key hurdle in the fabrication of better batteries is overcoming capacity fade in cathode electrodes.[2] Lithium manganese oxide (LMO) is a promising cathode material due to its high theoretical energy density, environmental benignity, low cost, and low toxicity.[3] However, LMO suffers from significant capacity fade due to manganese dissolution,[4–12] instability at the cathode electrolyte interface (CEI),[13–15] particle fracture,[16,17] and Jahn-Teller distortion.[18–21]

The intercalation of Li^+ ions, as well as the transition of active material phases, causes mechanical failure of the electrodes.[16] Specifically, in Li_XMn2O4 spinel systems, where $0<x<1$, Li^+ ions are extracted from or inserted into the interstitial sites in the host Mn_2O_4 framework.[22–25] $LiMn_2O_4$ spinel undergoes phase transitions to the empty λ-Mn_2O_4 spinel, resulting in a 6.8 % volume change in the cubic lattice.[26] In situ X-ray diffraction (XRD) shows the LMO spinel electrode experiences one cubic phase transition occurring during the 3.96 V plateau and another during the 4.07 V plateau.[23] Jahn-Teller distortion occurs when $Li_xMn_2O_4$ is further lithiated between $1<x<2$, resulting in an additional 5.6 % lattice volume expansion.[19–21] Phase transitions result in abrupt changes in the lattice parameter and cause misfit strain at the interface between the growing and consumed cubic phases, which leads to crack formation in the cathode.[27–32] Particle fracture results in the isolation of the degraded electrode particles which eventually results in loss of grain-to-grain connectivity within the particles.[33,34] The generation of isolated, non-reactive particles alters the electrode kinetic and thermodynamic properties, such as charge transfer resistance and entropy in the electrode,[35–40] and increases the dissolution rate of Mn^{2+} ions into the electrolyte. Understanding property changes and mechanical deformations in the electrode particles may play an important role in improving the electrochemical properties of Li-ion cathodes.

The mechanical degradation of Li-ion battery electrodes has been investigated with various measurements such as scanning electron microscopy (SEM),[16,17] transmission electron microscopy,[34,41–44] acoustic emission,[31] atomic force microscopy,[45,46] strain measurements,[47–50] and stress curvature measurements.[51–55] Recently, we observed asynchronous in situ strain and stress in a composite graphite electrode during lithiation and combined these measurements to calculate the electrochemical stiffness in the anode by taking the derivative of stress with respect to strain.[51] The asynchrony upon lithiation was associated with stress buildup during the early stages of Li^+ intercalation into the graphite anode. We wondered whether the interaction of Li^+ with cathode electrodes might also give an asynchronous mechanical response.

In this study, we monitor in situ strain and stress in a composite LMO electrode. In situ strain in the electrode is calculated by using the optical, full-field digital image correlation (DIC) technique.[56–58] The progression of deformation is tracked by following the electrode's natural speckle pattern. The bending cantilever technique is applied to calculate in situ stress generation in the electrode by monitoring the changes in the cantilever curvature,[55] as explained in more detail in the Experimental Methods. Strain and stress are coordinated by applied potential and ratioed to calculate the electrochemical stiffness.

2.2 Experimental Methods

2.2.1 Electrode Fabrication

As-received lithium manganese oxide (LMO) powder (electrochemical grade, Sigma-Aldrich, St. Louis, MO) was ball-milled in a SPEX Mixer/Mill 8000D for 1 hour with a hardened steel vial (5 mL capacity) and balls (6.35 mm diameter) with a grinding medium to LMO ratio of 5:7 (mass basis). Average particle size of the LMO particles is less than 1 μm. LMO composite electrodes were fabricated from water based slurry with a composition of 8:1:1 weight percent of LMO, carboxymethylcellulose sodium salt binder (Aldrich), and carbon black (Super P Li, Timcal). Electrodes for stress measurements were fabricated on a cantilever using a doctor blade yielding an electrode thickness of 2.1± 0.8 microns. Prior to casting, the cantilever (3 mm x 30 mm x 150 micron glass coverslip) was coated with a Ti adhesion layer (20 nm) followed by an Al current collector (100 nm) by using electron beam deposition. Electrodes for strain measurements

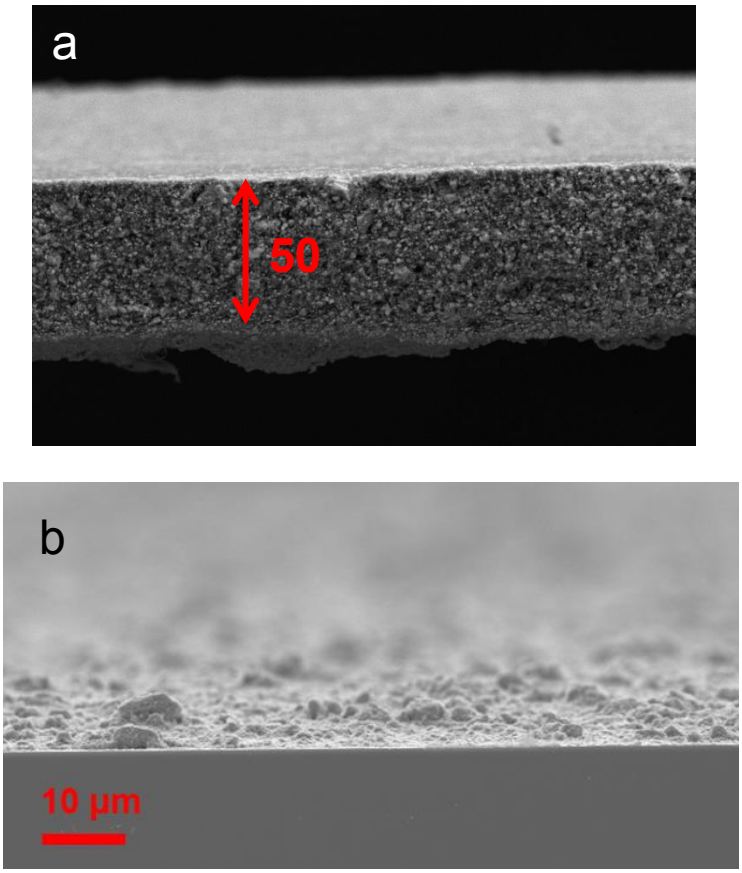

Figure 2.1. Cross-sections of a) a free-standing LMO electrode for strain measurements and b) a supported LMO electrode on a glass cantilever for stress measurements.

were free-standing and cast with a doctor blade to ca. 50 micron thickness and cut to a dimension of ca. 3 mm x 7 mm (Figure 2.1).

2.2.2 Electrochemical Cycling

Electrolyte components were used as received. The electrodes were analyzed by cyclic voltammetry in 1 M $LiPF_6$ (98%, Sigma-Aldrich) in 1:1 ethylene carbonate (anhydrous 99%, Sigma-Aldrich)/ dimethyl carbonate (anhydrous 99+%, Sigma-Aldrich) during strain and stress measurements in custom cells.[47,48] The cells were sealed under an Ar atmosphere and the counter/reference electrode was made from Li foil (Alfa Aesar). All potentials are with respect to the Li/Li^+ couple. The cells were cycled from 3.5 to 4.5 V, starting at open circuit potential followed by delithiation at 25µV s^{-1}. The average particle diameter and electrode thickness and morphology were analyzed by SEM (JEOL, JSM-7000F and Philips XL30 ESEM-FEG) before and after cycling. The refractive index of the electrolyte solution was found to be 1.338 by using a Mettler Toledo Refracto 30GS refractometer.

2.2.3 Strain and Stress Measurements

The digital image correlation (DIC) technique was used to track the evolution of strain (ε) in an unconstrained electrode during electrochemical cycling.[56–58] DIC is a full field optical method, which measures deformation by tracking the changes in gray value pattern in small neighborhoods called subsets during deformation. The surface of composite LMO electrodes has a natural speckle pattern that is suitable for tracking by the DIC technique. Images of 3 by 7 mm (1392 by 1040 pixels) field of view were captured every 10 minutes during cycling using an Aqua camera and 12X zoom lens (Navitar). The composite LMO electrode was assumed to be homogeneous and isotropic, following the method established by Jones et al.[47] Correlations to calculate strains and displacements were performed using the commercial software VIC2D using a subset size of 60 μm by 60 μm.

An optical bending cantilever technique[55] was used to monitor the evolution of the stress-thickness ($\sigma \cdot t$) in a constrained electrode during electrochemical cycling. Curvature changes of the reflective cantilever backside were recorded using an optical stress measurement setup described previously[59] and were used to determine stress-thickness in the sample using Stoney's equation;

$$\sigma \cdot t = \int_0^t \sigma_{ij} dz = {Y h_s^2 d\kappa}\Big/{6(1-\nu_s)} \qquad (2.1)$$

where $d\kappa$ is the cantilever curvature; h_s, Y, and ν_s are the thickness, Young's modulus (=75.9 GPa for glass), and Poisson's ratio (=0.22) of the cantilever substrate, respectively; and σ_{ij} is the integrated stress through t, the sample thickness. Reported stress-thickness values are changes relative to the pristine electrode.

2.3. Results and Discussion

2.3.1. Strain and Stress Development

In situ strain and stress measurements were performed under the same electrochemical conditions. Figure 2.2 shows typical voltammetry and the corresponding strain and stress response of composite LMO electrodes at a scan rate of 25 μV s^{-1}. During delithiation (anodic scan) between 3.5 and 3.8 V, a small contraction is observed in the unconstrained electrode (Figure 2.2b) and stress in the constrained electrode becomes slightly tensile (Figure 2.2c). At more positive potentials, there are two distinct current peaks, labeled α (4.03 V) and γ (4.16 V).[60] α represents

the cubic I to cubic II phase transition, and γ represents the cubic II to cubic III phase transition in LMO. The corresponding reverse transitions upon lithiation (cathodic scan) are labeled α' (3.96 V) and γ' (4.09 V). The current peaks occur simultaneously with these transitions.[23] In the same potential regime (ca. 3.8 to 4.3 V), strain and stress exhibit changes in slope also associated with lithiation and delithiation events. At potentials above 4.3 V, both the expansion of the unconstrained electrode and evolution of stress in the constrained electrode remain nearly constant.

During delithiation, the electrode contracts as seen by the evolution of strain (Figure 2.2b) and tensile stress (Figure 2.2c). During lithiation, tensile stress is relieved and the electrode expands. Compressive stress-thickness of ca. -3 N m^{-1} and expansive strain of ca. 0.1 % at the end of the cycle (3.5 V) are due to the generation of irreversible strain and stress. The irreversible electrode response is associated with irreversible processes such as CEI formation[61,62] or Mn^{2+} ion dissolution.[11,63–65]

In order to understand the potential dependent variations in strain and stress, we calculated the derivatives of strain and stress with respect to potential in Figure 2.3b,c (delithiation) and

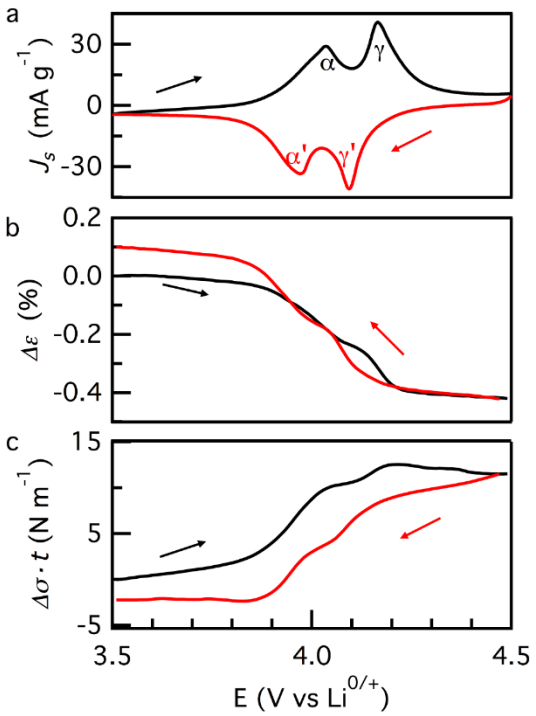

Figure 2.2. Potential-dependent mechanical response of a LMO electrode during cyclic voltammetry (CV). a) Current density (J_s) for the fourth cycle CV at 25 μV s^{-1} with corresponding in situ b) changes in strain ($\Delta\varepsilon$) and c) stress-thickness ($\Delta\sigma \cdot t$). Strain and stress-thickness values are shifted to start from zero. The black line (—) represents the anodic scan whereas the red line (—) indicates the cathodic scan. Arrows indicate the direction of the scans.

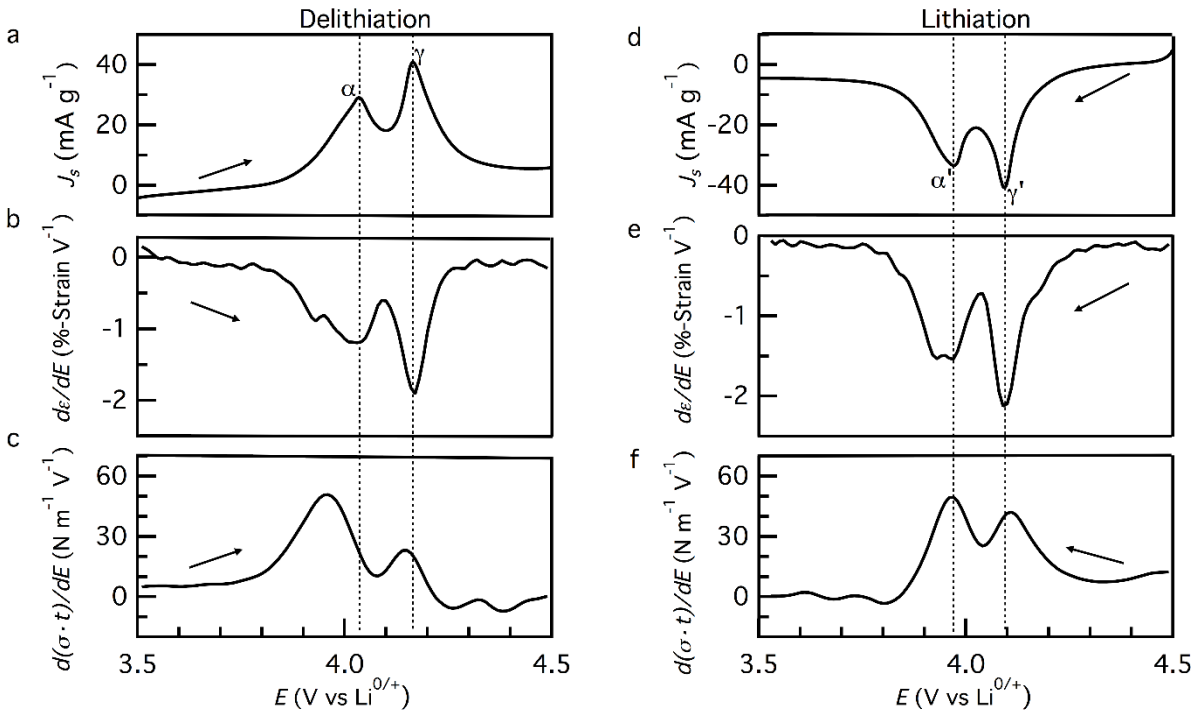

Figure 2.3. Stress and strain derivatives with respect to potential for fourth cycle CV at 25 μV s^{-1}. a) Current density (J_s), b) corresponding strain derivative ($d\varepsilon/dE$), and c) stress derivative ($d(\sigma \cdot t)/dE$) during delithiation; d) current density, e) corresponding strain derivative, and c) stress derivative during lithiation.

Figure 2.3e,f (lithiation). Figure 2.3b,c shows the presence of two dominant peaks in the strain and stress derivatives during delithiation. Interestingly, the maxima of the strain derivative match with the α and γ current peaks to within 0.01 V. The coupling of volumetric changes in the electrode with respect to the degree of lithiation is described in the literature.[66–68] Alternatively, the maximum of the stress derivative occurs more negative of the α peak. A similar asynchronous response between strain and stress was previously observed during lithiation of a graphite electrode.[51]

During lithiation and delithiation, the LMO lattice expands and contracts. Figure 2.4 compares the strain derivative obtained in this work to LMO lattice parameter changes, reproduced from a prior XRD study by Sun et al.[23] During delithiation, sharp changes in the lattice parameter are well aligned (within 0.01 V) with the strain derivative peaks, located at 4.03 and 4.17 V. The cubic I to II (α) and cubic II to III (γ) phase transitions change the lattice parameter by 0.029 Å and 0.114 Å, respectively. Interestingly, the magnitude of the strain derivative aligned with the γ transition is larger than that corresponding to the α transition.

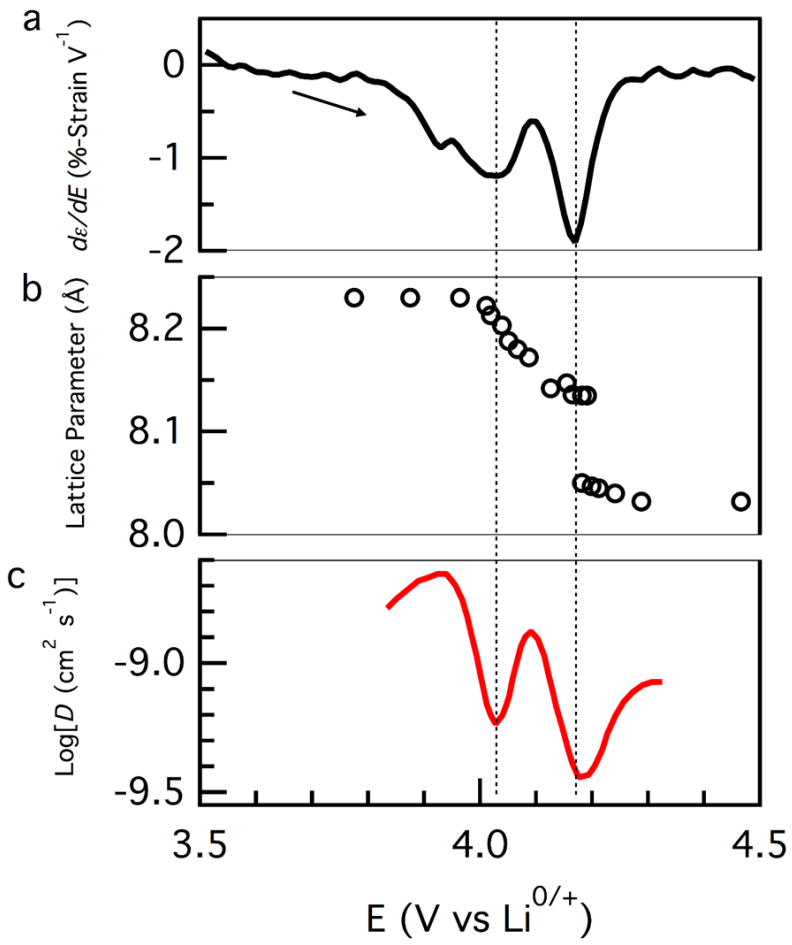

Figure 2.4. Relationship between strain evolution and LMO structural changes during delithiation. a) Strain derivative *(dε/dE)* (black line) during the fourth CV cycle at 25 μV s^{-1} is plotted with b) changes in the lattice parameter (black circles) observed during in situ diffraction studies from Sun et al.[23] and c) chemical diffusion coefficients (red line) calculated from impedance studies by Crain et al.[69]

Figure 2.4 also compares the derivative of strain with respect to potential from the current work to the Li^+ ion diffusion coefficient, *D*, calculated from impedance measurements by Crain et al.[69] As reported previously by Saidi et al.[70], the diffusion coefficient of Li^+ ions in LMO decreases due to repulsive Coulombic interactions as the α and γ transitions occur and Li^+ ion diffusion through the bulk becomes limited as available sites fill. Li^+ ion hopping from site to site becomes dependent on the availability of open sites and is slowed by ion repulsions.[70] Similar to the phase transitions, the local minima in the strain derivative (Figure 2.4a) coincide exactly with the local minima in the diffusion coefficient (Figure 2.4c). Additionally, density functional theory (DFT) calculations show the bulk diffusion of Li^+ ions is affected by strain.[71] Therefore, phase transformation-induced strain is well correlated with Li^+ ion diffusivity in the bulk.

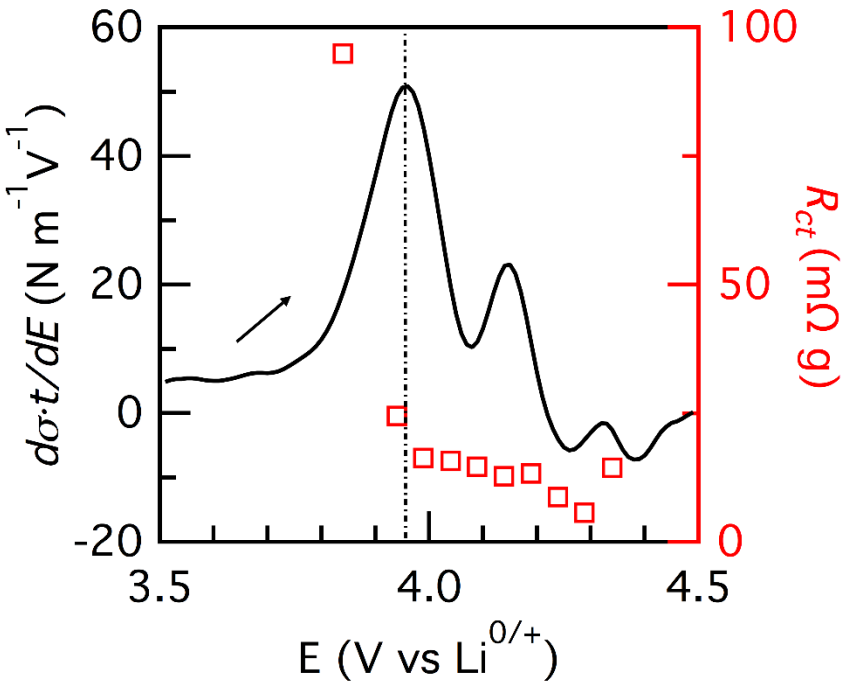

Figure 2.5. Relationship between stress evolution and surface kinetics. The charge transfer resistance (R_{ct}) (red squares) as calculated from electrochemical impedance spectroscopy by Crain et al.[69] indicates a decrease in R_{ct} in conjunction with the appearance of the stress derivative ($d(\sigma \cdot t)/dE$) (black line) peak at 3.95 V which precedes the corresponding current peak (Figure 2.3a). The vertical dashed line does not correspond to α and γ, but is used to draw the eye to a particular derivative feature.

Figure 2.3c shows two significant peaks in the stress derivative during delithiation, located at 3.95 and 4.15 V. Interestingly, the initial stress derivative peak (at 3.95 V) precedes the initial strain derivative and the α current peak, indicating the sharp change in the stress derivative is not correlated to bulk phase changes in the electrode. Furthermore, the initial stress derivative peak cannot be related to CEI formation since an electrochemical quartz crystal microbalance study reported detectable CEI growth during the first cycle only.[72] In Figure 2.5, we compare the stress derivative measured in this work during delithiation with the charge transfer resistance, R_{ct}, reproduced from an impedance study by Crain et al.[69] A dramatic decrease in R_{ct} coincides with the significant jump in the stress derivative. We hypothesize that the asynchronous development of stress reflects the influence of Li^+ ion kinetics at the LMO interface.

Figure 2.3e shows the strain derivative peaks during lithiation (at 3.95 and 4.09 V) are well aligned with the α' and γ' current peaks and again correspond well with the LMO phase transformations.[23] In great contrast to our asynchronous observations during delithiation, the stress

derivative peaks (located at 3.97 and 4.11 V) measured during lithiation coincide roughly with the current peaks in Figure 2.3f.

2.3.2. Electrochemical Stiffness

Strain and stress-thickness are normalized and plotted with respect to each other in Figure 2.6 to directly compare changes in strain and stress. To create the plot, we normalized stress-thickness and strain as follows,

$$\sigma_N(E) = \left[\sigma(E) - \sigma_{min}/\sigma_{max} - \sigma_{min}\right] \cdot t \quad (2.2)$$

$$\varepsilon_N(E) = \left[\varepsilon(E) - \varepsilon_{min}/\varepsilon_{max} - \varepsilon_{min}\right] \quad (2.3)$$

where $\sigma_N(E)$ and $\varepsilon_N(E)$ are the normalized stress-thickness and strain and σ_{min}, σ_{max}, ε_{min}, and ε_{max} are the maximum and minimum stress-thickness and strain values during delithiation and lithiation from Figure 2.2, respectively. Variations in curves are due to the asynchronous evolution of strain and stress during delithiation and lithiation. Tavassol et al. also observed similar variations in the stress-strain curves for a graphite negative electrode.[51] Upon delithiation, graphite experiences large changes in stress with minimal changes in strain until ca. 0.1 V, and the opposite occurs between 0.20 V to 0.25 V.[51]

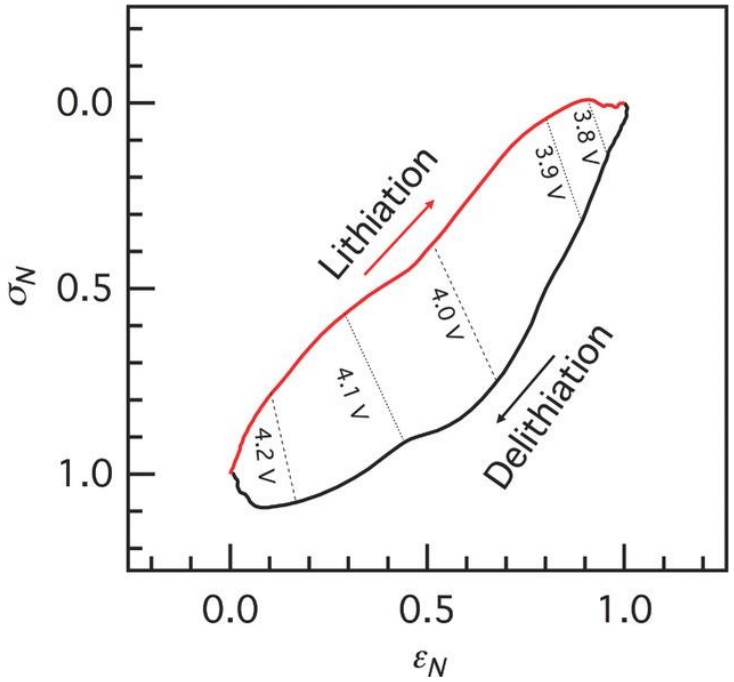

Figure 2.6. Stress evolution as a function of strain. The normalized stress and strain (see Equation (2.2) and (2.3), respectively) responses from the fourth cycle CV at 25 μV s^{-1} (from Figure 2.2), matched at various potential values. The dashed lines represent the potentials. The black line (—) represents delithiation whereas the red line (—) indicates lithiation. Arrows indicate the direction of the scans.

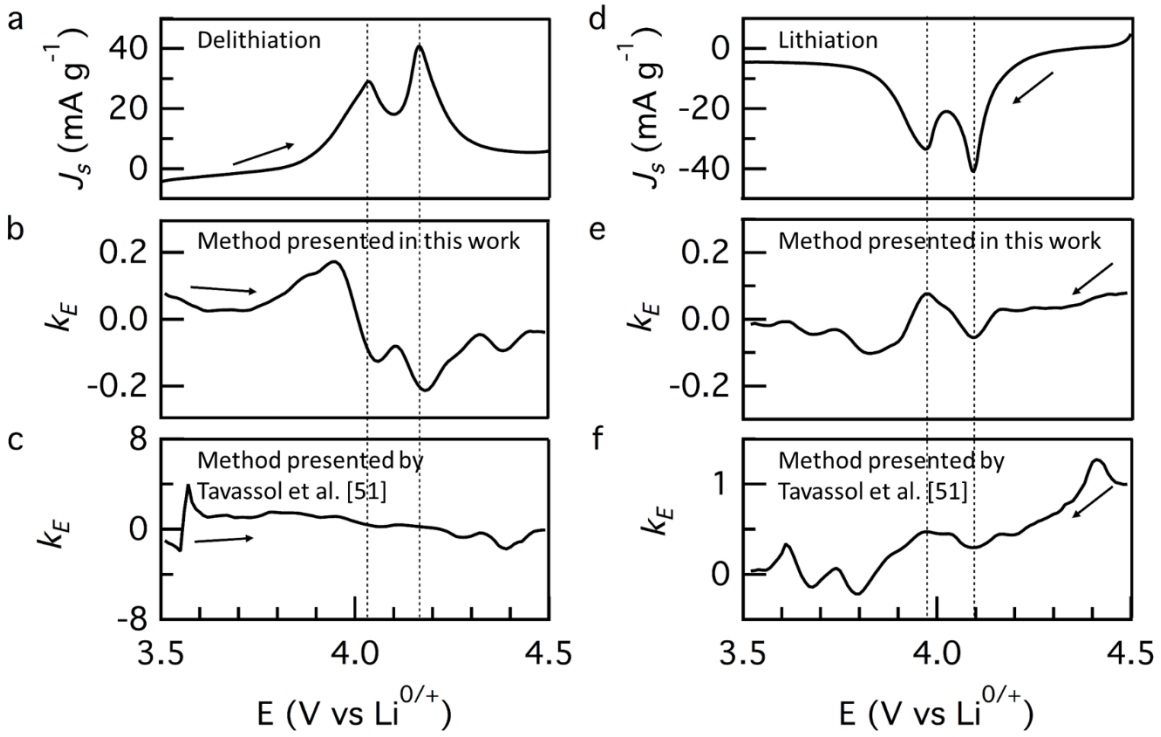

Figure 2.7. Comparison of two different approaches to calculate electrochemical stiffness, k_E, from data reported in this paper. a,d) Fourth cycle CV at 25 μV s^{-1}. b,e) Electrochemical stiffness calculated using the methods described in this paper. c,f) Electrochemical stiffness calculated using the methods described previously by Tavassol et al.[51]

The electrochemical stiffness of the electrode is related to incremental changes in strain and stress induced by the lithiation-delithiation process. The electrochemical stiffness is not a traditional material property, such as the Young's modulus, but instead is dependent on the state of charge. Previously, the electrochemical stiffness in graphite was calculated by taking the derivative of stress with respect to strain.[51]

$$k_E(E) = \frac{\partial(-\Delta\sigma)}{\partial\varepsilon} \tag{2.4}$$

In comparison to graphite, the stress-strain curve for LMO is more oblate and contains vertical asymptotes, the derivative of which results in false peaks that dominate the potential-dependent stiffness response. Figure 2.6 shows key features of interest including portions of the stress vs. strain plot in which the derivative cannot be defined. When a derivative is computed at such a point, the resulting k_E plot contains a vertical asymptote as seen in Figure 2.7. The vertical asymptote dwarfs any features of interest near the α (α') and γ (γ') current peaks during delithiation (lithiation).

Since the previous calculation method of Tavassol et al.[51] is not compatible with sharp changes in the stress-strain curves, an alternate method is adopted for this work. The stress and strain derivatives are normalized by dividing by the maximum derivative values from each measurement. The normalized stress and strain derivatives are also shifted vertically to avoid negative values in the calculation and to ensure numbers in the range $0 \leq x < 1$ are not in the denominator. The electrochemical stiffness, $k_E(E)$ is then calculated from the normalized stress and strain derivatives ($(d\sigma(E)/dE)_N$ and $(d\varepsilon(E)/dE)_N$, respectively) as follows,

$$k_E(E) = \frac{\left(d\sigma(E)/dE\right)_N}{\left(d\varepsilon(E)/dE\right)_N} - 1 \tag{2.5}$$

The stiffness is shifted by 1 such that when $k_E(E) = 0$, strain and stress are equally opposing one another and there is "zero" stiffness. When $k_E(E)$ is positive, the stiffness is dominated by stress at a given potential. When $k_E(E)$ is negative, stiffness is strain-dominated. Therefore, the electrochemical stiffness provides insight into the relative influence of strain and stress on the mechanical response of the electrode at a particular stage of lithiation or delithiation.

The relative magnitudes of stress and strain (Figure 2.2, ca. 12 N/m vs ca. -0.4%, respectively) are difficult to compare because the magnitudes are so dissimilar and have different units. Consequentially, the stress and strain derivative calculations are different by more than an order of magnitude. Therefore, before the ratio of the derivatives is calculated, the derivatives must first be normalized. Both the stress and strain derivatives are divided by their respective maximum peak value. As a rough example, the strain derivative from Figure 2.3b would be normalized by ca. -2 and the stress derivative from Figure 2.3c would be normalized by ca. 50. Both derivatives are then shifted up by the value of 2 to avoid negative values in the calculation and to ensure numbers in the range $0 \leq x < 1$ are not in the denominator.

Figure 2.8 shows the evolution of stiffness upon delithiation and lithiation of the electrode with the corresponding current response. Standard deviations are calculated from three measurements. Reproducible stiffness maxima and minima are marked numerically. During delithiation of the LMO electrode, four stiffness peaks are observed at 3.94 V, 4.06 V, 4.11 V and 4.18 V (Figure 2.8b). Interestingly, peak ① at 3.94 V precedes the initial current peak at 4.03 V while peak ④ more closely corresponds to the γ current peak. During lithiation, stiffness peaks ⑤, ⑥, and ⑦ are observed at 4.09, 3.96, and 3.87 V (Figure 2.8d). While peaks ⑤ and ⑥

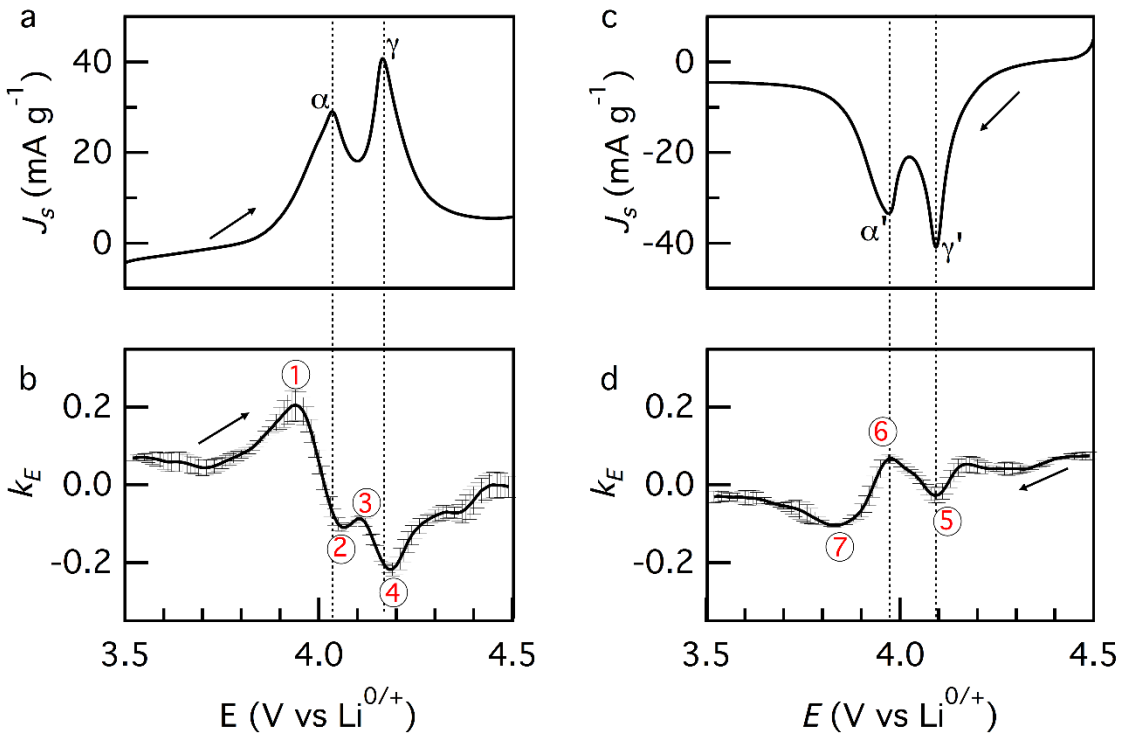

Figure 2.8. Electrochemical stiffness evolution. a) Current density (J_s) with corresponding b) electrochemical stiffness during delithiation; c) current density with corresponding d) electrochemical stiffness during lithiation for fourth cycle CV at 25 μV s^{-1}. Electrochemical stiffness is calculated by taking the ratio of the normalized derivatives (Equation 2.5). Vertical dashed lines represent the phase transformations. Arrows indicate the direction of the scans.

correspond with the γ' (4.09 V) and α' (3.96 V) current peaks, peak ⑦ is offset relative to the α' current peak.

The proposed driving forces for stress and strain evolution during delithiation and lithiation are shown schematically in Figure 2.9. Delithiation occurs primarily as a "surface" reaction, in which the extraction of Li^+ ions from the active material takes places. Initially surface resistance restrains the outflux of Li^+ ions into the electrolyte.[35,36,69] In the measurements reported here, this resistance is manifested as an increase in stress-dominated stiffness corresponding to peak ① in Figure 2.8b. Previous calculations also show an increase in stress during the early delithiation process due to higher pressure in the outer part of the particle.[73] Once Li^+ ions overcome the kinetic barrier at the surface; removal of ions from the LMO lattice begins and initiates the α phase transformation. The transition leads to an increase in strain which results in reduced stiffness values (peak ②). Peak ③ corresponds to the Li^+ ion diffusivity maximum (Figure 2.4). Finally,

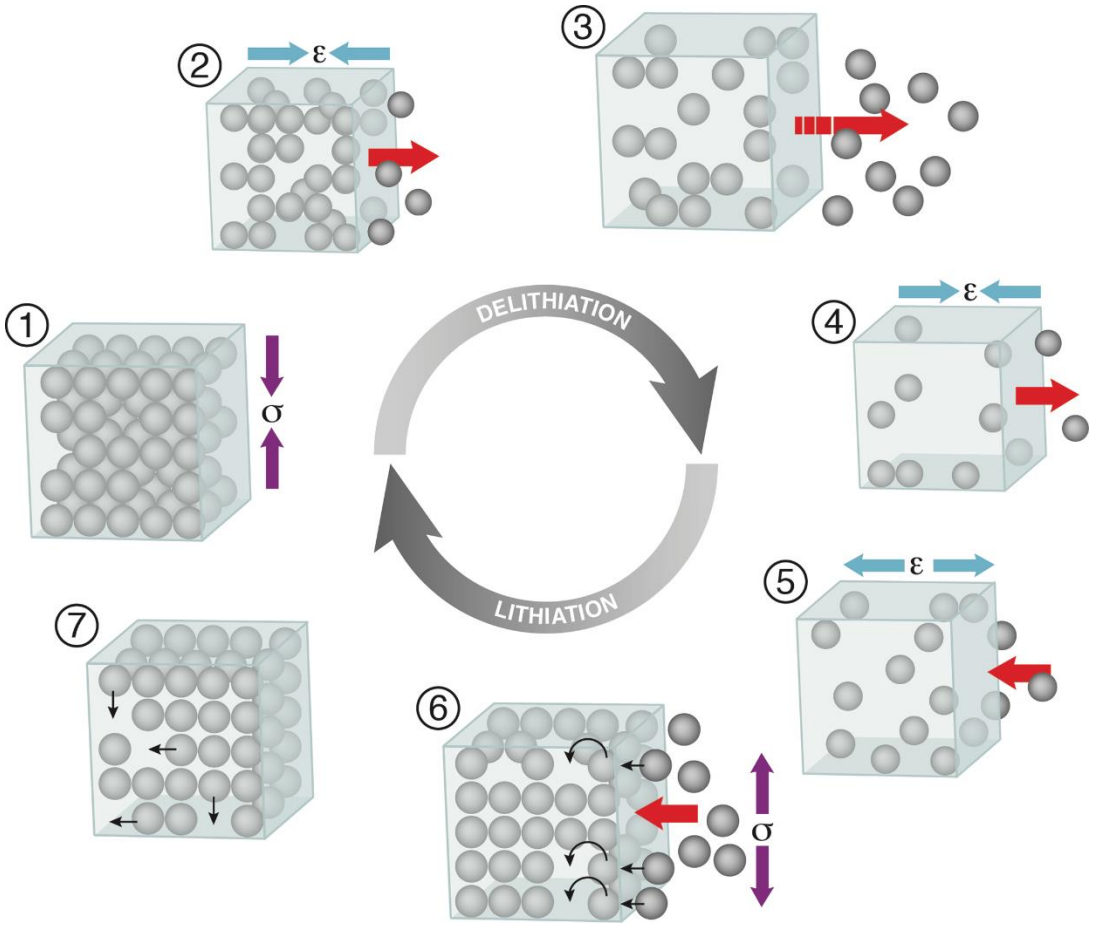

Figure 2.9. Schematic representation of the dominant strain and stress contributions to electrical stiffness during delithiation and lithiation. *Proposed mechanisms related to strain and stress during delithiation*: ① Increase in tensile stress due to charge transfer resistance at the surface, ② electrode contraction during α phase transition, ③ increase in Li^+ ion diffusivity, ④ electrode contraction during γ phase transition. *Proposed mechanisms related to strain and stress during lithiation*: ⑤ Electrode expansion during γ' phase transition, ⑥ increase in compressive stress caused by the difference between the Li^+ ion hopping and insertion rates, ⑦ relaxation of electrode by Li^+ ion rearrangement in the lattice. Red arrows represent the in- and out-flux of Li^+ ions. Black arrows show specific Li^+ ion movements into and through the lattice. Blue arrows show an increase in strain-dominated stiffness caused by expansion and shrinkage or the increase of stress in the electrode. Purple arrows show an increase in stress-dominated stiffness. Grey spheres represent Li^+ ions.

strain-dominated peak ④ reflects the rapid change in lattice parameter during the γ phase transformation. Thus, changes in the electrochemical stiffness correspond closely with processes occurring during delithiation.[51]

Variations in stiffness during charge and discharge (Figure 2.8b,d) reveal that delithiation and lithiation of LMO proceed via different mechanisms. Figure 2.9 illustrates the Li^+ ion insertion mechanism. During lithiation of the cubic III (lithium-depleted) phase, Li^+ ions rapidly diffuse into available sites in the LMO lattice with minimal resistance.[69] The γ' phase transformation induces

a large change in strain generation which causes a decrease in stiffness and leads to the appearance of a strain-dominated stiffness peak at 4.10 V (peak ⑤, Figure 2.8d). However, as the LMO lattice is filled, Coulombic repulsions between Li^+ ions reduce their diffusion into the electrode.[35,69] Li^+ ion-occupied sites in the LMO lattice must be vacated to create space for incoming ions, and so Li^+ ions hop from occupied to unoccupied neighboring sites.[62,74] Differences between the Li^+ ion hopping and insertion rates result in increased repulsive forces and leads to an increase in stress. This exothermic process between incoming Li^+ ions and Li^+-occupied sites escalates the disorder of the electrode, increasing the entropy of the system.[37–40] This hopping mechanism induces the formation of stress, which results in an increase in stiffness and brings about the appearance of a stress-dominated stiffness peak at 3.96 V (peak ⑥, Figure 2.8d). At potentials below ca. 3.9 V, the $Li_xMn_2O_4$ electrode is almost fully lithiated (x approaches 1).[23] As available Li^+ ion sites become filled, the reversible heat generation rate due to bulk phase changes decreases[38,39] and Li^+ ions rearrange in the lattice.[75] The broad stiffness peak ⑦ is associated with the lattice relaxation energy arising from the reduction of localized Mn^{4+} ions to Mn^{3+} ions. The strain-dominated sign of stiffness peak ⑦ is a consequence of electrode relaxation and the relatively low rate of lithiation.

Interestingly, stiffness variations during delithiation are greater than those associated with lithiation (Figure 2.8). Computational studies suggest different mechanical responses of electrodes during lithiation and delithiation.[31,32,76,77] A diffusion-induced stress model shows that variations in Young's modulus with respect to lithium concentration results in asymmetric stress profiles during lithiation and delithiation.[77] Also, microcrack generation occurs near the surface of the particle during delithiation and in the center of the particle during lithiation.[77,78] Lastly, a dynamic lattice spring model and experimental acoustic measurements found that the electrode experiences larger energy release due to brittle fracture during delithiation compared to lithiation.[31] As we and others have shown, delithiation causes larger mechanical changes in the particle compared to lithiation.[31,32,76]

2.4 Conclusion

Coordinated in situ strain and stress measurements were combined for the first time to calculate electrochemical stiffness changes in LMO. We extended the capability of the electrochemical stiffness calculation beyond that previously reported by comparing strain and

stress derivatives with respect to potential.[51] Li^+ ion intercalation mechanisms induce asynchronous stress and strain development in LMO. Changes in the electrochemical stiffness reveal that the underlying mechanisms governing stress and strain are intrinsically different. The state of charge and phase transitions of the electrode govern strain generation in LMO during delithiation and lithiation. However, stress is governed by surface resistance against lithium removal from the electrode into the electrolyte during delithiation and repulsive interactions between already occupied Li^+ ions and new inserted Li^+ ions during lithiation. During delithiation, the change in the stiffness magnitude is larger compared to that during lithiation and might be a contributing factor to the degradation of the electrode. We anticipate that every electrode will display unique stiffness features during lithiation and delithiation. Therefore, electrochemical stiffness provides a powerful tool for characterizing chemo-mechanical processes in different electrodes.

2.5 References

(1) Marom, R.; Amalraj, S. F.; Leifer, N.; Jacob, D.; Aurbach, D. *J. Mater. Chem.* **2011**, *21*, 9938.

(2) Etacheri, V.; Marom, R.; Elazari, R.; Salitra, G.; Aurbach, D. *Energy Environ. Sci.* **2011**, *4*, 3243.

(3) Yi, T.-F.; Zhu, Y.-R.; Zhu, X.-D.; Shu, J.; Yue, C.-B.; Zhou, A.-N. *Ionics (Kiel).* **2009**, *15*, 779.

(4) Zhan, C.; Lu, J.; Kropf, A. J.; Wu, T.; Jansen, A. N.; Sun, Y.-K.; Qiu, X.; Amine, K. *Nat. Commun.* **2013**, *4*, 2437.

(5) Aurbach, D.; Markovsky, B.; Salitra, G.; Markevich, E.; Talyossef, Y.; Koltypin, M.; Nazar, L.; Ellis, B.; Kovacheva, D. *J. Power Sources* **2007**, *165*, 491.

(6) Gummow, R. J.; de Kock, A.; Thackeray, M. M. *Solid State Ionics* **1994**, *69*, 59.

(7) Lu, J.; Zhan, C.; Wu, T.; Wen, J.; Lei, Y.; Kropf, A. J.; Wu, H.; Miller, D. J.; Elam, J. W.; Sun, Y.-K.; Qiu, X.; Amine, K. *Nat. Commun.* **2014**, *5*, 5693.

(8) Guan, D.; Jeevarajan, J. A.; Wang, Y. *Nanoscale* **2011**, *3*, 1465.

(9) Bai, Y.; Wu, F.; Yang, H.; Zhong, Y.; Wu, C. *Adv. Mater. Res.* **2011**, *391–392*, 1069.

(10) Li, C.; Zhang, H. P.; Fu, L. J.; Liu, H.; Wu, Y. P.; Rahm, E.; Holze, R.; Wu, H. Q. *Electrochim. Acta* **2006**, *51*, 3872.

(11) Esbenshade, J. L.; Fox, M. D.; Gewirth, A. A. *J. Electrochem. Soc.* **2014**, *162*, A26.

(12) Jaber-Ansari, L.; Puntambekar, K. P.; Kim, S.; Aykol, M.; Luo, L.; Wu, J.; Myers, B. D.; Iddir, H.; Russell, J. T.; Saldaña, S. J.; Kumar, R.; Thackeray, M. M.; Curtiss, L. A.; Dravid, V. P.; Wolverton, C.; Hersam, M. C. *Adv. Energy Mater.* **2015**, *5*, 1500646.

(13) Goodenough, J. B.; Kim, Y. *Chem. Mater.* **2010**, *22*, 587.

(14) Goodenough, J. B.; Park, K.-S. *J. Am. Chem. Soc.* **2013**, *135*, 1167.

(15) Kim, D.; Park, S.; Chae, O. B.; Ryu, J. H.; Kim, Y.-U.; Yin, R.-Z.; Oh, S. M. *J. Electrochem. Soc.* **2012**, *159*, A193.

(16) Wang, D.; Wu, X.; Wang, Z.; Chen, L. *J. Power Sources* **2005**, *140*, 125.

(17) Lim, M.-R.; Cho, W.-I.; Kim, K.-B. *J. Power Sources* **2001**, *92*, 168.

(18) Thackeray, M. M.; David, W. I. F.; Bruce, P. G.; Goodenough, J. B. *Mater. Res. Bull.* **1983**, *18*, 461.

(19) Ohzuku, T.; Kitagawa, M.; Hirai, T. *J. Electrochem. Soc.* **1990**, *137*, 769.

(20) Ohzuku, T.; Kitagawa, M.; Hirai, T. *J. Electrochem. Soc.* **1989**, *136*, 3169.

(21) Ohzuku, T.; Kato, J.; Sawai, K.; Hirai, T. *J. Electrochem. Soc.* **1991**, *138*, 2556.

(22) David, W. I. F.; Thackeray, M. M.; De Picciotto, L. A.; Goodenough, J. B. *J. Solid State Chem.* **1987**, *67*, 316.

(23) Sun, X.; Yang, X. Q.; Balasubramanian, M.; McBreen, J.; Xia, Y.; Sakai, T. *J. Electrochem. Soc.* **2002**, *149*, A842.

(24) Yang, X. Q.; Sun, X.; Lee, S. J.; McBreen, J.; Mukerjee, S.; Daroux, M. L.; Xing, X. K. *Electrochem. Solid-State Lett.* **1999**, *2*, 157.

(25) Liu, W.; Kowal, K.; Farrington, G. C. *J. Electrochem. Soc.* **1998**, *145*, 459.

(26) Qi, Y.; Hector, L. G.; James, C.; Kim, K. J. *J. Electrochem. Soc.* **2014**, *161*, F3010.

(27) Van der Ven, A.; Garikipati, K.; Kim, S.; Wagemaker, M. *J. Electrochem. Soc.* **2009**, *156*, A949.

(28) Hu, Y.; Zhao, X.; Suo, Z. *J. Mater. Res.* **2011**, *25*, 1007.

(29) Lee, S.; Oshima, Y.; Hosono, E.; Zhou, H.; Kim, K.; Chang, H. M.; Kanno, R.; Takayanagi, K. *J. Phys. Chem. C* **2013**, *117*, 24236.

(30) Zhao, K.; Pharr, M.; Vlassak, J. J.; Suo, Z. *J. Appl. Phys.* **2010**, *108*, 073517.

(31) Barai, P.; Mukherjee, P. P. *J. Electrochem. Soc.* **2014**, *161*, F3123.

(32) Woodford, W. H.; Chiang, Y.-M.; Carter, W. C. *J. Electrochem. Soc.* **2010**, *157*, A1052.

(33) Narayanrao, R.; Joglekar, M. M.; Inguva, S. *J. Electrochem. Soc.* **2013**, *160*, A125.

(34) Miller, D. J.; Proff, C.; Wen, J. G.; Abraham, D. P.; Bareño, J. *Adv. Energy Mater.* **2013**, *3*, 1098.

(35) Dokko, K.; Mohamedi, M.; Umeda, M.; Uchida, I. *J. Electrochem. Soc.* **2003**, *150*, A425.

(36) Zhuang, Q.-C.; Wei, T.; Du, L.-L.; Cui, Y.-L.; Fang, L.; Sun, S.-G. *J. Phys. Chem. C* **2010**, *114*, 8614.

(37) Thomas, K. E.; Bogatu, C.; Newman, J. *J. Electrochem. Soc.* **2001**, *148*, A570.

(38) Kobayashi, Y.; Mita, Y.; Seki, S.; Ohno, Y.; Miyashiro, H.; Nakayama, M.; Wakihara, M. *J. Electrochem. Soc.* **2008**, *155*, A14.

(39) Kim, J.-S.; Prakash, J.; Selman, J. R. *Electrochem. Solid-State Lett.* **2001**, *4*, A141.

(40) Wong, W. C.; Newman, J. *J. Electrochem. Soc.* **2002**, *149*, A493.

(41) Wang, H.; Jang, Y.-I.; Huang, B.; Sadoway, D. R.; Chiang, Y.-M. *J. Electrochem. Soc.* **1999**, *146*, 473.

(42) Zhou, J.; Notten, P. H. L. *J. Power Sources* **2008**, *177*, 553.

(43) Gabrisch, H.; Wilcox, J.; Doeff, M. M. *Electrochem. Solid-State Lett.* **2008**, *11*, A25.

(44) Liu, X. H.; Liu, Y.; Kushima, A.; Zhang, S.; Zhu, T.; Li, J.; Huang, J. Y. *Adv. Energy Mater.* **2012**, *2*, 722.

(45) Jesse, S.; Kumar, A.; Arruda, T. M.; Kim, Y.; Kalinin, S. V.; Ciucci, F. *MRS Bull.* **2012**, *37*, 651.

(46) Yoon, I.; Abraham, D. P.; Lucht, B. L.; Bower, A. F.; Guduru, P. R. *Adv. Energy Mater.* **2016**, *6*, 1600099.

(47) Jones, E. M. C.; Silberstein, M. N.; White, S. R.; Sottos, N. R. *Exp. Mech.* **2014**, *54*, 971.

(48) Schiffer, Z. J.; Cannarella, J.; Arnold, C. B. *J. Electrochem. Soc.* **2015**, *163*, A427.

(49) Qi, Y.; Harris, S. J. *J. Electrochem. Soc.* **2010**, *157*, A741.

(50) Glazer, M. P. B.; Cho, J.; Almer, J.; Okasinski, J.; Braun, P. V.; Dunand, D. C. *Adv. Energy Mater.* **2015**, *5*, 1500466.

(51) Tavassol, H.; Jones, E. M. C.; Sottos, N. R.; Gewirth, A. A. *Nat. Mater.* **2016**, *15*, 1182.

(52) Tavassol, H.; Cason, M. W.; Nuzzo, R. G.; Gewirth, A. A. *Adv. Energy Mater.* **2015**, *5*, 1400317.

(53) Tavassol, H.; Chan, M. K. Y.; Catarello, M. G.; Greeley, J.; Cahill, D. G.; Gewirth, A. A. *J. Electrochem. Soc.* **2013**, *160*, A888.

(54) Mukhopadhyay, A.; Kali, R.; Badjate, S.; Tokranov, A.; Sheldon, B. W. *Scr. Mater.* **2014**, *92*, 47.

(55) Mukhopadhyay, A.; Sheldon, B. W. *Prog. Mater. Sci.* **2014**, *63*, 58.

(56) Pan, B.; Qian, K.; Xie, H.; Asundi, A. *Meas. Sci. Technol.* **2009**, *20*, 062001.

(57) Chu, T. C.; Ranson, W. F.; Sutton, M. A.; Peters, W. H. *Exp. Mech.* **1985**, *25*, 232.

(58) Sutton, M. A.; Cheng, M.; Peters, W. H.; Chao, Y. J.; McNeill, S. R. *Image Vis. Comput.* **1986**, *4*, 143.

(59) Zhang, X.; Cahill, D. G. *Langmuir* **2006**, *22*, 9062.

(60) Thackeray, M. M. *Prog. Solid State Chem.* **1997**, *25*, 1.

(61) Das, S. R.; Majumder, S. B.; Katiyar, R. S. *J. Power Sources* **2005**, *139*, 261.

(62) Aurbach, D.; Gamolsky, K.; Markovsky, B.; Salitra, G.; Gofer, Y.; Heider, U.; Oesten, R.; Schmidt, M. *J. Electrochem. Soc.* **2000**, *147*, 1322.

(63) Jang, D. H.; Shin, Y. J.; Oh, S. M. *J. Electrochem. Soc.* **1996**, *143*, 2204.

(64) Tu, J.; Zhao, X. B.; Cao, G. S.; Tu, J. P.; Zhu, T. J. *Mater. Lett.* **2006**, *60*, 3251.

(65) Benedek, R.; Thackeray, M. M. *Electrochem. Solid-State Lett.* **2006**, *9*, A265.

(66) Oh, K.-Y.; Siegel, J. B.; Secondo, L.; Kim, S. U.; Samad, N. A.; Qin, J.; Anderson, D.; Garikipati, K.; Knobloch, A.; Epureanu, B. I.; Monroe, C. W.; Stefanopoulou, A. *J. Power Sources* **2014**, *267*, 197.

(67) Cannarella, J.; Leng, C. Z.; Arnold, C. B. In *SPIE Sensing Technology + Applications*; Dhar, N. K.; Balaya, P.; Dutta, A. K., Eds.; International Society for Optics and Photonics, 2014; p. 91150K.

(68) Sommer, L. W.; Raghavan, A.; Kiesel, P.; Saha, B.; Schwartz, J.; Lochbaum, A.; Ganguli, A.; Bae, C.-J.; Alamgir, M. *J. Electrochem. Soc.* **2015**, *162*, A2664.

(69) Crain, D.; Zheng, J.; Sulyma, C.; Goia, C.; Goia, D.; Roy, D. *J. Solid State Electrochem.* **2012**, *16*, 2605.

(70) Saïdi, M. Y.; Barker, J.; Koksbang, R. *J. Solid State Chem.* **1996**, *122*, 195.

(71) Dathar, G. K. P.; Sheppard, D.; Stevenson, K. J.; Henkelman, G. *Chem. Mater.* **2011**, *23*, 4032.

(72) Uchiyama, T.; Nishizawa, M.; Itoh, T.; Uchida, I. *J. Electrochem. Soc.* **2000**, *147*, 2057.

(73) Zhu, M.; Park, J.; Sastry, A. M. *J. Electrochem. Soc.* **2012**, *159*, A492.

(74) Lu, D.; Li, W.; Zuo, X.; Yuan, Z.; Huang, Q. *J. Phys. Chem. C* **2007**, *111*, 12067.

(75) Ammundsen, B.; Rozière, J.; Islam, M. S. *J. Phys. Chem. B* **1997**, *101*, 8156.

(76) García, R. E.; Chiang, Y.-M.; Craig Carter, W.; Limthongkul, P.; Bishop, C. M. *J. Electrochem. Soc.* **2005**, *152*, A255.

(77) Deshpande, R.; Qi, Y.; Cheng, Y.-T. *J. Electrochem. Soc.* **2010**, *157*, A967.

(78) Grantab, R.; Shenoy, V. B. *J. Electrochem. Soc.* **2011**, *158*, A948.

Chapter 3: Cathode/Electrolyte Interface-Dependent Changes in Stress and Strain in Lithium Iron Phosphate Composite Cathodes

Adapted with permission from Bassett, K. L.; Çapraz, Ö. Ö.; B. Özdogru, Gewirth, A. A.; Sottos, N. R. Cathode/Electrolyte Interface-Dependent Changes in Stress and Strain in Lithium Iron Phosphate Composite Cathodes. In preparation, 2019.

3.1 Introduction

Chemo-mechanical changes in battery electrodes during lithiation and delithiation affect the lifetime and performance of Li-ion batteries. Mechanical changes in Li-ion electrodes are known to cause electrode cracking.[1,2] Cracks not only create new surfaces which lead to increased electrolyte decomposition but also cause active material particles to break off from the electrode and become electrochemically isolated from the current collector. The repeated formation of surface films on the newly developed crack surfaces along with particle isolation may cause a decrease in electrode capacity and eventual battery failure.[3] In general, phase transformations during electrochemical lithiation and delithiation, active material cracking and degradation, and surface film formation may all contribute to mechanical changes (measured as stress and strain) in Li-ion electrode active materials.[2,4]

$LiFePO_4$ (LFP) is an inexpensive and environmentally benign Li-ion cathode commonly employed in technologies requiring fast discharges for operation (e.g., power tools).[5] Upon delithiation, the olivine phase $LiFePO_4$ forms $FePO_4$ and experiences significant triaxial strain along the *a* (strain = 5.0%), *b* (3.7%), and *c* (-1.9%) axes.[6] The lattice experiences a reversible -6.8% volume change during delithiation.[7] LFP particles with diameters larger than ca. 100 nm delithiate in a two-phase system with growing and shrinking domains of $LiFePO_4$ and $FePO_4$, respectively, and vice versa during lithiation.[8–15] A large amount of strain exists at the $LiFePO_4$/$FePO_4$ reaction front because of the lattice mismatch between the two phases.[16] Additionally, LFP particles have been shown to crack during cycling.[6] Therefore, increasing our understanding of the mechanical changes in LFP composite cathodes remains important to the pursuit of longer-lasting cathodes.

Previous methods to interrogate strain (volume change) and stress (pressure due to mismatched strain) in LFP include in-situ XRD[3] and ex-situ TEM and X-ray tomography

measurements.[1,17,18] The in-situ XRD measurement reported on lattice changes during lithiation and delithiation, but did not describe dynamic changes at the LFP/electrolyte interface. The insight from these ex-situ measurements is used in calculations and simulations to evaluate the relationship between stress, crack formation, and particle size in LFP electrodes.[19–22] None of these measurements, however, report on stress and strain occurring at the LFP/electrolyte interface, and thus do not evaluate the interplay of the cathode with the electrolyte. In particular, there is little understanding regarding electrode/electrolyte interactions at the LFP/electrolyte interface and how they affect the mechanical response of the electrode.

One dominant interaction at the electrode/electrolyte interface is the formation of films comprised of electrolyte decomposition products.[23–27] Films deposited at the cathode/electrolyte and anode/electrolyte interface during cycling are called the cathode/electrolyte interface (CEI) and solid electrolyte interphase (SEI), respectively. The electrolyte components may decompose in solution or at the electrode/electrolyte interface to form the inorganic and organic components of both the CEI and SEI.

Mechanical changes in a cathode caused by intercalation, degradation, or CEI formation can be described by the stress and strain changes occurring in the electrode. In-situ electrochemical stress measurements are typically performed by measuring changes in the cantilever substrate curvature. An electrode on a thin substrate expands or contracts and applies a force to deform the underlying substrate.[2,28] Change in cantilever curvature have been monitored by capacitance, interferometry, microbalance, atomic force microscopy, and laser beam reflection.[28–32] The reflected laser methods include measuring a single laser beam with a position sensitive detector and the spacing of multiple parallel beams created by an etalon.[28] Bending cantilever techniques have been used to measure the stress changes in Li-ion electrodes, including $LiCoO_2$, $Li_xMn_2O_4$ (LMO), Si, Sn, and graphite.[4,33–40] Strain evolution in Li-ion battery electrodes has been measured using transmission electron microscopy (TEM), atomic force microscopy, X-ray diffraction (XRD), tomography, or optical microscopy.[7,18,41,42] Digital image correlation (DIC) has been utilized to measure in-situ, full-field strains of composite electrodes during electrochemical cycling.[43–48] These methods have been used to report strain changes in Li-ion electrodes, including silicon, tin, graphite, and LMO.[33,41,42,49] Previously, we combined bending cantilever stress and DIC strain experiments to yield substantial new insight into electrode processes in LMO and graphite composite Li-ion electrodes.[33,49]

In this paper, we utilize bending cantilever electrochemical stress and DIC strain measurements to interrogate processes occurring during the lithiation and delithiation of LFP cathodes. We show that while stress and strain changes are associated with electrochemical lithiation and delithiation of the LFP material, there is an additional feature in the stress and strain related to the interaction of Li^+ with the CEI.

3.2 Experimental

3.2.1 Electrode Fabrication

Cathode slurries were fabricated by first mixing carboxymethylcellulose sodium salt (CMC) binder (Aldrich) in water in a 0.02:1 ratio by vortexing for 20 seconds and sonicating for 1 hour three times. Lithium iron phosphate ($LiFePO_4$, LFP) powder (Hanwha Chemicals) and carbon black (Super P Li, Timcal) were ground together in a mortar and pestle until homogenous in color. The resulting powder was mixed into the aqueous CMC slurry by vortexing and sonicating as described above. The final weight ratio of LFP to CMC to carbon black was 8:1:1. LFP particles observed with scanning electron microscopy (FEI Quanta FEG 450 ESEM) had diameters between 250-300 nm (Figure 3.1).

Electrode substrates for stress measurements were fabricated by electron beam depositing 20 nm Ti followed by 100 nm Al on a borosilicate glass coverslip (Gold Seal, # 1, 3 mm x 30 mm

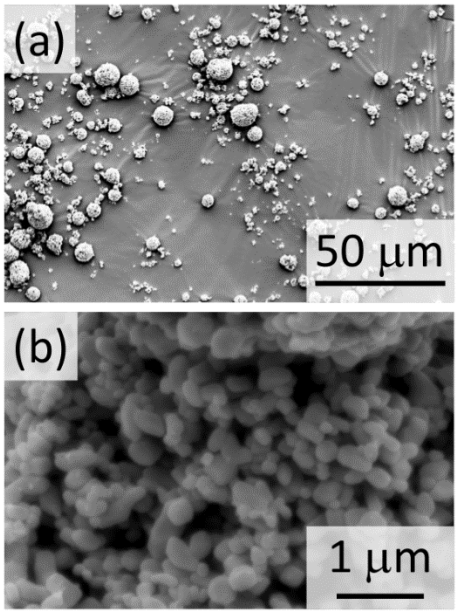

Figure 3.1. SEM of Hanwha LFP. Primary particles average diameter 260 ± 110 nm, measured across 75 particles.

x 150 μm). The cathode slurry was distributed on the stress cantilever substrate with a doctor blade to a thickness of ca. 2 μm. For strain cathodes, the slurry was first deposited on Cu foil to a thickness of ca. 50 μm. Once dry, free-standing electrodes were made by removing the slurry from the Cu foil and then cut to the dimensions of ca. 3 mm x 7 mm.

3.2.2 Electrochemical Cycling

Cyclic voltammetry (CV) on the LFP electrodes utilized for stress and strain measurements was performed in either 1 M solutions of $LiPF_6$ (98%, Sigma-Aldrich) or $LiClO_4$ dissolved in either 1:1 by volume in ethylene carbonate (EC, anhydrous 99%, Sigma-Aldrich)/dimethyl carbonate (DMC, anhydrous 99+%, Sigma-Aldrich) or propylene carbonate (PC, anhydrous 99.7%, Sigma-Aldrich). Stress and strain measurements were performed in separate custom cells with a single Li foil counter/reference electrode (Alfa Aesar).[43,50] All potentials reported herein are in reference to the Li/Li^+ electrochemical couple. Cells were assembled in an Ar atmosphere glovebox. The cells were cycled at 25 μV/s between 2.6 V and 4.4 V, commencing in the anodic direction from the open circuit potential (OCP, 3.44 V) using a CH Instruments potentiostat (model 6002E) or Arbin battery cycler (Model LBT). The refractive indices of the electrolytes were measured to be 1.338, 1.414, 1.409, and 1.426 for 1 M $LiPF_6$ in EC/DMC, 1 M $LiPF_6$ in PC, 1 M $LiClO_4$ in EC/DMC, and 1 M $LiClO_4$ in PC, respectively, by using a Mettler Toledo Refracto 30GC refractometer.

3.2.3 Stress and Strain Measurements

The stress-thickness product (σ·t) in the constrained cathode was measured using a bending cantilever technique as described previously.[2,49,51,52] The previously described optical stress measurement configuration was used to record changes in the cantilever curvature during cycling.[51] The stress-thickness was calculated using the Stoney's equation,

$$\sigma \cdot t = \int_0^t \sigma_{ij} dz = \frac{Y h_s^2 d\kappa}{6(1-\upsilon_s)} \tag{3.1}$$

in which Y, h_s, and ν_s are the Young's modulus (= 75.9 GPa for glass), thickness, and Poisson's ratio (= 0.22 for glass) of the cantilever substrate, respectively. dκ is the cantilever curvature and σ_{ij} is the integrated stress through the sample thickness, t. The reported stress-thickness values are relative to the initial electrode stress-thickness upon immersion at OCP. The strain (ε) in an unconstrained electrode was measured by digital image correlation (DIC) as described previously.[43,48] DIC is a full field optical method, which correlates changes in the grayscale values

of a surface speckle pattern to measure deformation of the composite cathode.[43] We used the natural speckle pattern of the composite electrode for DIC analysis. The surface of the electrode was illuminated with white light. A CCD camera (EXi Aqua, Q-imaging) equipped with a 12X zoom lens (Navitar) was used to capture images of a 2.5 x 3.5 mm region of interest (ROI) on a scale of 3.24 μm/pixel. Images were acquired every 8 min. The 8-bit images were 1392 pixels x 1040 pixels. Images were acquired at every 1 and 8 min when the electrodes were cycled at 200 and 25 μV/s, respectively. The commercial software VIC2D was used to calculate displacements and strains using a subset size of 60 μm by 60 μm.

3.2.4 Electrochemical Impedance Spectroscopy Measurements

Electrochemical impedance spectroscopy (EIS) measurements were performed on electrodes made of LFP/CMC/Super P (8:1:1) slurry cast onto Al foil (Sigma, MiniBin) with a doctor blade to a thickness of ca. 0.1 mm. Cells were assembled in CR2032 coin cells (MTI) with a stainless steel spacer (MTI), LFP cathode, 2 drops of electrolyte, Celgard separator, 2 more drops of electrolyte, Li foil (Alfa Aesar), another spacer, and a waveform spring (MTI). Cells were assembled with either 1 M $LiPF_6$ or $LiClO_4$ in EC/DMC. Each EIS measurement was performed by first holding at the target potential for 20 minutes followed by EIS between 1000 kHz–10 mHz with an amplitude of 30 mV. EIS was performed first at OCP (usually between 2.75 V–3.05 V) followed by linear potential sweeps between 4.4 V and 2.6 V at 0.1 mV/s for three cycles. EIS was performed at 4.4 V and 2.6 V during each cycle. The high- and mid-frequency region of the EIS was fit with RelaxIS3 software. All fits achieved $R^2 \geq 0.996$.

3.3 Results

3.3.1 In-situ Stress and Strain Measurements

Figure 3.2a shows the CV of a LFP composite cathode cantilever electrode at 25 μV/s in 1 M $LiPF_6$ in EC/DMC. The anodic CV current peaks at 3.62 V and the cathodic CV current peaks at 3.25 V with a peak splitting of 0.37 V and $E_{1/2}$ of 3.44 V, consistent with prior literature.[53–59]

Previous in-situ diffraction studies demonstrate that LFP particles with diameters larger than ca. 100 nm (in this work the particles are 250–300 nm in diameter) delithiate in a two-phase system with growing and shrinking domains of $LiFePO_4$ and $FePO_4$, respectively, and vice versa during lithiation.[8–15] The bulk phase transitions between $LiFePO_4$ and $FePO_4$ produce the typical

single electrochemical couple observed in Figure 3.2a.[53–59] Two regions (① and ②) are highlighted and will be discussed below.

Figure 3.2b shows the normalized in-situ stress-thickness observed in $LiPF_6$ in EC/DMC electrolyte. The stress-thickness is normalized so that the beginning of the anodic sweep at 2.6 V is at 0 N/m. During delithiation (anodic sweep), tensile stress in the electrode increases from 0 N/m to 3.3 N/m which indicates a contraction in the electrode. During lithiation (cathodic sweep),

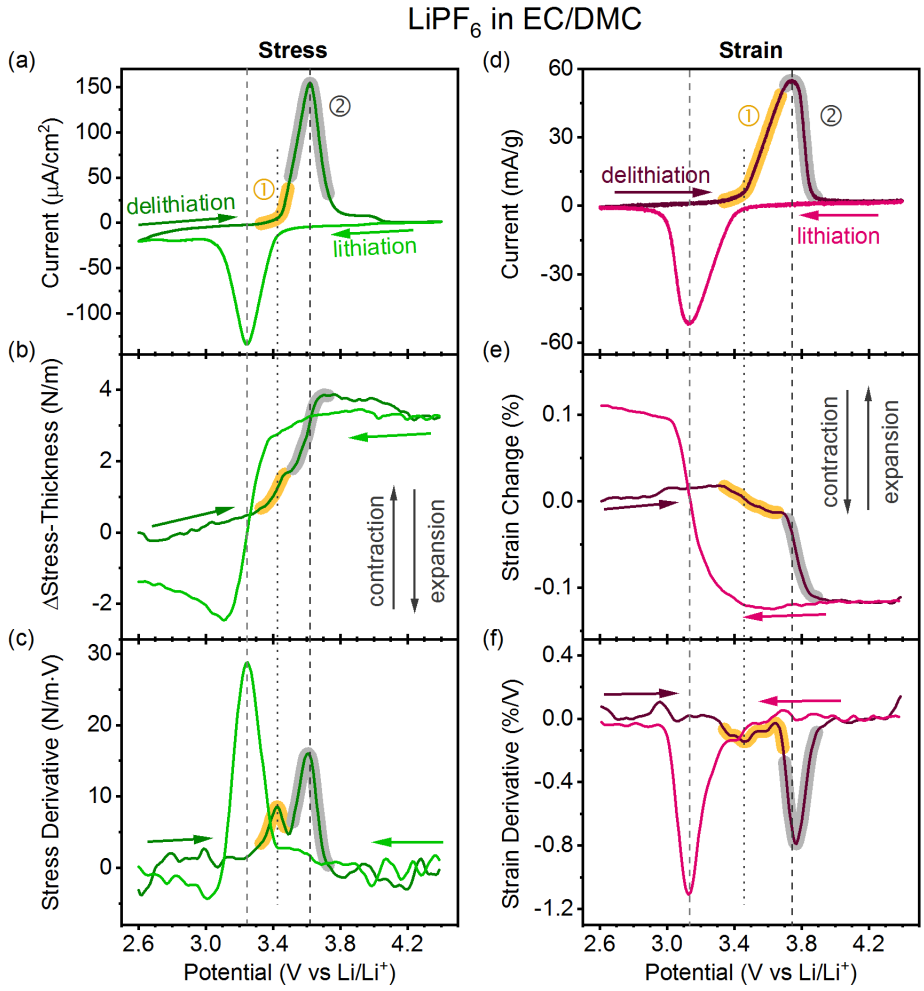

Figure 3.2. In-situ CV, stress, and strain data for a LFP cathode in $LiPF_6$ in EC/DMC. (a-f) Performed in 1 M $LiPF_6$ in EC/DMC electrolyte at 25 μV/s. In-situ 3rd cycle (a) CV, (b) stress-thickness, (c) stress-thickness derivative with respect to potential collected using cantilever-type LFP cathodes in the custom stress cell. In-situ 3rd cycle (d) CV, (e) strain change, and (f) strain change derivative with respect to potential collected using free-standing LFP cathodes in the custom strain cell. Regions ① (3.30 V–3.50 V in the stress data and 3.34 V–3.69 V in the strain data, highlighted in yellow) and ② (3.50 V–3.73 V in the stress data and 3.69 V–3.89 V in the strain data, highlighted in grey) during delithiation call attention to two separate features in the stress and strain and their corresponding current and derivative features within these potential ranges. Dashed lines aid in comparing CV peak locations and stress and strain features. The dotted line aids in comparing stress and strain features in (b) and (e) with the corresponding features at the same potential in the corresponding CVs and derivative plots. The colored arrows indicate the direction of the potential sweeps.

the accumulated tensile stress relaxes from 3.3 N/m and compressive stress builds to -1.4 N/m in the electrode due to the expansion of the electrode. Previous reports on stress evolution in $LiMn_2O_4$ (LMO) also show an increase in tensile stress during delithiation and compressive stress during lithiation,[34,35,49] but equivalent data for LFP is not available. There is a difference in stress-thickness between the beginning and the end of the cycle at 2.6 V of -1.4 N/m. We also observed similar irreversible stress in LMO composite electrodes[49] and attributed the phenomenon to irreversible processes during cycling such as CEI formation[60,61] and metal ion dissolution.[62–65] We speculate that similar processes are operative in the LFP system. Indeed, both CEI formation and metal ion dissolution occur in LFP electrodes.[66–72]

Figure 3.2c shows the derivative of stress-thickness with respect to potential. Interestingly, during delithiation (anodic sweep), two derivative peaks at 3.42 V (region ①) and 3.61 V (region ②) appear. The stress derivative peak at 3.61 V (region ②) reaches a maximum within 0.01 V of the corresponding current peak (Figure 3.2a). In contrast, the stress derivative peak at 3.42 V (region ①) corresponds to a potential in the anodic CV at which the current starts to increase. These three derivative features were reproducible among the different cycles obtained (Figure 3.3–3.5) and at all scan rates interrogated (25–100 μV/s).

Figure 3.2d shows the CV obtained at a scan rate 25 μV/s for LFP collected during in-situ strain measurements. The same phase changes described above govern the single electrochemical couple shown. The CV current peaks at 3.74 V during delithiation and 3.13 V during lithiation. The peak splitting (0.61 V) is larger than that found in the stress-related CV (0.38 V, Figure 3.2a) mostly due to resistance in the cathode caused by the electrode construction. Two regions (① and ②) are highlighted and will be discussed below.

Figure 3.2e shows the normalized in-situ strain change during CV. The strain change is normalized so that the beginning of the anodic sweep at 2.6 V is at zero strain. During delithiation (anodic sweep), the strain decreases by 0.11%, consistent with a decrease in electrode volume. The charge passed during the anodic sweep is 151 mAh/g (i.e., 89% of the theoretical capacity of LFP, 170 mAh/g). X-ray diffraction studies measured 6.8% reduction in particle volume when $LiFePO_4$ is fully delithiated to $FePO_4$.[2,7,12] The difference in strain evolution between composite electrode and particles originates from morphological factors associated with porosity, the volume fraction of the active material, and random orientation of the particles in the composite electrode. Previously, we developed an analytical model by incorporating these factors to calculate strain in

a composite electrode. The model successfully predicted experimentally measured strain evolution in the composite graphite electrode.[43] Upon lithiation, the strain change increases from -0.11% to 0.11% (a total change of 0.22%), consistent with an increase in electrode volume. CEI formation and transition metal dissolution could all contribute to the irreversible strain change of +0.11% seen in Figure 3.2e.[66–72]

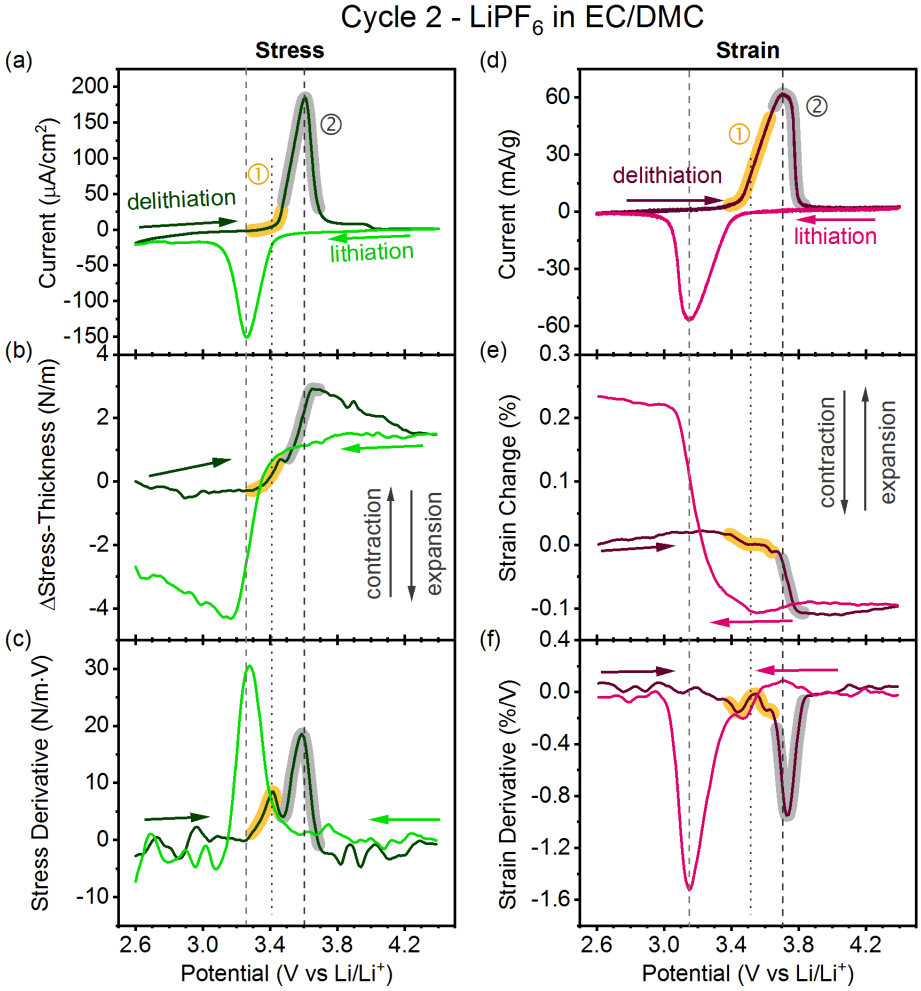

Figure 3.3. Cycle 2 of in-situ CV, stress, and strain experiments in $LiPF_6$ in EC/DMC. (a-f) Performed in 1 M $LiPF_6$ in EC/DMC electrolyte at 25 μV/s. In-situ 2nd cycle (a) cyclic voltammetry, (b) stress-thickness, (c) stress-thickness derivative with respect to potential collected using cantilever-type LFP cathodes in the custom stress cell. In-situ 2nd cycle (d) cyclic voltammetry, (e) strain change, and (f) strain change derivative with respect to potential collected using free-standing LFP cathodes in the custom strain cell Regions ① (3.27 V–3.48 V in the stress data and 3.35 V–3.68 V in the strain data, highlighted in yellow) and ② (3.48 V–3.71 V in the stress data and 3.68 V–3.86 V in the strain data, highlighted in grey) during delithiation call attention to two separate features in the stress and strain and their corresponding current and derivative features within these potential ranges. Dashed lines aid in comparing CV peak locations and stress and strain features. The dotted line aids in comparing stress and strain features in (b) and (e) with the corresponding features at the same potential in the corresponding CVs and derivative plots. The colored arrows indicate the direction of the potential sweeps.

Figure 3.2f shows the strain change derivative with respect to potential. Peaks in the strain derivative occur at 3.76 V during delithiation and 3.13 V during lithiation, within 0.02 V and 0 V of the corresponding current peaks, respectively. Just as in the stress derivative, only three peaks in the strain derivative are observed. Figure 3.3–3.5 show these features are retained in all scans examined. The peak positions of the anodic current are found to be negative of the coincident strain

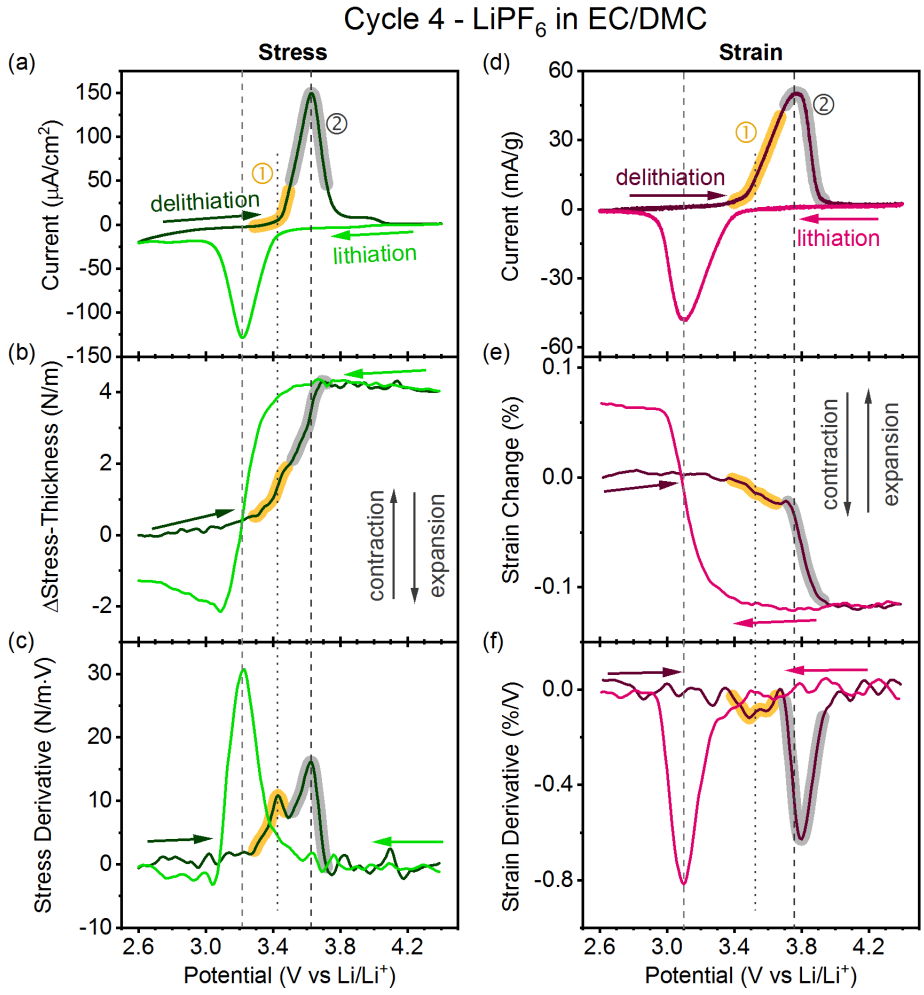

Figure 3.4. Cycle 4 of in-situ CV, stress, and strain experiments in $LiPF_6$ in EC/DMC. (a-f) Performed in 1 M $LiPF_6$ in EC/DMC electrolyte at 25 μV/s. In-situ 4th cycle (a) cyclic voltammetry, (b) stress-thickness, (c) stress-thickness derivative with respect to potential collected using cantilever-type LFP cathodes in the custom stress cell. In-situ 4th cycle (d) cyclic voltammetry, (e) strain change, and (f) strain change derivative with respect to potential collected using free-standing LFP cathodes in the custom strain cell. Regions ① (3.25 V–3.50 V in the stress data and 3.35 V–3.69 V in the strain data, highlighted in yellow) and ② (3.50 V–3.74 V in the stress data and 3.69 V–3.97 V in the strain data, highlighted in grey) during delithiation call attention to two separate features in the stress and strain and their corresponding current and derivative features within these potential ranges. Dashed lines aid in comparing CV peak locations and stress and strain features. The dotted line aids in comparing stress and strain features in (b) and (e) with the corresponding features at the same potential in the corresponding CVs and derivative plots. The colored arrows indicate the direction of the potential sweeps.

derivative features for all presented cycles by -0.03 ± 0.01 V, while the current peak during the cathodic sweep occurs at the same potential as the strain derivative peak.

Regions ① (3.34 V–3.69 V) and ② (3.69 V–3.89 V) during delithiation have been highlighted (in yellow and grey, respectively) in Figure 3.2d-f to correspond with two distinct strain and strain derivative features. The strain in region ① is characterized by an increase in strain

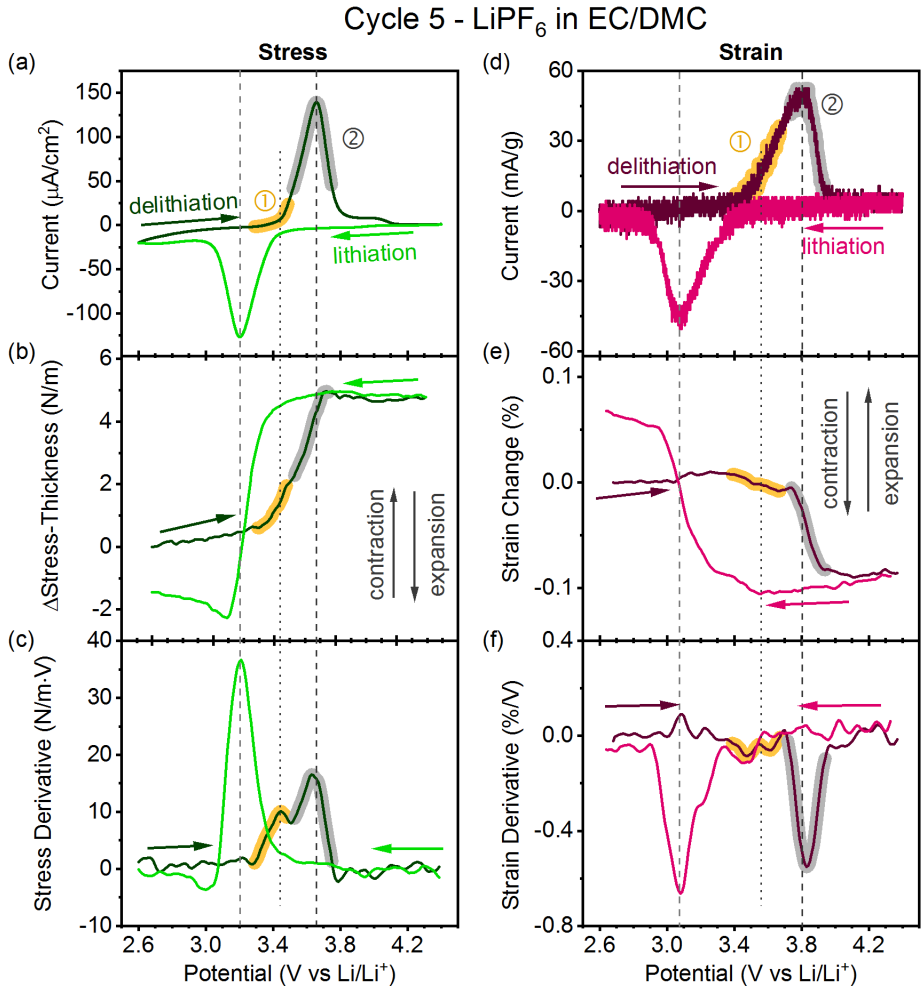

Figure 3.5. Cycle 5 of in-situ CV, stress, and strain experiments in $LiPF_6$ in EC/DMC. (a-f) Performed in 1 M $LiPF_6$ in EC/DMC electrolyte at 25 μV/s. In-situ 5th cycle (a) cyclic voltammetry, (b) stress-thickness, (c) stress-thickness derivative with respect to potential collected using cantilever-type LFP cathodes in the custom stress cell. In-situ 5th cycle (d) cyclic voltammetry, (e) strain change, and (f) strain change derivative with respect to potential collected using free-standing LFP cathodes in the custom strain cell. Regions ① (3.25 V–3.51 V in the stress data and 3.36 V–3.71 V in the strain data, highlighted in yellow) and ② (3.51 V–3.78 V in the stress data and 3.71 V–3.97 V in the strain data, highlighted in grey) during delithiation call attention to two separate features in the stress and strain and their corresponding current and derivative features within these potential ranges. Dashed lines aid in comparing CV peak locations and stress and strain features. The dotted line aids in comparing stress and strain features in (b) and (e) with the corresponding features at the same potential in the corresponding CVs and derivative plots. The colored arrows indicate the direction of the potential sweeps.

with a smaller rate of change than in region ②. The smaller slope makes this region difficult to identify in the strain derivative although it is also present here, in other cycles (Figures 3.3–3.4), and at other scan rates interrogated (25–100 μV/s). If the integrated area under the current and strain in regions ① and ② are compared, then region ① accounts for 48% of the charge and 28% of the strain while region ② accounts for 52% of the charge and 72% of the strain reported between 3.34 V–3.89 V. The strain generation lags behind the current, which is also evident by the 0.03 V difference in potential between the region ② delithiation strain derivative peak and current peak.

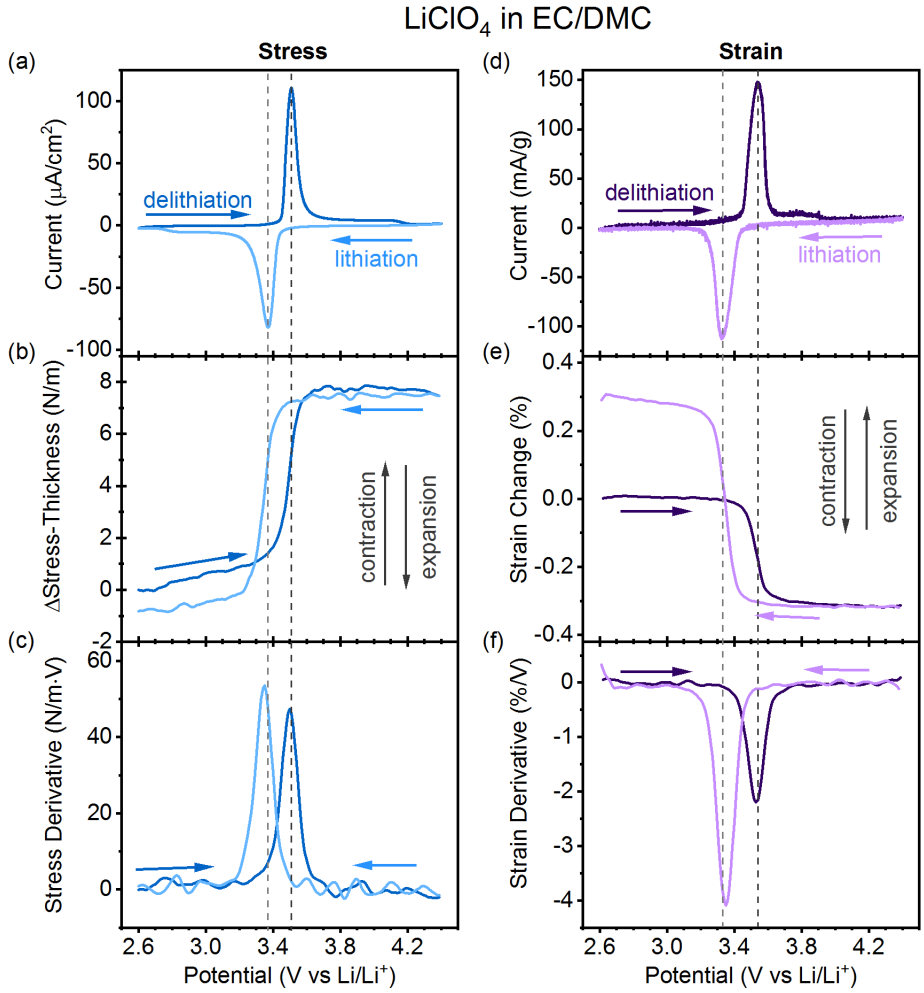

Figure 3.6. In-situ CV, stress, and strain data for a LFP cathode in $LiClO_4$ in EC/DMC. (a-f) Performed in 1 M $LiClO_4$ in EC/DMC electrolyte at 25 μV/s. In-situ 3rd cycle (a) CV, (b) stress-thickness, (c) stress-thickness derivative with respect to potential collected using cantilever-type LFP cathodes in the custom stress cell. In-situ 3rd cycle (d) CV, (e) strain change, and (f) strain change derivative with respect to potential collected using free-standing LFP cathodes in the custom strain cell. Dashed lines aid in comparing CV peak locations and stress and strain features. The colored arrows indicate direction of potential sweep.

The most interesting feature in the data presented here is the presence of an additional peak in both the stress-thickness derivative and the strain derivative (region ①) in $LiPF_6$ in EC/DMC during delithiation. The additional stress and strain features are not observed in LMO.[49] LMO electrodes exhibit two current peaks, two strain derivative peaks, and two stress derivative peaks during delithiation.[49] In contrast, LFP displays one characteristic current peak, two stress derivative peaks, and two strain derivative peaks during delithiation. In LMO, the stress and strain features are asynchronous; that is they occur at different potentials relative to the current peaks, a behavior found also for graphite anodes.[33,49] In LMO, the asynchronous behavior was associated with

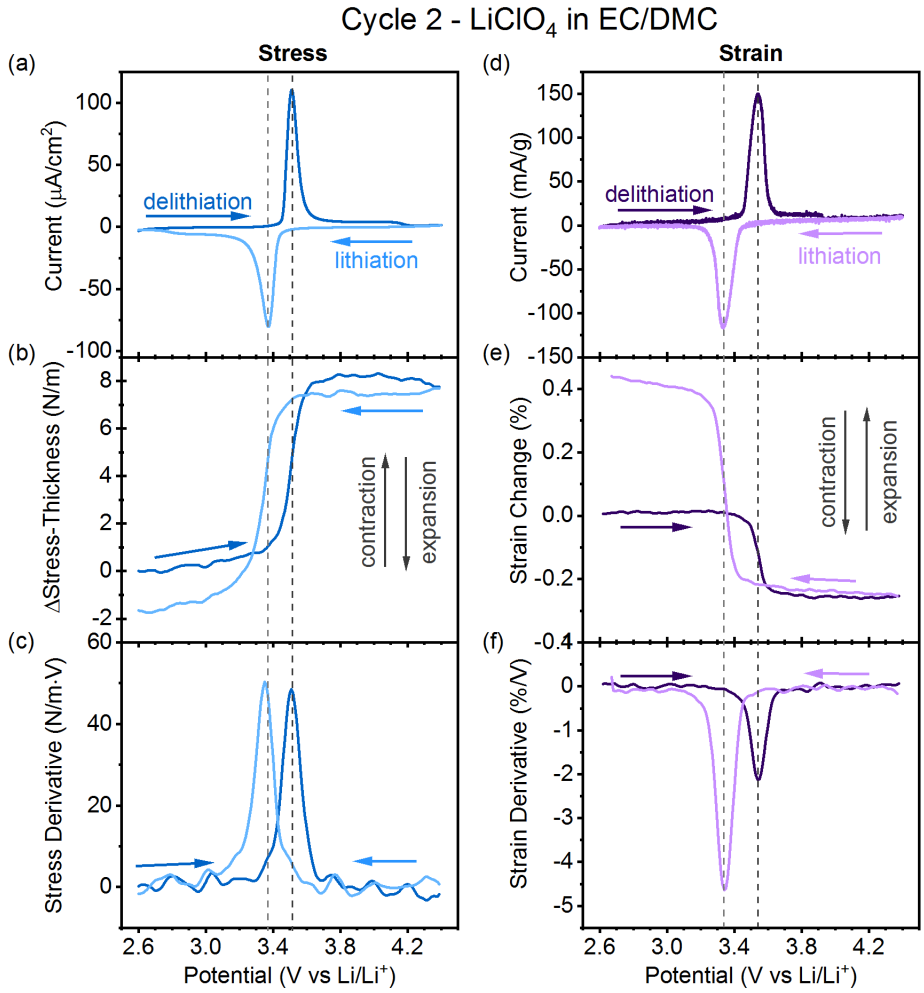

Figure 3.7. Cycle 2 of in-situ CV, stress, and strain experiments in $LiClO_4$ in EC/DMC. (a-f) Performed in 1 M $LiClO_4$ in EC/DMC electrolyte at 25 μV/s. In-situ 2nd cycle (a) cyclic voltammetry, (b) stress-thickness, (c) stress-thickness derivative with respect to potential collected using cantilever-type LFP cathodes in the custom stress cell. In-situ 2nd cycle (d) cyclic voltammetry, (e) strain change, and (f) strain change derivative with respect to potential collected using free-standing LFP cathodes in the custom strain cell. Dashed lines aid in comparing CV peak locations and stress and strain features. The colored arrows indicate direction of potential sweep.

changes in charge transfer resistance at potentials just prior to the lower potential delithiation peak. The presence of stress and strain derivative peaks coincident with both the onset of delithiation and the current peak maximum during delithiation differentiate LFP from LMO.

In order to evaluate the origin of the additional feature in the stress and strain, we examined the effect of different electrolytes on LFP mechanical changes. Figure 3.6a shows the 3rd cycle CV obtained from LFP during in-situ stress measurements in 1 M $LiClO_4$ in EC/DMC electrolyte obtained at a scan rate of 25 μV/s. The current peaks at 3.51 V during delithiation and 3.37 V during lithiation with a peak splitting of 0.14 V. The average potential between the two current

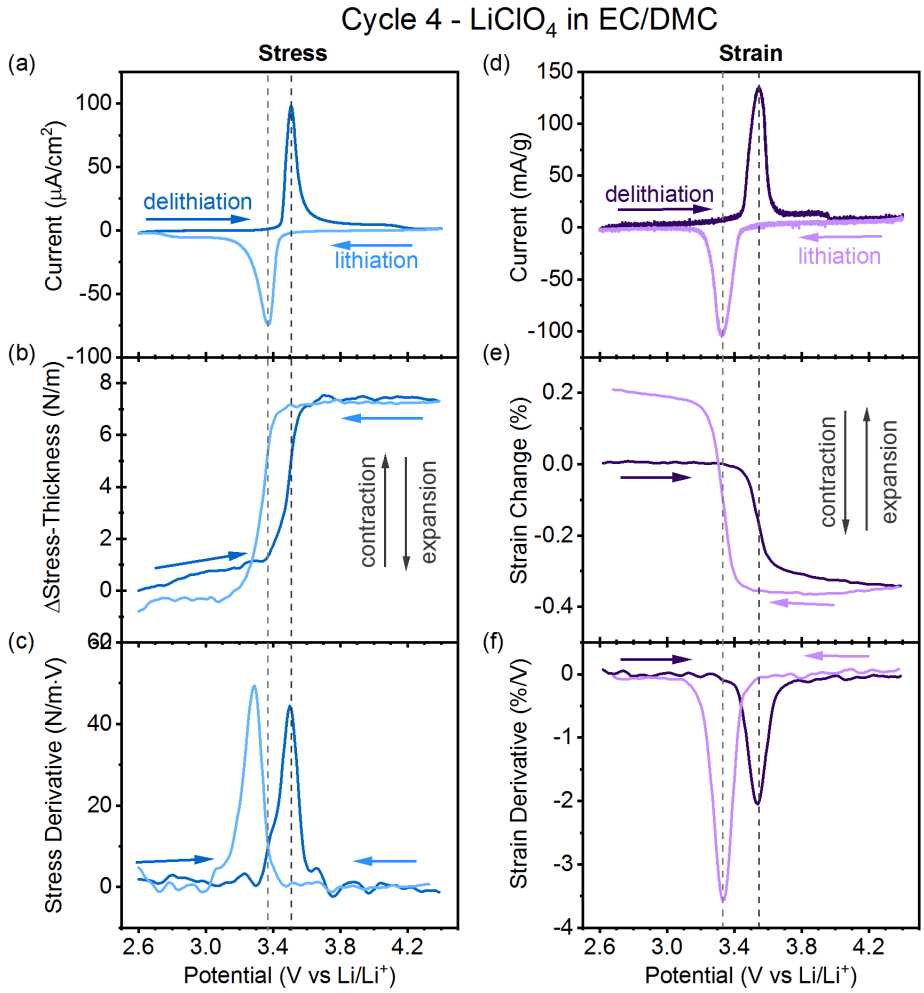

Figure 3.8. Cycle 4 of in-situ CV, stress, and strain experiments in $LiClO_4$ in EC/DMC. (a-f) Performed in 1 M $LiClO_4$ in EC/DMC electrolyte at 25 μV/s. In-situ 4th cycle (a) cyclic voltammetry, (b) stress-thickness, (c) stress-thickness derivative with respect to potential collected using cantilever-type LFP cathodes in the custom stress cell. In-situ 4th cycle (d) cyclic voltammetry, (e) strain change, and (f) strain change derivative with respect to potential collected using free-standing LFP cathodes in the custom strain cell. Dashed lines aid in comparing CV peak locations and stress and strain features. The colored arrows indicate direction of potential sweep.

peaks ($E_{1/2}$ = 3.44 V) in $LiClO_4$ in EC/DMC agrees with that reported above for $LiPF_6$ in EC/DMC and with the literature.[53–59] The average peak splitting over 5 cycles in $LiClO_4$ in EC/DMC compared to in $LiPF_6$ in EC/DMC is 0.15 ± 0.02 V and 0.38 ± 0.05 V, respectively. A smaller peak splitting is indicative of lower resistance in the cell, which we examine in more detail later. Figure 3.6b shows the change in normalized stress-thickness during CV. During delithiation, tensile stress increases by 7.49 N/m, indicating a contraction of the electrode. Upon lithiation, the tensile stress decreases and compressive stress builds in the electrode. The stress decreases by 8.28 N/m resulting in an irreversible change in stress of -0.82 N/m at the end of lithiation. As before, we

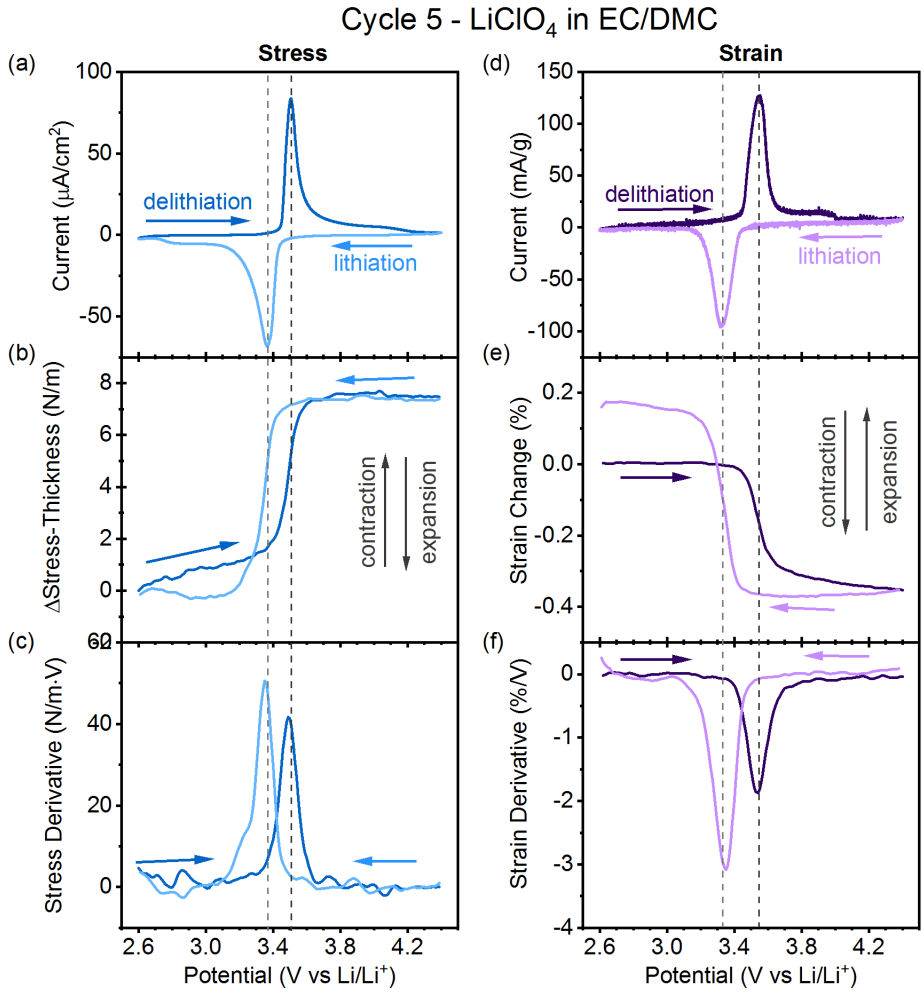

Figure 3.9. Cycle 5 of in-situ CV, stress, and strain experiments in $LiClO_4$ in EC/DMC. (a-f) Performed in 1 M $LiClO_4$ in EC/DMC electrolyte at 25 μV/s. In-situ 5th cycle (a) cyclic voltammetry, (b) stress-thickness, (c) stress-thickness derivative with respect to potential collected using cantilever-type LFP cathodes in the custom stress cell. In-situ 5th cycle (d) cyclic voltammetry, (e) strain change, and (f) strain change derivative with respect to potential collected using free-standing LFP cathodes in the custom strain cell. Dashed lines aid in comparing CV peak locations and stress and strain features. The colored arrows indicate direction of potential sweep.

attribute the irreversible change in stress-thickness to CEI formation and metal ion dissolution. Figure 3.6c shows the derivative of stress-thickness with respect to potential. Unlike the stress derivative in $LiPF_6$ in EC/DMC electrolyte (Figure 3.2c), the stress derivative in $LiClO_4$ in EC/DMC exhibits only one derivative peak during delithiation. The peak reaches a maximum at 3.50 V, within 0.01 ± 0.01 V of the corresponding current peak. During lithiation, one stress derivative peak arises, as in $LiPF_6$ in EC/DMC, at 3.35 V, within 0.02 ± 0.03 V of the related current peak.

Figure 3.6d shows the 3rd cycle CV of LFP during in-situ strain measurements. The current peaks at 3.54 V during delithiation and 3.33 V during lithiation with a 0.21 V peak splitting. Once again, the CV obtained during electrochemical strain measurements shows less reversible cycling due to impedance inherent in the electrode design. The integrated charge during delithiation is 148 mAh/g, which is 87% of the LFP theoretical capacity. Figure 3.6e shows the strain change during

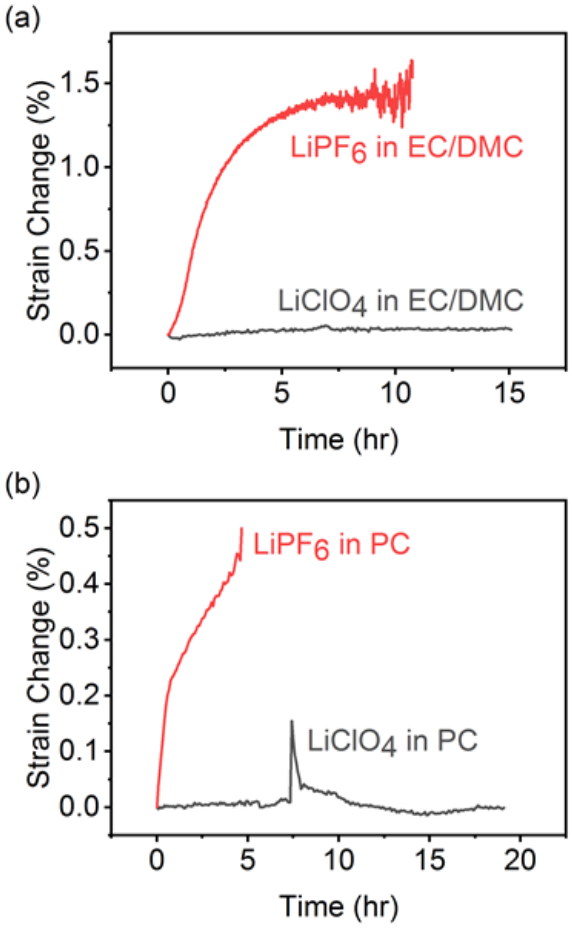

Figure 3.10. LFP strain changes in $LiPF_6$ and $LiClO_4$ in either EC/DMC or PC at open circuit potential. Free-standing strain electrodes measured in custom strain cell immersed in $LiPF_6$ or $LiClO_4$ in (a) EC/DMC or (b) PC at OCP.

the 3rd cycle CV in $LiClO_4$ in EC/DMC. After delithiation, the strain has decreased to -0.32%, indicating a decrease in the overall electrode volume. Upon lithiation, the electrode volume increases as evidenced by an increase to 0.29% from -0.32% or an overall 0.61% increase. CEI formation, metal ion dissolution, and electrode swelling could all contribute to the irreversible strain of 0.29%. Figure 3.6f shows the strain derivative with respect to potential. One large peak occurs during both delithiation and lithiation at 3.53 V and 3.35 V, respectively, within 0.02 ± 0.01 V of their corresponding current peaks. Stress and strain features were found to be consistent in cycles 2–5 (Figure 3.7–3.9).

At the end of delithiation (at 4.4 V), Figure 3.6e shows the strain evolved in $LiClO_4$ in EC/DMC (-0.32%) is larger than that seen in $LiPF_6$ in EC/DMC (-0.11%) in Figure 3.2e. Likewise, at the end of lithiation (at 2.6 V), the strain evolved in $LiClO_4$ in EC/DMC (0.29%) is also larger than that in $LiPF_6$ in EC/DMC (0.11%). Figure 3.10 shows the strain change during OCP in both

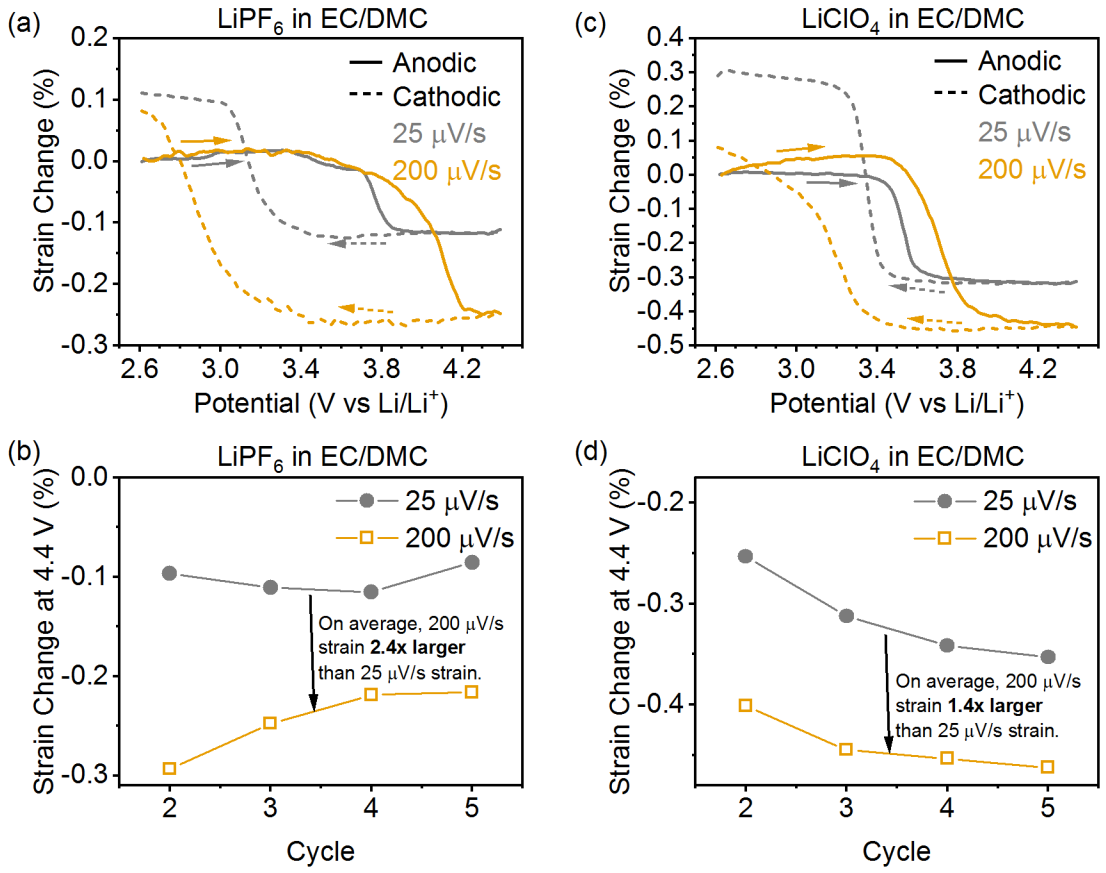

Figure 3.11. Rate-dependent strain changes in $LiPF_6$ and $LiClO_4$ in EC/DMC. Strain changes at 25 μV/s and 200 μV/s during the 3rd cycle CV in (a) 1 M $LiPF_6$ and (c) $LiClO_4$ in EC/DMC. The strain change at the end of delithiation (at 4.4 V) at 25 μV/s and 200 μV/s during cycles 2-5 in (b) 1 M $LiPF_6$ and (d) $LiClO_4$ in EC/DMC. On average, the strain change increases by 2.4x and 1.4x in $LiPF_6$ and $LiClO_4$ in EC/DMC, respectively upon increasing the scan rate from 25 μV/s and 200 μV/s.

$LiPF_6$ and $LiClO_4$-containing electrolytes. At OCP, the electrode immersed in $LiPF_6$-containing electrolytes expands significantly more than those in $LiClO_4$-containing electrolytes (1.56% versus 0.04%, respectively, in EC/DMC). The larger volume expansion at OCP suggests the electrode in $LiPF_6$-containing electrolytes swells and results in an increase in porosity of the composite electrode. Previous work by Jones et al. employed a strain model for composite electrodes that incorporates the volume fraction of the active material and polymer/carbon black matrix.[43] The

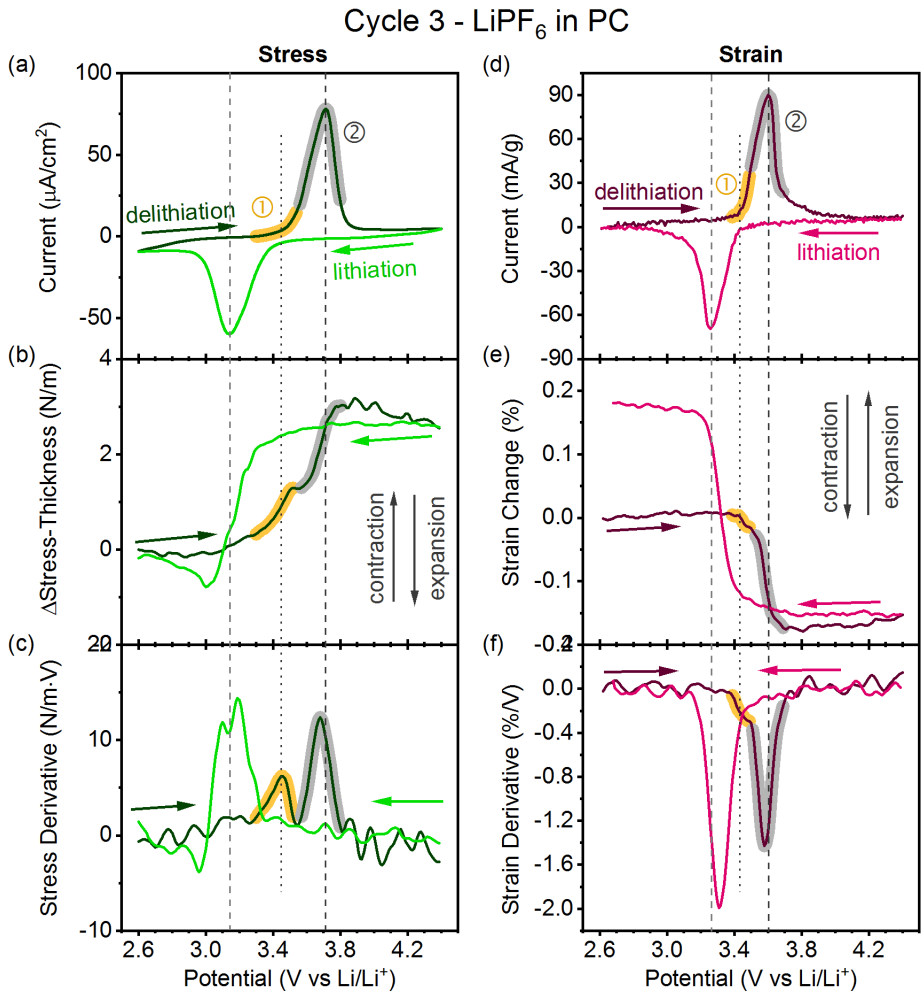

Figure 3.12. In-situ CV, stress, and strain experiments in $LiPF_6$ in PC. (a-f) Performed in 1 M $LiPF_6$ in PC electrolyte at 25 μV/s. In-situ 3rd cycle (a) cyclic voltammetry, (b) stress-thickness, (c) stress-thickness derivative with respect to potential collected using cantilever-type LFP cathodes in the custom stress cell. In-situ 3rd cycle (d) cyclic voltammetry, (e) strain change, and (f) strain change derivative with respect to potential collected using free-standing LFP cathodes in the custom strain cell. Regions ① (3.27 V–3.55 V in the stress data and 3.35 V–3.49 V in the strain data, highlighted in yellow) and ② (3.55 V–3.80 V in the stress data and 3.49 V–3.70 V in the strain data, highlighted in grey) during delithiation call attention to two separate features in the strain and their corresponding current and strain derivative features within these potential ranges. Dashed lines aid in comparing CV peak locations and stress and strain features. The dotted line aids in comparing a stress derivative peak in (c) with the corresponding features at the same potential in the (a) CV and (b) stress-thickness. The colored arrows indicate direction of the potential sweeps.

model suggests that strain changes proportionally with volume fraction. Upon swelling of the electrode in electrolyte, the volume fraction of the composite electrode decreases and consequently the measured strain decreases as well.[43] Therefore, greater porosity in the composite electrodes in $LiPF_6$-containing electrolyte would result in smaller observed strain changes during CV.

Figure 3.11 shows that the amount of strain evolved at the end of delithiation increases by 2.4x in $LiPF_6$ and by 1.4x in $LiClO_4$ in EC/DMC upon increasing the CV scan rate from 25 μV/s to 200 μV/s. Like the increased current peak splitting, larger strain changes at higher scan rates may indicate increased resistance in the cell in $LiPF_6$ compared to $LiClO_4$-containing electrolytes.

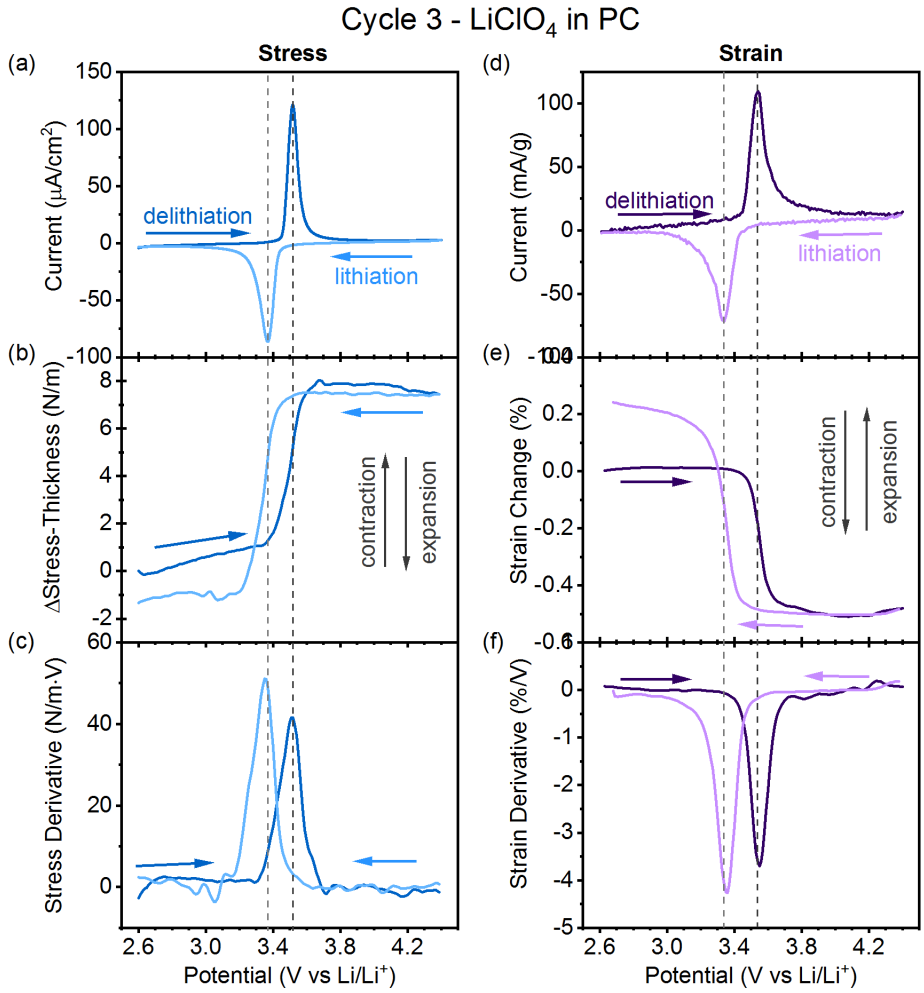

Figure 3.13. In-situ CV, stress, and strain experiments in $LiClO_4$ in PC. (a-f) Performed in 1 M $LiClO_4$ in PC electrolyte at 25 μV/s. In-situ 3rd cycle (a) cyclic voltammetry, (b) stress-thickness, (c) stress-thickness derivative with respect to potential collected using cantilever-type LFP cathodes in the custom stress cell. In-situ 3rd cycle (d) cyclic voltammetry, (e) strain change, and (f) strain change derivative with respect to potential collected using free-standing LFP cathodes in the custom strain cell. Dashed lines aid in comparing CV peak locations and stress and strain features. The colored arrows indicate direction of potential sweep.

We next examine the effect of solvent on the presence of two stress and strain peaks during delithiation of LFP. Figures 3.12 and 3.13 report the stress and strain obtained in an electrolyte consisting of $LiPF_6$ in propylene carbonate (PC) (Figure 3.12) $LiClO_4$ in PC (Figure 3.13). The stress results in PC mimic those found in EC/DMC. The stress derivative in $LiPF_6$ in PC electrolyte again exhibits two peaks during delithiation and one during lithiation (Figure 3.12). The more negative stress derivative peak during delithiation at 3.45 V is shifted ca. 0.26 V from the current peak (at 3.71 V), while the stress derivative peaks at 3.68 V and 3.17 V are closer in potential to the related current peaks at 3.71 V and 3.14 V, respectively. The stress derivative in $LiClO_4$ electrolytes exhibit one peak during each sweep (Figure 3.13) which are within 10 mV of the current peak, and the strain derivatives in either electrolyte show only one large peak during each sweep (Figure 3.13) within 0.05 V of the current peak. In $LiPF_6$ in PC electrolyte, there is a two-step strain event during delithiation, although the first step is less evident relative to the strain measured in $LiPF_6$ in EC/DMC. The current peak splitting also yields wider peak splitting in $LiPF_6$ in PC compared to $LiClO_4$ in PC.

3.3.2 Electrochemical Impedance Measurements

In order to further evaluate the origin of the additional stress and strain peak observed in $LiPF_6$ electrolyte we performed EIS measurements on LFP cathodes. Figure 3.14a shows the high- to mid-frequency region obtained from EIS measurements of LFP cathodes in 1 M $LiPF_6$ in EC/DMC. The spectra were collected at the minimum (2.6 V) and maximum (4.4 V) potentials during the first three CV cycles. The inset to Figure 3.14a shows the equivalent circuit used to describe the high- to mid-frequency region and the fit to the data are shown in pink. The equivalent circuit features three main elements (literature reports of LFP impedance spectra vary and exhibit between one to three semi-circles; the low frequency region was not considered in our analysis).[53,55,56,68,73,74] The first element, R_s, corresponds to the solution resistance. The second element describes the LFP cathode/Al current collector interface with a resistor ($R_{LFP/Al)}$ and a capacitor ($C_{LFP/Al)}$ in parallel. The third element describes charge transfer at the LFP/electrolyte interface and is modeled by the charge transfer resistance (R_{ct}) in parallel with a constant phase

element (CPE_{ct}). In the EIS, $R_{LFP/Al}$ and $C_{LFP/Al}$ are manifested in a small state-of-charge (SOC) independent, high-frequency semi-circle denoted by an arrow in Figure 3.14a (fit values in Table 3.1).[73–75] The larger, mid-frequency semi-circle corresponds to the charge transfer resistance (R_{ct}) between the electrolyte and cathode particles and exhibits potential-dependent changes such that the semi-circle is larger at 2.6 V than at 4.4 V. The SOC-dependent features in the mid-frequency region associate them strongly with the cathode/electrolyte interface in our cell.

Figure 3.14b shows the value of the R_{ct} fitting parameter at different points in the CV corresponding to 4.4 V (black) and 2.6 V (green). The R_{ct} observed at 4.4 V and 2.6 V occurs at an average of 39 ± 2 Ω and 191 ± 12 Ω, respectively. The average difference between the R_{ct} at 4.4 V and 2.6 V within each cycle (indicated with grey arrows) is 152 ± 14 Ω. Figure 3.14c shows the

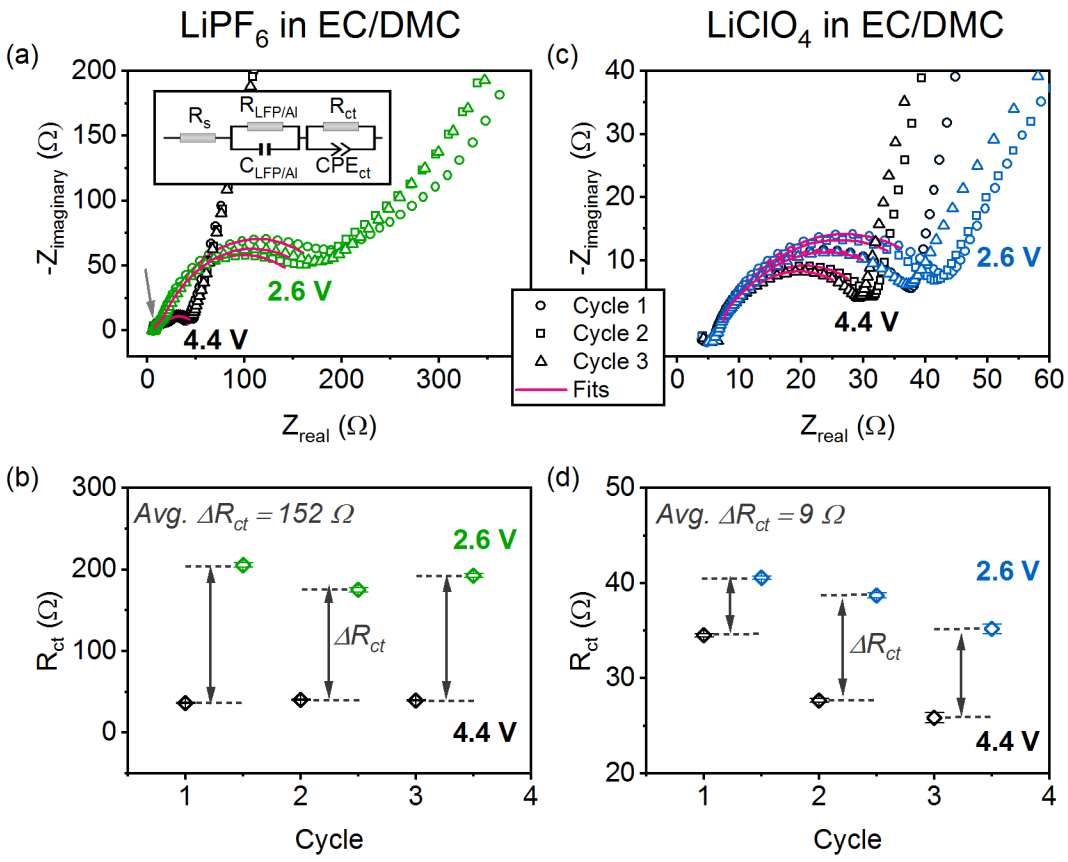

Figure 3.14. EIS measurements in $LiPF_6$ and $LiClO_4$ in EC/DMC. EIS measurements at 2.6 V (green or blue) and 4.4 V (black) of LFP in (a) 1 M $LiPF_6$ in EC/DMC and (c) 1 M $LiClO_4$ in EC/DMC during 3 cycles of CV at 0.1 mV/s. The inset of (a) shows the equivalent circuit used to fit both sets of data and the result of these fits are shown in pink. Charge transfer resistance (R_{ct}) values from fitting the mid- to high-frequency region of the impedance in (b) 1 M $LiPF_6$ in EC/DMC and (c) 1 M $LiClO_4$ in EC/DMC. Error bars show the fit error, and the gray arrows aid in comparing changes in R_{ct} at 2.6 V (green or blue) and 4.4 V (black) within the same CV cycle.

mid- to high-frequency EIS region of LFP in 1 M $LiClO_4$ in EC/DMC. The equivalent circuit presented in Figure 3.14a was also used to fit this data. Table 3.1 shows all the fit parameters and corresponding errors. The mid-frequency, R_{ct}-related semicircle also exhibits potential-dependent fluctuations such that R_{ct} is generally larger at 2.6 V than at 4.4 V. Figure 3.14d shows the value of R_{ct} at 4.4 V (black) and 2.6 V (blue). The R_{ct} observed at 4.4 V and 2.6 V occur at an average of 26 ± 4 Ω and 35 ± 3 Ω, respectively. Interestingly, the average difference between the

Table 3.1. EIS fit parameters. Fit parameters from fitting the mid- to high- frequency of LFP in 1 M $LiPF_6$ or $LiClO_4$ in EC/DMC. The errors were given from the RelaxIS fitting program.

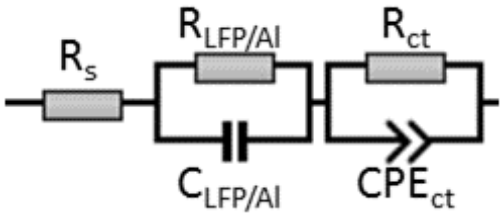

Electrolyte	Time (s)	Potential (V)	R_s (Ω)	$R_{LFP/Al}$ (Ω)	$C_{LFP/Al}$ (μF)	R_{ct} (Ω)	CPE_{ct} (μF)
1 M $LiPF_6$ in EC/DMC	0	3.048	7.44±0.07	1.5±0.1	1.2±0.1	356±7	19.2±0.6
	17705	4.4	7.00±0.09	2.7 ± 0.3	1.0±0.1	36.2±0.9	90±10
	39900	2.6	7.15±0.06	3.8±0.2	0.86±0.04	206±3	19.5±0.9
	62094	4.4	7.18±0.06	5.8±0.2	0.72±0.02	40±1	140±20
	84290	2.6	6.95±0.06	4.5±0.2	0.86±0.03	175±3	24±1
	106484	4.4	7.07±0.07	6.2±0.2	0.74±0.03	40±1	190±20
	128679	2.6	7.09±0.05	5.1±0.2	0.84±0.03	193±3	28±1
1 M $LiClO_4$ in EC/DMC	0	2.75	5.7±0.1	1.4±0.1	5±1	45.7±0.2	15±2
	20706	4.4	5.44±0.07	1.26±0.06	5±1	34.5±0.2	14±2
	42901	2.6	5.89±0.05	1.24±0.05	6±2	40.6±0.2	12±1
	65098	4.4	5.70±0.06	1.23±0.05	4.0±0.9	27.7±0.2	16±3
	87293	2.6	6.01±0.05	1.29±0.05	5±1	38.7±0.3	14±2
	109489	4.4	6.04±0.06	1.26±0.09	3.2±0.5	25.8±0.5	22±4
	131684	2.6	5.80±0.09	1.45±0.09	3.7±0.6	35.2±0.05	19±3

R_{ct} at 4.4 V and 2.6 V within each cycle is much lower in $LiClO_4$ electrolyte (9 ± 2 Ω) than in $LiPF_6$ electrolyte (152 ± 14 Ω). Smaller impedance for LFP in 1 M $LiClO_4$ in EC/DMC compared to 1 M $LiPF_6$ in EC/DMC (albeit at 60°C) has been previously reported[53] A report by Tang et al. also shows that R_{ct} depends on the SOC.[55] Thus, EIS data indicate that R_{ct} is lower and changes less as a function of SOC in $LiClO_4$ relative to $LiPF_6$-containing electrolyte.

The linear sweep voltammetry performed between the EIS experiments shows larger peak splittings for LFP cycled in $LiPF_6$ than $LiClO_4$-containing electrolytes (Figure 3.15), in agreement with the voltammetry collected during in-situ stress and strain measurements.

3.4. Discussion

The additional feature seen in the stress and strain obtained from LFP evaluated in $LiPF_6$ is not found in $LiClO_4$. Additionally, the voltammetry in $LiPF_6$ exhibits greater peak splitting and wider peaks relative to $LiClO_4$. These voltammetric changes are mirrored in higher impedance changes and the overall higher impedance seen in $LiPF_6$ electrolytes compared to $LiClO_4$. These observations imply that there is an electrolyte-dependent increase in resistance at the cathode/electrolyte interface in $LiPF_6$ relative to $LiClO_4$.

Several electrolyte properties could contribute to the extra stress and strain derivative feature, increased peak splitting, wider current peaks, and increased impedance in $LiPF_6$ compared to $LiClO_4$ electrolytes, including: ionic conductivity, transference number, coordination number,

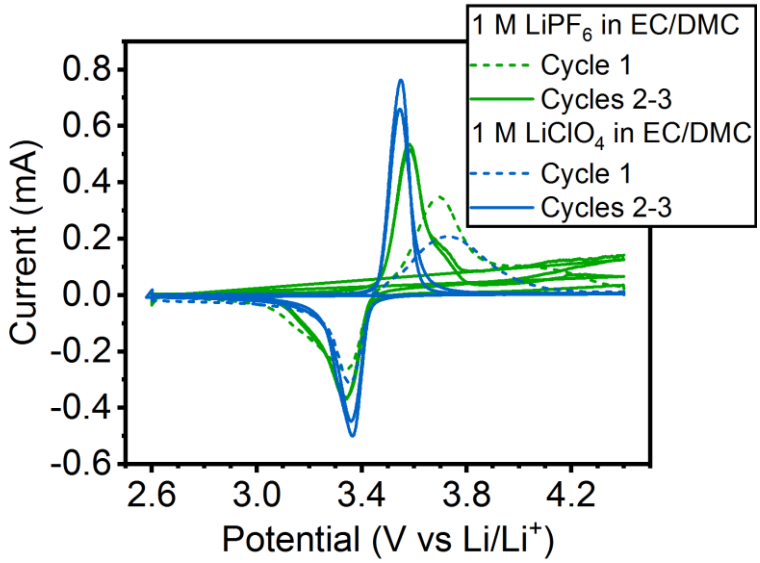

Figure 3.15. Linear sweep voltammetry performed between EIS experiments in coin cells. LSV performed at 0.1 mV/s in either 1 M $LiPF_6$ in EC/DMC (green) or 1 M $LiClO_4$ in EC/DMC (blue) for three cycles. The first cycle is shown as a dashed line. EIS was performed at the top (4.4 V) and bottom (2.6 V) of each LSV.

transition metal dissolution, and decomposition products. The ionic conductivity of $LiPF_6$ in EC/DMC (10.7 mS/cm) is larger than that for $LiClO_4$ in EC/DMC (8.4 mS/cm) and therefore is not contributing to higher impedance in $LiPF_6$ in EC/DMC.[76] Li^+ transference numbers in $LiPF_6$ and $LiClO_4$ in PC electrolytes range from 0.31–0.41 and 0.29–0.44, respectively, and are therefore essentially the same.[77–80] The coordination numbers of $LiPF_6$ and $LiClO_4$ are ca. 2.75 and 2.25 in DMC and 3.5 and 3.25 in PC, respectively.[81] The similarity in coordination number between the two electrolyte salts suggests that coordination number effects are not the origin of the stress, strain, peak splitting, and impedance changes seen here. Another possible explanation for the increased current peak splitting, increased impedance, and extra stress and strain derivative peaks in $LiPF_6$–containing electrolytes is Fe dissolution from LFP.[53,68,82] Indeed, higher concentrations of Fe dissolution from LFP occurs after electrode storage in $LiPF_6$ in EC/DMC compared to $LiClO_4$ in EC/DMC, albeit only by ca. 2 ppm.[83]

Finally, another possible origin of the differences between $LiClO_4$ and $LiPF_6$ is the CEI formed in the different electrolytes. Most carbonate-containing electrolytes decompose to form Li_2CO_3, polyethers, carboxylates, ROLi, and $ROCO_2Li$ on Li-air and Li-ion cathodes.[27,84–88] Specifically, the CEI in $LiPF_6$ exhibits F-containing species–such as LiF, Li_xPF_y, and $Li_xPO_yF_z$–because of the reactivity of $LiPF_6$ decomposition byproducts (such as HF).[26,53,89] $LiClO_4$ in PC or tetraethylene glycol dimethyl ether electrolytes decomposes to LiCl and other $LiClO_x$ compounds on cathodes in Li-air batteries. LiCl, however, does not form on cathodes in $LiClO_4$ in EC/DMC.[86,87] Finally, while the organic components of the CEI may be similar in electrolytes containing either $LiClO_4$ or $LiPF_6$, the CEI formed in $LiClO_4$ is thinner than that formed in $LiPF_6$.[76,90]

Our impedance studies suggest that the CEI in $LiPF_6$ is more resistive relative to that in $LiClO_4$. The value of the R_{ct} at 2.6 V is an order of magnitude greater in $LiPF_6$ compared to $LiClO_4$. The conductivity of LiF near 2.6 V is ca. 10^{-32} S/cm.[91] In contrast, LiCl and Li_2CO_3 exhibit conductivities near 10^{-9} S/cm and 10^{-15} S/cm, respectively.[92,93] We also showed that the impedance of the LFP-containing cell differs with changing SOC, with the more discharged cells exhibiting higher impedance. There are several possible reasons for this change. First, the conductivity of LiF changes depending on electrode potential. Near 4.5 V, the conductivity (near 10^{-12} S/cm) is comparable to other CEI but plummets to 10^{-32} S/cm below ca. 2.75 V vs Li/Li^+.[91] Second, the CEI does not grow linearly throughout cycling but instead partially dissolves and deposits depending

on SOC.[94–96] Dedryvnère et al. demonstrated increased O-containing CEI on lithiated LFP compared to delithiated cathodes;[95] and Sina et al. showed that a thicker, LiF-containing CEI formed on lithiated versus delithiated FeF_2 cathodes.[96]

In this work, the larger current peak splitting, wider current peaks, and higher impedance changes in $LiPF_6$ containing electrolytes suggest the formation of a thicker, more resistive CEI formed on LFP cathodes in $LiPF_6$ electrolytes. The observation of a similar stress and strain derivative peak in $LiPF_6$ in PC electrolyte further supports the anion dependence of this behavior. We suggest that the potential-dependent formation of high impedance degradation products formed on the LFP surface in $LiPF_6$ electrolytes is associated with the additional feature in the stress and strain derivatives during cathode delithiation and the larger strain change at faster CV scan rates. Prior work in LMO shows the same number of stress and strain derivative peaks as

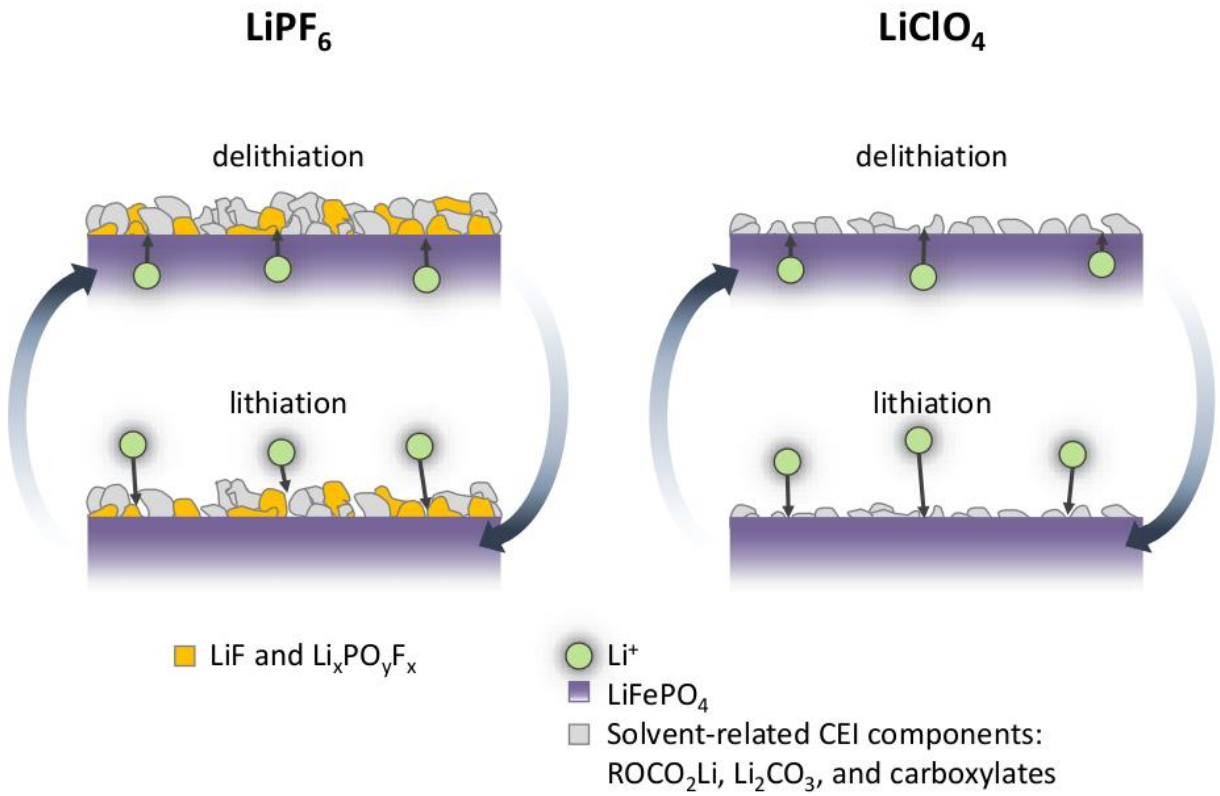

Figure 3.16. CEI effect on Li^+ diffusion at the LFP/electrolyte interface during delithiation and lithiation. Comparison of Li^+ diffusion through the CEI during delithiation and lithiation in $LiPF_6$ versus $LiClO_4$ electrolytes. During delithiation, the Li^+ break through a thick and highly resistive CEI. This process causes stress at the interface, possibly causing cracks that would allow more facile Li^+ diffusion during lithiation. Li^+ diffusion at the LFP/electrolyte interface in $LiClO_4$ electrolytes occurs more freely through the thinner and less resistive CEI. The CEI is thinner during lithiation compared to delithiation in both electrolytes. The polymeric hydrocarbons (polyethylene glycol) that also contribute to the cathode CEI are not pictured here for clarity. LiCl formation on cathodes only occurs in some $LiClO_4$ + solvent electrolytes and so is also excluded.

voltammetric peaks;[49] here we observe one more stress and strain derivative peak compared to the current peak during delithiation. Since the CEI on LMO is likely not much different from that on LFP, we suggest that overlapping peaks in the stress and strain is the reason this additional feature is not individually observed in LMO.

The higher R_{ct} seen at 2.6 V suggests that the CEI becomes thicker by the end of discharge. During cathode delithiation, the highly resistive CEI on the cathode formed at low potentials in $LiPF_6$ electrolytes forms a barrier against delithiation. Li^+ must break through the thicker and more resistive CEI in order to diffuse to the CEI/electrolyte interface and solvate in the electrolyte (Figure 3.16). The interaction between Li^+ and the CEI would cause an increase in strain and compressive stress–indicating electrode expansion–as the delithiation process begins. The beginning of delithiation during CV and the extra stress and strain derivative features occur within the same potential window (region ① in Figure 3.2).

While Li^+ interactions with the CEI probably influence the extra stress and strain derivative peaks in $LiPF_6$ electrolytes, bulk lattice changes are most likely associated with the stress and strain derivative peaks during lithiation and during region ② of delithiation in $LiPF_6$ electrolytes because Li^+ no longer needs to break through a thick CEI. Bulk lattice changes would also be associated with the stress and strain derivative peaks in $LiClO_4$ electrolytes during lithiation and delithiation.

3.5 Conclusion

In this work we show that stress and strain derivatives exhibit an extra feature in $LiPF_6$–containing electrolytes, likely associated with the presence of a thicker and more resistive CEI formed in $LiPF_6$ relative to $LiClO_4$. The current peak splitting during CV and impedance at 2.6 V of LFP in $LiPF_6$ in EC/DMC or PC are larger than those found in $LiClO_4$ in EC/DMC or PC electrolytes. We propose that the potential-dependent growth of a thick and resistive CEI in $LiPF_6$ electrolytes causes the extra stress and strain derivative features, the larger current peak splitting, and the higher impedance. Li^+ has to interact with the thicker and more resistive CEI formed in $LiPF_6$ electrolytes to delithiate LFP and in turn create stress and strain in the LFP composite electrode at the onset of delithiation. The contribution of CEI to mechanical forces acting in a Li-ion cells further proves that understanding the composition and morphology of surface films is paramount to designing longer lasting Li-ion batteries.

3.6 References

(1) Chen, G.; Song, X.; Richardson, T. J. *Electrochem. Solid-State Lett.* **2006**, *9*, A295.

(2) Mukhopadhyay, A.; Sheldon, B. W. *Prog. Mater. Sci.* **2014**, *63*, 58.

(3) Wang, D.; Wu, X.; Wang, Z.; Chen, L. *J. Power Sources* **2005**, *140*, 125.

(4) Tokranov, A.; Sheldon, B. W.; Lu, P.; Xiao, X.; Mukhopadhyay, A. *J. Electrochem. Soc.* **2014**, *161*, A58.

(5) Whittingham, M. S. *Chem. Rev.* **2004**, *104*, 4271.

(6) Wang, D.; Wu, X.; Wang, Z.; Chen, L. *J. Power Sources* **2005**, *140*, 125.

(7) Padhi, A. K.; Nanjundaswamy, K. S.; Goodenough, J. B. *J. Electrochem. Soc.* **1997**, *144*, 1188.

(8) Liu, H.; Strobridge, F. C.; Borkiewicz, O. J.; Wiaderek, K. M.; Chapman, K. W.; Chupas, P. J.; Grey, C. P. *Science (80-.).* **2014**, *344*, 1480.

(9) Laffont, L.; Delacourt, C.; Gibot, P.; Wu, M. Y.; Kooyman, P.; Masquelier, C.; Tarascon, J. M. *Chem. Mater.* **2006**, *18*, 5520.

(10) Wang, J.; Chen-Wiegart, Y. K.; Wang, J. *Nat. Commun.* **2014**, *5*, 4570.

(11) Niu, J.; Kushima, A.; Qian, X.; Qi, L.; Xiang, K.; Chiang, Y.-M.; Li, J. *Nano Lett.* **2014**, *14*, 4005.

(12) Andersson, A. S.; Kalska, B.; Häggström, L.; Thomas, J. O. *Solid State Ionics* **2000**, *130*, 41.

(13) Orikasa, Y.; Maeda, T.; Koyama, Y.; Minato, T.; Murayama, H.; Fukuda, K.; Tanida, H.; Arai, H.; Matsubara, E.; Uchimoto, Y.; Ogumi, Z. *J. Electrochem. Soc.* **2013**, *160*, A3061.

(14) Li, D.; Zhou, H. *Mater. Today* **2014**, *17*, 451.

(15) Malik, R.; Abdellahi, A.; Ceder, G. *J. Electrochem. Soc.* **2013**, *160*, A3179.

(16) Lv, W.; Niu, Y.; Jian, X.; Zhang, K. H. L.; Wang, W.; Zhao, J.; Wang, Z.; Yang, W.; He, W. *Appl. Phys. Lett.* **2016**, *108*, 083901.

(17) Gabrisch, H.; Wilcox, J.; Doeff, M. M. *Electrochem. Solid-State Lett.* **2008**, *11*, A25.

(18) Wu, L.; De Andrade, V.; Xiao, X.; Zhang, J. *J. Electrochem. Energy Convers. Storage* **2019**, 1.

(19) Shadow Huang, H.-Y.; Wang, Y.-X. *J. Electrochem. Soc.* **2012**, *159*, A815.

(20) Hu, Y.; Zhao, X.; Suo, Z. *J. Mater. Res.* **2010**, *25*, 1007.

(21) Lu, Y.; Ni, Y. *Mech. Mater.* **2015**, *91*, 372.

(22) Kim, S.; Huang, H.-Y. S. *J. Mater. Res.* **2016**, *31*, 3506.

(23) Vetter, J.; Novák, P.; Wagner, M. R.; Veit, C.; Möller, K.-C.; Besenhard, J. O.; Winter, M.; Wohlfahrt-Mehrens, M.; Vogler, C.; Hammouche, A. *J. Power Sources* **2005**, *147*, 269.

(24) Gauthier, M.; Carney, T. J.; Grimaud, A.; Giordano, L.; Pour, N.; Chang, H.-H.; Fenning, D. P.; Lux, S. F.; Paschos, O.; Bauer, C.; Maglia, F.; Lupart, S.; Lamp, P.; Shao-Horn, Y. *J. Phys. Chem. Lett.* **2015**, *6*, 4653.

(25) Kabir, M. M.; Demirocak, D. E. *Int. J. Energy Res.* **2017**, *41*, 1963.

(26) Yu, X.; Manthiram, A. *Energy Environ. Sci.* **2018**, *11*, 527.

(27) Edström, K.; Gustafsson, T.; Thomas, J. O. *Electrochim. Acta* **2004**, *50*, 397.

(28) Abadias, G.; Chason, E.; Keckes, J.; Sebastiani, M.; Thompson, G. B.; Barthel, E.; Doll, G. L.; Murray, C. E.; Stoessel, C. H.; Martinu, L. *J. Vac. Sci. Technol. A Vacuum, Surfaces, Film.* **2018**, *36*, 020801.

(29) Koch, R.; Leonhard, H.; Thurner, G.; Abermann, R. *Rev. Sci. Instrum.* **1990**, *61*, 3859.

(30) Klokholm, E. *Rev. Sci. Instrum.* **1969**, *40*, 1054.

(31) Jaeckel, L.; Láng, G.; Heusler, K. E. *Electrochim. Acta* **1994**, *39*, 1031.

(32) Brunt, T. A.; Rayment, T.; O'Shea, S. J.; Welland, M. E. *Langmuir* **1996**, *12*, 5942.

(33) Tavassol, H.; Jones, E. M. C.; Sottos, N. R.; Gewirth, A. A. *Nat. Mater.* **2016**, *15*, 1182.

(34) Chung, K. Y.; Kim, K.-B. *J. Electrochem. Soc.* **2002**, *149*, A79.

(35) Sheth, J.; Karan, N. K.; Abraham, D. P.; Nguyen, C. C.; Lucht, B. L.; Sheldon, B. W.; Guduru, P. R. *J. Electrochem. Soc.* **2016**, *163*, A2524.

(36) Pyun, S.-I.; Go, J.-Y.; Jang, T.-S. *Electrochim. Acta* **2004**, *49*, 4477.

(37) Shin, J. W.; Chason, E. *Phys. Rev. Lett.* **2009**, *103*, 056102.

(38) Sheth, J.; Karan, N. K.; Abraham, D. P.; Nguyen, C. C.; Lucht, B. L.; Sheldon, B. W.; Guduru, P. R. *J. Electrochem. Soc.* **2016**, *163*, A2524.

(39) Bucci, G.; Swamy, T.; Bishop, S.; Sheldon, B. W.; Chiang, Y.-M.; Carter, W. C. *J. Electrochem. Soc.* **2017**, *164*, A645.

(40) Kumar, R.; Woo, J. H.; Xiao, X.; Sheldon, B. W. *J. Electrochem. Soc.* **2017**, *164*, A3750.

(41) Liu, X. H.; Huang, J. Y. *Energy Environ. Sci.* **2011**, *4*, 3844.

(42) Beaulieu, L. Y.; Eberman, K. W.; Turner, R. L.; Krause, L. J.; Dahn, J. R. *Electrochem.*

Solid-State Lett. **2001**, *4*, A137.

(43) Jones, E. M. C.; Silberstein, M. N.; White, S. R.; Sottos, N. R. *Exp. Mech.* **2014**, *54*, 971.

(44) Eastwood, D. S.; Yufit, V.; Gelb, J.; Gu, A.; Bradley, R. S.; Harris, S. J.; Brett, D. J. L.; Brandon, N. P.; Lee, P. D.; Withers, P. J.; Shearing, P. R. *Adv. Energy Mater.* **2014**, *4*, 1300506.

(45) Gonzalez, J.; Sun, K.; Huang, M.; Lambros, J.; Dillon, S.; Chasiotis, I. *J. Power Sources* **2014**, *269*, 334.

(46) Qi, Y.; Harris, S. J. *J. Electrochem. Soc.* **2010**, *157*, A741.

(47) Xin, N.; Sun, Y.; He, M.; Radke, C. J.; Prausnitz, J. M. *Fluid Phase Equilib.* **2018**, *461*, 1.

(48) Çapraz, Ö. Ö.; Rajput, S.; White, S.; Sottos, N. R. *Exp. Mech.* **2018**, *58*, 561.

(49) Çapraz, Ö. Ö.; Bassett, K. L.; Gewirth, A. A.; Sottos, N. R. *Adv. Energy Mater.* **2016**, 1601778.

(50) Schiffer, Z. J.; Cannarella, J.; Arnold, C. B. *J. Electrochem. Soc.* **2016**, *163*, A427.

(51) Zhang, X.; Cahill, D. G. *Langmuir* **2006**, *22*, 9062.

(52) Tavassol, H.; Chan, M. K. Y.; Catarello, M. G.; Greeley, J.; Cahill, D. G.; Gewirth, A. A. *J. Electrochem. Soc.* **2013**, *160*, A888.

(53) Koltypin, M.; Aurbach, D.; Nazar, L.; Ellis, B. *Electrochem. Solid-State Lett.* **2007**, *10*, A40.

(54) Köhler, M.; Berkemeier, F.; Gallasch, T.; Schmitz, G. *J. Power Sources* **2013**, *236*, 61.

(55) Tang, K.; Yu, X.; Sun, J.; Li, H.; Huang, X. *Electrochim. Acta* **2011**, *56*, 4869.

(56) Takahashi, M.; Tobishima, S.; Takei, K.; Sakurai, Y. *Solid State Ionics* **2002**, *148*, 283.

(57) Liu, H.; Li, C.; Zhang, H. P.; Fu, L. J.; Wu, Y. P.; Wu, H. Q. *J. Power Sources* **2006**, *159*, 717.

(58) Yang, S.; Zhou, X.; Zhang, J.; Liu, Z. *J. Mater. Chem.* **2010**, *20*, 8086.

(59) Churikov, A. V.; Ivanishchev, A. V.; Ushakov, A. V.; Romanova, V. O. *J. Solid State Electrochem.* **2014**, *18*, 1425.

(60) Das, S. R.; Majumder, S. B.; Katiyar, R. S. *J. Power Sources* **2005**, *139*, 261.

(61) Aurbach, D.; Gamolsky, K.; Markovsky, B.; Salitra, G.; Gofer, Y.; Heider, U.; Oesten, R.; Schmidt, M. *J. Electrochem. Soc.* **2000**, *147*, 1322.

(62) Esbenshade, J. L.; Fox, M. D.; Gewirth, A. A. *J. Electrochem. Soc.* **2014**, *162*, A26.

(63) Jang, D. H.; Shin, Y. J.; Oh, S. M. *J. Electrochem. Soc.* **1996**, *143*, 2204.

(64) Tu, J. P.; Zhao, X. B.; Cao, G. S.; Tu, J. P.; Zhu, T. J. *Mater. Lett.* **2006**, *60*, 3251.

(65) Benedek, R.; Thackeray, M. M. *Electrochem. Solid-State Lett.* **2006**, *9*, A265.

(66) Li, Z.; Zhang, D.; Yang, F. *J. Mater. Sci.* **2009**, *44*, 2435.

(67) Wu, H.-C.; Su, C.-Y.; Shieh, D.-T.; Yang, M.-H.; Wu, N.-L. *Electrochem. Solid-State Lett.* **2006**, *9*, A537.

(68) Amine, K.; Liu, J.; Belharouak, I. *Electrochem. commun.* **2005**, *7*, 669.

(69) Striebel, K.; Shim, J.; Sierra, A.; Yang, H.; Song, X.; Kostecki, R.; McCarthy, K. *J. Power Sources* **2005**, *146*, 33.

(70) Rauhala, T.; Jalkanen, K.; Romann, T.; Lust, E.; Omar, N.; Kallio, T. *J. Energy Storage* **2018**, *20*, 344.

(71) Yang, W.; Wang, Z.; Chen, L.; Chen, Y.; Zhang, L.; Lin, Y.; Li, J.; Huang, Z. *RSC Adv.* **2017**, *7*, 33680.

(72) Cao, W.; Li, J.; Wu, Z. *Ionics (Kiel).* **2016**, *22*, 1791.

(73) Schmidt, J. P.; Chrobak, T.; Ender, M.; Illig, J.; Klotz, D.; Ivers-Tiffée, E. *J. Power Sources* **2011**, *196*, 5342.

(74) Illig, J.; Ender, M.; Chrobak, T.; Schmidt, J. P.; Klotz, D.; Ivers-Tiffee, E. *J. Electrochem. Soc.* **2012**, *159*, A952.

(75) Gaberscek, M.; Moskon, J.; Erjavec, B.; Dominko, R.; Jamnik, J. *Electrochem. Solid-State Lett.* **2008**, *11*, A170.

(76) Xu, K. *Chem. Rev.* **2004**, *104*, 4303.

(77) Croce, F.; D'Aprano, A.; Nanjundiah, C.; Koch, V. R.; Walker, C. W.; Salomon, M. *J. Electrochem. Soc.* **1996**, *143*, 154.

(78) Mauro, V.; D'Aprano, A.; Croce, F.; Salomon, M. *J. Power Sources* **2005**, *141*, 167.

(79) Verbrugge, M. W.; Koch, B. J.; Schneider, E. W. *J. Appl. Electrochem.* **2000**, *30*, 269.

(80) Zhao, J.; Wang, L.; He, X.; Wan, C.; Jiang, C. *J. Electrochem. Soc.* **2008**, *155*, A292.

(81) Chapman, N.; Borodin, O.; Yoon, T.; Nguyen, C. C.; Lucht, B. L. *J. Phys. Chem. C* **2017**, *121*, 2135.

(82) Choi, W.; Manthiram, A. *J. Electrochem. Soc.* **2006**, *153*, A1760.

(83) Koltypin, M.; Aurbach, D.; Nazar, L.; Ellis, B. *J. Power Sources* **2007**, *174*, 1241.

(84) Yang, L.; Ravdel, B.; Lucht, B. L. *Electrochem. Solid-State Lett.* **2010**, *13*, A95.

(85) Liu, Y.-M.; G. Nicolau, B.; Esbenshade, J. L.; Gewirth, A. A. *Anal. Chem.* **2016**, *88*,

7171.

(86) Veith, G. M.; Nanda, J.; Delmau, L. H.; Dudney, N. J. *J. Phys. Chem. Lett.* **2012**, *3*, 1242.

(87) Younesi, R.; Hahlin, M.; Edström, K. *ACS Appl. Mater. Interfaces* **2013**, *5*, 1333.

(88) Aurbach, D.; Markovsky, B.; Salitra, G.; Markevich, E.; Talyossef, Y.; Koltypin, M.; Nazar, L.; Ellis, B.; Kovacheva, D. *J. Power Sources* **2007**, *165*, 491.

(89) Malmgren, S.; Ciosek, K.; Hahlin, M.; Gustafsson, T.; Gorgoi, M.; Rensmo, H.; Edström, K. *Electrochim. Acta* **2013**, *97*, 23.

(90) Kanamura, K.; Tamura, H.; Shiraishi, S.; Takehara, Z. *J. Electroanal. Chem.* **1995**, *394*, 49.

(91) Pan, J.; Cheng, Y.-T.; Qi, Y. *Phys. Rev. B* **2015**, *91*, 134116.

(92) Mogensen, M. B.; Hennesø, E. *Acta Chem. Slov.* **2016**, *63*, 519.

(93) Shi, S.; Qi, Y.; Li, H.; Hector, L. G. *J. Phys. Chem. C* **2013**, *117*, 8579.

(94) Yoon, T.; Lee, T.; Soon, J.; Jeong, H.; Jurng, S.; Ryu, J. H.; Oh, S. M. *J. Electrochem. Soc.* **2018**, *165*, A1095.

(95) Dedryvère, R.; Maccario, M.; Croguennec, L.; Le Cras, F.; Delmas, C.; Gonbeau, D. *Chem. Mater.* **2008**, *20*, 7164.

(96) Sina, M.; Thorpe, R.; Rangan, S.; Pereira, N.; Bartynski, R. A.; Amatucci, G. G.; Cosandey, F. *J. Phys. Chem. C* **2015**, *119*, 9762.

Chapter 4: Operando Observations and First Principles Calculations of Reduced Lithium Insertion in Au-Coated $LiMn_2O_4$

Reproduced with permission from Bassett, K. L.; Warburton, R. E.; Deshpande, S.; Fister, T. T.; Ta, K.; Esbenshade, J. L.; Kinaci, A.; Chan, M. K. Y.; Wiaderek, K. M.; Chapman, K. W.; Greeley, J. P.; Gewirth, A. A. Operando Observations and First Principles Calculations of Reduced Lithium Insertion in Au-Coated $LiMn_2O_4$. Adv. Mater. Interfaces 2019, 6, 1801923. Copyright 2019 Advanced Materials Interfaces.

4.1 Introduction

Lithium-ion batteries drive the portable electronics industry and appear increasingly in electric and hybrid vehicles. However, Li-ion cathodes remain a stumbling block toward longer-lasting devices and longer-range vehicles due to long term capacity fade.[1,2] $LiMn_2O_4$ (LMO) is a common cathode material with low toxicity, high thermal stability, and a high voltage (ca. 4.1 V vs. Li/Li^+). However, LMO exhibits capacity fade upon extended cycling, which is primarily attributed to (1) the formation of a Jahn-Teller distorted $Li_2Mn_2O_4$ tetragonal phase at low voltages, (2) electrolyte oxidation at high voltages, and (3) Mn ion dissolution from the electrode surface.[3–5] While formation of tetragonal $Li_2Mn_2O_4$ and electrolyte oxidation can be mitigated by cycling in a restricted voltage window, other innovative solutions are needed to address Mn dissolution from the LMO surface.

Many approaches have been developed to protect LMO from these mechanisms, such as bulk or surface doping[6–8] and deposition of protective coatings on the electrode surface.[9–16] Oxides,[9,12,13] fluorides,[14] graphene,[10] and metals[11,15] have previously been employed as LMO coatings. These coatings sustain capacity upon cycling by mitigating Mn dissolution and decreasing electrolyte decomposition. Although semiconductor coatings, including oxides and fluorides, are predicted to have high electrochemical stability, HF scavenging characteristics, and have been shown to effectively suppress Mn dissolution, their Li^+ and electrical conductivity is often poor, which can lead to resistance in the battery.[17,18] Metal coatings are good candidates to improve electrical conductivity, although many metals will oxidize well below 4.5 V vs Li/Li^+. Au coatings, however, remain oxidatively stable under these conditions[15,19] and therefore function as a promising model system to study the influence of a metallic protective coating on LMO. While

Au coatings are unlikely to be economically viable for a commercial battery system, these coatings do provide an interesting model system with which to study the effect of conductive coatings more generally.

One possible effect attendant deposition of a conductive surface coating is changes in the intercalation chemistry of the bulk material. Therefore, examining LMO with a bulk measurement, such as powder X-ray diffraction (XRD), could provide valuable insight into the interactions between an electrode and its coating. Previously, ex-situ and in-situ XRD studies comparing coated and uncoated LMO observed increased peak broadening, formation of defect phases after extended cycling, and irreversible changes to the lattice parameter for the coated materials.[20–34] This prior work, however, left unclear how conductive coatings influence LMO intercalation chemistry, which is directly related to the lattice parameter during charge and discharge. It is also unclear how those lattice parameter changes correlate with electrochemical performance. Moreover, very few studies have used theoretical calculations, such as density functional theory (DFT), to directly evaluate physical properties of the interface formed between an electrode and protective coatings.[35–37] Information regarding the chemical nature of the electrode-coating interface may be able to provide specific insights into experimentally measurable properties, such as the lattice parameter changes and overall electrochemical cycling performance. For instance, one might anticipate contact between a semiconducting cathode and a reducing metal, such as Au, may lead to interfacial charge transfer, which could in turn influence the intercalation chemistry. Such effects can be probed using a combination of operando characterization and theoretical chemistry calculations.

The intent of this work is to develop an understanding of the interactions between the LMO surface and a model conductive Au coating using operando XRD followed by Rietveld analysis and DFT calculations. These techniques help elucidate properties of an electrode-coating interface, and how these interfacial effects may influence bulk intercalation chemistry in coated Li-ion cathodes. A more comprehensive description of the electronic and geometric features of electrode-coating interfaces can aid in the design of future functional coatings and other solid-solid interfaces in Li-ion batteries.

4.2 Experimental Methods

4.2.1 Electrochemistry and Operando Diffraction

All chemicals were used as received without further purification. Electroless deposition of a continuous Au shell on LMO was performed as previously described.[15] In summary, $LiMn_2O_4$ (LMO) (electrochemical grade, Sigma-Aldrich), $AuCl_3 \cdot 3H_2O$ (99.9+% metals basis, Sigma-Aldrich), and ethanol (200 proof, Decon Laboratories Inc.) were heated to 60 °C with stirring. A solution of hydroquinone (0.4 g, Sigma-Aldrich) in ethanol (5 mL) was added drop-wise. The mixture was allowed to stir for 10-15 minutes then removed from heat. The resulting solid was isolated, washed three times with ethanol, and dried at 90 °C under vacuum overnight. As-received (bare) LMO was used to compare with the Au-coated material. Previous reports contain further characterization of Au-coated LMO, and scanning electron micrographs show continuous Au films that are ca. 3.5 nm thick with a few additional islands between 5-20 nm in diameter on the LMO surface.[15]

Electrodes for operando studies were constructed by mixing carbon black (Vulcan XC-72, Cabot Corporation), graphite (300 mesh, 99%, Alfa Aesar), PTFE binder (Sigma-Aldrich), and as-received or Au-coated LMO in a mass ratio of 1:1:2:6 in a mortar and pestle. Approximately 0.024-0.028 g of slurry were pressed into a 10 mm diameter die at 18-28 thousand PSI for two seconds. The cells were reweighed before cycling, and all cyclic voltammograms are reported with respect to the active material mass in each electrode.

Operando X-ray diffraction (XRD) patterns were collected during cyclic voltammetry (CV). CVs commenced at open circuit potential and were cycled between 3.5-4.5 V vs Li/Li^+ at 25 or 50 $\mu V\ s^{-1}$ in 1 M $LiPF_6$ (98%, Sigma-Aldrich) in 1:1 (v/v) ethylene carbonate (anhydrous, 99%, Sigma-Aldrich)/ dimethyl carbonate (anhydrous, ≥99%, Sigma-Aldrich) against a Li counter/reference electrode (99.9%, Alfa Aesar) with a glass fiber separator with CH Instruments potentiostats (models 760D, 660E, 60002E, 610E, and 760E). Potentials are reported with respect to Li/Li^+. The battery stack was constructed inside a custom AMPIX cell.[38] The AMPIX cell models a coin cell electrode configuration and is equipped with X-ray transmissive windows for in-situ and operando studies. Kapton tape protected the glassy carbon window from Li exposure. Graphite and window peaks seen in the XRD were identical with those reported previously.[38]

Operando XRD was performed in transmission mode at beamline 17 BM at the Advanced Photon Source (APS) with a wavelength of 0.72768 Å. Multiple samples were analyzed in parallel

using the AMPIX multi-cell holder. A diffraction pattern was collected for each sample every 10 min with a collection time of 10 sec using a Perkin Elmer a-Si Flat Panel PE1621 detector. The beam size was 0.3 x 0.3 mm.

Datasets were analyzed with GSAS II, an open source crystallography package.[39] 2D images were masked and integrated using LaB_6 for calibration. The background scans were performed on cells with the anode, electrolyte, and separator but without a cathode. Rietveld refinements were performed on select 1D diffraction data to evaluate the lattice parameters based on structural models from the Inorganic Crystal Structure Database. Differences between

Table 4.1. Goodness of fit indicators for all Rietveld refinements performed. Cycle 0 refers to immediately before the first delithiation at 3.6 V.

Sample	Cycle number	R_p	R_{wp}	R_{exp}	(Reduced $\chi^2)^{1/2}$
Lithiated Bare LMO	OCP	3.27	4.82	0.95	5.11
	0	2.95	4.67	0.94	5.02
	1	2.12	3.55	1.10	3.24
	2	2.54	4.19	0.99	4.26
	3	2.54	4.35	1.12	3.93
	4	2.94	5.31	1.15	4.64
	5	2.82	4.45	1.07	4.20
	6	2.50	4.24	0.95	4.51
Lithiated Au-coated LMO	OCP	2.65	4.36	1.02	4.30
	0	3.12	4.66	1.00	4.67
	1	2.69	4.35	1.25	3.66
	2	3.23	5.70	1.02	5.62
	3	3.17	4.94	1.14	4.36
	4	2.98	5.07	1.17	4.38
	5	3.17	5.09	1.10	4.65
	6	4.07	6.30	1.01	4.97
Delithiated Bare LMO	1	3.49	4.59	1.00	4.62
	2	2.47	3.99	1.35	2.97
	3	2.25	3.57	0.97	3.70
	4	2.33	3.67	1.15	3.23
	5	2.42	4.01	1.13	3.57
	6	2.93	4.31	1.03	4.21
Delithiated Au-coated LMO	1	2.62	3.62	1.08	3.37
	2	3.36	4.60	1.54	3.01
	3	3.46	4.82	1.04	4.67
	4	2.74	4.13	1.16	3.58
	5	3.10	4.51	1.15	3.96
	6	2.40	3.79	1.07	3.57

calculated and observed peak heights are largely due to masking the original 2D detector image to remove single crystal reflections from the Li counter electrode which overlapped multiple LMO reflections. Therefore, Rietveld structural parameters pertaining to peak height are not reported or analyzed. Rietveld refinements were carried to a weighted profile R-factor (R_{wp}) value of no greater than 6.30. The R_{wp} is the minimized sum of squared differences between the model and data that has been scaled by the weighted intensities.[40] R-factors for all Rietveld refinements performed are reported in Table 4.1.

4.2.2 Density Functional Theory Calculations

Periodic, spin-polarized, DFT calculations were performed using the Vienna Ab initio Simulation Package (VASP).[41–43] The electronic cores are treated using the projector augmented wave (PAW) method,[44,45] with [He] and [Ne]$3s^2$ effective core potentials for oxygen and manganese, respectively. All lithium electrons are treated explicitly using the small-core pseudopotential. The generalized gradient approximation of Perdew-Burke-Ernzerhof (PBE) is used as the exchange and correlation functional,[46] with a Hubbard *U*[47–49] correction of 3.5 eV applied to the Mn 3d states. A plane wave kinetic energy cutoff of 520 eV was used in all calculations. Total energies were converged to 0.10 meV per unit cell, with a force criterion of 20 meV $Å^{-1}$ imposed for geometry relaxations.

Delithiation calculations were performed starting from the Li-terminated LMO(001) surface described in our previous work.[50] To reduce spurious supercell interactions, oxygen atoms at the bottom of the slab were passivated with hydrogens, which are initially subject to full ionic relaxation. As in previous work,[51–53] part of the slab was fixed to represent the LMO bulk (Figure 4.1). The delithiation sampling is therefore limited to the range of atoms that are subject to ionic relaxation. Delithiation free energies ($\Delta G_{Li_xMO \rightarrow Li_yMO}$) between LMO slabs of two different lithium contents (Li_xMO and Li_yMO) were calculated as a function of cell voltage with respect to the Li/Li^+ reference electrode (U_{Li/Li^+}) using the electrochemical potential $\left(g_{Li}^{bulk} - eU_{Li/Li^+}\right)$, where g_{Li}^{bulk} is the intensive bulk Li free energy and e is the charge of an electron of the lithium ions removed from LMO.

$$\Delta G_{Li_xMO \rightarrow Li_yMO} = [G_{Li_yMO} + (y - x)\left(g_{Li}^{bulk} - eU_{Li/Li^+}\right)] - G_{Li_xMO} \qquad (4.1)$$

Au-coated electrodes were modeled by introducing a two-layer, $2\sqrt{2}$ x $2\sqrt{2}$ Au(001) slab, which has a strain of less than 1% compared to the LMO(001) surface. We introduced a 20 Å vacuum

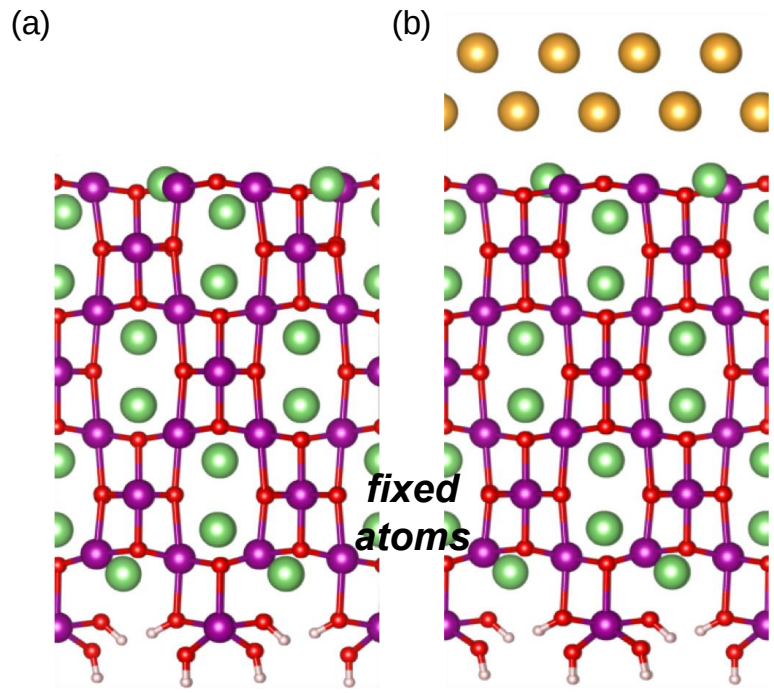

Figure 4.1. Starting lithiated structures for the (a) bare and (b) Au-coated LMO(001) surfaces. Delithiation calculations are limited to the region wherein atoms are allowed to relax. The stoichiometry of the delithiation region (as described in Methods of the main text) in the fully lithiated state is $Li_8Mn_{16}O_{32}$, which is reduced to $LiMn_2O_4$ in the remainder of paper in order to report formation energies with respect to the number of Mn_2O_4 formula units.

layer for slab calculations, with dipole corrections added into the total energy. Chemical bonding analysis was performed using the crystal orbital Hamilton population (COHP) method within the LOBSTER code.[54–58] Atom projected density of states (PDOS) calculations were performed by projecting wave function character onto the crystal orbitals determined from chemical bonding analysis. A Γ-centered 2 x 2 x 1 k-point sampling for geometry relaxations was employed, with a denser 4 x 4 x 1 grid applied for DOS, work function, and COHP calculations.

4.3 Results

Figure 4.2 shows the cyclic voltammetry (CV) of the bare and Au-coated LMO obtained at a scan rate of 50 μV s^{-1}. The two sets of reversible peaks shown are indicative of phase transformations from fully lithiated $LiMn_2O_4$ (cubic I) to $Li_{0.5}Mn_2O_4$ (cubic II) to λ-MnO_2 (cubic III) during the anodic sweep and vice versa during the cathodic sweep.[59] Additional capacity in the first cycle (dotted line) at 4.0 V is likely due to irreversible Mn loss from the cathode and solid electrolyte interphase (SEI) formation.[60–63] During cycling, the charge associated with both the

Au-coated and bare LMO decreases, which may be due to various capacity fade mechanisms previously documented in the literature, e.g., Mn loss, SEI formation, oxygen loss, and decoupling of the active material from the conductive support.[60–63] By the end of 6 cycles, the charge capacity of the bare LMO (defined as the integrated charge in the CV from 3.5 to 4.4 V) has decreased by an additional 9% from the second charging cycle. The observed capacity fade in our half cells is consistent with our previous work on Au-coated LMO full cells which also shows a consistent drop in capacity through the first ca. 75 cycles.[15]

The similar peak oxidation/reduction potentials and peak splittings for the coated and bare samples suggest that the Au coatings do not greatly influence kinetics, which agrees with previous results.[15] Figure 4.3 shows that the DFT-calculated Li^+ diffusion barriers in bulk Au are very low, confirming minimal kinetic resistance due to the presence of the coating. The Li^+ diffusion kinetics are expected to be further enhanced for grain boundary diffusion compared to the bulk DFT predictions.[64] The bare LMO current peak broadening at ca. 3.8 V during the cathodic cubic II to I transition, however, suggests kinetic limitations upon lithiation of the cubic I phase. This hypothesis is supported by the absence of a similar feature during CV at a slower scan rate of 25 $\mu V\ s^{-1}$ (Figure 4.4).

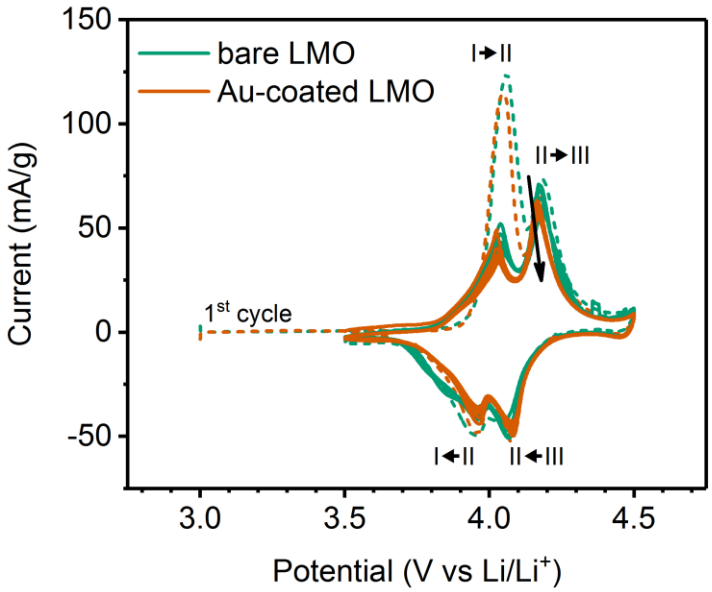

Figure 4.2. Operando CV of Au-coated (orange) and bare (teal) LMO at 50 $\mu V\ s^{-1}$. Current is normalized by the mass of LMO in the electrode pellet. The dotted line shows the first cycle, while the arrow shows the direction of capacity and voltage evolution during cycling.

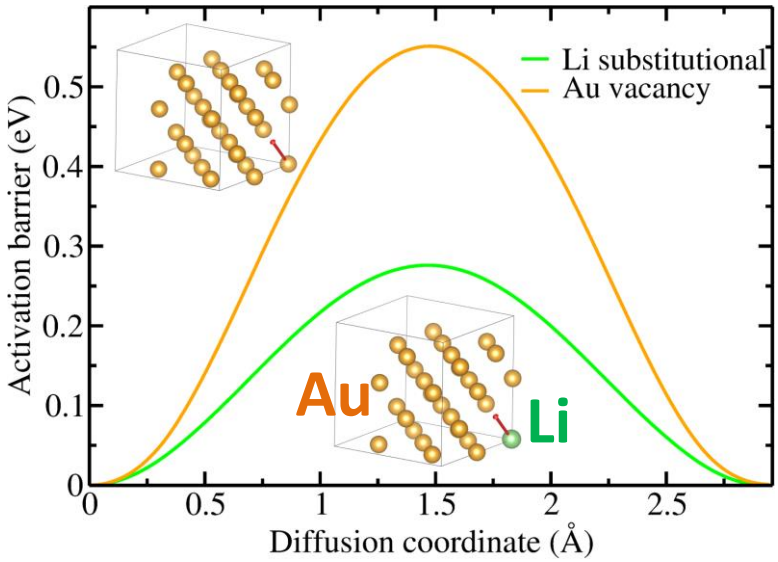

Figure 4.3. Vacancy-mediated diffusion of Au and Li^+ in bulk Au. The low diffusion barrier of 0.28 eV for Li^+ in Au suggests that the Au coating is not limiting in terms of Li^+ ion conductivity of Au-coated LMO.

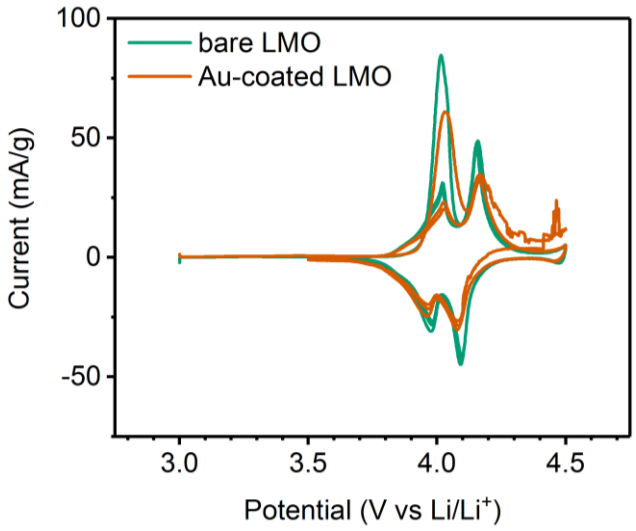

Figure 4.4. Operando CV of Au-coated (orange) and bare (teal) LMO at 25 μV/s. Current is normalized by the mass of LMO in the electrode pellet.

Figure 4.5 shows the in-situ XRD of the bare (Figure 4.5a) and Au-coated LMO (Figure 4.5b) at open circuit potential (OCP) in fully assembled cells before cycling. The background (yellow line in Figure 4.5) was collected separately and includes diffraction through a cell constructed with a Li anode, separator, and electrolyte. Due to changes in incident flux throughout the experiment, the background was scaled to fit the data.

Figure 4.5 shows that the LMO diffraction peaks are unchanged between the bare and Au-coated samples, where the only new reflections in the Au-coated sample are associated with Au.

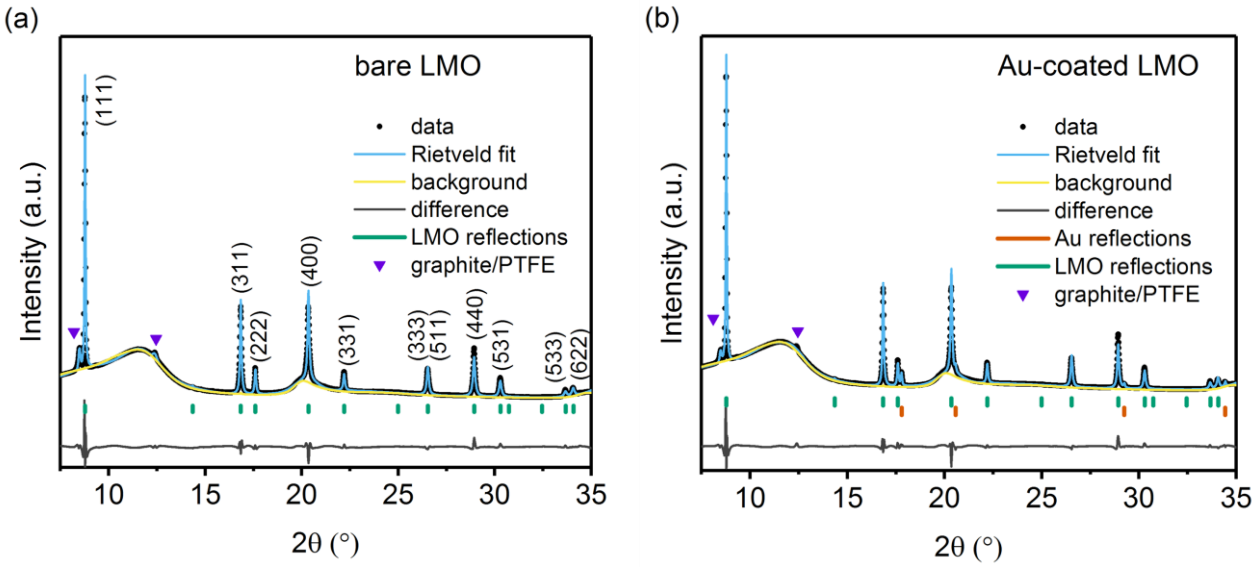

Figure 4.5. Powder diffraction patterns with Rietveld refinements for (a) bare LMO and (b) Au-coated LMO in the AMPIX cell at OCP before cycling at 50 μV s^{-1}. The differences calculated are the Rietveld fits subtracted from the collected data. Visible LMO peaks are indexed.

Rietveld refinement of the LMO-associated peaks gave a lattice parameter of 8.241 (1) Å, consistent with the LMO cubic I phase (8.238-8.248 Å).[65–67] These data show that the Au coating does not change the initial LMO structure.

Figure 4.6 shows the potential-dependent XRD obtained at a scan rate of 50 μV s^{-1} from both bare (Figure 4.6b) and Au-coated (Figure 4.6c) LMO along with the potential utilized during data collection (Figure 4.6a). For clarity, the spectra in the heat maps are normalized by the integration of the entire spectra and then background subtracted. Figure 4.6 shows there are no changes in both the bare and Au-coated LMO diffraction patterns for the first 5.14 hours corresponding to a potential sweep between 3 and 3.9 V. After 3.9 V, the cubic I phase begins to delithiate to the cubic II phase.

During the first cycle delithiation (starting at 5.3 hours and ending at 7.1 hours, corresponding to potentials between 3.95 and 4.28 V) for both the bare and Au-coated LMO, the 2θ values of the LMO-related peaks ((111), (311), (222), (400), and (331) at 8.76°, 16.84°, 17.59°, 20.34°, and 22.22°, respectively) begin to increase as the fully lithiated cubic I phase begins to delithiate and moves through the cubic II to cubic III phase. During delithiation, the Rietveld refinements give a lattice parameter change from 8.241(1) to 8.042(1) Å for both the bare and Au-coated LMO. Upon the cathodic sweep (from 8.3 to 13.0 hours corresponding to a voltage sweep

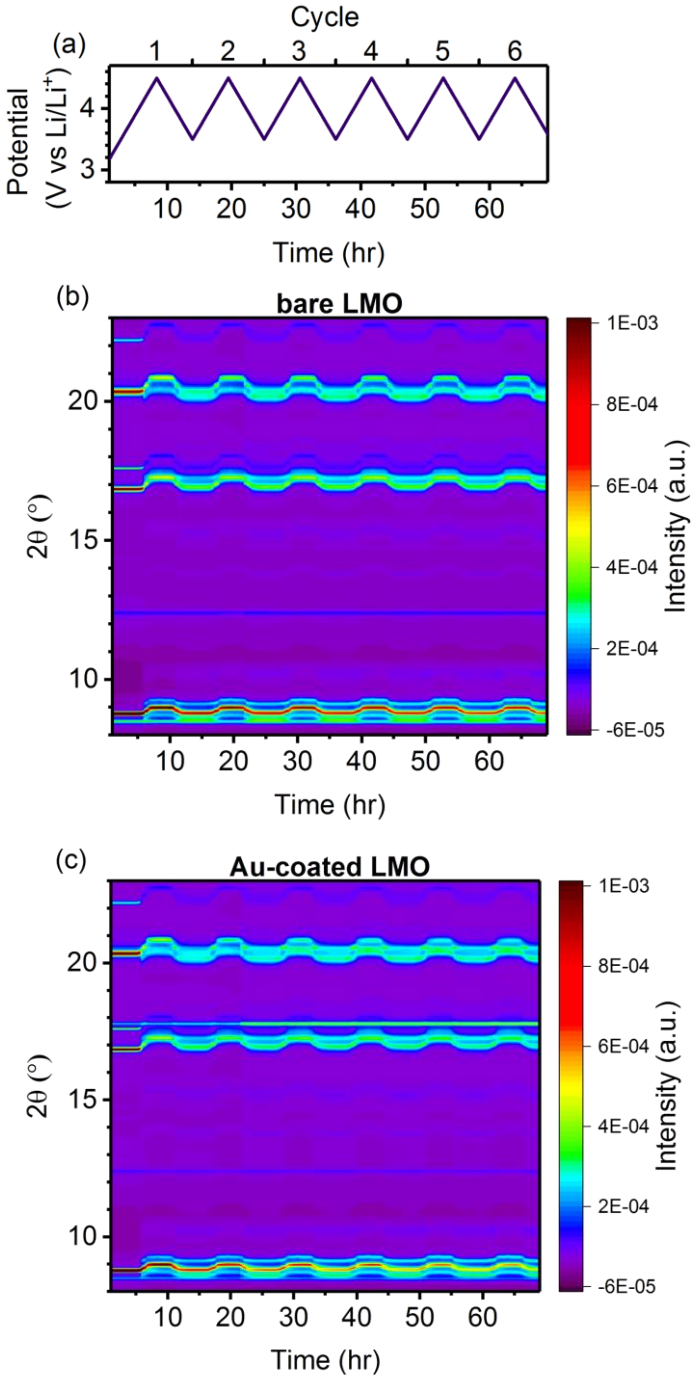

Figure 4.6. Operando XRD performed on bare and Au-coated LMO during CV at 50 μV s^{-1}. (a) Potential, (b) bare LMO 2θ (in degrees), and (c) Au-coated LMO 2θ changes with time and cycle number. A 2θ range of 8-23° is chosen to highlight higher intensity reflections. Diffraction peak intensities at time of 0 hrs correspond to those at OCP shown in Figure 4.5.

from 4.5 to 3.5 V), the cubic III → II → I transitions occur and the peaks shift back to lower 2θ values. The behavior during delithiation and lithiation seen for the bare LMO is consistent with

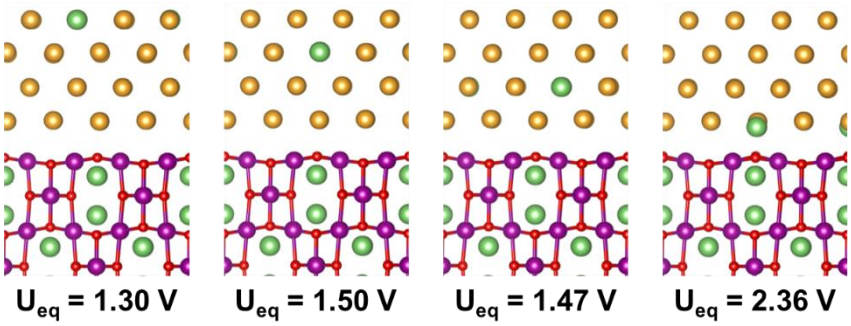

Figure 4.7. Equilibrium potentials for Li substitution within a 4 layer Au film on $Li_{0.75}Mn_2O_4$, calculated for when the ΔG in Equation 4.1 is equal to zero. As the Li substitution position moves from the Au surface (far left) to the LMO/Au interface (far right), the substitution becomes more favorable. However, even the highest substitution equilibrium potential (U_{eq} = 2.36 V vs. Li/Li^+ at the LMO/Au interface) is well outside the normal operation of LMO as a cathode and would instead be closer to anodic potentials.

previous reports.[59,68] Other persistent peaks include a PTFE peak at 8.49°, conductive carbon (graphite) peak at 12.38°, and the strong cubic Au peak at 17.78°.[69] Based on XRD, graphite and Au do not undergo any significant changes during cycling, as is expected at these positive potentials. The Au diffraction peaks originate from larger islands (ca. 20 nm diameter) and not the ca. 3.5 nm film that coats the majority of the LMO particle surface. Additionally, DFT calculations show that Li-Au alloy coatings are unstable at these potentials (Figure 4.7). This is in agreement with previous work from our groups indicating that Li-Au intermetallic surface alloy formation occurs at potentials less than 2.0 V vs. Li/Li^+.[70]

During the first delithiation, several new peaks grow in above and below the (111) peak at 8.72° and 9.27°, above the (311) peak at 17.50°, and below the (440) peak at 20.43°. The peaks at 8.72° and 9.27° also change in 2θ during cycling and are most likely defect spinel phases or Li_2MnO_3, as reported previously.[20,27–31,71] Those at 17.5° and 20.43° are most likely due to compounds within the SEI, such as LiF.[27] Strain, metastable structure, potential texturing, and even degree of crystallinity could contribute to difficulties in indexing these phases.[72,73]

After the first delithiation and lithiation cycle, individual Gaussian fits show the peak areas in the XRD patterns decrease while the peak widths grow wider (Figure 4.8), consistent with previous reports.[68] This change is likely caused by the formation of the electrochemically active defect phases seen near the LMO(111) peak or increased strain.[72] After the first CV cycle, the full width half maximum (FWHM) of the (111) peak has increased by ca. 2.4x relative to that found at OCP for the bare LMO; the corresponding change is 2x for the Au-coated LMO. The area of the same peak has decreased by ca. 2.4x and 2.6x for the bare and Au-coated LMO, respectively.

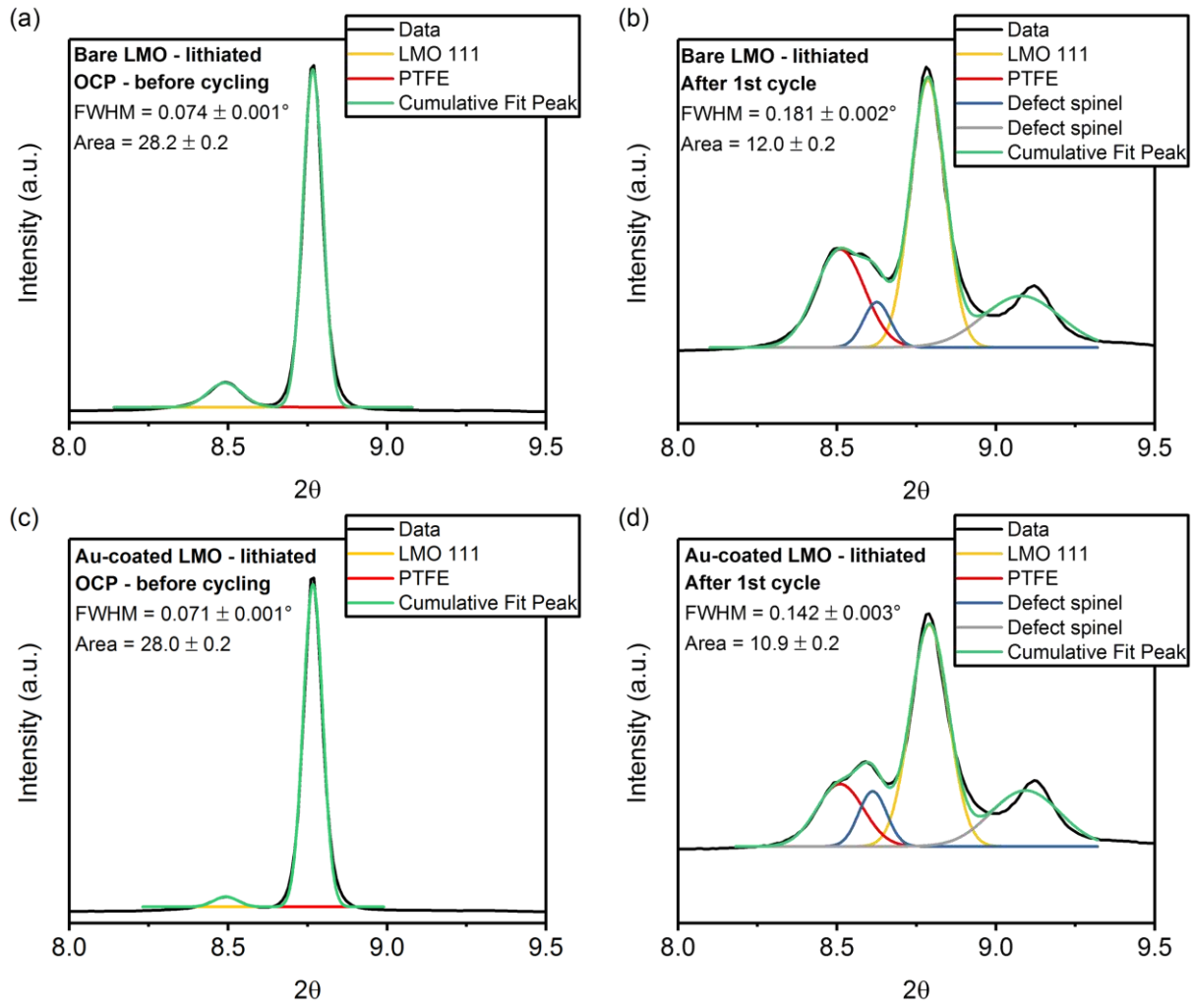

Figure 4.8. Gaussian fits of background subtracted diffraction of (a) bare LMO at OCP, (b) lithiated bare LMO after the first CV cycle, (c) Au-coated LMO at OCP, and (d) Au-coated LMO after the first CV cycle. After the 1st CV cycle, the FWHM of the (111) peak has increased by 2.4x and 2x for the bare and Au-coated LMO, respectively. The area has decreased by 2.4x and 2.6x for the bare and Au-coated LMO, respectively. Although the Rietveld refinement parameters pertaining to height are not examined because of masking the original area detector image, the same mask was used for every diffraction pattern for a given sample. Therefore, it's valid to examine peak height changes over time for a particular peak of a sample.

Likewise, the Rietveld scale factor decreased by an average of ca. 2.7x and 2.2x for the bare and Au-coated LMO, respectively, when comparing the uncycled (at OCP) and cycled (cycles 1-6) lithiated LMO.

Figure 4.9 shows the change in lattice parameter of the lithiated and delithiated Au-coated and bare LMO during cycling at 50 $\mu V\ s^{-1}$. The lattice parameter was calculated at OCP, just prior to the first delithiation at 3.6 V (at t = 8.2 hr), and at 4.5 V and 3.5 V vs Li/Li^+ during the CV.

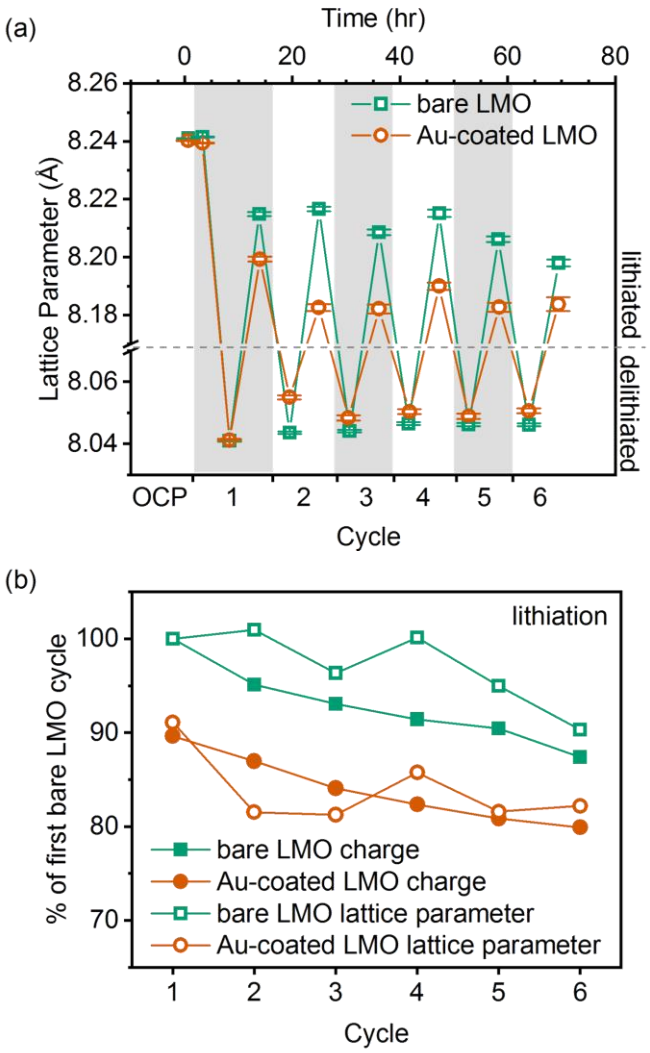

Figure 4.9. Lattice parameter and charge changes during cycling. (a) Lattice parameters from Rietveld refinements of selected XRD patterns of the lithiated and delithiated LMO phase at OCP, just prior to the first delithiation at 3.6 V (at t = 8.2 hr), at 3.5 V at the end of a lithiation CV half cycle, and at 4.5 V after a delithiation half cycle. (b) The relative lattice parameter and relative charge of each cycle compared to the initial bare LMO values after a full lithiation sweep for bare and Au-coated LMO. Charge was calculated without subtracting a capacitive background. Original charge values are plotted in Figure 4.10.

Rietveld refinements produced the lattice parameters and error bars (uncorrected estimated standard deviations produced by those refinements). Figure 4.9a shows that at OCP and before the first delithiation at 3.6 V, both samples exhibited a lattice parameter of 8.241(1) Å which then decreased to 8.040(1) Å after the first delithiation. Upon the first operando lithiation (Figure 4.9a, cycle 1, t = 13.8 hr), the lattice parameters of the two samples diverge, with the bare LMO lattice parameter increasing more than that of the Au-coated LMO. During the rest of cycling, the bare LMO exhibits both larger lattice parameters upon lithiation and smaller lattice parameters upon delithiation. Table 4.2 provides the lattice parameters for each cycle.

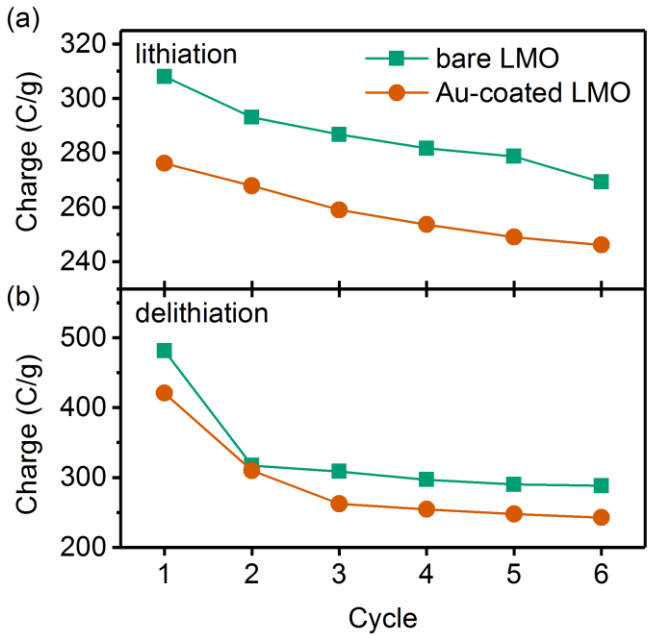

Figure 4.10. Charge calculated for each sweep in the CV for both (a) lithiation and (b) delithiation. The charge was calculated without subtracting a capacitive background and by integrating between 3.5 to 4.4 V vs Li/Li^+.

Figure 4.9b shows the relative lattice parameter and relative charge on each cycle compared to the initial bare LMO values after a full lithiation sweep for bare and Au-coated LMO. For lattice parameters, the percentage is calculated relative to the lattice parameters of 8.241 Å at OCP and 8.040 Å following the first delithiation (Figure 4.9a, cycle 1) of bare LMO. Figure 4.9b shows that the relative lattice parameter tracks with the relative charge closely for both the bare and Au-coated LMO samples. This shows that changes in lattice parameter reflect changes in the degree of lithiation each sample experiences. Based on the lower lithiated lattice constant and decreased charge, we conclude that Au-coated is less likely to be re-lithiated to the same extent as bare LMO due to the modified properties of the interface between LMO and the Au coating. To exclude the possibility of kinetic effects driving the observed charge difference between bare and Au-coated LMO at 50 $\mu V\ s^{-1}$ (ca. C/5.5), we applied the same approach to data collected at a slower scan rate of 25 $\mu V\ s^{-1}$ (ca. C/11) and found the difference negligible. However, we note that while the operando half-cell measurements suggest a decrease in capacity for Au-coated LMO that the coating is still effective in reducing Mn dissolution and enhances capacity retention in full cells, as shown when cycled against graphite anodes in our previous work.[15] Additionally, the selected diffraction patterns in Figure 4.11 show a tail on the LMO(111) peak during the first lithiation.

The tail indicates phase heterogeneity due to slower lithiation in the Au-coated LMO.[69] Figure 4.12 shows that the integrated area of the LMO (111) peak decreases with a trend similar to the charge during lithiation as well. We note, however, that this correlation is not maintained for delithiation of LMO (Figure 4.13); we suggest that during delithiation other processes are active, including SEI formation and Mn dissolution.

Table 4.2. Lattice parameters of Au-coated and bare LMO as shown in Figure 4.9a and 4b. The reported lattice parameters have been rounded to the accuracy of the 17-BM set-up. The calculated estimated standard deviations were generally calculated to 10^{-4}, and so these too have been rounded up to 1 x 10^{-3}. Cycle 0 refers to immediately before the first delithiation at 3.6 V.

Sample	Cycle number	Time, hr	Potential, V vs Li/Li^+	Lattice Parameter, Å
Lithiated Bare LMO	OCP	0.6722	3.120	8.241(1)
	0	3.3389	3.600	8.242(1)
	1	13.8389	3.510	8.215(1)
	2	24.9539	3.509	8.217(1)
	3	36.1111	3.501	8.209(1)
	4	47.2944	3.511	8.215(1)
	5	58.2611	3.509	8.206(1)
	6	69.4611	3.501	8.198(1)
Lithiated Au-coated LMO	OCP	0.6389	3.114	8.240(1)
	0	3.3056	3.594	8.239(1)
	1	13.9700	3.514	8.199(1)
	2	24.9150	3.516	8.183(1)
	3	36.0833	3.506	8.182(1)
	4	47.2555	3.504	8.190(1)
	5	58.4222	3.514	8.183(1)
	6	69.4222	3.506	8.184(1)
Delithiated Bare LMO	1	8.3389	4.500	8.041(1)
	2	19.5056	4.490	8.044(1)
	3	30.6222	4.489	8.044(1)
	4	41.6111	4.491	8.047(1)
	5	52.7611	4.499	8.046(1)
	6	63.9611	4.489	8.046(1)
Delithiated Au-coated LMO	1	8.3056	4.494	8.041(1)
	2	19.4722	4.496	8.055(1)
	3	30.4167	4.474	8.048(1)
	4	41.7555	4.486	8.050(1)
	5	52.7555	4.494	8.049(1)
	6	63.9222	4.496	8.051(1)

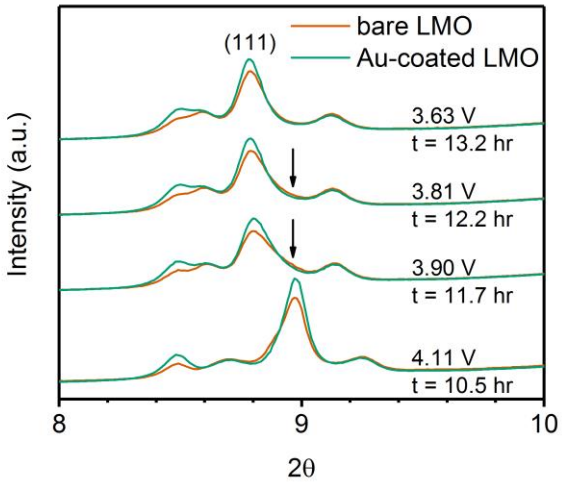

Figure 4.11. Selected diffraction patterns of bare and Au-coated LMO during the first lithiation at 50 μV/s. The arrows draw attention to a tail on the LMO(111) peak.

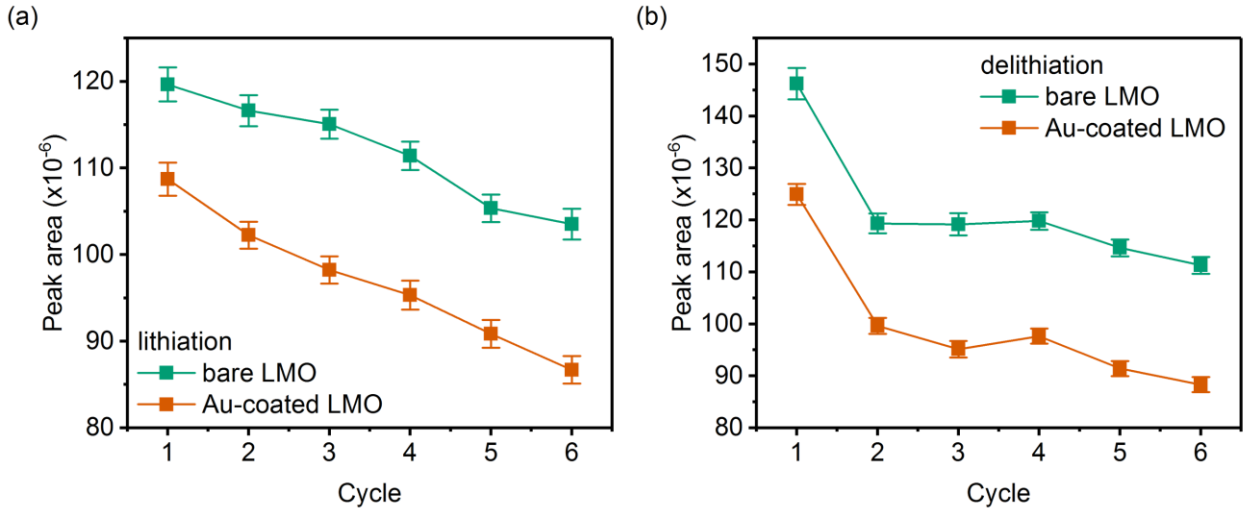

Figure 4.12. Gaussian fits of background subtracted (111) LMO peak of bare and Au-coated LMO after (a) lithiation and (b) delithiation.

DFT calculations are performed to further understand the nature of the LMO/Au interface at different lithium contents. To address this, we consider the delithiation of LMO(001) surfaces, with and without the Au coating, as discussed in the Methods section. Here, we apply a periodic model of the Au coating with two atomic layers in order to make the coated electrode computationally tractable to enable insights regarding the interface formed between LMO and the Au coating. We expect that a periodic model should sufficiently capture the effects of the Au coating, which deposits primarily as a film of ca. 3 nm in thickness with additional islands between 5 and 20 nm wide, sufficiently large in order to screen finite size effects in metal particles.[15,74–76]

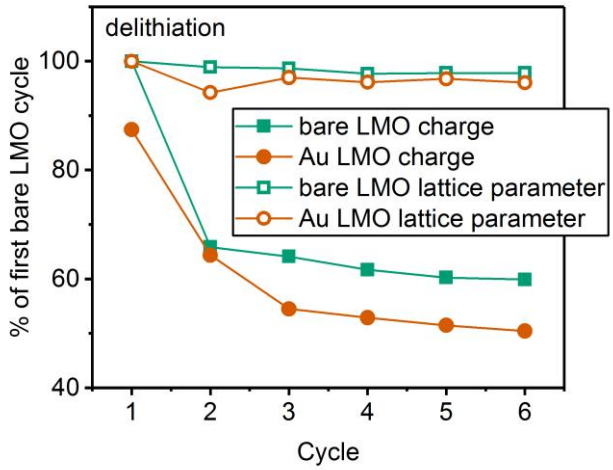

Figure 4.13. The relative lattice parameter and relative charge of each cycle compared to the initial bare LMO values after a full delithiation sweep for bare and Au-coated LMO. For this figure 100% of the lattice parameter is approximately 8.040(1) Å and any larger number is considered a decrease in percentage because the LMO material isn't fully delithiating and utilizing all available capacity.

Starting with a Li-terminated[50] LMO(001) surface, Li^+ are systematically removed from the near-surface region. Figure 4.14a and 4.14b show the most thermodynamically stable configurations at different Li^+ concentrations for bare and Au-coated LMO, respectively. The main difference between the Li^+ configurations of the bare and Au-coated LMO is that the Au coating appears to favor delithiation closer to the LMO/Au interface, whereas Li^+ removal from deeper into the sub-surface is thermodynamically favored for bare LMO. Figure 4.14c and 4.14d at 3.0 and 3.5 V, respectively, show the potential-dependent delithiation thermodynamics for both the bare and Au-coated LMO(001) surfaces, with voltage corrections applied by the formalism in Equation 4.1 (see Methods). The formation energies are reported with respect to the fully lithiated x = 1 phase, and are normalized by the fraction of Li^+ present per Mn_2O_4 formula unit in the near-surface region in which we allow our delithiation calculations to proceed. There are variations in the most thermodynamically favorable Li^+ configurations (filled symbols in Figure 4.14c and 4.14d) due to the effect of Au. Figure 4.14c and 4.14d show that the Au coating stabilizes more Li^+-deficient surfaces, with respect to the fully lithiated (x = 1 in the $Li_xMn_2O_4$ delithiation region of the slab model as shown in Figure 4.1) phase. Notably, we observe that there is a thermodynamic energy barrier against full re-lithiation of LMO back to x = 1 even at $\boldsymbol{U_{Li/Li^+}}$ = 3 V (Figure 4.14c). Moreover, the enhanced thermodynamic stability of Li^+-deficient surfaces in the presence of the

coating may suggest suppressed formation of the near surface $Li_2Mn_2O_4$ static Jahn-Teller tetragonal phase or other defect phases.[77] These trends are consistent with the decreased charge and Li^+ content for the Au-coated LMO (Figure 4.9b), although we note that these calculated near-surface effects cannot fully account for the extent of charge and Li^+ deficiency observed in experiment. These calculations do suggest, however, a general thermodynamic driving force for decreased Li^+ concentration in Au-coated LMO in comparison to bare LMO, an effect which is

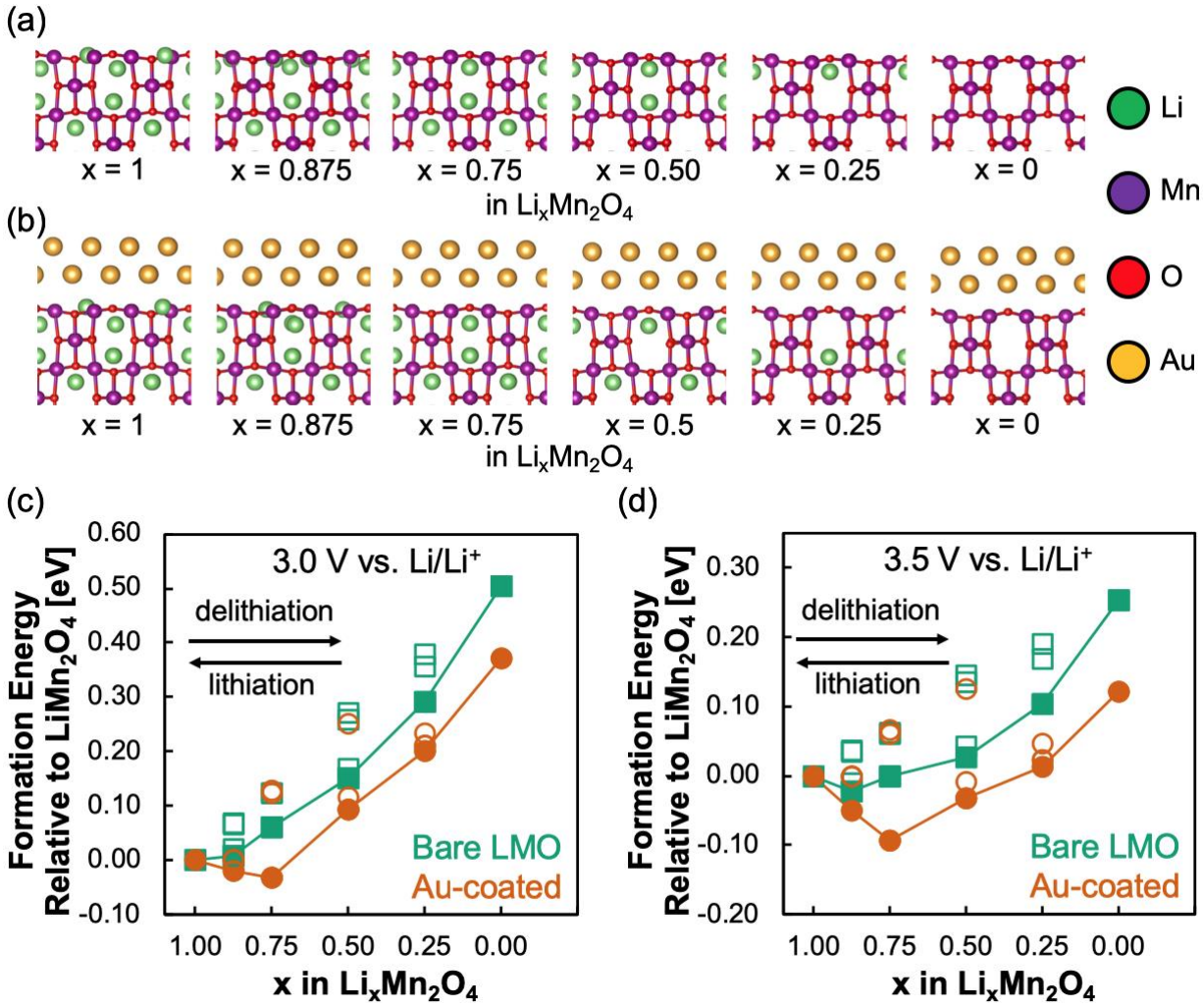

Figure 4.14. DFT-calculated thermodynamics for near surface lithiation and delithiation of bare and Au-coated LMO. Low-energy structures at different lithium contents for (a) bare and (b) Au-coated LMO(001) surfaces. The bottom of the slab is fixed, and (a-b) shows only atoms that are relaxed within the permitted lithium removal region. The stoichiometries presented correspond only to the near-surface region in which delithiation is allowed to occur in the calculations, such that the *x*-values correspond to fractional lithium content with respect to $LiMn_2O_4$ stoichiometry. A legend of the different atoms types is presented to the right of (a) and (b). Relative energies of bare (teal) and Au-coated (orange) LMO at (c) 3.0 V and (d) 3.5 V vs. Li/Li^+. The filled in shapes represent the most thermodynamically stable configuration for a given stoichiometry, whose structures are represented in (a-b) and are connected by solid lines, whereas metastable lithium configurations are represented by unfilled shapes.

evident from the significant decrease in lattice constant for the lithiated LMO phase seen in Figure 4.9a. Analogous plots for lithiation/delithiation thermodynamics at higher potentials can be found in Figure 4.15. We also obtain similar thermodynamic results using three- and four-layer Au films, the results of which can be found in Figure 4.16.

Figure 4.17 shows the projected density of states (PDOS) and projected crystal orbital Hamilton populations (pCOHP) of near-surface electronic states for the bare (Figure 4.17a and 4.17b) and Au-coated (Figure 4.17c and 4.17d) LMO(001) surfaces. In each of these plots, the Fermi energy (E_f) is set to the valence band maximum (VBM). In Figure 4.17, the DOS projections are on a surface Mn ion (other topmost layer Mn ions are related by symmetry), the five O ions to

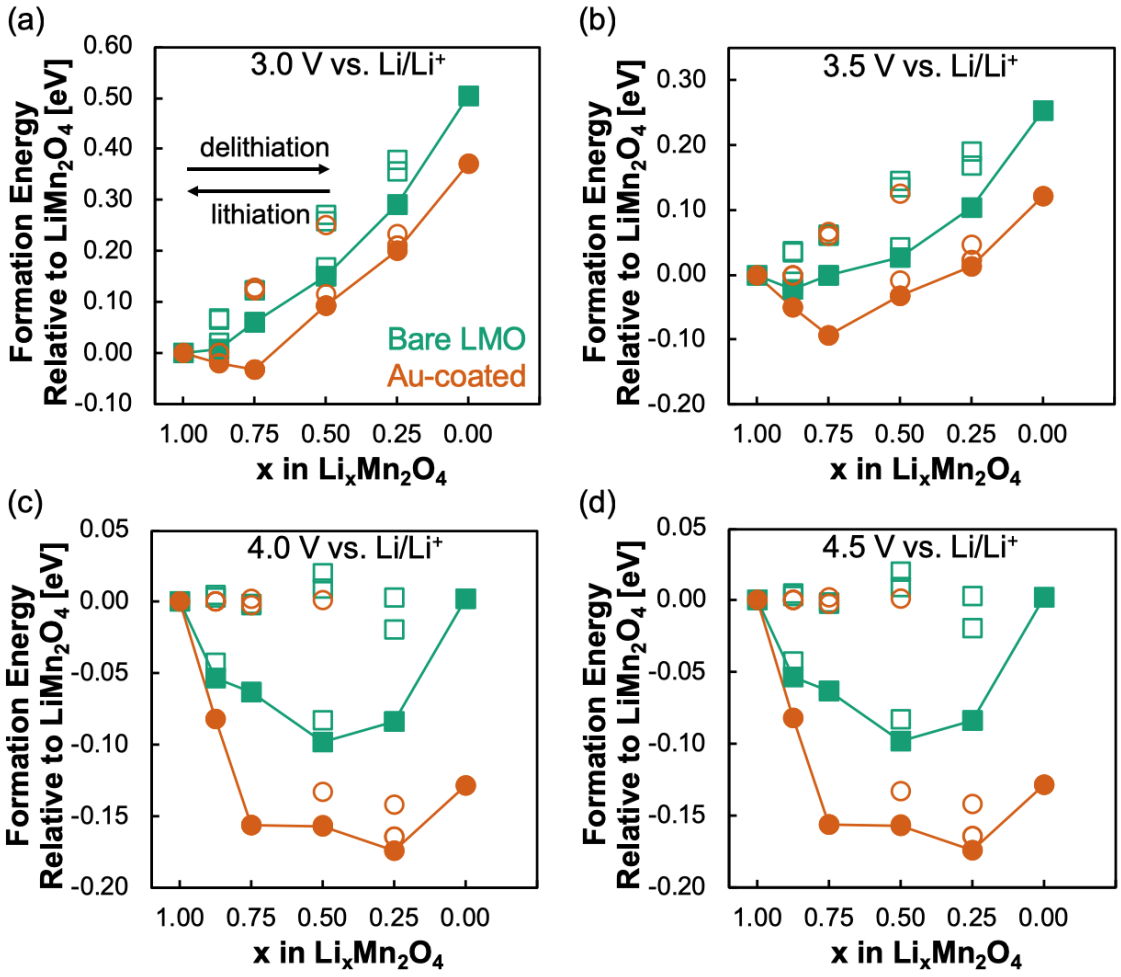

Figure 4.15. Relative energies of bare (teal) and Au-coated (orange) LMO at (a) 3.0 V, (b) 3.5 V, (c) 4.0 V, and (d), 4.5 V vs. Li/Li$^+$. The filled in shapes represent the most thermodynamically stable configuration for a given stoichiometry, whose structures are represented in Figures 5a and 5b of the main text, and are connected by solid lines, whereas metastable lithium configurations are represented by unfilled shapes.

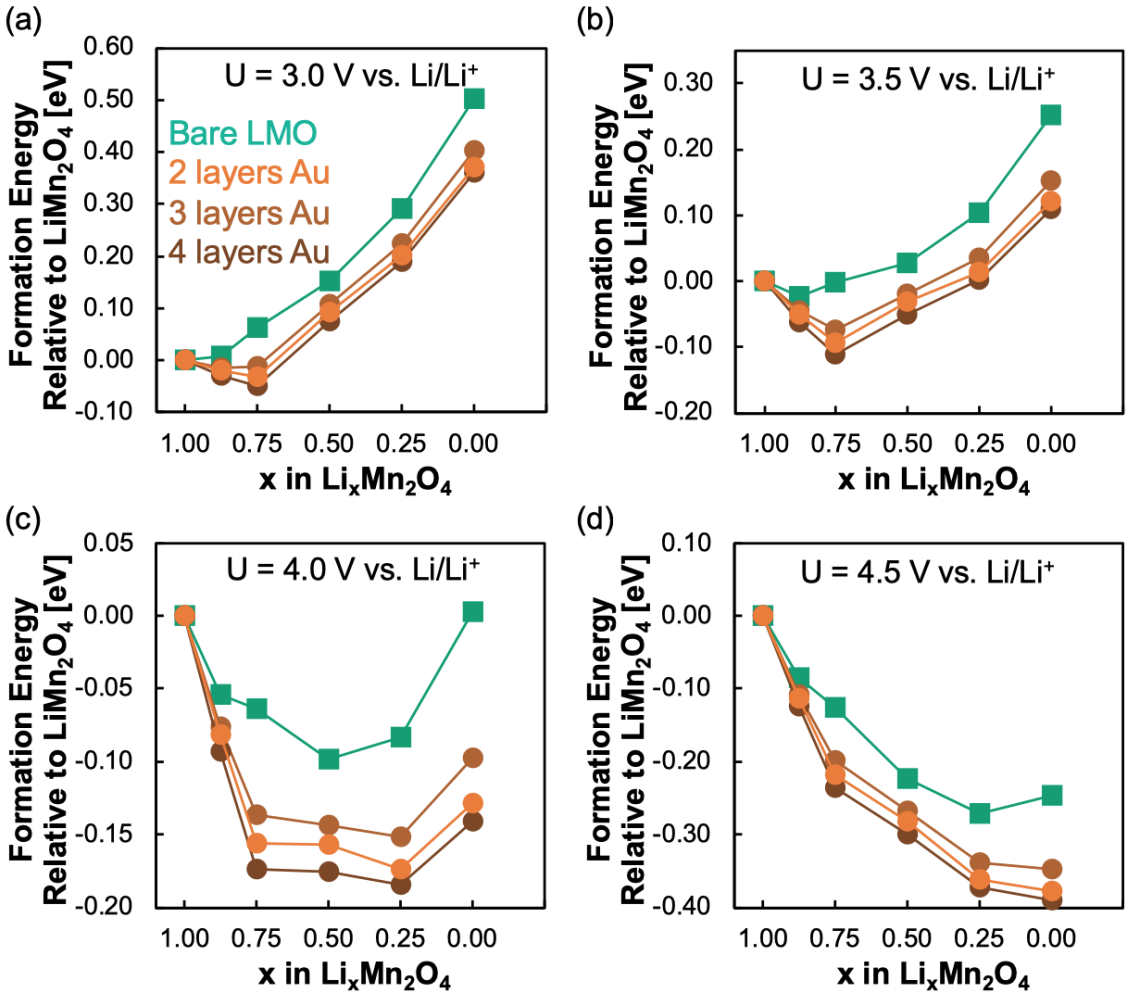

Figure 4.16. Relative energies of bare (teal) and Au-coated (orange) LMO with different Au layer thicknesses (different shades of orange, as labeled in (a)) at (a) 3.0 V, (b) 3.5 V, (c) 4.0 V, and (d) 4.5 V vs. Li/Li^+. The data points represent the most thermodynamically stable configuration for a given stoichiometry.

which it is coordinated, and the Au atoms in the film. pCOHP pairs are considered to analyze crystal orbital hybridization of Mn-O and Au-O states. Figure 4.17a and 4.17b show the PDOS and pCOHP of bare LMO upon delithiation from x = 1 (Figure 4.17a) to x = 0.75 (Figure 4.17b). Upon Li^+ removal, electron depletion causes the E_f to move lower into Mn states, which become oxidized. Figure 4.17b illustrates the shift of some Mn states of the x = 0.75 phase above the E_f (marked by *), in comparison to the PDOS of the x = 1 phase in Figure 4.17a. In this case, the hole is partially shared between two surface Mn ions, perhaps due to strain imposed by the fixed lattice constant. The states which shift above the Fermi level upon Li^+ removal are associated with Mn-O anti- or non-bonding states according to the pCOHP calculations (Figure 4.17b marked by *). The pCOHP calculations for bare LMO are in good agreement with previous work, showing the

anti-bonding Mn-O nature of valence states directly below E_f, whereas Mn-O bonding states occur at lower energies.[78]

Figure 4.17c and 4.17d show the PDOS and pCOHP analysis for the Au-coated LMO(001) surface. Contrary to trends observed for bare LMO in Figure 4.17a and 4.17b, Li^+ removal from x = 1 (Figure 4.17c) to x = 0.75 (Figure 4.17d) shifts neither the Mn-O anti-bonding states above the Fermi level, based on Mn PDOS, nor the corresponding Mn-O pCOHP between the two states of

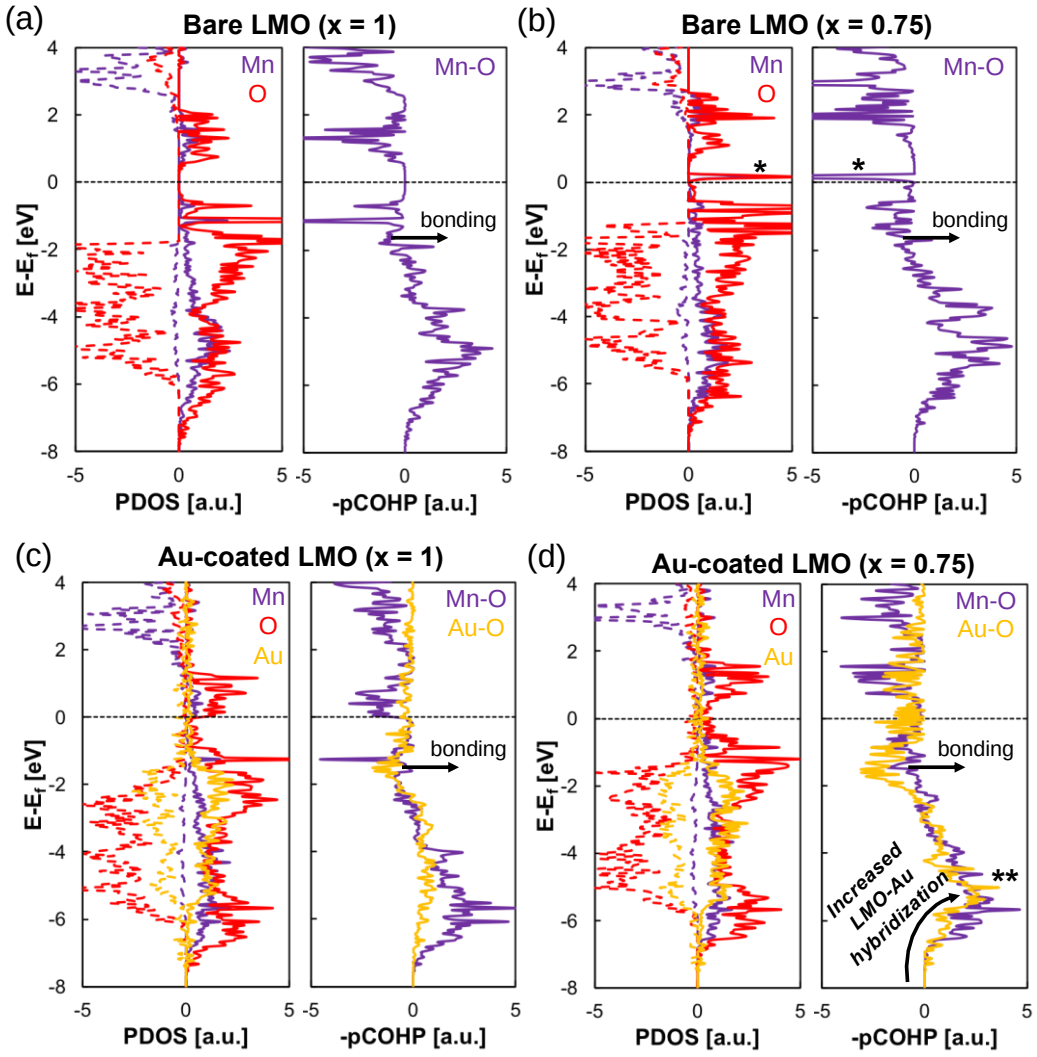

Figure 4.17. (a-d) Atom projected density of states (PDOS) and projected crystal orbital Hamilton population (pCOHP) analysis of surface Mn-O and Au-O bonds for bare $Li_xMn_2O_4$ at (a) x = 1 and (b) x = 0.75, as well as Au-coated LMO at (c) x = 1 and (d) x = 0.75. The Fermi level (E_f) is denoted by the dashed black line in each plot. In the PDOS plots, positive PDOS values (solid lines) correspond to the majority spin channel, whereas negative PDOS values (dashed lines) correspond to the minority spin channel. In the pCOHP plots, positive values along the -pCOHP axis correspond to bonding states, as shown by the horizontal arrows on the plots, whereas negative values correspond to states that are associated with either anti- or non-bonding orbitals.

charge. These observations suggest a lack of charge neutrality between the electronic states of Li, Mn, and O alone. Instead, the pCOHP analysis in Figure 4.17d shows Au-O anti-bonding states around the Fermi level. This suggests that Li^+ removal is associated with partial oxidation of Au, rather than isolated oxidation at the Mn centers as seen in the bare LMO. Moreover, the Au-O pCOHP is comparatively flat at x = 1 (Figure 4.17c), indicating minimal hybridization between Au and O orbitals. However, upon delithiation to x = 0.75 the pCOHP analysis (Figure 4.17d) describes Au-O bonding states at low energies (centered ca. -5 eV below E_f and marked by **) as well as anti-bonding hybridization character directly below E_f. The low energy of the Au-O bonding states with respect to the Fermi level suggests strong binding between Au and LMO upon Li^+ removal, stabilizing a Li^+-deficient region near the LMO/Au interface. This observation is consistent with the relevant thermodynamic stability of these configurations shown in Figure 4.14c and 4.14d, where we can further attribute the thermodynamic driving forces for decreased Li^+ content in lithiated LMO to the partial oxidation of the Au coating as it interacts with Li^+-deficient LMO surfaces.

To further investigate the surface redox process upon Li^+ removal from Au-coated LMO, we perform a charge density difference analysis to determine the nature of charge transfer between the LMO surface and the Au coating. Figure 4.18a shows the planar-averaged charge transfer between the composite LMO/Au interfacial system with respect to its isolated components, determined using the DFT-calculated charge densities (ρ).

$$\boldsymbol{charge\ transfer} = \boldsymbol{\rho_{LMO/Au} - (\rho_{LMO} + \rho_{Au})} \tag{4.2}$$

In Equation 4.2 and Figure 4.18a, a positive value of the charge transfer corresponds to an increase in electron density, or rather, a buildup of negative charge. Figure 4.18a shows a planar-averaged cross-section of this data for the Au-coated x = 0.75 phase to demonstrate charge transfer normal to the LMO/Au interface. Figure 4.18b shows the integrated charge density difference to illustrate the magnitude of negative and positive charge buildup on LMO and the Au film, respectively. The integrated charge density in Figure 4.18b is determined from integration of the charge transfer (Equation 4.2) from the fixed end of the LMO slab to the vacuum region. The formation of the interface with Au leads to an increase in electron density in the LMO near-surface region, suggesting that the Au film must be partially oxidized to satisfy charge neutrality. We also observe a deviation in the average Mn magnetic moment of the system between bare and Au-coated LMO (Figure 4.19). More specifically, the average Mn magnetic moment is consistently

higher in the Au-coated LMO surface than that of bare LMO, suggesting a lower average oxidation state for Au-coated LMO since lower-valence Mn ions have more unpaired 3d electrons. These interpretations are consistent with the PDOS and pCOHP analyses of Au-coated LMO in Figure 4.17c and 4.17d. These findings further suggest a potential energy driving force for LMO

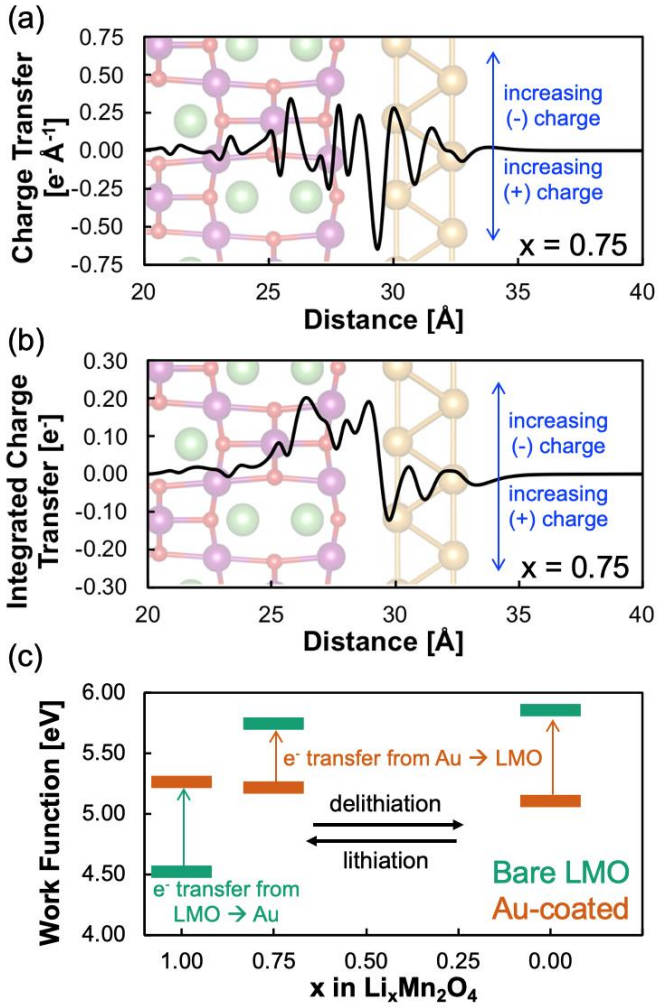

Figure 4.18. Charge transfer and work function shifts from LMO/Au interface formation. (a-b) Charge transfer between Au and LMO(001) surface with x = 0.75 lithium content, including (a) planar-averaged charge density difference between Au-coated and bare LMO and (b) integrated charge transfer between LMO and Au, starting from the fixed end of the LMO slab up to the vacuum. Positive charge transfer in (a) and (b) refers to an increase in electron density, or, negative charge accumulation. Further details regarding these calculations are provided in the main text. (c) Work functions of the most thermodynamically stable x = 1, x = 0.75, and x = 0 surfaces for the bare (teal) and Au-coated (orange) LMO(001) surfaces. The colored arrows in (c) represent the average electron transfer direction when LMO is brought into contact with the Au film. For example, when the Au-coated LMO work function is lower than bare LMO, as it is for stable surfaces ($x \leq 0.75$), the Fermi level is higher in energy, which suggests an electron accumulation in the LMO near-surface and electron depletion in Au is needed to satisfy charge neutrality. This is consistent with the charge density calculations in (a-b).

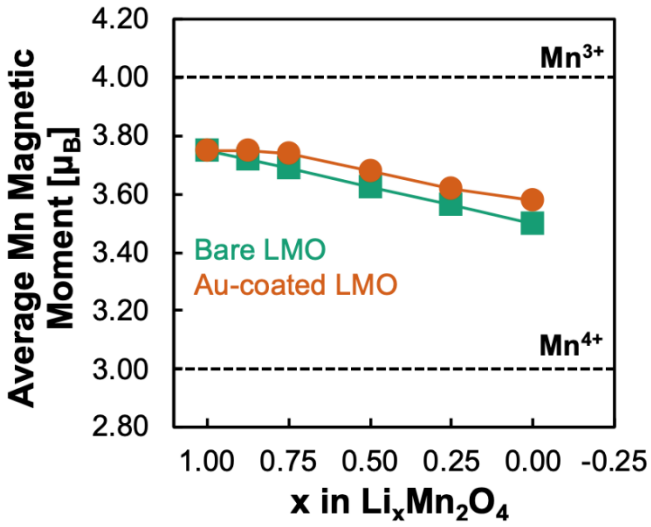

Figure 4.19. Average Mn oxidation states for bare (teal) and Au-coated (orange) LMO as a function of Li^+ content. The dashed lines correspond to the magnetic moment reference for Mn^{3+} (which has four unpaired 3d electrons) and Mn^{4+} (which has three unpaired electrons).

conduction states to become populated upon contact with the Au coating, which would seemingly be in competition upon lithiation with incoming ($Li^+ + e^-$) pairs which require empty conduction states for intercalation to occur.

Although the thermodynamics (Figure 4.14), chemical bonding analysis (Figure 4.17), and electrode-coating charge transfer (Figure 4.18a and 4.18b) calculations all provide an explanation for a Li^+-deficient near-surface, they do not fully explain how this could lead to a measurable change in the bulk Li^+ content and lattice parameter as determined from the XRD lattice parameter refinement (Figure 4.9). Thus, we address these interfacial electronic structure effects and consider how they may influence the bulk properties of Au-coated LMO. While the individual Fermi levels of isolated LMO and Au are different, the composite system E_f is pinned when they are brought into contact. This will force the valence and conduction bands of LMO to bend to adjust to the E_f of the composite system. The direction and extent to which the band bending occurs will be driven by the relative work function between bare LMO and the Au coating to determine driving forces for electron transfer, which may protrude further into the bulk of the LMO electrode.

Figure 4.18c shows how the work function (ϕ) of the LMO surface varies between the bare and Au-coated LMO surfaces. Full electrostatic potentials, as well as the electrostatic potential differences between bare and Au-coated LMO, are included in Figure 4.20. The bare and Au-coated LMO ϕ values are estimated at different states of charge (refer to Figure 4.14c-d for relevant

potential ranges for each surface) by the potential energy difference between the vacuum level and E_f. As in the PDOS/pCOHP analysis in Figure 4.17, the E_f is set to the VBM in this analysis. While the exact position of E_f between the VBM and the conduction band minimum (CBM) cannot be directly identified for a surface model without rigorous quantification of bulk intrinsic defect levels, we expect that Li^+ vacancies are the dominant defect that determine E_f during delithiation, justifying its positioning at the VBM. Moreover, we further emphasize that this approach should sufficiently enable trend-based analyses of charge transfer processes at the LMO/Au interface. Compared to the bare LMO, the Au-coated LMO has a lower overall ϕ at both the x = 0.75 and x = 0 states of charge. While the x = 1 phase shows the opposite trend, we note that this state of charge is unlikely to exist in the presence of the Au coating based on our thermodynamic calculations shown in Figure 4.14c and 4.14d. This trend is consistent with the formation of a metal-semiconductor junction, wherein $\phi_{Au} < \phi_{LMO}$, and electrons are transferred from Au to LMO

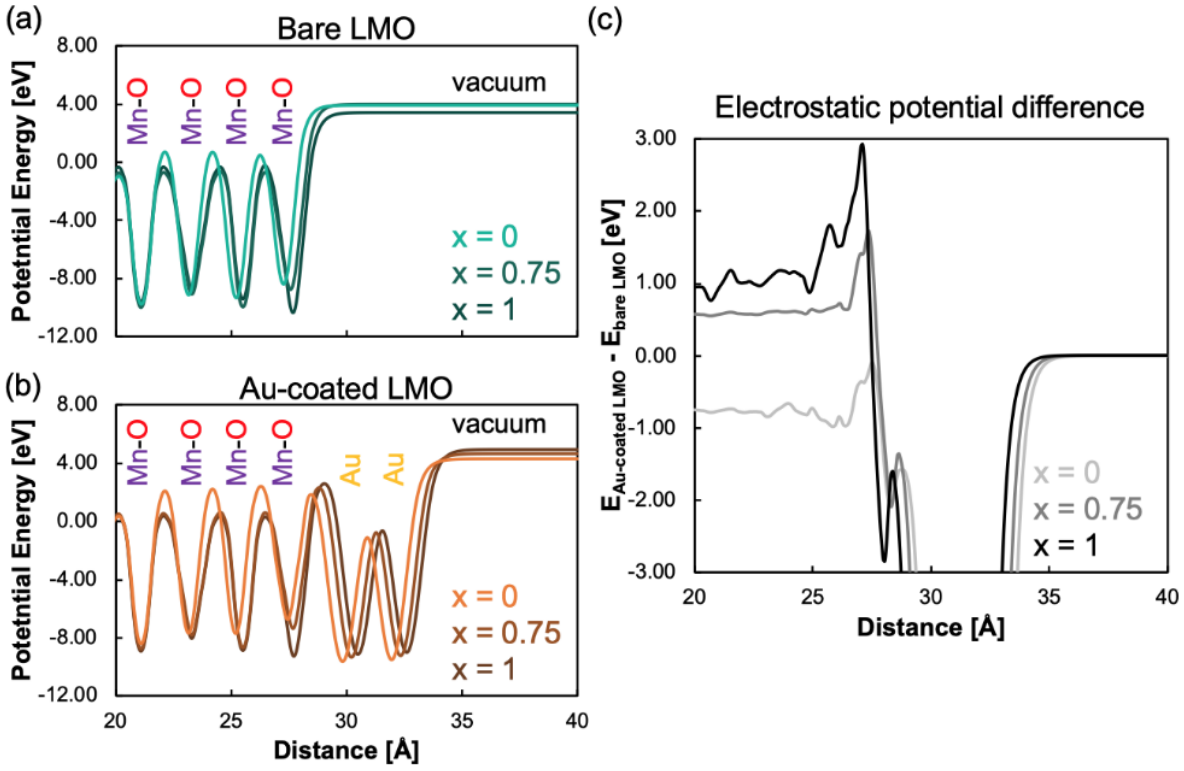

Figure 4.20. Electrostatic potentials for (a) bare and (b) Au-coated LMO for x = 0, 0.75, and 1 in $Li_xMn_2O_4$. The vacuum level is used to determine work functions plotted in Figure 4.21 of the main text. (c) Difference in the electrostatic potential between Au-coated and bare LMO, each normalized to the vacuum level, which is equivalent in all six systems by definition. The negative end of the plot is cut off to focus on the electrostatic potential differences between the Mn-O layers of the bare and Au-coated LMO, as labeled in (a) and (b). We note that oscillations in the difference function may also be partially due to slight geometric differences in the relaxed bare and Au-coated structures for a given Li^+ content.

due to Fermi level pinning between LMO and Au. The downward band-bending of LMO conduction states in a near-interface electron accumulation region could, in principle, propagate below the surface on the scale of nanometers.[79] As the delithiation calculations (Figure 4.14c-d) suggest, the electronic population of LMO conduction states may make lithiation less favorable for the Au-coated surfaces since these electrochemical reactions require a (Li^+ + e^-) pair for insertion.

4.4 Conclusion

Figure 4.21 demonstrates the proposed effect of the Au coating, where the Li^+-deficient near-surface region leads to an overall decrease in bulk Li^+ concentration as suggested by a decrease in the observed lattice parameter and overall charge transferred to Au-coated LMO. The Li^+-deficient region near the LMO/Au interface– stabilized by a strong interaction and

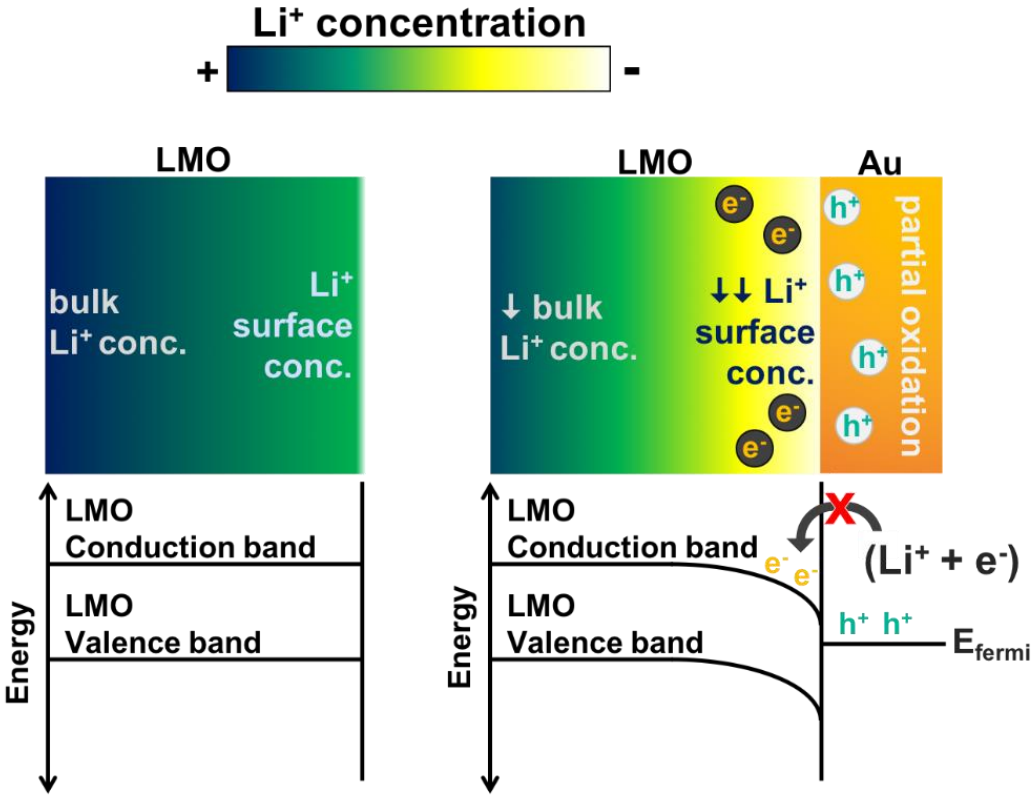

Figure 4.21. Influence of Au coating on LMO electrochemistry. The difference in work function between LMO and Au in Au-coated LMO leads to the near-surface accumulation of electrons. This effect also results in partial oxidation of the Au coating near the interface and inhibited reaction of (Li^+ + e^-) pairs, leading to an overall reduction in Li^+ concentration in Au-coated LMO as compared to bare LMO. This change in the near-surface solubility limit may reduce the bulk Li^+ concentration due to reduced concentration gradients in LMO particles.

hybridization between Au and O orbitals– likely leads to an electron accumulation region hindering full lithiation upon discharge.

The region of electron accumulation from the downward bending of LMO conduction states near the metal-semiconductor junction may only protrude into the bulk at the nanometer scale, which would not directly account for the experimentally observed changes in lattice parameter. This interfacial effect, however, could present a kinetic challenge to Li^+ proceeding into the LMO bulk due to a lower Li^+ concentration boundary condition at the surface.[80] Li^+ transport upon lithiation is governed by Fickian diffusion, wherein the driving forces are primarily the surface-to-bulk concentration gradients, in the absence of a significant intraparticle potential gradient: $J_{Li} = -D\nabla c_{Li}$. This effect, depicted in Figure 4.21, inhibits bulk lithiation up to the concentration of stoichiometric $LiMn_2O_4$, leading to the reduction in electrode lattice parameter and capacity (Figure 4.14).

The findings in this work on a model Au-coated LMO system suggest that, while protective coatings may be effective in suppressing transition metal dissolution from Li-ion battery cathodes,[15] interfacial potential energy effects may limit the Li^+ solubility in the near-surface. Future coatings, conductive or not, will need to balance these potential energy effects with other well-established coating design parameters, such as ionic/electrical conductivity and chemical reactivity with compounds in the organic electrolyte. Additionally, our findings suggest that extensive experimental and theoretical investigations of solid-solid interfaces in Li-ion batteries are necessary in order to tune the performance of the interfaces between electrodes and protective coatings, as well as those between electrodes and solid electrolytes.

4.5 References

(1) Thackeray, M. M.; Wolverton, C.; Isaacs, E. D. *Energy Environ. Sci.* **2012**, *5*, 7854.

(2) Whittingham, M. S. *Chem. Rev.* **2004**, *104*, 4271.

(3) Dai, Y.; Cai, L.; White, R. E. *J. Electrochem. Soc.* **2013**, *160*, A182.

(4) Gummow, R. J.; de Kock, A.; Thackeray, M. M. *Solid State Ionics* **1994**, *69*, 59.

(5) Thackeray, M. M.; Shao-Horn, Y.; Kahaian, A. J.; Kepler, K. D.; Skinner, E.; Vaughey, J. T.; Hackney, S. A. *Electrochem. Solid-State Lett.* **1998**, *1*, 7.

(6) He, X.; Li, J.; Cai, Y.; Wang, Y.; Ying, J.; Jiang, C.; Wan, C. *J. Power Sources* **2005**, *150*, 216.

(7) Lu, J.; Zhan, C.; Wu, T.; Wen, J.; Lei, Y.; Kropf, A. J.; Wu, H.; Miller, D. J.; Elam, J. W.; Sun, Y.-K.; Qiu, X.; Amine, K. *Nat. Commun.* **2014**, *5*, 5693.

(8) Wang, G. X.; Bradhurst, D. H.; Liu, H. K.; Dou, S. X. *Solid State Ionics* **1999**, *120*, 95.

(9) Li, C.; Zhang, H. P.; Fu, L. J.; Liu, H.; Wu, Y. P.; Rahm, E.; Holze, R.; Wu, H. Q. *Electrochim. Acta* **2006**, *51*, 3872.

(10) Jaber-Ansari, L.; Puntambekar, K. P.; Kim, S.; Aykol, M.; Luo, L.; Wu, J.; Myers, B. D.; Iddir, H.; Russell, J. T.; Saldaña, S. J.; Kumar, R.; Thackeray, M. M.; Curtiss, L. A.; Dravid, V. P.; Wolverton, C.; Hersam, M. C. *Adv. Energy Mater.* **2015**, *5*, 1500646.

(11) Son, J. T.; Park, K. S.; Kim, H. G.; Chung, H. T. *J. Power Sources* **2004**, *126*, 182.

(12) Kim, J.-S.; Johnson, C. S.; Vaughey, J. T.; Hackney, S. A.; Walz, K. A.; Zeltner, W. A.; Anderson, M. A.; Thackeray, M. M. *J. Electrochem. Soc.* **2004**, *151*, A1755.

(13) Ha, H.-W.; Yun, N. J.; Kim, K. *Electrochim. Acta* **2007**, *52*, 3236.

(14) Chen, Q.; Wang, Y.; Zhang, T.; Yin, W.; Yang, J.; Wang, X. *Electrochim. Acta* **2012**, *83*, 65.

(15) Esbenshade, J. L.; Fox, M. D.; Gewirth, A. A. *J. Electrochem. Soc.* **2014**, *162*, A26.

(16) Mahmood, N.; Hou, Y. *Adv. Sci.* **2014**, *1*, 1400012.

(17) Aykol, M.; Kirklin, S.; Wolverton, C. *Adv. Energy Mater.* **2014**, *4*, 1400690.

(18) Aykol, M.; Kim, S.; Hegde, V. I.; Snydacker, D.; Lu, Z.; Hao, S.; Kirklin, S.; Morgan, D.; Wolverton, C. *Nat. Commun.* **2016**, *7*, 13779.

(19) Trabelsi, S. K.; Tahar, N. B.; Trabelsi, B.; Abdelhedi, R. *J. Appl. Electrochem.* **2005**, *35*, 967.

(20) Tu, J.; Zhao, X. B.; Cao, G. S.; Zhuang, D. G.; Zhu, T. J.; Tu, J. P. *Electrochim. Acta* **2006**, *51*, 6456.

(21) Liu, D.; Liu, X.; He, Z. *J. Alloys Compd.* **2007**, *436*, 387.

(22) Lee, S.-W.; Kim, K.-S.; Lee, K.-L.; Moon, H.-S.; Kim, H.-J.; Cho, B.-W.; Cho, W.-I.; Park, J.-W. *J. Power Sources* **2004**, *130*, 233.

(23) Hwang, B. J.; Santhanam, R.; Huang, C. P.; Tsai, Y. W.; Lee, J. F. *J. Electrochem. Soc.* **2002**, *149*, A694.

(24) Park, S.-C.; Han, Y.-S.; Kang, Y.-S.; Lee, P. S.; Ahn, S.; Lee, H.-M.; Lee, J.-Y. *J. Electrochem. Soc.* **2001**, *148*, A680.

(25) Cho, J.; Kim, T.-J.; Kim, Y. J.; Park, B. *Chem. Commun.* **2001**, *0*, 1074.

(26) Chan, H.-W.; Duh, J.-G.; Sheu, H.-S. *J. Electrochem. Soc.* **2006**, *153*, A1533.

(27) Lee, J.-W.; Park, S.-M.; Kim, H.-J. *Electrochem. commun.* **2009**, *11*, 1101.

(28) Kim, C.-S.; Kwon, S.-H.; Yoon, J.-W. *J. Alloys Compd.* **2014**, *586*, 574.

(29) Tu, J.; Zhao, X. B.; Xie, J.; Cao, G. S.; Zhuang, D. G.; Zhu, T. J.; Tu, J. P. *J. Alloys Compd.* **2007**, *432*, 313.

(30) Sun, Y.-K.; Hong, K.-J.; Prakash, J. *J. Electrochem. Soc.* **2003**, *150*, A970.

(31) Xiong, L.; Xu, Y.; Tao, T.; Du, X.; Li, J. *J. Mater. Chem.* **2011**, *21*, 4937.

(32) Kannan, A. M.; Manthiram, A. *Electrochem. Solid-State Lett.* **2002**, *5*, A167.

(33) Lin, Y.-M.; Wu, H.-C.; Yen, Y.-C.; Guo, Z.-Z.; Yang, M.-H.; Chen, H.-M.; Sheu, H.-S.; Wu, N.-L. *J. Electrochem. Soc.* **2005**, *152*, A1526.

(34) Lee, S.-W.; Kim, K.-S.; Moon, H.-S.; Lee, J.-P.; Kim, H.-J.; Cho, B.-W.; Cho, W.-I.; Park, J.-W. *J. Power Sources* **2004**, *130*, 227.

(35) Leung, K.; Qi, Y.; Zavadil, K. R.; Jung, Y. S.; Dillon, A. C.; Cavanagh, A. S.; Lee, S.-H.; George, S. M. *J. Am. Chem. Soc.* **2011**, *133*, 14741.

(36) Tebbe, J. L.; Holder, A. M.; Musgrave, C. B. *ACS Appl. Mater. Interfaces* **2015**, *7*, 24265.

(37) Chen, L.; Warburton, R. E.; Chen, K.-S.; Libera, J. A.; Johnson, C.; Yang, Z.; Hersam, M. C.; Greeley, J. P.; Elam, J. W. *Chem* **2018**, *4*, 2418.

(38) Borkiewicz, O. J.; Shyam, B.; Wiaderek, K. M.; Kurtz, C.; Chupas, P. J.; Chapman, K. W. *J. Appl. Crystallogr.* **2012**, *45*, 1261.

(39) Toby, B. H.; Dreele, R. B. Von. *J. Appl. Crystallogr.* **2013**, *46*, 544.

(40) Toby, B. H. *Powder Diffr.* **2006**, *21*, 67.

(41) Kresse, G.; Furthmüller, J. *Comput. Mater. Sci.* **1996**, *6*, 15.

(42) Kresse, G.; Hafner, J. *Phys. Rev. B* **1993**, *47*, 558.

(43) Kresse, G.; Furthmüller, J. *Phys. Rev. B* **1996**, *54*, 11169.

(44) Blöchl, P. E. *Phys. Rev. B* **1994**, *50*, 17953.

(45) Kresse, G.; Joubert, D. *Phys. Rev. B* **1999**, *59*, 1758.

(46) Perdew, J. P.; Burke, K.; Ernzerhof, M. *Phys. Rev. Lett.* **1996**, *77*, 3865.

(47) Anisimov, V. I.; Zaanen, J.; Andersen, O. K. *Phys. Rev. B* **1991**, *44*, 943.

(48) Anisimov, V. I.; Solovyev, I. V.; Korotin, M. A.; Czyżyk, M. T.; Sawatzky, G. A. *Phys. Rev. B* **1993**, *48*, 16929.

(49) Liechtenstein, A. I.; Anisimov, V. I.; Zaanen, J. *Phys. Rev. B* **1995**, *52*, R5467.

(50) Warburton, R. E.; Iddir, H.; Curtiss, L. A.; Greeley, J. *ACS Appl. Mater. Interfaces* **2016**, *8*, 11108.

(51) Chan, M. K. Y.; Long, B. R.; Gewirth, A. A.; Greeley, J. P. *J. Phys. Chem. Lett.* **2011**, *2*, 3092.

(52) Long, B. R.; Chan, M. K. Y.; Greeley, J. P.; Gewirth, A. A. *J. Phys. Chem. C* **2011**, *115*, 18916.

(53) Chan, M. K. Y.; Wolverton, C.; Greeley, J. P. *J. Am. Chem. Soc.* **2012**, *134*, 14362.

(54) Dronskowski, R.; Bloechl, P. E. *J. Phys. Chem.* **1993**, *97*, 8617.

(55) Deringer, V. L.; Tchougréeff, A. L.; Dronskowski, R. *J. Phys. Chem. A* **2011**, *115*, 5461.

(56) Maintz, S.; Deringer, V. L.; Tchougréeff, A. L.; Dronskowski, R. *J. Comput. Chem.* **2013**, *34*, 2557.

(57) Maintz, S.; Esser, M.; Dronskowski, R. *Acta Phys. Pol. B* **2016**, *47*, 1165.

(58) Maintz, S.; Deringer, V. L.; Tchougréeff, A. L.; Dronskowski, R. *J. Comput. Chem.* **2016**, *37*, 1030.

(59) Sun, X.; Yang, X. Q.; Balasubramanian, M.; McBreen, J.; Xia, Y.; Sakai, T. *J. Electrochem. Soc.* **2002**, *149*, A842.

(60) Vetter, J.; Novák, P.; Wagner, M. R.; Veit, C.; Möller, K.-C.; Besenhard, J. O.; Winter, M.; Wohlfahrt-Mehrens, M.; Vogler, C.; Hammouche, A. *J. Power Sources* **2005**, *147*, 269.

(61) Arora, P.; White, R. E.; Doyle, M. *J. Electrochem. Soc.* **1998**, *145*, 3647.

(62) Tang, C.-Y.; Ma, Y.; Haasch, R. T.; Ouyang, J.-H.; Dillon, S. J. *J. Phys. Chem. Lett.* **2017**, *8*, 6226.

(63) Wang, L.-F.; Fang, B.-J.; Chen, J.-S. *J. Power Sources* **2005**, *150*, 1.

(64) Balluffi, R. W.; Allen, S. M.; Carter, W. C. *Kinetics of Materials*; John Wiley & Sons, Inc.: Hoboken, New Jersey, 2005.

(65) Thackeray, M. M. *Prog. Solid State Chem.* **1997**, *25*, 1.

(66) Akimoto, J.; Takahashi, Y.; Gotoh, Y.; Mizuta, S. *J. Cryst. Growth* **2001**, *229*, 405.

(67) Akimoto, J.; Takahashi, Y.; Gotoh, Y.; Mizuta, S. *Chem. Mater.* **2000**, *12*, 3246.

(68) Lee, Y. J.; Wang, F.; Mukerjee, S.; McBreen, J.; Grey, C. P. *J. Electrochem. Soc.* **2000**, *147*, 803.

(69) Grenier, A.; Liu, H.; Wiaderek, K. M.; Lebens-Higgins, Z. W.; Borkiewicz, O. J.; Piper,

L. F. J.; Chupas, P. J.; Chapman, K. W. *Chem. Mater.* **2017**, *29*, 7345.

(70) Tavassol, H.; Chan, M. K. Y.; Catarello, M. G.; Greeley, J.; Cahill, D. G.; Gewirth, A. A. *J. Electrochem. Soc.* **2013**, *160*, A888.

(71) Thackeray, M. M.; Kock, A. de; Rossouw, M. H.; Liles, D.; Bittihn, R.; Hoge, D. *J. Electrochem. Soc.* **1992**, *139*, 363.

(72) *Powder Diffraction: Theory and Practice*; Dinnebier, R. E.; Billinge, S. J. L., Eds.; Royal Society of Chemistry: Cambridge, 2008.

(73) Shi, F.; Pei, A.; Vailionis, A.; Xie, J.; Liu, B.; Zhao, J.; Gong, Y.; Cui, Y. *Proc. Natl. Acad. Sci.* **2017**, *114*, 12138.

(74) Kleis, J.; Greeley, J.; Romero, N. A.; Morozov, V. A.; Falsig, H.; Larsen, A. H.; Lu, J.; Mortensen, J. J.; Dułak, M.; Thygesen, K. S.; Nørskov, J. K.; Jacobsen, K. W. *Catal. Letters* **2011**, *141*, 1067.

(75) Li, L.; Larsen, A. H.; Romero, N. A.; Morozov, V. A.; Glinsvad, C.; Abild-Pedersen, F.; Greeley, J.; Jacobsen, K. W.; Nørskov, J. K. *J. Phys. Chem. Lett.* **2013**, *4*, 222.

(76) Mistry, H.; Reske, R.; Zeng, Z.; Zhao, Z.-J.; Greeley, J.; Strasser, P.; Cuenya, B. R. *J. Am. Chem. Soc.* **2014**, *136*, 16473.

(77) Ben, L.; Yu, H.; Chen, B.; Chen, Y.; Gong, Y.; Yang, X.; Gu, L.; Huang, X. *ACS Appl. Mater. Interfaces* **2017**, *9*, 35463.

(78) Lee, Y. K.; Park, J.; Lu, W. *J. Electrochem. Soc.* **2016**, *163*, A1359.

(79) Zhang, Z.; Yates, J. T. *Chem. Rev.* **2012**, *112*, 5520.

(80) Van der Ven, A.; Bhattacharya, J.; Belak, A. A. *Acc. Chem. Res.* **2013**, *46*, 1216.

Appendix A: Operando X-ray Tomography of Li-Ion Solid Electrolytes

A.1 Introduction

Solid-electrolytes (SE) are a potential replacement for traditional Li-ion liquid electrolytes. SE are non-flammable and might allow for the use of higher energy density Li anodes in place of the traditional graphite anodes first commercialized by Sony in 1991.[1] Although many improvements to SE conductivity have been made in recent years, SE have not been living up to expectations associated with blocking Li dendrite growth.[2] Monroe and Newman predicted that high shear modulus materials (like many SE) would block dendritic Li growth.[3,4] Still, many papers report shorting and crack formation in SE during cycling.[5–7]

Dendritic Li growth in SE is difficult to observe during cycling because of limited optical access within a solid material contained within a cell. Porz et al. have used optical microscopy to view Li plating at the electrode/SE interface.[5] Sun et al. performed synchrotron X-ray tomography at the SE/electrode interface.[8] Still the effect of dendritic Li growth throughout the bulk has not been visualized during battery operation. Here, I describe efforts to use operando X-ray tomography to monitor SE morphology changes during cyclic voltammetry (CV). Unfortunately, due to the small X-ray cross-section of Li at the X-ray energies needed to penetrate both a SE pellet and a custom cell (ca. 30 keV or more), Li is mostly transparent in these measurements. Please refer to Chapter 1 for more details on X-ray tomography.

In general, sulfide SE are more conductive and are easier to process than garnet-type SE.[2,5] $Li_{10}GeP_2S_{12}$ (LGPS) and $Li_7P_3S_{11}$ (LPS) are sulfide SE of interest because the ionic conductivity of LGPS approaches that of the commercially used 1 M $LiPF_6$ in EC/DMC liquid electrolyte, and LPS exhibits better conductivity than many other sulfide SE and better structural stability in comparison to LGPS.[2]

Unfortunately, poor interfacial contact and degradation at the SE/electrode interface leads to less than ideal ionic conductivities.[9,10] The voltage stability window of LGPS and LPS are between 2–3 V vs Li/Li^+, far below the 4–5 V Li-ion batteries commercially in use today.[11] In order to mitigate problems with interfacial contact, our group employs a thin liquid electrolyte interlayer between the SE and electrode.[12] Other efforts within our group have involved improving the SE voltage stability window by the application of different coatings.[9]

A.2 Experimental

LGPS (99.99%, MSE Supplies LLC) and LPS (99.99%, MSE Supplies LLC) pellets were pressed in a 2 mm diameter die with a hydraulic press (seen in Figure A.1, International Crystal Laboratories) at 1500 psi for 3 min and 1000 psi for 5 min, respectively. Before pressing, the LGPS or LPS powder was ground in an agate mortar and pestle. A single red gasket (included with die) was used to make thin pellets (ca. 150 μm thick). Thicker pellets can be made by using two gaskets, although these thicker pellets were never used as experiment samples. The metal die pieces were sonicated in ethanol, dried in a 150° oven, and cooled in the glovebox before use. To press the pellets, first a gasket then the collar are placed around the central die post. Then the flat side of a dry metal spatula is used to press the powder into the die to its maximum capacity such that no obvious voids or inconsistencies are visible in the packed powder. If excess material is left on the surface of the collar it should be removed to ensure the surface of the collar is as flat as possible while pressing the pellet. Once the powder has been added, the shiny side of the cylindrical top is placed in contact with the metal collar and pellet material. The sides of the cell are wrapped in Parafilm to prevent the top coming off and to help mitigate exposure to air. The entire die is placed inside an Al-coated plastic bag, sealed, and removed from the box for pressing. Once the prescribed pressing sequence is complete the die must be returned to the glove box before opening. As the

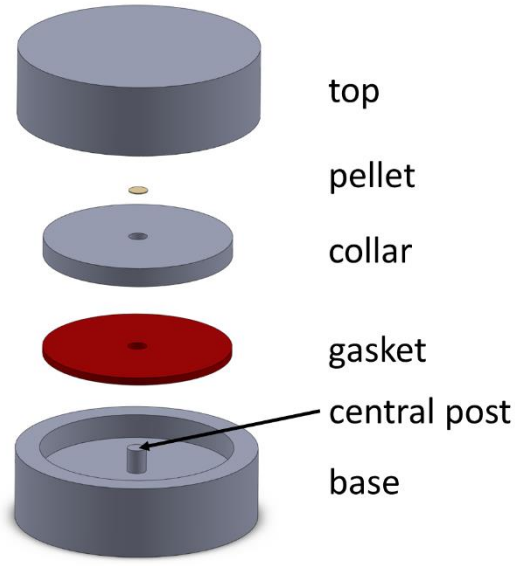

Figure A.1. Exploded view of die used to make SE pellets for tomography experiments. Die purchased from International Crystal Laboratories.

Al-coated bag has remained sealed since being removed from the glovebox there is the abject possibility that pulling vacuum on the bag will cause it to expand and pop open, thus jostling the die and pressed pellet. To preclude this, the bag is opened and rapidly transferred into the ante-chamber before pulling vacuum. The pellets are released from the die inside the glovebox by first removing the collar (with pellet inside) and gasket, then placing the collar back on face up and using the post to press the pellet out of the collar. Between pellets of the same type, the die (especially in the parts contacting pellet material) is wiped clean inside the glovebox. When switching between the two materials, the die is sonicated in ethanol and again dried at 150°C for a minimum of 5 minutes. The agate mortar and pestle are also cleaned with ethanol and dried at 150°C.

CV was performed on LGPS or LPS in custom cells between two Li electrodes. CV was performed starting at 0 V then cycling between ±0.1 V or ±0.5 V at 0.2 mV/s. Usually cycling was performed first within the narrower voltage range followed by cycling within the wider voltage range. The custom cell is described in more detail in section A.3.

Li electrodes were made by first scratching a piece of Li (Alfa Aesar) until shiny and removing a small piece slightly larger than the area of the stainless-steel plunger. This piece was set atop one plunger and pressed into place with the back of the tweezers. Excess Li was removed from the edges by scraping around the circumference with the flat edge of the tweezers such that no Li hung over the edges of the plunger. The lithium film was then pressed onto a clean glass pane to flatten any surface irregularities The Li is alternatively cleaned up and pressed until a smooth, flat, and shiny piece of Li is affixed to the plunger end. The Li must be thick enough to clear a burr left on the plunger, and it is of utmost importance that the Li is both smooth and flat. Any errant pieces of Li (e.g., pieces protruding perpendicular to the Li surface) can short a cell, and a surface that is not flat will cause the pellet to break during cell construction. The second Li electrode is made in the same way but on one end of an "I" piece.

The cell is constructed by first inserting the Li-coated plunger through the cell body and tightening the first nut such that the plunger can be moved up and down but remains held in place without assistance. The SE pellet is gently placed atop the plunger and centered on the Li electrode. The plunger is then retracted so that the pellet is recessed within the cylindrical section of the cell body by several mm. The "I' piece is gently placed Li side down on top of the pellet. The plunger is then retracted more such that the pellet is situated just below where the middle nut on the body

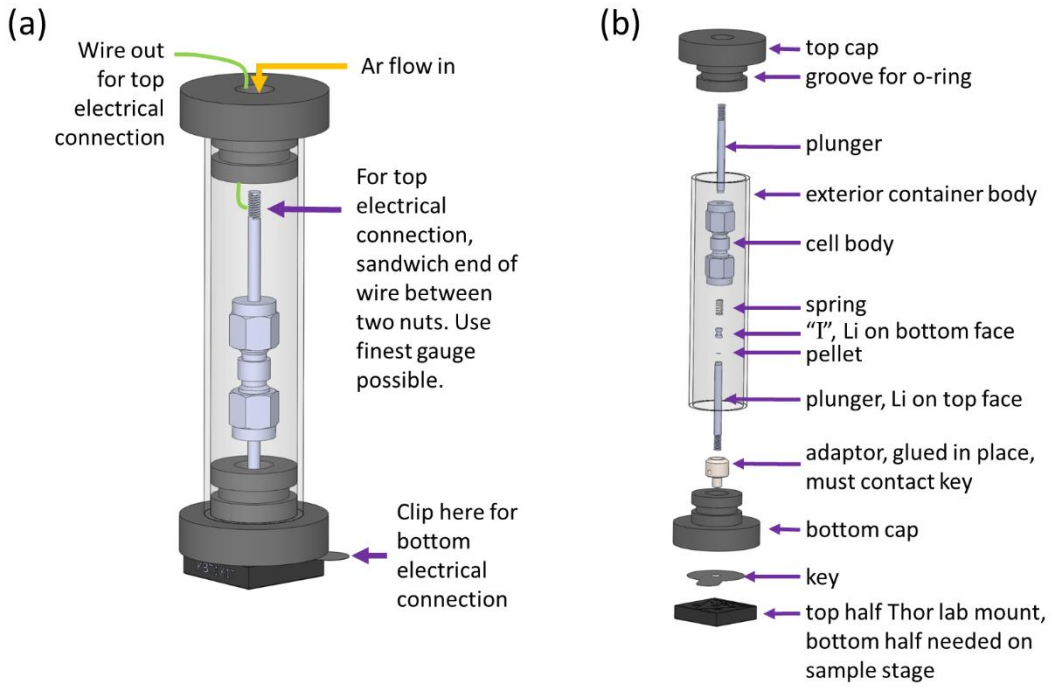

Figure A.2. Operando custom tomography cell. (a) The assembled cell and (b) the exploded view.

was before being ground off. It is important to make sure that the "I" piece follows the pellet down smoothly. Avoid dropping the "I" heavily onto the pellet. It is also important to position the pellet such that any changes in the width of the cell body do not intersect it. A change in cell wall thickness through the pellet will make high-quality reconstructions impossible. Once the pellet has been positioned, fully tighten the lower ferrule around the plunger to lock the plunger in place. Then a spring followed by another plunger is placed on top of the "I" piece. Put the top ferrules and nuts into place, gently compress the cell so that you can feel the spring compress, but not so much as to fully compress the spring, and then tighten the nuts. After construction, the cell should read near 0 V with a resistance of 1-15 kΩ with a multimeter.

The operando tomography experiments performed in March 2018 used a monochromatic beam near 30 keV with a 500 μm Si filter and 750 μm Be window. A 100 μm LuAG:Ce scintillator, 5x microscope objective, and Grasshopper 3 camera with an pixel size of 5.86 μm (effectively 1.172 μm with the 5x lens) were used to collect images. The images were saved as HDF5 files. The CV current and potential were saved in the HDF5 metadata channels 3 and 4, respectively. CV was performed using CH Instruments potentiostats. A USB extender connected the CHI inside the hutch to a laptop outside. Using network cables resulted in dropped signal between the CHI

and computer mid-experiment and are not recommended. Tim Fister owns a 9-pin to BNC adaptor for saving the CHI current and potential in the metadata. The current in the metadata probably needs to be converted to account for every CHI auto-sensitivity change. It's easiest to not use the current collected in the metadata. Instead, use the potential and time stamps in the metadata to correlate the images with the current recorded with the CHI. The potential was recorded correctly and doesn't need to be converted. Commonly, the potential is saved with the opposite sign.

A.3 Cell Design

A tomography cell needs to be symmetrical around the vertical axis of rotation. If the cell is larger than the field of view then ideally the cell will be made out of a low-Z material that will not contribute largely to the background scans. In pursuit of designing such a cell for tomography of SE, a modified nylon Swagelok cell was fabricated with the help of the SCS machine shop (see Figure A.2 for a schematic of the cell and Table A.1 for a list of parts). After the first beamtime, we discovered that a nylon Swagelok doesn't seal well enough around the stainless steel plungers, so an external container was also fabricated. Into this cell, we flowed a constant stream of Ar. While the external container isn't air tight, the constant stream of Ar does prevent visible degradation of the SE, which reacts with O_2 and H_2O.

The 7BM beamline staff provide the hardware to mount the external container and cell at the beamline. This hardware includes four optical posts in the smallest diameter available and a base plate with a threaded hole in the middle. A screw is used to fix the bottom half of the kinematic base to the baseplate. Additional posts are used to hold the Ar line in place and to support the wire that connects to the top electrode.

A.4 Data Workup

I will now describe all the steps I might take to transform raw fly scan images into reconstructed slices and calculated crack volumes. A fly scan is all the images collected from either a 180° or 360° rotation. Figure A.3 gives a brief overview of these steps.

A.4.1 Processing Raw Tomography Images with TomoPy on the UIUC SCS Cluster

A.4.1.1 Using the UIUC SCS Cluster to Run TomoPy Code

Beginning side note: when I give directions on what to type into a command prompt, type everything within the quotes but do not include the quotation marks themselves.

Table A.1. List of parts, the suppliers, and any modifications made to the original part for cell and external cell container.

Part	Supplier	Part #	Modifications
Cell body with end caps, Union, nylon 1/8" OD	Swagelok	NY-200-6	Machine shop counterbored the center to 1/8”
Nylon ferrule set for 1/8” Swagelok tube fittings	Swagelok	NY-200-SET	Round off hex on body to OD 0.25”
Spring, 302 Stainless Steel Precision Compression Spring, ASTM A313, 0.25" Overall length, 0.12" OD, 0.088" ID	McMaster-Carr	9435K11	None
Plungers and “I” pieces, 1/8” 316 Stainless Steel Rod	SCS Machine Shop		Only cut with wire electrical discharge machining (EDM). For plungers: Cut rod to length 1.5”, turn down one end to 0.107” then thread for 4-40’s. Turn down other end to 3 mm diameter to a depth of 1 mm. “I”: Turn down rod diameter to 3 mm. Cut rod to length of 0.16”. Centered on length of rod, cut groove of diameter 2 mm and 0.062” height along length of rod.
External container body, Clear Acrylic Round Tube, 1" OD x 7/8" ID, 6’ Long	McMaster-Carr	8532K21	Cut to length of 3.5”
External container top and bottom cap, Delren	SCS Machine Shop		Pieces manufactured by the SCS Machine Shop

Table A.1., continued

Chemical-Resistant Viton Fluoroelastomer O-Ring, 3/32 Fractional Width, Dash Number 115	McMaster-Carr	9464K28	None
Mini-Series Adapter with External 8-32 Threads and Internal 4-40 Threads	ThorLabs	MSA8	None
Key, 0.008" thick stainless steel sheet	SCS Machine Shop		Key shape cut by machine shop
Thor labs mount: Alternate Top Plate for KB1X1 Kinematic Base, Four 8-32 Taps and Bottom Plate Only for 1" x 1" Kinematic Base	ThorLabs	KBT1X1T and KBB1X1	None
4-40 Hex nuts	Unknown		None
Ultra-Flexible Miniature High-Temperature Wire	McMaster-Carr	9564T1	None

TomoPy, an open-source Python-based program, is used to reconstruct the raw HDF5 (file type) images collected at APS. As seen in Figure A.4, a reconstruction involves taking the collected projection images and processing them to yield horizontal slices or views of the object imaged. Because the original HDF5 files are so large, a significant amount of RAM (32 GB minimum, much more preferred) and a fast processor is needed to process this data. The UIUC School of Chemical Sciences (SCS) Computing Center's High Performance Computational (HPC) Cluster provides the appropriate infrastructure for this data workup and allows for as many reconstructions to be run as they have computers open. This guide is for people, like myself, who are rather new to using Python and secure shell (SSH) interfaces. If you are an experienced user, you'll notice that I do things in the easy-to-understand but not fastest way (e.g., creating the submit.sh file in Notepad then converting the file instead of creating it directly in the cluster command prompt).

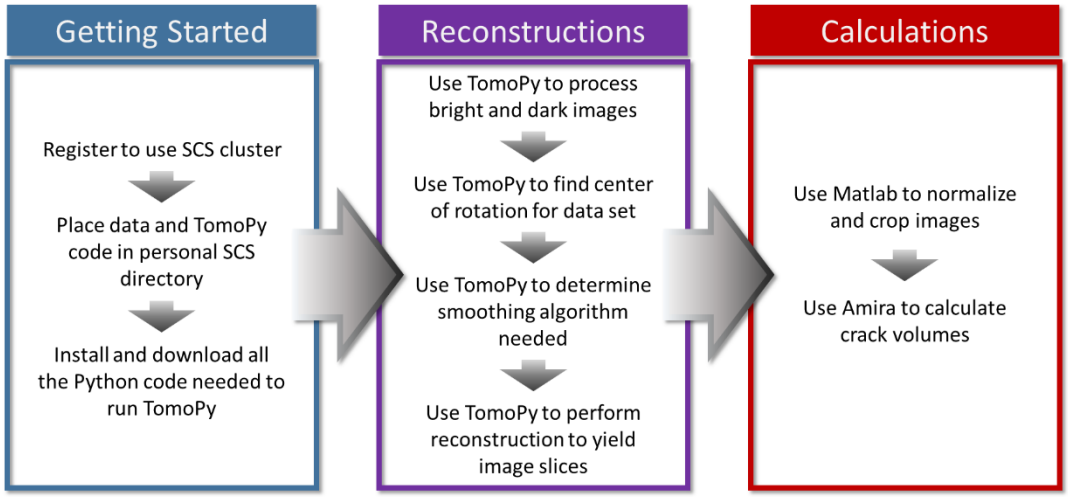

Figure A.3. Data processing workflow

You'll probably also notice that all of my vocabulary isn't completely accurate. The fine people of the SCS Computer Center can help you if my directions aren't making sense.

The cluster runs code and processes data saved in an individual's SCS network drive. First, contact the Computing Center and make an SCS account with them. To establish a link between your own computer and the network drive first VPN into the UIUC network if you are off campus, then map the network drive "\\homes.scs.illnois.edu\SCSusername" using your SCS username (usually UIUC NetID) and password. If you are on campus but not within the SCS network, enter "scs\SCSusername" for your username. Put any data or TomoPy code you want to use in your network drive.

One can connect to the SCS cluster in one of two ways. First, if on a PC, download PuTTY, a free SSH client. This client was recommended to me by the Computing Center staff. Then open PuTTY on your computer, and SSH into the cluster by entering "lipid.scs.illinois.edu" into the

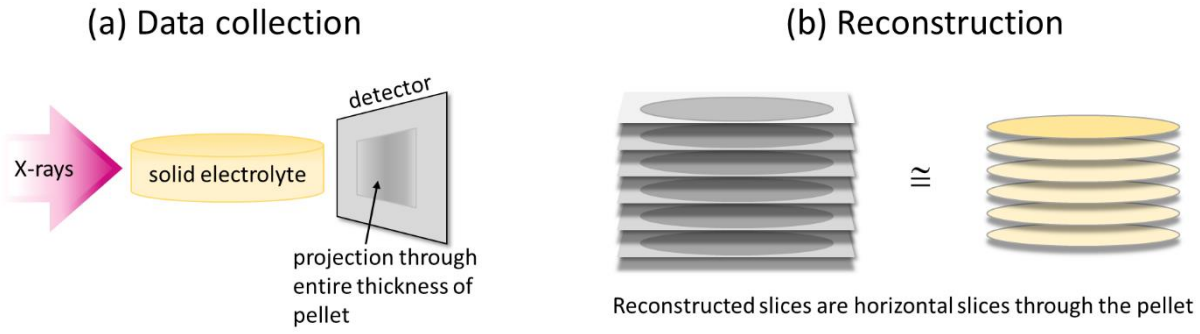

Figure A.4. Diagram showing the difference in the (a) raw data collected during a fly scan and (b) the horizontal slices resulting from reconstruction of the raw data.

Host Name box, click Open, then login using your SCS username and password. Secondly, if one is on a Linux computer and on the UIUC network, simply type the following into the command prompt: “ssh -Y SCSusername@lipid.scs.illinois.edu”.

Now you must download the correct Python version and supporting code onto the cluster to run TomoPy. You should only have to do these six steps once. To be honest, I think the Computing Center staff did this for me. You may need to request certain permissions to perform these steps. In the command screen that appears after logging into the cluster, do the following:

(1) Enable Anaconda in your environment by typing “module load anaconda”;

(2) Create the Anaconda environment by typing “conda create -n tomopy -c conda-forge tomopy”. This step will take quite a while.

(3) Enable the environment by typing first “bash”, enter, then “source activate tomopy” and enter.

(4) If you already have a simple TomoPy script in your network drive, test the script by typing “python NameOfScript.py” using an actual script such as Tomo_Preprocess_SingleThread.py or TomoPy_DiagnoseCenter.py. In this step, use a script that won’t be very resource heavy. Either use the Preprocess script or use the DiagnoseCenter script but only analyze a line of data (i.e., make end_row-start_row = 1).

(5) Create a text file in Notepad, name it “submit.sh” and put the following in it (exclude quotes):

“#!/bin/bash
#$ -S /bin/bash
#$ -cwd

module load anaconda
source activate tomopy

python TomoPy_DiagnoseCenter.py”
(change TomoPy_DiagnoseCenter.py to another .py name if you’d like to run a different piece of code)

(6) Python will throw an error if you use a Notepad file created in Windows. To fix this type “dos2unix submit.sh” into the cluster command prompt. Every time you make changes to the submit.sh file, you will have to rerun “dos2unix submit.sh”.

Before telling you how to execute TomoPy code, first I’ll give you a series of general commands you will need to move around the cluster prompt. There are many more commands available to use, but I don’t know them. Before starting, I highly recommend reading the “UnixPrimer” found at https://scs.illinois.edu/resources/computing/tutorials. Talk to the Computing Center if you need more direction. I’ll give a description of the command and then the command within quotation marks. Once again, don’t type the quotation marks.

- To see what’s in your current directory: “ls”
- To move into a subdirectory “cd [folder name]” where [folder name] should be replaced with the pertinent information, no brackets
- To see what computing resources are open on the cluster: “qstat -f”
- To open a file in the cluster prompt that is contained in the current working directory: “less [file name]” where [file name] should be replaced with the pertinent information, no brackets
- To see your currently running jobs: “qstat”

  qstat outputs something that looks like the following:

  ob-ID prior name user **state** submit/start at queue slots ja-task-ID

  19379 1.00588 submit.sh mhallock **r** 05/11/2018 16:08:04 gpu@compute-1-0.local 16

  The first column (in red) is the job ID number. The state column (in blue) will typically be only one of two things: 'qw' = waiting to run or 'r' = running. Other readouts indicate an error.

  The job automatically generate some files pertinent how the job proceeded. These outputs get saved to a file (by default) named the same as the job name, with .o and the job ID attached to it. So the output from this job was written to submit.sh.o19379. The file that ends in “.e###” (where ### is the job ID) will give you information if an error occurs and

the execution fails. This file will not tell you if you did a good job performing a reconstruction, only if you executed the code in a way that doesn't throw errors.

- If for any reason you need to stop the job, you can type: "qdel ###" where ### is the job ID.
- To open any text file: "less [filename]" and substitute [filename] for an actual value, no brackets. I use this to look at the .e### file.
- To close the file opened: "q"

To run TomoPy code, go the appropriate working directory that contains your relevant code and data and run: "qsub -pe default 32 submit.sh". If a number larger than 32 is used then one of the 128 GB RAM computers will be used instead. These are much more highly subscribed, I don't recommend using them because the queue list is longer. The 32 GB computers will be sufficient if the chunk size in the TomoPy code is low enough (30 hasn't ever thrown memory errors for me).

A.4.1.2 Using the TomoPy Code

First, you will need a way to look at the raw fly scan HDF5 files. There are two different programs I use, but for this stage of the data workup, I prefer the first:

Method (1), Use ImageJ/Fiji with HDF5 plugin: Download Fiji. This is a bundled version of ImageJ that performs somewhat better with large file sizes. (That being said, PCs are not usually happy to open files bigger than their RAM cards. In other words, if you're on a 32 GB RAM computer with 4 x 8 GB RAM cards, then it might get mad at you for trying to open a 10 GB file.) Google "Fiji ImageJ download" to find and download Fiji. Then download the HDF5 plugin. Google "HDF5 plugin for ImageJ" to find this. You'll eventually end up downloading this off of GitHub. In Fiji, install the HDF5 plugin by going to Plugins > Install > then choose the appropriate .jar file. To open an HDF5 file in Fiji/ImageJ go to File > Import > HDF5. For these specific image files choose "/exchange/data" and the option to load as individual stacks. This should open an image stack of all of the images in the HDF5 file. There's a scroll bar at the bottom of the window that allows you to quickly scroll through the images, which will come in handy. When your cursor is over the image, the x- and y-coordinates of that pixel will read out on the main Fiji/ImageJ bar. You will need these pixel values later on.

Method (2), Use HDFView: Download HDFView from hdfgroup.org. Download one of the Pre-built Binary Distributions. Once installed, you can drag an HDF5 file from your file

explorer into the left column of HDFView to import a file. To see the images, click the arrow next to “exchange”, right click on “data”, select “Open As”, under “Display As” choose “Image”, then below set “Height” to “dim 1” and “Width” to “dim 2”.

This next section describes how to process data for which bright and dark HDF5 images were collected and saved separately from the fly scan HDF5 files. I will shorthand the two types of code and call the TomoPy_DiagnoseCenter.py code “DiagnoseCenter” and the Tomo_Preprocess_SingleThread.py code “Preprocess”.

General comments about TomoPy code:

1. Most of the code you will need to change in DiagnoseCenter or Preprocess are within the General/User settings sections.
2. The SCS cluster cannot output images. Either comment out lines of code that try to open a picture or change the code to save the images. I’ve done the former in the code I’ve left. These include statements like “plt.show()” and “print (X)”.
3. If monochromatic X-rays are used during the experiment, then the beam hardening routine can be commented out in the code. I’ve commented out the following lines in DiagnoseCenter:

   ~line 500: projection_data_subset =

   fapply_beam_hardening_projection(projection_data_subset)

   ~line 282: temp_dataset =

   fapply_beam_hardening_projection(dataset[:,0:1,:].copy())

   If you remove beam hardening, then your images are now in units of intensity instead of transmission. i.e., Without beam hardening, lower density areas are brighter.
4. Comment out lines dealing with auto-centering routines if you don’t want to use them in DiagnoseCenter (I never did because they weren’t working properly). I commented out:
   a. ~lines 284-286:

      284: arg_180deg = np.argmin(np.abs(theta - (np.pi - theta[0])))

      285: new_rotation_center =

      tomopy.find_center_pc(temp_dataset[0,...],

      temp_dataset[arg_180deg,...], tol=0.5)

286: print(new_rotation_center)

5. Because you're working on a cluster and you don't know how many CPUs you will be allotted, anywhere "ncore-multiprocess.cpu_count()-10" appears, a more flexible statement will need to replace it. I used:

   "try:
   ncore=int(os.environ["NSLOTS"])
   except KeyError:
   ncore=multiprocessing.cpu_count()-10
   print("Using ncore=%d"%ncore)"

6. There are a couple of pixels that don't save properly during data collection and generally save as "0" value. This becomes a problem in the Denoising code when the program tries to divide by the smallest pixel value. To fix this, lines 166, 167, 171, and 172 have been changed to force some integer values. That being said, I don't use the denoising routine often so you man not run into this problem. Changes made to:

   166: yf=yf.astype(int)
   167: zf=zf.astype(int)
   171: yf0 = yf0.astype(int); yf1 = yf1.astype(int);
   172: zf0 = zf0.astype(int); zf1 = zf1.astype(int);

Step (1): Use Preprocess to average together all the bright images, all the dark images, and remove zingers (overly bright pixels). The only thing you should need to change in this code is "bright_images_filename" and dark_images_filename". Make sure the submit.sh file contains the name of the Preprocess code and not the DiagnoseCenter code. The Tomopy code will look in the current working directory for the original files and will write the new files in the same directory. The new files will have "Prefiltered.hdf5" at the end of the file name. You only need to do this step once for a given set up bright and dark images. You can copy and paste the resulting files into directories where they still apply. Don't use bright and dark images for random data sets. Use those that apply.

Step (2): Use DiagnoseCenter to find the center of rotation in your images. All directions I'm about to give will be in the User Settings portion of the code.

1. Change the “bright_filename”, “dark_filename” and “data_filename” to the correct values.
2. Open a raw HDF5 file in either ImageJ or HDF5Viewer. Find a horizontal row of pixels that intersects the entire pellet horizontally–somewhere in the middle. Note the y-pixel value of this row, and in DiagnoseCenter enter this number for start_row and this number+1 for end_row.
3. In ImageJ, you might be able to approximate where the center of rotation is (within a hundred pixels or so) by quickly scrolling through the images. This will help speed things along. Enter your approximate center of rotation x-pixel value in for rotation_center. Turn diagnose_rotation_center to “True”. At first set search_margin to a large number (10-100, depending your confidence in the center of rotation estimate). DiagnoseCenter will produce images with centers at positions of rotation_center ± search_margin in step sizes of search_step. The larger search_margin is, the larger search_step should be. You will rerun DiagnoseCenter multiple times until you are using search_step = 0.5 to ascertain your final rotation_center value.
4. Look at your raw images in ImageJ or HDFViewer. Pick a region of the image (e.g., upper right, lower left) that has a stable set of features. This means the region brightness should stay relatively consistent throughout the fly images and features should not pass through it. Change I0_box_loc to indicate where this region is located.
5. You will know from your experiments whether you did 180° or 360° fly scans. Change the number in theta_span to 1.0 for 180° scans and 2.0 for 360° scans.
6. In output_path_tiffstack, change the string in quotes to “/DiagnoseCenter/”
7. Now you can run the DiagnoseCenter code with “qsub -pe default 32 submit.sh”. Make sure the submit.sh file is referencing the DiagnoseCenter and not Preprocess.
8. The output of this code should be a folder of TIFF images called “DiagnoseCenter” containing 2*(search_margin/search_step)+1 images. Open these images in ImageJ as a stack (drag folder into ImageJ bar). Each image name contains the center x-pixel value used to produce that image. Use the bottom scroll bar to look through the images. Your image with an ideal center will contain minimum artifacts shaped

like crescent moons and minimum anomalous lines of different contrast radiating out from the center. You may find that none of your images are perfectly centered but look like they're starting to converge at one extreme or between two images. Revisit step 3 and change your rotation_center, search_margin, and search_step appropriately. Delete your current DiagnoseCenter folder of images and reexecute the code. You will need to do this iteratively until your search step is of size 0.5 and you've found the best rotation_center possible.

Step (3): Use DiagnoseCenter code to perform a full reconstruction.

1. Determine the y-range of the object in the image to be reconstructed. Use ImageJ to scroll through your original HDF5 image file and identify two y-pixel values, one above and one below your pellet or object of interest. Make sure you scroll through the images to confirm that your pellet stays within these two values. Always give yourself some wiggle room (an extra 30-100 pixels of extra padding). Place the smaller y-axis value into start_row and the larger into end_row.
2. Change rotation_center to the optimized center value you found in Step (2). Change diagnose_rotation_center to "False".
3. Change the string in output_path_tiffstack to "/Recon/"
4. Run the DiagnoseCenter code. The output will be a new folder called Recon in your current working directory. These are your finished reconstruction TIFF images.

- Instead of first working up the entire y-range of the fly scan, you may want to play around with a smaller stack of images (e.g., end_row-start_row ≅ 5) and test different ring and stripe removal techniques. These options can be found near line 228. The first line reads "def fremove_stripes(dataset,method='sf'):". The string in single quotes (here: 'sf') determines which algorithm is used to remove artifacts. In the original TomoPy code supplied to me by the 7BM staff, this string was 'sf'and the else statement pertaining to 'sf' read: "dataset = tomopy.prep.stripe.remove_stripe_sf(dataset, 10, ncore=1) # Smoothing filter stripe removal". I have found it advantageous to us 'fw'(the Fourier Wavelet Method) and to experiment with the level and sigma values associated with it. Figure A.5 shows a comparison between these two methods and the parameters employed. Münch et al. provide details on how these algorithms affect the final

reconstructed images.[13] A word of warning: The more smoothing one applies, the more data contrast one removes from the image. So remember that as you smooth, you lose data. Tread lightly and compare many different outcomes.

A.4.2 Using MATLAB and Amira to Normalize, Crop, and Calculate Crack Volume

If you're using data for which bright and dark images were not collected for every fly scan, then you have a problem with images darkening throughout an experiment that contains many fly scans. As data collection continues, the microscope objective darkens and changes the mean values of the images you're collecting. My goal is to be able to use the same thresholding numbers in Amira to determine crack volumes. In order for this to work, the images must be normalized in the same way, and I perform these normalizations in MATLAB. Otherwise thresholding values for the first fly scan will not work for the last fly scan. I also use MATLAB to mask and/or crop images before analyzing them in Amira. This allows the user to carefully control what regions of the images are analyzed in Amira. You'll find that edge effects and ringing cause difficulty in working up the entire image in one go because they contribute anomalously to crack volumes. MATLAB contains built in masking functions that I choose not to use. The cracks in my reconstructions are darker than the pellet and after normalization some of the crack pixel values are 0, and MATLAB sets mask values at 0. So instead my code creates masks that are the maximum value for a 16-bit image, instead of the minimum.

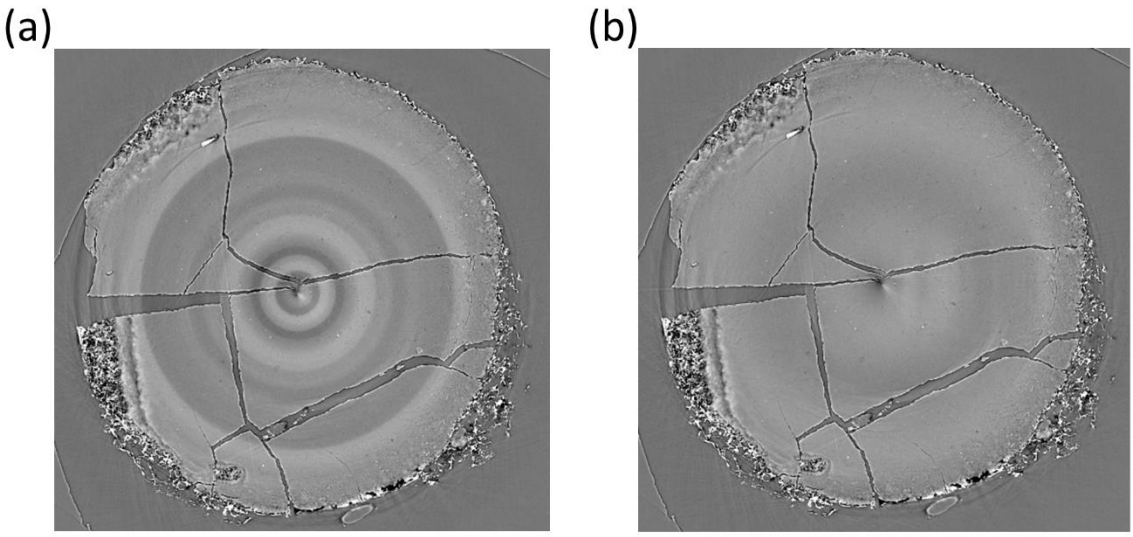

Figure A.5. Comparison of two smoothing algorithms used. (a) employs the 'sf' option with this line of code: "dataset = tomopy.prep.stripe.remove_stripe_sf(dataset, 10, ncore=1) # Smoothing filter stripe removal". (b) uses the 'fw' method with this line of code: "dataset = tomopy.prep.stripe.remove_stripe_fw(dataset,level=8,wname='sym16',sigma=5,pad=True,ncore=ncore) # Fourier Wavelet method".

Amira is image processing software designed specifically to work with tomography data slices. It can't perform reconstructions, but it can perform operations on the slices resulting from reconstructions. The larger your image file sizes when working in Amira, the slower your calculations will run. Therefore, we will use MATLAB to crop images to desirable regions of interest.

I use computers in the Beckman Institute's Imaging Technology Group Vislab to process tomography images with MATLAB and Amira. Occasionally I'll use the best Linux computer for data viewing. Mostly, I use a Windows 7 computer with 16 cores and 128 GB of RAM. There's a list of computers online that states whether or not Amira is already loaded onto a specific computer, and I use one of these.

A.4.2.1 MATLAB code for Normalizing and Cropping Tomography Slices

```
close all
clear all

%% Import data
read_dir = 'Z:\Documents\2018_tomo\LPS-
GC_3_insitu\Dering_Amira_41stack_0029\original_lvl-15_sig-5';
```

```
write_dir = 'Z:\Documents\2018_tomo\LPS-GC_3_insitu\Dering_Amira_41stack_0029\rec_crop_lvl-15_sig-5_8oclock';
cd(read_dir);

% Options section
cropping = 2; % 1 for circle crop; 2 for rectangular crop
import = 1; % 1 if you want to import
process = 1; % 1 if you want to process images, incl. normalize and crop
export = 1; % 1 if you want to export tiff

% A collection of crop values I've used previously
% % for LGPS 6
% outter_x = 1250;
% outter_y = 1250;
% outter_radius = 750;
% inner_x = 1225;
% inner_y = 1225;
% inner_radius = 100;

% for LPS-GC 3
outter_x = 1460;
outter_y = 1460;
outter_radius = 750;
inner_x = 1460;
inner_y = 1460;
inner_radius = 150;


% for rectangular area
% x_origin = 1443;
% y_origin = 1710;
```

```
% x_size = 360;
% y_size = 441;
x_origin = 890;
y_origin = 1760;
x_size = 240;
y_size = 200;

x_mask_origin = 1443;
y_mask_origin = 1710;
x_mask_size = 220;
y_mask_size = 170;

%% import data

if import == 1 % 1 to import data, 0 to skip import

    % Imports all files with .tiff at the end from the directory above
    imageFiles = dir('*.tiff');
    numfiles = length(imageFiles); % counts number of files uploaded
    raw_data = cell(1, numfiles);  % creates cell to hold data

    for k = 1:numfiles
      raw_data{k} = imread(imageFiles(k).name);
    end
end

%% figure out masks

if cropping == 1 % uses circle crop
    figure; imagesc(raw_data{1});
    viscircles([outter_x outter_y],outter_radius);
```

```
    viscircles([inner_x inner_y], inner_radius);

    figure; imagesc(raw_data{end});
    viscircles([outter_x outter_y],outter_radius);
    viscircles([inner_x inner_y], inner_radius);
end % end if

if cropping == 2 % uses rectangle crop
    figure; imagesc(raw_data{1});
    rectangle('Position', [x_origin y_origin x_size y_size]);
    rectangle('Position', [x_mask_origin y_mask_origin x_mask_size y_mask_size]);
end
%% do everything else

if process == 1



% find dimension of image
[dimx, dimy] = size(raw_data{1});
norm_dim = 200; % size of normalization
norm_x = 10; % 0 is left hand, dimx is right hand side of image
norm_y = dimy - norm_dim - 10; % 0 is top and dimy is bottom of image

% figure; imagesc(raw_data{1});

figure;
m = 5; %rows
n = ceil(numfiles/m); %columns
% plot raw images
for k = 1:numfiles
    h(k) = subplot(m,n,k);
```

```
    histogram(raw_data{k});
end
linkaxes(h, 'xy');
suptitle('raw images');
%     figure; imagesc(raw_data{k}); needs loop?


% find minimum value of each image, make positive, then add 1.1 so above 1

for k = 1:numfiles
    min_val(k) = min(raw_data{k}(:));
end
mintotal = min(min_val(:));

if mintotal <= 0
    for k = 1:numfiles
        use_data{k} = raw_data{k} + abs(mintotal) + 1.001 ;
        min_val_post(k) = min(use_data{k}(:));
    end
end


% output max, min, and mean of data shifted above 1
a = max(use_data{1}(:));
b = min(use_data{1}(:));
c = mean(use_data{1}(:));
disp(['shift data above 1.... max = ' num2str(a) '; min = ' num2str(b) '; mean = ' num2str(c)])

%     figure; imagesc(use_data{k}); needs loop?
```

```
% crop area for normalization and perform normalization
figure;
for k = 1:numfiles
    norm_area{k} = imcrop(use_data{k}, [norm_x, norm_y, norm_dim, norm_dim]);
    norm_factor(k) = mean2(norm_area{k}(:));
    use_data{k} = use_data{k}./norm_factor(k);
    h(k) = subplot(m,n,k);
    histogram(use_data{k});
end
linkaxes(h, 'xy');
suptitle('normalized images');
clear norm_area norm_factor

% output max, min, and mean of normalized data
a = max(use_data{1}(:));
b = min(use_data{1}(:));
c = mean(use_data{1}(:));
disp(['normalized images.... max = ' num2str(a) '; min = ' num2str(b) '; mean = ' num2str(c)])

% shift data to prepare for conversion to 16 bit
figure;
for k = 1:numfiles
    use_data{k} = (use_data{k} -0.6)./0.7;% for LPS-GC 3 %         -0.5);% for LGPS6
    h(k) = subplot(m,n,k);
    histogram(use_data{k});
end
linkaxes(h, 'xy');
suptitle('after shifting data to prep for 16 bit conversion');

% output max, min, and mean of data prepped for 16 bit conversion
a = max(use_data{1}(:));
```

```
b = min(use_data{1}(:));
c = mean(use_data{1}(:));
disp(['after shifting data to prep for 16 bit conversion.... max = ' num2str(a) '; min = ' num2str(b)
'; mean = ' num2str(c)])

%% create masks, crop, and change to 16-bit data

if cropping == 1 % *******circular cropping with masks
   % inner mask has zeros inside
   outter_mask = ones(dimx, dimy);
   RGB = insertShape(outter_mask,'FilledCircle',[outter_x outter_y outter_radius],'LineWidth',1,
'Color', 'black');
   outter_mask = rgb2gray(RGB);
   maskmax = max(outter_mask(:));
   outter_mask = outter_mask - maskmax;
   clear RGB
   maskmin = min(outter_mask(:));
   if maskmin > 1
      maskfix = 1/maskmin;
   else
      maskfix = 1/maskmin;
   end
   outter_mask = outter_mask.*maskfix;
   % figure; imagesc(outter_mask); title('outter mask');

   inner_mask = ones(dimx, dimy);
   RGB = insertShape(inner_mask,'FilledCircle',[inner_x inner_y inner_radius],'LineWidth',1,
'Color', 'black');
   maskmin = min(RGB(:));
   inner_mask = rgb2gray(RGB)-maskmin;
   clear RGB
```

```
maskmax = max(inner_mask(:));
if maskmax > 1
   maskfix = 1/maskmax;
else
   maskfix = 1/maskmax;
end
inner_mask = inner_mask.*maskfix;
% figure; imagesc(inner_mask); title('inner mask');

figure;
for k = 1:numfiles
   use_data{k} = use_data{k} .* outter_mask .* inner_mask;
   h(k) = subplot(m,n,k);
   histogram(use_data{k});
%     figure; imagesc(use_data{k}); title('masked');
end
linkaxes(h, 'xy');
suptitle('after mask applied');

a = max(use_data{1}(:));
b = min(use_data{1}(:));
c = mean(use_data{1}(:));
disp(['after mask applied.... max = ' num2str(a) '; min = ' num2str(b) '; mean = ' num2str(c)])

% crop image and change to 16-bit
row_start = outter_y - outter_radius - 10;
row_end = outter_y + outter_radius + 10;
col_start = outter_x - outter_radius - 10;
col_end = outter_x + outter_radius +10;
figure;
for k = 1:numfiles
```

```
        use_data{k} = uint16(65535*use_data{k}(row_start:row_end, col_start:col_end)); % crops and changes to better 16-bit range
        h(k) = subplot(m,n,k);
        histogram(use_data{k});
    end
    linkaxes(h, 'xy');
    suptitle('ready for saving , w/ 16-bit conversion');

    a = max(use_data{1}(:));
    b = min(use_data{1}(:));
    c = mean(use_data{1}(:));
    disp(['ready for saving , w/ 16-bit conversion.... max = ' num2str(a) '; min = ' num2str(b) '; mean = ' num2str(c)])
    end % end if

end


if cropping == 2 % ********* crop rectangular area of interest

    row_start = y_origin;
    row_end = y_origin + y_size - 1;
    col_start = x_origin;
    col_end = x_origin + x_size - 1;

    figure;
    for k = 1:numfiles
        use_data{k} = use_data{k}(row_start:row_end, col_start:col_end); % crops and changes to better 16-bit range
%         use_data{k} = uint16(65535*use_data{k}(row_start:row_end, col_start:col_end)); % crops and changes to better 16-bit range
```

```
    h(k) = subplot(m,n,k);
    histogram(use_data{k});
  end
  linkaxes(h, 'xy');
  suptitle('cropped');

  figure; imagesc(use_data{1});

  rec_mask = ones(y_size, x_size);
  RGB = insertShape(rec_mask,'FilledRectangle',[x_origin-x_mask_origin y_origin-
y_mask_origin x_mask_size y_mask_size],'LineWidth',1, 'Color', 'black');
  rec_mask = (rgb2gray(RGB)-1)*-10/6*5;
  figure; imagesc(rec_mask);



%   figure; % use this if you don't want to perform 16 bit conversion
%   for k = 1:numfiles
% %       use_data{k} = use_data{k}(row_start:row_end, col_start:col_end); % crops and
changes to better 16-bit range
%       use_data{k} = use_data{k}  + rec_mask); % crops and changes to better 16-bit range
%       h(k) = subplot(m,n,k);
%       histogram(use_data{k});
%   end
%   linkaxes(h, 'xy');
%   suptitle('masked');
% end

  figure;
  for k = 1:numfiles
%       use_data{k} = use_data{k}(row_start:row_end, col_start:col_end); % crops and changes
to better 16-bit range
```

```
        use_data{k} = uint16(65535*use_data{k}); % crops and changes to better 16-bit range
        h(k) = subplot(m,n,k);
        histogram(use_data{k});
    end
    linkaxes(h, 'xy');
    suptitle('masked and 16 bit');
end

figure; imagesc(use_data{1});
%% save tiff images with old names

if export == 1

cd(write_dir);



for k = 1:numfiles
    name = imageFiles(k).name;
    imwrite(use_data{k}, name);
end
end % end if
```

A.4.2.2 Using Amira to Calculate Crack Volume

In order to prevent human bias in the crack volume calculations, I look through several different fly scans and then decide on thresholding values that I can use on all fly scans performed during a particular CV.

When saving Amira projects, I usually choose the Minimize project size option. This way Amira saves all of the original data imported and the manipulations you've performed but not the computed surfaces. This option saves a fair amount of data storage space but requires time to recompute your data manipulations upon opening the file. You will also save the .labels files separately. Save often.

To calculate crack volumes:

1. Start Amira, click “Open Data”, and select all TIFF image files you want to examine. I recommend using data sets smaller than the originally reconstructed data. The larger the files imported, the slower all Amira actions will take. As far as I know, you can’t easily crop images or make masks in Amira, so do all of that with MATLAB.
2. If prompted, read complete volume into memory if there's enough RAM.
3. Change object name to something useful like the fly scan name. Check to make sure x and y dimensions of pixels are equal (1 x 1 x 1). Click ok.
    a. If the Project tab is selected, the left side of the screen shows the data stack in green and any visualizations and calculations you’ve performed. This is where Amira catalogues any data you’ve uploaded, modified, or analyzed. The middle panel shows your images as an Ortho Slice. The right side might show the results of calculations you’ve performed.
    b. The Ortho Slice shows you one slice at a time. To activate/deactivate whether or not you can see Ortho Slice, click on the small square next to the Ortho Slice label. When this box is white, Ortho Slice will not view in your middle panel. Vice versa when it’s orange. To change which slice you’re viewing, to change the color map, or visualize slices from another orthogonal view point, click on the orange Ortho Slice box. Below you’ll see viewing options you can change in the Property dialogue.
4. If you want to quickly visualize the 3D data, right click on the green data label, select Favorites > Volren. Click on the new yellow Volren box and activate the square (turn orange) next to the Volren label. In the Property dialogue will be options for changing what you see. Use your left mouse button to click and drag to rotate the sample view. If you want to save an image on the screen, use the camera icon above the image to save the current view. You can also have multiple viewing options (like Ortho Slice and Volren) activated at the same time.
5. The bulk of the useful work we do towards calculating crack volumes will be performed in the Segmentation tab. The purpose of the Segmentation tab is to decide what voxels (3D pixels) belong to a different phase, component, or material of your system. Amira calls them materials. In our work, we will identify the voxels that make up the cracks.

a. In the Segmentation Editor box, select the data set you want to work up in the Image drop down. You will also establish your first .labels file in the Label Field. The .labels files record what pixels you assign to which materials. If you have never performed any segmentation in the current Amira job, there should automatically be a .labels file available.
b. Under Materials, you'll find the default materials you can assign pixels to. You don't assign pixels to Exterior. Right click on Inside and rename to Cracks. You can also add or delete materials by right clicking or using the buttons below.
c. In the Display Control box, you'll find different ways to manipulate the images you're viewing. Underneath your image on the right, there's a slide bar you can use to scroll through and view all the uploaded slices in the stack.

6. Under Selection, you will find all of the various tools used to choose and assign pixels to different materials. Make sure you have the correct material selected above in the Materials box. Choose the volume radio button to apply your selection parameters to the entire volume and not just a single slice. You will use the + and – buttons to add or subtract the pixels you've selected to the chosen material.
    a. I prefer to use the threshold tool (symbol looks like you have all of your cell phone network bars). To try and remove human bias from the pixel picking process, I will do the following process for several different data sets, settle on a thresholding maximum and minimum, and apply those values to all data sets.
    b. To use the threshold tool, click on the tool symbol, select All slices, then move the range of selection with the sliders or by typing values into the boxes on either side of the histogram. As you change these values, you will see more or fewer blue-tinted pixels on your image. Make sure you're scrolling through different slices before settling on final threshold bounds. To apply the blue pixels to the selected material, click Select Masked Voxels (then blue pixels become purple), then click the + symbol (another color change will occur corresponding to the color assigned to that material). You've now added these pixels to your material. Save your work!
7. If you need to remove some pixels that are not a part of your cracks you have two options. One is less bias prone because you can apply the same settings to all of your data files and the other one completely relies on human selection.

a. The first method will remove islands or fill holes in your data set. You can set the limits and apply those same limits to other data sets. In the toolbar, click Segmentation > Remove islands. In the Islands Filter box, chose the island size or smaller that you would like to exclude. Under Apply To, chose Current Slice to remove 2D islands made of voxels only within a single slice. Chose All slices to remove 2D islands from all slices. Choose 3D volume if you want your island size to include voxels connected in three dimensions. I typically chose 3D volume. Click on Highlight all islands to preview what will be removed. Change the parameters until you're happy. You can't undo this step. Make a note of the parameters used. Amira won't save these for you. Click Apply to apply your changes.
b. The second method uses human choice to remove errant islands of pixels. In the Segmentation Tab, under Segment Editor > Selection> choose Magic Wand. With the Magic Wand you will click on voxels in your material and then the – button to remove them from the currently selected material. If you want to select only islands on the slice currently in view, unselect All slices. If you want to be selecting 3D islands to remove, make sure All slices is selected. Save your work!

8. Once you have satisfactorily assigned the different materials for your .labels file, go back to the Project Tab. You will now see a new green box with the new .labels file you created. We will now create a 3D surface which can then be integrated. Right click on .labels box, then select Compute > Generate Surface > Create.
9. Choose the new red Generate Surface box. Below in the Properties dialogue, do not select Compactify, keep Minimum Edge Length at 0, and change Smoothing to None. Click Apply. This might take a while depending on your file size.
10. Once the surface is computed (yields green box, .surf file), right click on the green box, and choose Measure And Analyze > Surface Area Volume > Create. In the Properties dialogue, check materials under Mode, and choose Apply. Choose the new .statistics green box and next to Spreadsheet, select Show. This will open a tab in the Tables window on the right side of the screen and report volumes in numbers of voxels for the materials you assigned in the .labels file. Save!

A.5 Preliminary Results

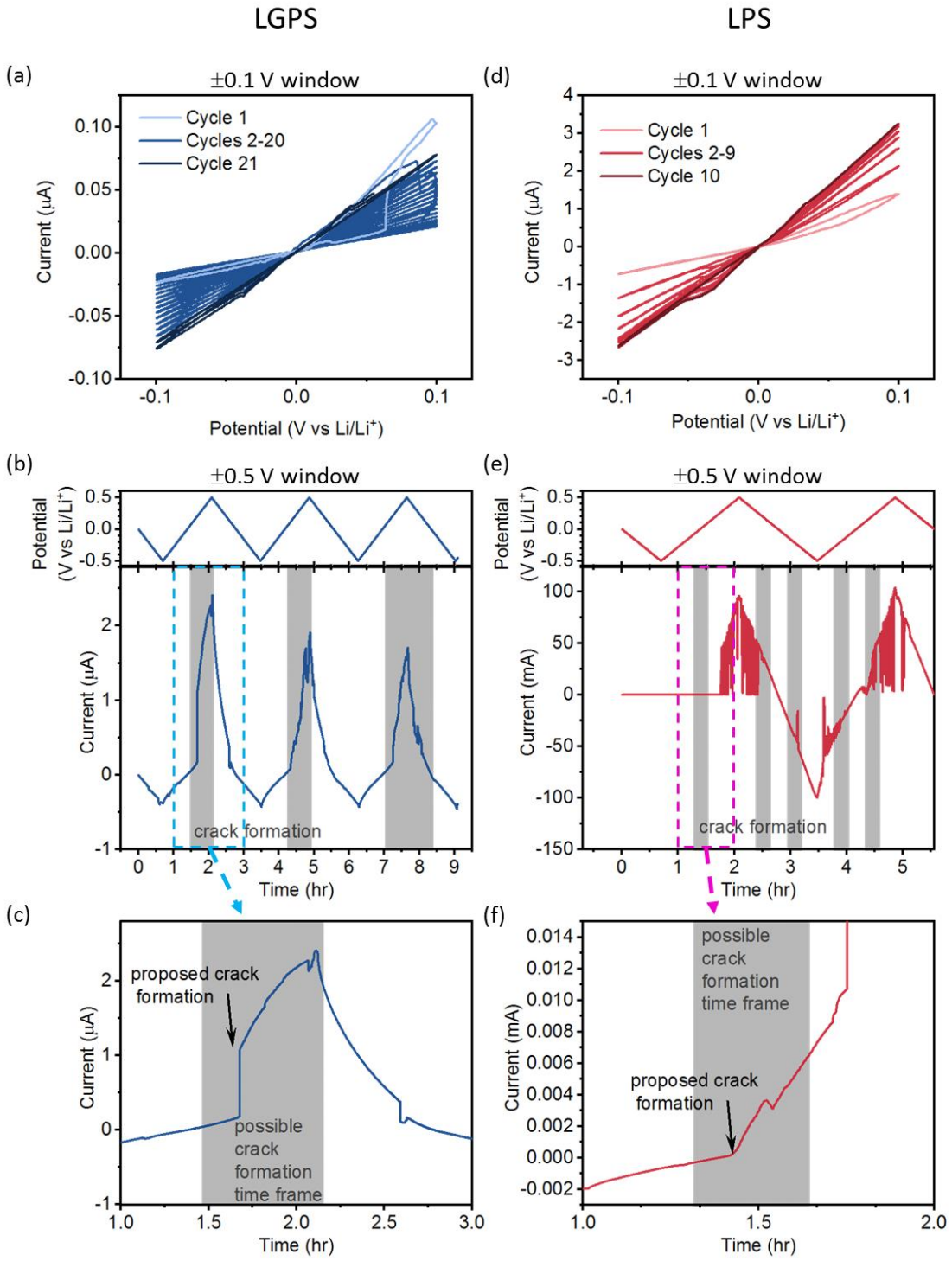

Figure A.6. CV at 0.2 mV/s collected during operando tomography on (a-c) Li/LGPS/Li and (d-f) Li/LPS/Li cells. (a,d) show CV cycled between ±0.1 V, (b,e) show CV cycled between ±0.5 V, and (c,f) show magnified portions of (b) and (e), respectively. The grey regions indicate regions in which cracks form, as observed by operando tomography.

Figure A.6 shows CV performed at 0.2 mV/s on Li/SE/Li (SE was either LPS or LGPS) housed in custom tomography cells. First, the cells were cycled from 0 V in a negative direction to -0.1 V and then between ±0.1 V for 21 (LGPS, Figure A.6a) or 10 (LPS, Figure A.6b) cycles. Then the CV window was changed to ±0.5 V for 3 cycles. The number of cycles for LPS cycled between ±0.1 V was decreased from 21 to 10 cycles because an ex-situ experiment in which a Li/LPS/Li cell was run inside an Ar box did not short during 30 cycles. The number of cycles was decreased to expedite data collection.

Figure A.6a shows CV of LGPS between ±0.1 V. During cycle 1, the current at -0.1 V is near -0.025 μA and increases over 21 cycles to -0.075 μA. During cycle 1, the current at 0.1 V is near 0.1 μA. The current at 0.1 V is 0.06 μA during cycle 2, drops to 0.02 μA during cycle 3, and then slowly increases over 21 cycles to 0.08 μA, indicating an increase in resistance in the cell, probably from surface decomposition.[9] There are no telltale signs of shorting during cycling between ±0.1 V such as short current spikes or sudden increase in current.

Figure A.6b shows CV of LGPS between ±0.5 V. The grey regions indication time frames in which cracks formed as observed with operando tomography. The beginning of a grey region marks the beginning of one tomography scan, and the end of the grey region marks the beginning of a later scan (usually the next sequential scan). The grey region starting at 7 hours contains two of these regions because cracking was seen between two sets of scans. Within these regions, the current jumps from ca. 0.1 μA to above 1.5 μA. Figure A.6c shows the first grey region between 1.46 and 2.16 hr (0.05 V and 0.45 V) in which the first new cracks were observed. I hypothesize that the steep jump in current at 1.68 hr (0.22 V) occurs as a crack forms. The new crack might reveal more surface area on which Li may plate.

Figure A.6d shows CV of LPS between ±0.1 V. During cycle 1, the current at -0.1 V is near -0.72 μA and increases steadily over 10 cycles to -2.59 μA, indicating an increase in resistance in the cell, probably from surface decompostion.[9] During cycle 1, the current at 0.1 V is near 1.40 μA. The current at 0.1 V slowly increases to 3.25 μA after 10 cycles.

Figure A.6e shows CV of LPS between ±0.5 V. Within the grey regions, the current jumps up and down, sometimes by as much as 75 mA. These sudden increases and decreases in current are considered to be signs of temporary shorting in the cell. A dendrite forms, passes extra current, degrades, and then ceases to act as a short. Figure A.6f shows the first grey region between 1.26

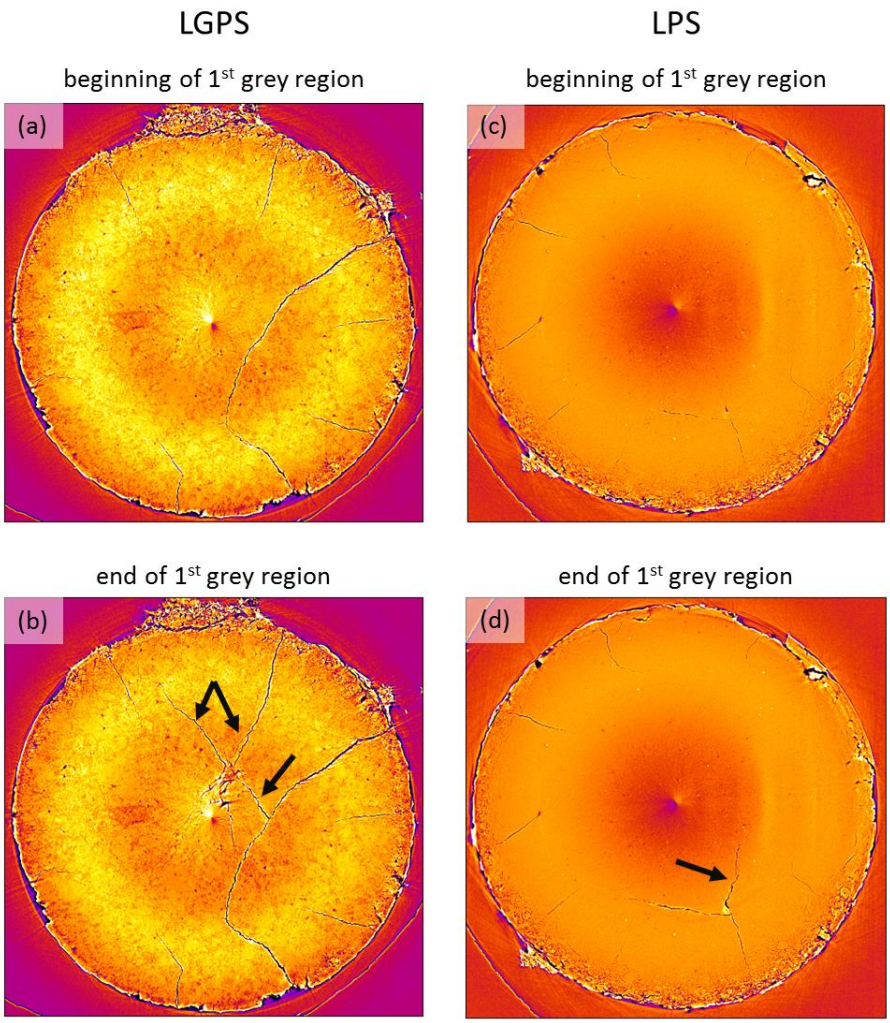

Figure A.7. Slices of (a,b) LGPS and (c,d) LPS at the (a,c) beginning and (b,d) end of the grey regions shown in Figure A.6. Black arrows point to newly formed cracks. These slices come from the middle of the pellet, not from one of the SE/Li interfaces.

hr and 1.54 hr (-0.09 V and 0.11 V). I hypothesize that the small jump in current at 1.43 hr (0.40 V) occurs as a crack forms. Here it is possible to distinguish the current response due to crack formation from the large mA jumps in current, often associated with battery shorting.

Figure A.7 shows single horizontal slices of LGPS (left column) and LPS (right column) before and after the first new cracks form. The LGPS pellet presents in higher contrast to its surrounds because of its larger electron density, due to the presence of Ge. As a comparison, at 30 keV the absorption length of LGPS is 0.152 cm (assuming ρ = 2.0 g/cm^3) and that of LPS is 0.285 cm (assuming ρ = 1.9 g/cm^3); meaning that less LGPS material is needed to attenuate the beam by a factor of 1/e. The new cracks seen in Figure A.7b and Figure A.7b originate from preexisting cracks. Unfortunately, near 30 keV, the contrast between Li and Ar is low enough that we cannot

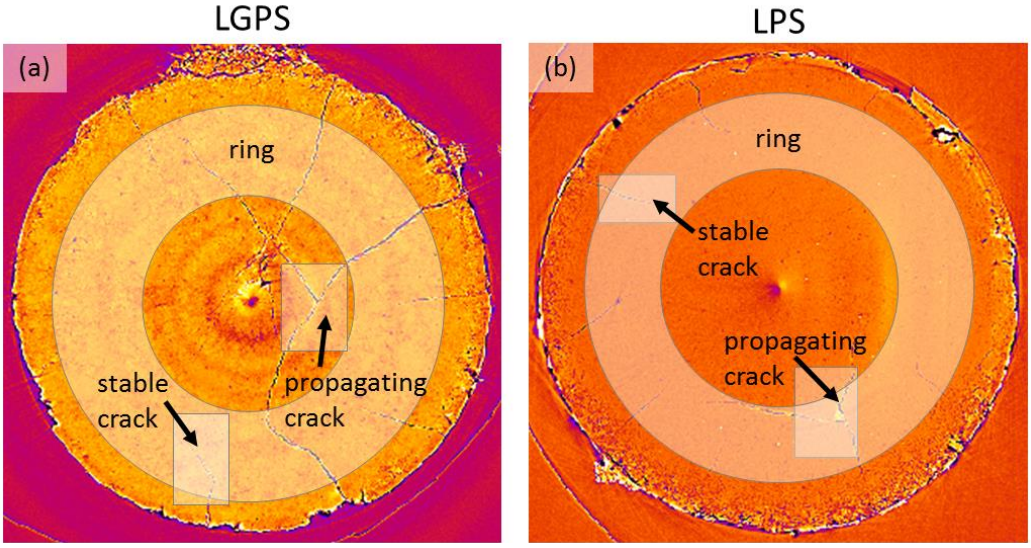

Figure A.8. Shows three regions of interest used when calculating crack volume changes in (a) LGPS and (b) LPS with Amira. The integrated crack volumes are shown in Figure A.9. The images here are the same as those used in Figure A.7b and A.7d.

prove the presence or absence of Li in the cracks. In the raw images, the interface between the bulk Li electrode and Ar can be seen, but such sharp interfaces are not available for imaging within the pellets.

Figure A.8 shows different regions of interest used for calculating crack volumes. The ring region was chosen because artifacts in the reconstruction lead to pronounced rings that are brighter or darker than nearby regions. By integrating a ring volume, I can analyze an area all the way around the pellet and obtain decent statistics without including fluctuating pixel values that don't represent reality. Cropping away the outside edges of the pellet eliminates edge effects and crumbling from contributing to the crack volumes. The rectangular propagating and stable crack regions were chosen to monitor cracks that do or do not propagate with extended cycling. The regions are also chosen to minimize the contribution of ring artifacts.

Figure A.9 shows the results of integrating the crack volume through forty-three LGPS slices and twenty-five LPS slices in the three different regions shown in Figure A.8. The slices used for integration were chosen such that no SE/Li interfaces were included in the integration. These interfaces contain artifacts that artificially change the calculated crack volume. Improvements could be made to these calculations by figuring out how to rotate the pellet in MATLAB to be more horizontal. Amira only performs integration calculations in the planes of slices and won't do so at an angle, cutting through many slices.

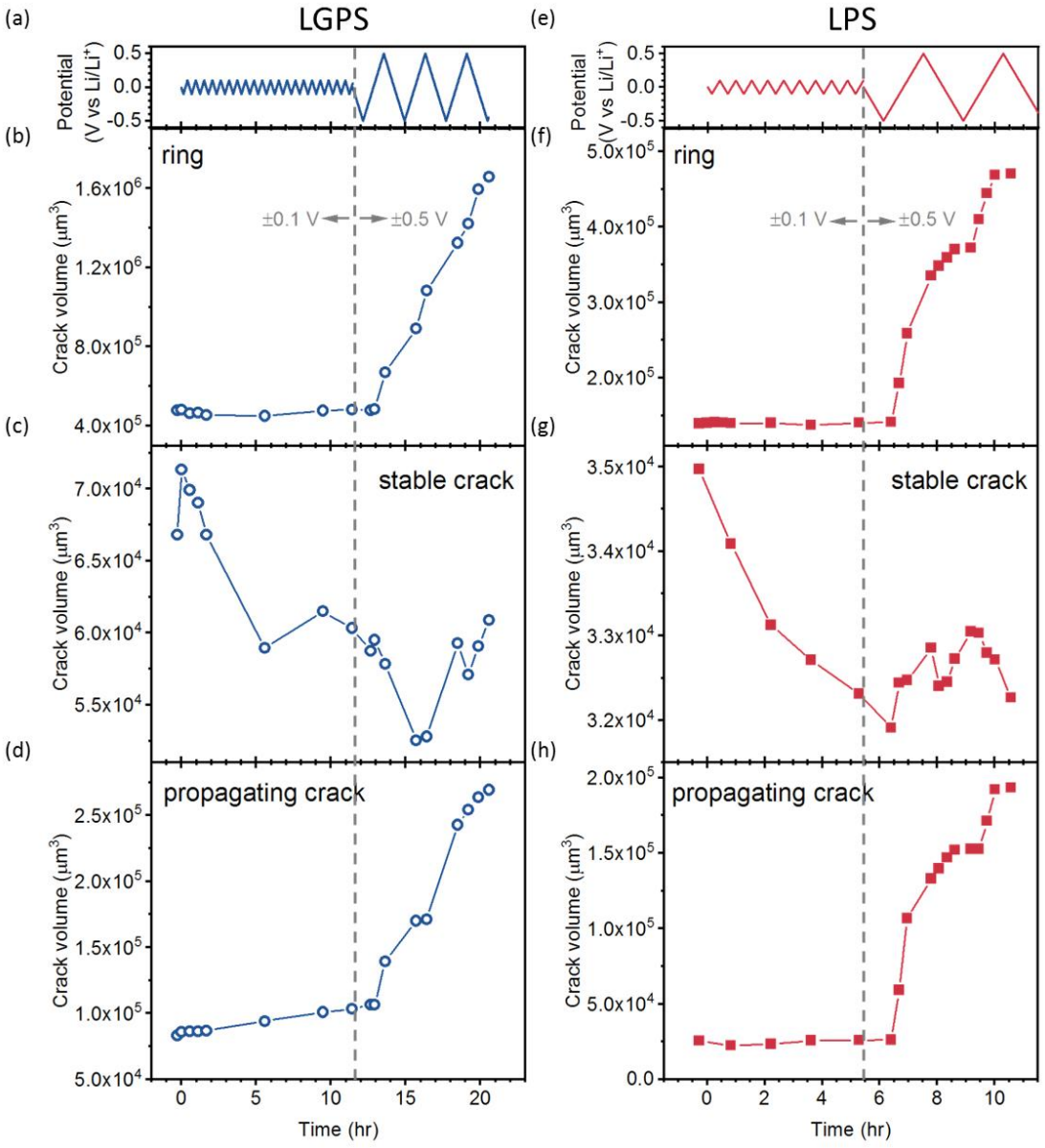

Figure A.9. (b-d, f-h) Calculated crack volumes in (a-d) LGPS and (e-h) LPS pellets during (a,e) potential control. The integrated crack volumes were within (b,f) ring areas that catch crack behavior around the entire circumference of the pellet, (c,g) in rectangular areas around a stable crack, and (d,h) in a rectangular area around a crack that propagates further during cycling.

The ring integrations for LGPS (Figure A.9b) and LPS (Figure A.9f) were performed to give a statistical overlook of how cracks are changing through a large pellet volume. These areas contain multiple cracks that contribute to the overall computed crack volume. In both LGPS and LPS, the initiation of new cracks can be seen after 12.9 hr and 6.4 hr, respectively, after cycling between ±0.5 V begins. The crack volume then steadily grows for the rest of cycling.

Figure A.9c and Figure A.9g show the volume change of cracks in LGPS and LPS, respectively, that were present at OCP before cycling and that do not propagate further during CV. Interestingly, the volume of these cracks decreases at first and then levels off. I hypothesize that degradation occurring on the inside faces of these cracks form products that make the crack volume decrease.

Figure A.9d and Figure A.9h show the volume change of cracks in LGPS and LPS, respectively, that were both present at OCP before cycling and also further propagate after the potential window is widened to ±0.5 V. The volume of propagating cracks in both LGPS and LPS does not decrease during the ±0.1 V CV, as seen in Figure A.9c and Figure A.9g. Instead the crack volume steadily increases (LGPS) or stays approximately constant (LPS) during cycling in the ±0.1 V window. The crack volume in LGPS steadily increases from the start of ±0.1 V cycling until the first new crack appears (0–12.9 hr). It is possible that Li plating in the crack is forcing the crack open, creating stress at the interface that is released upon crack propagation.

In conclusion, more crack volume calculations need to be performed on various individual cracks. MATLAB code needs to be developed to tilt the tomography images such that the circular faces of the pellet are near horizontal. This will allow better integration statistics by using more slices in crack volume calculations while still avoiding the inclusion of interfaces and the edge effects present there.

A.6 References

(1) Kim, J. G.; Son, B.; Mukherjee, S.; Schuppert, N.; Bates, A.; Kwon, O.; Choi, M. J.; Chung, H. Y.; Park, S. *J. Power Sources* **2015**, *282*, 299.

(2) Bachman, J. C.; Muy, S.; Grimaud, A.; Chang, H.-H.; Pour, N.; Lux, S. F.; Paschos, O.; Maglia, F.; Lupart, S.; Lamp, P.; Giordano, L.; Shao-Horn, Y. *Chem. Rev.* **2016**, *116*, 140.

(3) Monroe, C.; Newman, J. *J. Electrochem. Soc.* **2004**, *151*, A880.

(4) Monroe, C.; Newman, J. *J. Electrochem. Soc.* **2005**, *152*, A396.

(5) Porz, L.; Swamy, T.; Sheldon, B. W.; Rettenwander, D.; Frömling, T.; Thaman, H. L.; Berendts, S.; Uecker, R.; Carter, W. C.; Chiang, Y.-M. *Adv. Energy Mater.* **2017**, *7*, 1701003.

(6) Ren, Y.; Shen, Y.; Lin, Y.; Nan, C.-W. *Electrochem. commun.* **2015**, *57*, 27.

(7) Cheng, E. J.; Sharafi, A.; Sakamoto, J. *Electrochim. Acta* **2017**, *223*, 85.

(8) Sun, F.; Dong, K.; Osenberg, M.; Hilger, A.; Risse, S.; Lu, Y.; Kamm, P. H.; Klaus, M.; Markotter, H.; Garcia-Moreno, F.; Arlt, T.; Manke, I. *J. Mater. Chem. A* **2018**, *ASAP*.

(9) Sang, L.; Bassett, K. L.; Castro, F. C.; Young, M. J.; Chen, L.; Haasch, R. T.; Elam, J. W.; Dravid, V. P.; Nuzzo, R. G.; Gewirth, A. A. *Chem. Mater.* **2018**, *30*, 8747.

(10) Ma, J.; Chen, B.; Wang, L.; Cui, G. *J. Power Sources* **2018**, *392*, 94.

(11) Richards, W. D.; Miara, L. J.; Wang, Y.; Kim, J. C.; Ceder, G. *Chem. Mater.* **2016**, *28*, 266.

(12) Philip, M. A.; Sullivan, P. T.; Zhang, R.; Wooley, G. A.; Kohn, S. A.; Gewirth, A. A. *ACS Appl. Mater. Interfaces* **2019**, *11*, 2014.

(13) Münch, B.; Trtik, P.; Marone, F.; Stampanoni, M. *Opt. Express* **2009**, *17*, 8567.

Appendix B: MATLAB Code for Processing Stress Data, Strain Data, and Calculating Electrochemical Stiffness

B.1 MATLAB Code for Processing Stress and Strain Together and Calculating Electrochemical Stiffness

```
% This script imports data from the original labview file, divides it up
% into individual anodic and cathodic sweeps for each cycle, smooths the
% data, takes the derivative, and plots the echem, stress, and dstress for
% all cycles.

% OPTIONS: There are two derivative options in this script. Comment out the
% one you don't want to use.
%
% Choose to plot the echem from the potentiostat or labview. Script needs to
% be changed in the plotting section for this to occur.

close all


%% ******The Options Section!******
data_import_choice = 1; % if = 1 then data is imported and cut up into its sweeps
find_file = 1; % 0 = use windows explorer, 1 = use file paths below
   stress_path = 'C:\Users\Kimberly\Dropbox\Grad
school\LFP\LFP_Stress_Hanwha\paper_170707_HanwhaLFP_OCP_25uVs_ClO4_PC';
   stress_echem_file = '02_echem25uVs_170707_HanwhaLFP_OCP_25uVs_ClO4_PC.txt';
   stress_file = '02_stress25uVs_170707_HanwhaLFP_OCP_25uVs_ClO4_PC';

   strain_path = 'C:\Users\Kimberly\Dropbox\Grad school\LFP\LFP_Strain_Hanwha\paper';
   strain_file = 'matlab_171211_LiClO4_PC.xlsx';

% electrode area
stress_area = 0.788;       % in cm^2
current_conversion = 1e6;  % to make A into mA (1e3) or uA (1e6) etc
index_refraction_old = 1.338;  % keep both index of refraction numbers 1 if no correction
needed
index_refraction_new = 1.426;  % LiPF6 EC/DMC 1.338, LiClO4 EC/DMC 1.409, LiPF6 PC
1.414, LiClO4 PC 1.426,

% pick potential range which will be used throughout plotting and
% interpolation sections (this has not been implemented yet)
material = 4;  % 0 if LMO with range 3.5-4.5 V
            % 1 if LFP with range 2.6-4.2 V
            % 2 if PAQ with range 1.8-2.6 V
```

```
        % 3 if ITO with range 1.0-4.0 V
        % 4 if LFP with range 2.6-4.4 V

% how much smoothing of original stress data do you want?
stress_smooth_kernel = 7;
% how big of an interval should the derivative be performed over?
stress_deriv_kernel = 11;

% how much smoothing of original strain data do you want?
strain_smooth_kernel = 7;
% how big of an interval should the derivative be performed over?
strain_deriv_kernel = 11;

% Perform certain fuctions?
resistance_correction = 0; % 1 = do correction. Referes to shifts detailed immediately below

    % Shift potential by a constant
      %If stress values need to be shifted
      Vstress = 0; % in volts

      %If strain values need to be shifted
      Vstrain = 0; % in volts

    % Uses V_new = V_original - IR to shift potential, non-linear shift
      % If stress values need to be shifted
      rstress = 0; % in Ohms

      % If strain values need to be shifted
      rstrain = 0; % in Ohms

peak_splitting_choice = 0;     % 1 = find out peak splitting between stress and strain echem,
depending on how noisy the data is, this section my require extra attentio
ratio_derivatives_choice = 1;  % 1 = perform all manipulations and plotting for ratio of
derivatives calculation
flip_stress_choice = 1;        % 1 = use for ratio of derivative calculations. multiplies stress
derivative by -1

% Plotting?
plot1 = 0;  % 1 = plot original stress and smoothed stress together
plot2 = 0;  % 1 = plot original strain and smoothed strain together
plot3 = 0;  % 1 = plot stress and strain ECHEM together
plot4 = 0;  % 1 = plot STRESS and STRAIN together
plot5 = 0;  % 1 = plot echem and  stress and strain DERIVATIVES together in one panel
plot6 = 0;  % 1 = plot echem, strain, strain derivatives, old style
plot7 = 0;  % 1 = plot echem, stress, and strain
plot8 = 0;  % 1 = plot echem, stress, and stress derivative
```

```
plot9 = 0;  % 1 = plot echem, strain, and strain derivative
plot10 = 0; % 1 = integrate strain echem and compare strain and charge curve
%% Import and chop up potentiostat data related to stress
if data_import_choice == 1
%import stress echem data
if find_file ==0
   [file,path] = uigetfile('*.txt');
   echem = importdata(fullfile(path,file));
else
   echem = importdata(fullfile(stress_path, stress_echem_file));
end
data = echem.data;

% Parse original echem data
% MAY NEED TO BE CHANGED depending on how individual potentiostat exports
% data
org_echem_pot = data(:,1);
org_echem_cur = data(:,2)/stress_area*current_conversion;
org_echem_chrg = data(:,3);
org_echem_time = data(:,4);

clear data

num_data = numel(org_echem_pot); %total number of points in the data array

% Find line number for max and min of each cycle
[pot_max, maxind] = findpeaks(org_echem_pot, 'MinPeakProminence', .1);
DataInv = 1.01*max(org_echem_pot) - org_echem_pot;
[pot_min, minind] = findpeaks(DataInv, 'MinPeakProminence', .1);

% Combine max and min
maxmin = vertcat(maxind, minind);

% Sort max and min line numbers so each anodic/cathodic cycle can be
% accurately picked out
echem_cyclebounds =  sort(maxmin, 'ascend');
echem_sweep_num = numel(echem_cyclebounds);

% Chop up echem potential data into anodic and cathodic cycles
echem_pot = cell(1,echem_sweep_num);
i = 1;
x = 0;
y = echem_cyclebounds(i);
while echem_sweep_num - i +1 > 1
   echem_pot{i} = org_echem_pot(x + 1:y);
   x = echem_cyclebounds(i);
```

```
    i = i + 1;
    y = echem_cyclebounds(i);
end
echem_pot{i} = org_echem_pot(x:y); %gets the last bit of data
echem_pot{i+1} = org_echem_pot(y:num_data);

% Chop up echem current data into anodic and cathodic cycles
echem_cur = cell(1,echem_sweep_num);
i = 1;
x = 0;
y = echem_cyclebounds(i);
while echem_sweep_num - i + 1 > 1
    echem_cur{i} = org_echem_cur(x + 1:y);
    x = echem_cyclebounds(i);
    i = i + 1;
    y = echem_cyclebounds(i);
end
echem_cur{i} = org_echem_cur(x:y); %gets the last bit of data
echem_cur{i+1} = org_echem_cur(y:num_data);

end
%% Import and chop up labview data
if data_import_choice == 1
%import labview data
if find_file ==0
    [file,path] = uigetfile('*.');
    labview = importdata(fullfile(path,file));
else
    labview = importdata(fullfile(stress_path, stress_file));
end
data = labview.data;

% Parse original labview data
org_time = data(:,1);
org_pot = data(:,2);
org_cur = data(:,3)/stress_area*current_conversion;
org_stress = data(:,4)*index_refraction_old/index_refraction_new;
org_psd = data (:,5);

clear data

%get rid of duplicate potential values and the other values associated
%with them
[pot, ind_unique,~] = unique(org_pot);
ind_unique = sort(ind_unique, 'ascend');
    org_pot = org_pot(ind_unique);
```

```
    org_time = org_time(ind_unique);
    org_cur = org_cur(ind_unique);
    org_stress = org_stress(ind_unique);
    org_psd = org_psd(ind_unique);

    num_data = numel(org_time); %total number of points in the data array

% Find line number for max and min of each cycle
[pot_max, maxind] = findpeaks(org_pot, 'MinPeakProminence', .1);
DataInv = 1.01*max(org_pot) - org_pot;
[pot_min, minind] = findpeaks(DataInv, 'MinPeakProminence', .1);

% Combine max and min
maxmin = vertcat(maxind, minind);

% Sort max and min line numbers so each anodic/cathodic cycle can be
% accurately picked out
cyclebounds =  sort(maxmin, 'ascend');
sweep_num = numel(cyclebounds);

% Chop up time data into anodic and cathodic cycles
stress_time = cell(1,sweep_num);
org_cycle_time = cell(1,sweep_num);
i = 1;
x = 10; %start 10 data points in to avoid weird values
y = cyclebounds(i);
while sweep_num - i + 1 > 1
    stress_time{i} = org_time(x + 1:y); %this variable will change throughout program
    org_cycle_time{i} = stress_time{i};
    x = cyclebounds(i);
    i = i + 1;
    y = cyclebounds(i);
end
stress_time{i} = org_time(x:y); %gets the last bit of data
stress_time{i+1} = org_time(y:num_data-10);

% Chop up potential data into anodic and cathodic cycles
stress_pot = cell(1,sweep_num);
org_cycle_pot = cell(1,sweep_num);
i = 1;
x = 10;
y = cyclebounds(i);
while sweep_num - i + 1 > 1
    stress_pot{i} = org_pot(x + 1:y);
    org_cycle_pot{i} = stress_pot{i};
    x = cyclebounds(i);
```

```
    i = i + 1;
    y = cyclebounds(i);
end
stress_pot{i} = org_pot(x:y); %gets the last bit of data
stress_pot{i+1} = org_pot(y:num_data-10); %

% Chop up current data into anodic and cathodic cycles
stress_cur = cell(1,sweep_num);
org_cycle_cur = cell(1,sweep_num);
i = 1;
x = 10;
y = cyclebounds(i);
while sweep_num - i + 1 > 1
    stress_cur{i} = org_cur(x + 1:y);
    org_cycle_cur{i} = stress_cur{i};
    x = cyclebounds(i);
    i = i + 1;
    y = cyclebounds(i);
end
stress_cur{i} = org_cur(x:y); %gets the last bit of data
stress_cur{i+1} = org_cur(y:num_data-10);

% Chop up stress data into anodic and cathodic cycles
stress = cell(1,sweep_num);
org_cycle_stress{i} = cell(1,sweep_num);
i = 1;
x = 10;
y = cyclebounds(i);
while sweep_num - i + 1 > 1
    stress{i} = org_stress(x + 1:y);
    org_cycle_stress{i} = stress{i};
    x = cyclebounds(i);
    i = i + 1;
    y = cyclebounds(i);
end
stress{i} = org_stress(x:y); %gets the last bit of data
stress{i+1} = org_stress(y:num_data-10);

% NaN values
for i = 1:sweep_num
    stress_pot{i}(isnan(stress_pot{i})) = [];
    %echem_pot{i}(isnan(echem_pot{i})) = [];
    stress_cur{i}(isnan(stress_cur{i})) = [];
    %echem_cur{i}(isnan(echem_cur{i})) = [];
    stress{i}(isnan(stress{i})) = [];
end
```

```
end
%% Import and process Ozgur's strain data
if data_import_choice == 1
%import labview data
if find_file ==0
   [file,path] = uigetfile('*.');
   org_data = importdata(fullfile(path,file));
else
   org_data = importdata(fullfile(strain_path, strain_file));
end
data = org_data.data;

org_strain_echem_pot = data(:,1);
org_strain_echem_cur = data(:,2);
org_strain_pot = data(:,4);
org_strain_time = data(:,5);
org_strain = data(:,6);

clear data
%% Parse electrochemistry for strain

strain_num_data = numel(org_strain_echem_pot); %total number of points in the data array

% Find line number for max and min of each cycle
[~, maxind] = findpeaks(org_strain_echem_pot, 'MinPeakProminence', 0.4, 'MinPeakDistance',
10);
DataInv = 1.01*max(org_strain_echem_pot) - org_strain_echem_pot;
[~, minind] = findpeaks(DataInv, 'MinPeakProminence', 0.4, 'MinPeakDistance',10);

% Combine max and min
strain_maxmin = vertcat(maxind, minind);

% Sort max and min line numbers so each anodic/cathodic cycle can be
% accurately picked out
strain_echem_cyclebounds =  sort(strain_maxmin, 'ascend');
strain_echem_sweep_num = numel(strain_echem_cyclebounds);

% Chop up echem potential data into anodic and cathodic cycles
strain_echem_pot = cell(1,strain_echem_sweep_num);
i = 1;
x = 0;
y = strain_echem_cyclebounds(i);
while strain_echem_sweep_num - i +1 > 1
   strain_echem_pot{i} = org_strain_echem_pot(x + 1:y);
   x = strain_echem_cyclebounds(i);
   i = i + 1;
```

```
    y = strain_echem_cyclebounds(i);
end
strain_echem_pot{i} = org_strain_echem_pot(x:y); %gets the last bit of data
strain_echem_pot{i+1} = org_strain_echem_pot(y:strain_num_data);

% Chop up echem current data into anodic and cathodic cycles
strain_echem_cur = cell(1,strain_echem_sweep_num);
i = 1;
x = 0;
y = strain_echem_cyclebounds(i);
while strain_echem_sweep_num - i + 1 > 1
    strain_echem_cur{i} = org_strain_echem_cur(x + 1:y);
    x = strain_echem_cyclebounds(i);
    i = i + 1;
    y = strain_echem_cyclebounds(i);
end
strain_echem_cur{i} = org_strain_echem_cur(x:y); %gets the last bit of data
strain_echem_cur{i+1} = org_strain_echem_cur(y:strain_num_data);



%% Chop up strain data

strain_num_data = numel(org_strain); %total number of points in the data array

% Find line number for max and min of each cycle
[pot_max, maxind] = findpeaks(org_strain_pot, 'MinPeakProminence', 0.8);
DataInv = 1.01*max(org_strain_pot) - org_strain_pot;
[pot_min, minind] = findpeaks(DataInv, 'MinPeakProminence', 0.8);

% Combine max and min
maxmin = vertcat(maxind, minind);

% Sort max and min line numbers so each anodic/cathodic cycle can be
% accurately picked out
strain_cyclebounds =  sort(maxmin, 'ascend');
strain_sweep_num = numel(strain_cyclebounds);

% Chop up time data into anodic and cathodic cycles
strain_time = cell(1,strain_sweep_num);
org_strain_cycle_time = cell(1,strain_sweep_num);
i = 1;
x = 0;
y = strain_cyclebounds(i);
while strain_sweep_num - i + 1 > 1
    strain_time{i} = org_strain_time(x + 1:y); %this variable will change throughout program
```

```
    org_strain_cycle_time{i} = strain_time{i};
    x = strain_cyclebounds(i);
    i = i + 1;
    y = strain_cyclebounds(i);
end
strain_time{i} = org_strain_time(x:y); %gets the last bit of data
strain_time{i+1} = org_strain_time(y:strain_num_data);

% Chop up potential data into anodic and cathodic cycles
strain_pot = cell(1,strain_sweep_num);
org_strain_cycle_pot = cell(1,strain_sweep_num);
i = 1;
x = 0;
y = strain_cyclebounds(i);
while strain_sweep_num - i + 1 > 1
    strain_pot{i} = org_strain_pot(x + 1:y);
    org_strain_cycle_pot{i} = strain_pot{i};
    x = strain_cyclebounds(i);
    i = i + 1;
    y = strain_cyclebounds(i);
end
strain_pot{i} = org_strain_pot(x:y); %gets the last bit of data
strain_pot{i+1} = org_strain_pot(y:strain_num_data);

% Chop up stress data into anodic and cathodic cycles
strain = cell(1,strain_sweep_num);
org_cycle_strain = cell(1,strain_sweep_num);
i = 1;
x = 0;
y = strain_cyclebounds(i);
while strain_sweep_num - i + 1 > 1
    strain{i} = org_strain(x + 1:y);
    org_cycle_strain{i} = strain{i};
    x = strain_cyclebounds(i);
    i = i + 1;
    y = strain_cyclebounds(i);
end
strain{i} = org_strain(x:y); %gets the last bit of data
strain{i+1} = org_strain(y:strain_num_data);

% NaN values
for i = 1:strain_sweep_num +1
    strain_pot{i}(isnan(strain_pot{i})) = [];
    strain_time{i}(isnan(strain_time{i})) = [];
    strain{i}(isnan(strain{i})) = [];
    strain_echem_pot{i}(isnan(strain_echem_pot{i})) = [];
```

```
    strain_echem_cur{i}(isnan(strain_echem_cur{i})) = [];
end

end

%% Smooth stress data

% Resample stress and current data over an evenly spaced voltage vector
skip = 0.01;
if material == 0 % picks which interval to use
    stress_pot_even1 = 3.4:skip:4.6; % LMO
elseif material == 1
    stress_pot_even1 = 2.4:skip:4.3; % LFP
elseif material == 2
    stress_pot_even1 = 1.7:skip:2.7; % PAQ
elseif material == 3
    stress_pot_even1 = 1:skip:4;     % ITO
elseif material == 4
    stress_pot_even1 = 2.4:skip:4.5; % LFP range up to 4.4 V
end

stress_interp = cell(1,sweep_num+1);
cur_interp = cell(1,sweep_num+1);
echem_cur_interp = cell(1,sweep_num+1);
echem_pot_interp = cell(1,sweep_num+1);
for i = 1:sweep_num+1

    % Remove duplicate voltage values
    [stress_pot{i}, ind_unique,~] = unique(stress_pot{i});
    stress{i} = stress{i}(ind_unique);
    stress_cur{i} = stress_cur{i}(ind_unique);
%     [echem_pot{i}, ind_unique,~] = unique(echem_pot{i});
%     echem_pot{i} = echem_pot{i}(ind_unique);
%     echem_cur{i} = echem_cur{i}(ind_unique);

    % Interpolate the stress over an evenly spaced voltage vector
    stress_interp{i} = interp1(stress_pot{i}, stress{i}, stress_pot_even1);
    cur_interp{i} = interp1(stress_pot{i}, stress_cur{i}, stress_pot_even1);
%     echem_cur_interp{i} = interp1(echem_pot{i}, echem_cur{i}, stress_pot_even1);
%     echem_pot_interp{i} = interp1(echem_pot{i}, echem_pot{i}, stress_pot_even);

    % Plot new data
    %plot(ax_stress(1), stress_pot_even, stress_interp{i}, '.-r')

end
```

```
% Smooth stress data


stress_smooth = cell(1,sweep_num+1);
for i = 1:sweep_num+1

    % Smooth the stress
    stress_smooth{i} = smooth(stress_interp{i}, stress_smooth_kernel);

    %Remove any stress values that were extropolated during smoothing
    ind_nan = isnan(stress_interp{i}); % assign indices to NaN values in
    %the vector that are outside of potential range
    stress_smooth{i}(ind_nan) = NaN; % get rid of extrapolated values

end

if plot1 == 1
% Plot original stress and smoothed stress together
for i = 1:sweep_num+1
    figure;
    plot(stress_pot{i}, stress{i}, stress_pot_even1, stress_smooth{i});
    r = rem(i,2);
    if r == 0
        j = i/2;
        anod_cath = 'cathodic';
    else
        j = (i+1)/2;
        anod_cath = 'anodic';
    end

    cycletitle = (['Cycle ' num2str(j) ' ' anod_cath ' Stress']);
    title(cycletitle);
    legend('original', 'smoothed', 'Location', 'best');
end
end

% Flip stress so that all contractions are negative
if flip_stress_choice == 1
for i = 1:sweep_num+1

    stress_smooth{i} = -1*stress_smooth{i};

end
end
%% %% Smooth strain data
```

```
% Resample stress and current data over an evenly spaced voltage vector
skip = 0.01;
if material == 0 % picks which interval to use
   strain_pot_even1 = 3.4:skip:4.6; % LMO
elseif material == 1
   strain_pot_even1 = 2.4:skip:4.3; % LFP
elseif material == 2
   strain_pot_even1 = 1.7:skip:2.7; % PAQ
elseif material == 3
   strain_pot_even1 = 1:skip:4;     % ITO
elseif material == 4
   strain_pot_even1 = 2.4:skip:4.5; % LFP range up to 4.4 V
end

strain_interp = cell(1,strain_sweep_num+1);
strain_cur_interp = cell(1,strain_sweep_num+1);
for i = 1:strain_sweep_num+1

   % Remove duplicate voltage values
   [strain_pot{i}, ind_unique,~] = unique(strain_pot{i});
   strain{i} = strain{i}(ind_unique);
   [strain_echem_pot{i}, ind_unique,~] = unique(strain_echem_pot{i});
   strain_echem_cur{i} = strain_echem_cur{i}(ind_unique);
%     strain_echem_pot{i} = strain_echem_pot{i}(ind_unique);

   % Interpolate the strain over an evenly spaced voltage vector
   strain_interp{i} = interp1(strain_pot{i}, strain{i}, strain_pot_even1);
   strain_cur_interp{i} = interp1(strain_echem_pot{i}, strain_echem_cur{i}, strain_pot_even1);
   strain_cur_interp{i} = strain_cur_interp{i}';
   strain_pot_interp{i} = interp1(strain_echem_pot{i}, strain_echem_pot{i}, strain_pot_even1);
   strain_pot_interp{i} = strain_pot_interp{i}';
end
strain_pot_even1 = strain_pot_even1';

% Smooth strain data

strain_smooth = cell(1,strain_sweep_num+1);
for i = 1:strain_sweep_num+1

   % Smooth the stress
   strain_smooth{i} = smooth(strain_interp{i}, strain_smooth_kernel);

   %Remove any stress values that were extropolated during smoothing
   ind_nan = isnan(strain_interp{i}); % assign indices to NaN values in
   %the vector that are outside of potential range
```

```
    strain_smooth{i}(ind_nan) = NaN; % get rid of extrapolated values

end


A = gt(sweep_num, strain_sweep_num); %determine if more stress or strain data

if A == 1
    sweep = strain_sweep_num+1;
else
    sweep = sweep_num+1;
end

if plot2 == 1
% Plot original strain and smoothed strain together
for i = 1:strain_sweep_num+1
    figure;
    plot(strain_pot{i}, strain{i}, strain_pot_even1, strain_smooth{i});
    r = rem(i,2);
    if r == 0
        j = i/2;
        anod_cath = 'cathodic';
    else
        j = (i+1)/2;
        anod_cath = 'anodic';
    end

    cycletitle = (['Cycle ' num2str(j) ' ' anod_cath ' Strain']);
    title(cycletitle);
    legend('original', 'smoothed', 'Location', 'best');
end
end


%% Pick your derivative method!


% METHOD 1: Derivative of the smoothed stress

stress_deriv = cell(1,sweep_num+1);
% METHOD 1: Derivative of the smoothed stress
% for i = 1:sweep_num+1
%     stress_deriv{i} = gradient(stress_smooth{i},stress_pot_even);
% end

% METHOD 2: Elizabeth's alternative derivative method. n determines how large the
```

```
% interval over which the derivative is taken. n is odd.

for i = 1:sweep_num+1
   stress_deriv{i} = gradient_mod(stress_smooth{i}, stress_pot_even1, stress_deriv_kernel);

   %Remove any stress values that were extropolated during taking the
   %derivative
   ind_nan = isnan(stress_interp{i}); % assign indices to NaN values in
   %the vector that are outside of potential range
   stress_deriv{i}(ind_nan) = NaN; % get rid of extrapolated values
end

%% Pick your derivative method!

strain_deriv = cell(1,strain_sweep_num+1);

% METHOD 1: Derivative of the smoothed strain
% for i = 1:strain_sweep_num+1
%     strain_deriv{i} = gradient(strain_smooth{i},strain_pot_even);
% end

% METHOD 2: Elizabeth's alternative derivative method. n determines how large the
% interval over which the derivative is taken. n is odd.

for i = 1:strain_sweep_num+1
   strain_deriv{i} = gradient_mod(strain_smooth{i}, strain_pot_interp{i}, strain_deriv_kernel);

   %Remove any stress values that were extropolated during taking the
   %derivative
   ind_nan = isnan(strain_interp{i}); % assign indices to NaN values in
   %the vector that are outside of potential range
   strain_deriv{i}(ind_nan) = NaN; % get rid of extrapolated values
end

%% Resistance correction

if resistance_correction == 1
   % Shift potential by a constant
   for i = 1:sweep
      %If stress values need to be shifted
      stress_pot{i} = stress_pot{i}-Vstress;
      echem_pot{i} = echem_pot{i}-Vstress;

      %If strain values need to be shifted
      strain_echem_pot{i} = strain_echem_pot{i}-Vstrain;
      strain_pot_interp{i} = strain_pot_interp{i}-Vstrain;
```

```
end
stress_pot_even1 = stress_pot_even1-Vstress;
strain_pot_even1 = strain_pot_even1-Vstrain;

% Uses V_new = V_original - IR to shift potential, non-linear shift
for i = 1:sweep
    % If stress values need to be shifted
    stress_pot{i} = stress_pot{i}-rstress.*stress_cur{i}*10^-6;

    % If strain values need to be shifted
    strain_echem_pot{i} = strain_echem_pot{i}-rstrain.*strain_echem_cur{i}*10^-3;
    strain_pot_interp{i} = strain_pot_interp{i}-rstrain.*strain_cur_interp{i}*10^-3;
end
 stress_pot_even1 = stress_pot_even1-rstress.*cur_interp{4}*10^-6;
 strain_pot_even1 = strain_pot_even1-rstrain.*strain_cur_interp{4}*10^-3;



 %% Re-interpolate post potential correction

skip = 0.01;
if material == 0 % picks which interval to use
    stress_pot_even = 3.4:skip:4.6; % LMO
    strain_pot_even = 3.4:skip:4.6;
elseif material == 1
    stress_pot_even = 2.4:skip:4.3; % LFP
    strain_pot_even = 2.4:skip:4.3;
elseif material == 2
    stress_pot_even = 1.7:skip:2.7; % PAQ
    strain_pot_even = 1.7:skip:2.7;
elseif material == 3
    stress_pot_even = 1:skip:4;     % ITO
    strain_pot_even = 1:skip:4;
elseif material == 4
    stress_pot_even = 2.4:skip:4.5; % LFP range up to 4.4 V
    strain_pot_even = 2.4:skip:4.5;
end

    ind = find(isnan(stress_pot_even1));
    stress_pot_even1(ind)= [];
    ind = find(isnan(strain_pot_even1));
    strain_pot_even1(ind)= [];

for i = 1:sweep

    % Remove NaN values, make those cells empty
```

```
        ind = find(isnan(stress_smooth{i}));
        stress_smooth{i}(ind)= [];
        ind = find(isnan(stress_deriv{i}));
        stress_deriv{i}(ind)= [];
        ind = find(isnan(cur_interp{i}));
        cur_interp{i}(ind)= [];
        stress_pot_even2 = stress_pot_even1;
        stress_pot_even2(ind)= [];

        ind = find(isnan(strain_smooth{i}));
        strain_smooth{i}(ind)= [];
        ind = find(isnan(strain_deriv{i}));
        strain_deriv{i}(ind)= [];
        strain_pot_even2 = strain_pot_even1;
        strain_pot_even2(ind)= [];

        % Interpolate the stress over an evenly spaced voltage vector
        %stress_interp{i} = interp1(stress_pot_even1, stress_interp{i}, stress_pot_even);
        cur_interp{i} = interp1(stress_pot_even2, cur_interp{i}, stress_pot_even);
        echem_cur_interp{i} = interp1(echem_pot{i}, echem_cur{i}, stress_pot_even);
    %    echem_pot_interp{i} = interp1(echem_pot{i}, echem_pot{i}, stress_pot_even);
        stress_smooth{i} = interp1(stress_pot_even2, stress_smooth{i}, stress_pot_even);
        stress_deriv{i} = interp1(stress_pot_even2, stress_deriv{i}, stress_pot_even);

       % Interpolate the stress over an evenly spaced voltage vector
        strain_interp{i} = interp1(strain_pot{i}, strain{i}, strain_pot_even);
        strain_cur_interp{i} = interp1(strain_echem_pot{i}, strain_echem_cur{i}, strain_pot_even);
        strain_cur_interp{i} = strain_cur_interp{i}';
        strain_pot_interp{i} = interp1(strain_echem_pot{i}, strain_echem_pot{i}, strain_pot_even);
        strain_pot_interp{i} = strain_pot_interp{i}';
        strain_smooth{i} = interp1(strain_pot_even2, strain_smooth{i}, strain_pot_even);
        strain_deriv{i} = interp1(strain_pot_even2, strain_deriv{i}, strain_pot_even);

    end

    for i = 1:sweep
        strain_echem_check{i} = gradient_mod(strain_cur_interp{i}, strain_pot_even,
strain_deriv_kernel);
        stress_echem_check{i} = gradient_mod(cur_interp{i}, stress_pot_even,
stress_deriv_kernel);

        figure;
        hold on
        plotyy(stress_pot_even, stress_echem_check{i}, strain_pot_even, strain_echem_check{i})
        legend('stress CV', 'strain CV');
```

```
        plot(stress_pot_even, zeros(1,211),'k')

        r = rem(i,2);
        if r == 0
            j = i/2;
            anod_cath = 'cathodic';
        else
            j = (i+1)/2;
            anod_cath = 'anodic';
        end

        cycletitle = (['Cycle ' num2str(j) ' ' anod_cath]);
        title(cycletitle);


    end
else
        skip = 0.01;
    if material == 0 % picks which interval to use
        stress_pot_even = 3.4:skip:4.6; % LMO
        strain_pot_even = 3.4:skip:4.6;
    elseif material == 1
        stress_pot_even = 2.4:skip:4.3; % LFP
        strain_pot_even = 2.4:skip:4.3;
    elseif material == 2
        stress_pot_even = 1.7:skip:2.7; % PAQ
        strain_pot_even = 1.7:skip:2.7;
    elseif material == 3
        stress_pot_even = 1:skip:4;     % ITO
        strain_pot_even = 1:skip:4;
    elseif material == 4
        stress_pot_even = 2.4:skip:4.5; % LFP range up to 4.4 V
        strain_pot_even = 2.4:skip:4.5;
    end
end


    %% Compare stress and strain echem
if plot3 == 1

for i = 1:2:sweep

    j = i + 1;

    echemboth = figure('units','inch','position',[1.5,2,5,4], 'outerposition', [1,1,6,5.5]);
    axi(1) = subplot('position',[0.15, 0.2, 0.69, 0.7]);
```

```
    [ax, p1, p2] = plotyy([echem_pot{i}', echem_pot{j}'], [echem_cur{i}', echem_cur{j}'],...
        [strain_echem_pot{i}', strain_echem_pot{j}'], [strain_echem_cur{i}',
strain_echem_cur{j}']);
    hold on
    p1.Color = 'b';
    p2.Color = 'r';
    ax(1).YColor = 'b';
    ax(2).YColor = 'r';

    ylabel(ax(1), 'Stress Current, I ({\mu}A cm^{-2})')
    ylabel(ax(2), 'Strain Current, I (mA g^{-1})');
    xlabel(ax(1), 'Potential, E (V vs Li)');
    set(ax(1),'FontSize',15);
    set(ax(2),'FontSize',15);

    if material == 0 % pick which material
        ax(1).XLim = [3.5 4.5]; % LMO
        ax(2).XLim = [3.5 4.5];
        ax(1).XTick = [3.5 3.6 3.7 3.8 3.9 4.0 4.1 4.2 4.3 4.4 4.5];
        ax(1).XTickLabel = {'3.5','','','','4.0','','','','4.5'};
    elseif material == 1
        ax(1).XLim = [2.6 4.2]; % LFP
        ax(2).XLim = [2.6 4.2];
        ax(1).XTick = [2.6 2.7 2.8 2.9 3.0 3.1 3.2 3.3 3.4 3.5 3.6 3.7 3.8 3.9 4.0 4.1 4.2];
        ax(1).XTickLabel = {'2.6', '','','3.0','','','3.4', '','','3.8','','','4.2'};
        ax(2).XTick = [2.6 2.7 2.8 2.9 3.0 3.1 3.2 3.3 3.4 3.5 3.6 3.7 3.8 3.9 4.0 4.1 4.2];
    elseif material == 2
        ax(1).XLim = [1.8 2.6]; % PAQ
        ax(2).XLim = [1.8 2.6];
        ax(1).XTick = [1.8 1.9 2.0 2.1 2.2 2.3 2.4 2.5 2.6];
        ax(1).XTickLabel = {'1.8','','2.0','','2.2','','2.4','','2.6'};
        ax(2).XTick = [1.8 1.9 2.0 2.1 2.2 2.3 2.4 2.5 2.6];
    elseif material == 3
        ax(1).XLim = [1.0 4.0];   % ITO
        ax(2).XLim = [1.0 4.0];
        ax(1).XTick = [1.0 1.2 1.4 1.6 1.8 2.0 2.2 2.4 2.6 2.8 3.0 3.2 3.4 3.6 3.8 4.0];
        ax(1).XTickLabel = {'1.0', '', '', '', '', '2.0', '', '', '', '', '3.0', '', '', '', '', '4.0'};
        ax(2).XTick = [1.0 1.2 1.4 1.6 1.8 2.0 2.2 2.4 2.6 2.8 3.0 3.2 3.4 3.6 3.8 4.0];
    elseif material == 4
        ax(1).XLim = [2.6 4.4]; % LFP with limit up to 4.4 V
        ax(2).XLim = [2.6 4.4];
        ax(1).XTick = [2.6 2.7 2.8 2.9 3.0 3.1 3.2 3.3 3.4 3.5 3.6 3.7 3.8 3.9 4.0 4.1 4.2 4.3 4.4];
        ax(1).XTickLabel = {'2.6','','','2.9','','','3.2','','','3.5','','','3.8','','','4.1','','','4.4'};
        ax(2).XTick = [2.6 2.7 2.8 2.9 3.0 3.1 3.2 3.3 3.4 3.5 3.6 3.7 3.8 3.9 4.0 4.1 4.2 4.3 4.4];
    end
```

```
    k = j/2;
    cycletitle = (['Cycle ' num2str(k)]);
    title(cycletitle);

end
end


    %% Echem peak splitting
if peak_splitting_choice == 1
for i = 1:2:sweep

    j = i + 1;
    k = (i+1)/2;
    [stress_cur_max, maxind] = findpeaks(echem_cur{i}, 'MinPeakProminence', 0.2,
'MinPeakDistance', 10);
    stress_potmax_anod(k) = echem_pot{i}(maxind);
    stress_curmax_anod(k) = stress_cur_max;
    [stress_cur_max, maxind] = findpeaks(echem_cur{j}, 'MinPeakProminence', 0.2,
'MinPeakDistance', 10);
    stress_potmax_cath(k) = echem_pot{j}(maxind);
    stress_curmax_cath(k) = stress_cur_max;

    [strain_cur_max, maxind] = findpeaks(strain_cur_interp{i}, 'MinPeakProminence', 0.8,
'MinPeakDistance', 20);
    strain_potmax_anod(k) = stress_pot_even(maxind);
    strain_curmax_anod(k) = strain_cur_max;
    [strain_cur_max, maxind] = findpeaks(strain_cur_interp{j}, 'MinPeakProminence', 0.8,
'MinPeakDistance', 10);
    strain_potmax_cath(k) = stress_pot_even(maxind);
    strain_curmax_cath(k) = strain_cur_max;

    cycle(k) = k;
end

    stress_cur_split = stress_potmax_anod - stress_potmax_cath;
    strain_cur_split = strain_potmax_anod - strain_potmax_cath;


    figure('units','inch','position',[1.5,2,5,4], 'outerposition', [1,1,6,5.5]);
    subplot('position',[0.15, 0.2, 0.69, 0.7]);

    plot(cycle, stress_cur_split, cycle, strain_cur_split);
    hold on
```

```
    ylabel( 'Peak Split (V)')
    xlabel( 'Cycle');
    ax=gca;
    set(ax,'FontSize',15);
    legend(['stress', 'strain'])

    title('Peak Splitting');
end

%% Compare stress and strain
if plot4 == 1
for i = 1:2:sweep

    j = i + 1;

    both = figure; %make figure

    axis1 = axes('Parent', both, 'Ycolor', [0 0 1],...
        'FontSize', 15, 'position',[0.15, 0.2, 0.69, 0.7]);
    box(axis1, 'on');
    hold(axis1, 'on');

    plot(stress_pot_even', stress_smooth{i}, 'Parent', axis1, 'Color', [0 0 1]);
    plot(stress_pot_even', stress_smooth{j}, 'Parent', axis1, 'Color', [0 0 1]);
    xlabel('Potential (V vs Li/Li^{+})');
    ylabel('-1*Stress (N m^{-1})');
    hold on

    k = j/2;
    cycletitle = (['Cycle ' num2str(k)]);
    title(cycletitle);

   axis2 = axes('Parent',both,'HitTest','off','Color','none',...
        'YColor',[1 0 0],...
        'YAxisLocation','right',...
        'FontSize',15,...
        'Position',[0.15 0.2 0.69 0.7]);
    hold(axis2, 'on');

    if material == 0 % pick which material
        axis1.XLim = [3.5 4.5]; % LMO
        axis2.XLim = [3.5 4.5];
        axis1.XTick = [3.5 3.6 3.7 3.8 3.9 4.0 4.1 4.2 4.3 4.4 4.5];
        axis1.XTickLabel = {'3.5','','','','','4.0','','','','','4.5'};
        axis2.XTick = [3.5 3.6 3.7 3.8 3.9 4.0 4.1 4.2 4.3 4.4 4.5];
        axis2.XTickLabel = {'','','','','','','','','','',''};
```

```
    elseif material == 1
        axis1.XLim = [2.6 4.2]; % LFP
        axis2.XLim = [2.6 4.2];
        axis1.XTick = [2.6 2.7 2.8 2.9 3.0 3.1 3.2 3.3 3.4 3.5 3.6 3.7 3.8 3.9 4.0 4.1 4.2];
        axis1.XTickLabel = {'2.6', ','','3.0','','','3.4', ','','','3.8','','','4.2'};
        axis2.XTick = [2.6 2.7 2.8 2.9 3.0 3.1 3.2 3.3 3.4 3.5 3.6 3.7 3.8 3.9 4.0 4.1 4.2];
        axis2.XTickLabel = {'', ','','','','','','', ','','','','','','','','};
    elseif material == 2
        axis1.XLim = [1.8 2.6]; % PAQ
        axis2.XLim = [1.8 2.6];
        axis1.XTick = [1.8 1.9 2.0 2.1 2.2 2.3 2.4 2.5 2.6];
        axis1.XTickLabel = {'1.8','','2.0','','2.2','','2.4','','2.6'};
        axis2.XTick = [1.8 1.9 2.0 2.1 2.2 2.3 2.4 2.5 2.6];
        axis2.XTickLabel = {'','','','','','','','','};
    elseif material == 3
        axis1.XLim = [1.0 4.0];   % ITO
        axis2.XLim = [1.0 4.0];
        axis1.XTick = [1.0 1.2 1.4 1.6 1.8 2.0 2.2 2.4 2.6 2.8 3.0 3.2 3.4 3.6 3.8 4.0];
        axis1.XTickLabel = {'1.0', '', '', '', '', '2.0', '', '', '', '', '3.0', '', '', '', '', '4.0'};
        axis2.XTick = [1.0 1.2 1.4 1.6 1.8 2.0 2.2 2.4 2.6 2.8 3.0 3.2 3.4 3.6 3.8 4.0];
        axis2.XTickLabel = {'', '', '', '', '', '', '', '', '', '', '', '', '', '', '', ''};
    elseif material == 4
        axis1.XLim = [2.6 4.4]; % LFP with limit up to 4.4 V
        axis2.XLim = [2.6 4.4];
        axis1.XTick = [2.6 2.7 2.8 2.9 3.0 3.1 3.2 3.3 3.4 3.5 3.6 3.7 3.8 3.9 4.0 4.1 4.2 4.3 4.4];
        axis1.XTickLabel = {'2.6','','','2.9','','','3.2','','','3.5','','','3.8','','','4.1','','','4.4'};
        axis2.XTick = [2.6 2.7 2.8 2.9 3.0 3.1 3.2 3.3 3.4 3.5 3.6 3.7 3.8 3.9 4.0 4.1 4.2 4.3 4.4];
        axis2.XTickLabel = {'','','','','','','','','','','','','','','','','','','','','};
    end

    plot(strain_pot_even,strain_smooth{i},'Parent',axis2,'Color',[1 0 0]);
    plot(strain_pot_even, strain_smooth{j},'Parent',axis2,'Color',[1 0 0]);
    ylabel('Strain (%)');

end
end
%% Calculate ratio of derivatives
if ratio_derivatives_choice == 1

deriv_ratio{i} = cell(1,sweep+1);
for i = 1:sweep
    %  use if stress or strain needs to be flipped to make data work
    if rem(i,2) == 0 %for cathodic scans
        dstress = -1*stress_deriv{i}; % all peaks point in positive direction
        dstrain = -1*strain_deriv{i};
    else %for anodic scans
```

```
        dstress = stress_deriv{i};
        dstrain = strain_deriv{i};
    end

    stressmax = max(dstress); % normalize to a 0 to 1 ranges and shift up two
    dstress = dstress./stressmax+2;
    strainmax = max(dstrain);
    dstrain = dstrain./strainmax+2;

    deriv_ratio{i} = rdivide(dstress, dstrain)-1;

    %Plot the normalized data

    normalized = figure; %make figure

    axis1 = axes('Parent', normalized, 'Ycolor', [0 0 0],...
        'FontSize', 15,...
        'position',[0.15, 0.2, 0.69, 0.7]);
    box(axis1, 'on');
    hold(axis1, 'on');

    p1 = plot(strain_echem_pot{i}, strain_echem_cur{i}, 'Parent', axis1, 'DisplayName',
'Current',...
        'Color', [0 0 0], 'LineStyle', '--');
    xlabel('Potential, E (V vs Li)');
    ylabel('Current (\muA g^{-1})');
    hold on

   axis2 = axes('Parent',normalized,'HitTest','off','Color','none',...
        'YColor',[0 0 0],...
        'YAxisLocation','right',...
        'FontSize',15,...
        'Position',[0.15 0.2 0.69 0.7]);
    hold(axis2, 'on');

    if material == 0 % pick which material
        axis1.XLim = [3.5 4.5]; % LMO
        axis2.XLim = [3.5 4.5];
        axis1.XTick = [3.5 3.6 3.7 3.8 3.9 4.0 4.1 4.2 4.3 4.4 4.5];
        axis1.XTickLabel = {'3.5','','','','','4.0','','','','','4.5'};
        axis2.XTick = [3.5 3.6 3.7 3.8 3.9 4.0 4.1 4.2 4.3 4.4 4.5];
        axis2.XTickLabel = {'','','','','','','','','','',''};
    elseif material == 1
        axis1.XLim = [2.6 4.2]; % LFP
        axis2.XLim = [2.6 4.2];
        axis1.XTick = [2.6 2.7 2.8 2.9 3.0 3.1 3.2 3.3 3.4 3.5 3.6 3.7 3.8 3.9 4.0 4.1 4.2];
```

```
    axis1.XTickLabel = {'2.6', ','','3.0','','','3.4', ','','3.8','','','4.2'};
    axis2.XTick = [2.6 2.7 2.8 2.9 3.0 3.1 3.2 3.3 3.4 3.5 3.6 3.7 3.8 3.9 4.0 4.1 4.2];
    axis2.XTickLabel = {'', ','','','','','','', ','','','','','',''};
elseif material == 2
    axis1.XLim = [1.8 2.6]; % PAQ
    axis2.XLim = [1.8 2.6];
    axis1.XTick = [1.8 1.9 2.0 2.1 2.2 2.3 2.4 2.5 2.6];
    axis1.XTickLabel = {'1.8','','2.0','','2.2','','2.4','','2.6'};
    axis2.XTick = [1.8 1.9 2.0 2.1 2.2 2.3 2.4 2.5 2.6];
    axis2.XTickLabel = {'','','','','','','','',''};
elseif material == 3
    axis1.XLim = [1.0 4.0];   % ITO
    axis2.XLim = [1.0 4.0];
    axis1.XTick = [1.0 1.2 1.4 1.6 1.8 2.0 2.2 2.4 2.6 2.8 3.0 3.2 3.4 3.6 3.8 4.0];
    axis1.XTickLabel = {'1.0', '', '', '', '', '2.0', '', '', '', '', '3.0', '', '', '', '', '4.0'};
    axis2.XTick = [1.0 1.2 1.4 1.6 1.8 2.0 2.2 2.4 2.6 2.8 3.0 3.2 3.4 3.6 3.8 4.0];
    axis2.XTickLabel = {'', '', '', '', '', '', '', '', '', '', '', '', '', '', '', ''};
elseif material == 4
    axis1.XLim = [2.6 4.4]; % LFP with limit up to 4.4 V
    axis2.XLim = [2.6 4.4];
    axis1.XTick = [2.6 2.7 2.8 2.9 3.0 3.1 3.2 3.3 3.4 3.5 3.6 3.7 3.8 3.9 4.0 4.1 4.2 4.3 4.4];
    axis1.XTickLabel = {'2.6','','','2.9','','','3.2','','','3.5','','','3.8','','','4.1','','','4.4'};
    axis2.XTick = [2.6 2.7 2.8 2.9 3.0 3.1 3.2 3.3 3.4 3.5 3.6 3.7 3.8 3.9 4.0 4.1 4.2 4.3 4.4];
    axis2.XTickLabel = {'','','','','','','','','','','','','','','','','','','','',''};
end

    p2 = plot(stress_pot_even', dstress,'Parent', axis2, 'DisplayName', 'Stress derivative', 'Color', [0
0 1]);
    p3 = plot(strain_pot_even, dstrain,'Parent',axis2,'DisplayName', 'Strain derivative','Color', [1 0
0]);
    ylabel('Normalized Derivatives');

    M = [p1 p2 p3];
    legend1 = legend(M, 'Current', 'Stress derivative', 'Strain derivative');
    set(legend1, 'EdgeColor', 'none', 'Color', 'none');

    r = rem(i,2);
    if r == 0
        j = i/2;
        anod_cath = 'cathodic';
        axis1.YDir = 'reverse';
    else
        j = (i+1)/2;
        anod_cath = 'anodic';
    end
```

```
    cycletitle = (['Cycle ' num2str(j) ' ' anod_cath]);
    title(cycletitle);

end

% Plot ratio of derivatives
for i = 1:sweep

    stiff = figure;
    axis = axes('Parent', stiff, ...
        'FontSize', 15,...
        'position',[0.15, 0.2, 0.69, 0.7]);
    box(axis, 'on');
    hold(axis, 'on');

    if material == 0 % pick which material
        axis.XLim = [3.5 4.5]; % LMO
        axis.XTick = [3.5 3.6 3.7 3.8 3.9 4.0 4.1 4.2 4.3 4.4 4.5];
        axis.XTickLabel = {'3.5','','','','4.0','','','','4.5'};
    elseif material == 1
        axis.XLim = [2.6 4.2]; % LFP
        axis.XTick = [2.6 2.7 2.8 2.9 3.0 3.1 3.2 3.3 3.4 3.5 3.6 3.7 3.8 3.9 4.0 4.1 4.2];
        axis.XTickLabel = {'2.6', '','','3.0','','','3.4', '','','3.8','','','4.2'};
    elseif material == 2
        axis.XLim = [1.8 2.6]; % PAQ
        axis.XTick = [1.8 1.9 2.0 2.1 2.2 2.3 2.4 2.5 2.6];
        axis.XTickLabel = {'1.8','','2.0','','2.2','','2.4','','2.6'};
    elseif material == 3
        axis.XLim = [1.0 4.0];   % ITO
        axis.XTick = [1.0 1.2 1.4 1.6 1.8 2.0 2.2 2.4 2.6 2.8 3.0 3.2 3.4 3.6 3.8 4.0];
        axis.XTickLabel = {'1.0', '', '', '', '', '2.0', '', '', '', '', '3.0', '', '', '', '', '4.0'};
    elseif material == 4
        axis.XLim = [2.6 4.4]; % LFP with limit up to 4.4 V
        axis.XTick = [2.6 2.7 2.8 2.9 3.0 3.1 3.2 3.3 3.4 3.5 3.6 3.7 3.8 3.9 4.0 4.1 4.2 4.3 4.4];
        axis.XTickLabel = {'2.6','','','2.9','','','3.2','','','3.5','','','3.8','','','4.1','','','4.4'};
    end

    plot(stress_pot_even, deriv_ratio{i}, 'Parent', axis);
    hold on

    ylabel('Ratio of derivatives');
    xlabel('Potential, E (V vs Li)');

    % Build title
    r = rem(i,2);
    if r == 0
```

```
        j = i/2;
        sweepdirection = 'cathodic';
    else
        j = (i+1)/2;
        sweepdirection = 'anodic';
    end

    cycletitle = (['Cycle ' num2str(j) ' ' sweepdirection]);
    title(cycletitle);

end
end
%% Plot echem and strain and stress derivatives together in one panel
if plot5 == 1

ylabels{1} = 'Current';
ylabels{2} = 'Strain Derivative';
ylabels{3} = 'Stress Derivative';

for i = 1:sweep


    [ax, hlines] = plotyyy(echem_pot{i}, echem_cur{i},...
        strain_pot_interp{i}, strain_deriv{i},...
        stress_pot_even, stress_deriv{i}, ylabels);
    hlines(1).Color = 'k';
    hlines(1).LineStyle = '--';
    hlines(2).Color = 'r';
    hlines(3).Color = 'b';
    ax(1).YColor = 'k';
    ax(2).YColor = 'r';
    ax(3).YColor = 'b';
    ax(1).XLabel.String = 'Potential (V vs. Li)';
    ax(1).FontSize = 15;
    ax(2).FontSize = 15;
    ax(3).FontSize = 15;
    hold on

    r = rem(i,2);
    if r == 0
        j = i/2;
        anod_cath = 'cathodic';
        legend(hlines, 'Current','Strain derivative','Stress derivative', 'Location', 'southeast');
    else
        j = (i+1)/2;
        anod_cath = 'anodic';
```

```
        ax(3).YDir = 'reverse';
        ax(2).YDir = 'reverse';
        legend(hlines, 'Current','Strain','Stress', 'Location', 'northwest');
    end

    cycletitle = (['Cycle ' num2str(j) ' ' anod_cath]);
    title(cycletitle);

end
end


% Plot strain, strain derivative with echem
if plot6 == 1
for i = 1:2:strain_sweep_num+1

    % Allows last cycle to plot even if there's no cathodic sweep
    if i <= strain_sweep_num
        j = i + 1;
    else
            j = i;
    end


    % Stress figure
    hstrain = figure('units','inch','position',[1,0.5,5,6.3]);
    ax_strain(1) = subplot('position',[left, bot, width, height]);
    ax_strain(2) = subplot('position',[left, bot+height, width, height]);
    ax_strain(3) = subplot('position',[left, bot+height*2, width, height]);

    cycletitle = (['Cycle ' num2str((i+1)/2)]);

    % Plot stress
    plot(ax_strain(2), strain_pot_interp{i}, strain_interp{i}, 'linestyle', '-', 'Color', [.55 .51 .88]);
    hold(ax_strain(2), 'on');
    plot(ax_strain(2), strain_pot_interp{j}, strain_interp{j}, 'linestyle', '-', 'Color', [.4 .4 .4]);
    hold(ax_strain(2), 'on');

    % Plot echem
    plot(ax_strain(3), strain_pot_interp{i}, strain_cur_interp{i}, '-b')
    hold(ax_strain(3), 'on');
    plot(ax_strain(3), strain_pot_interp{j}, strain_cur_interp{j}, '-k') %labview data
    hold(ax_strain(3), 'on');
    title(cycletitle);
    legend('anodic', 'cathodic', 'Location', 'northwest');
```

```
    % Plot smoothed stress
    plot(ax_strain(2), strain_pot_interp{i}, strain_smooth{i}, '-b');
    hold(ax_strain(2), 'on');
    plot(ax_strain(2), strain_pot_interp{j}, strain_smooth{j}, '-k');
    hold(ax_strain(2), 'on');

    % Plot stress derivative
    plot(ax_strain(1), strain_pot_interp{i}, strain_deriv{i}, '-b');
    hold(ax_strain(1), 'on');
    plot(ax_strain(1), strain_pot_interp{j}, strain_deriv{j}, '-k');
    hold(ax_strain(1), 'on');

    % % Customize plot labels
    xlabel(ax_strain(1), 'Potential, E (V vs Li)');
    set (ax_strain(2), 'xtick', get(ax_strain(1),'xtick'), 'xticklabel', '');
    set (ax_strain(3), 'xtick', get(ax_strain(1),'xtick'), 'xticklabel', '');

    ylabel(ax_strain(2), 'Strain');
    ylabel(ax_strain(3), 'Current, I ({\mu}A)');
    ylabel(ax_strain(1), 'Strain Derivative');

    set(ax_strain(1),'FontSize',15);
    set(ax_strain(2),'FontSize',15);
    set(ax_strain(3),'FontSize',15);


    ax_strain(1).XLim = [2.6 4.4];
    ax_strain(2).XLim = [2.6 4.4];
    ax_strain(3).XLim = [2.6 4.4];
    ax_strain(1).XTick = [2.6 2.7 2.8 2.9 3.0 3.1 3.2 3.3 3.4 3.5 3.6 3.7 3.8 3.9 4.0 4.1 4.2 4.3 4.4];
    ax_strain(2).XTick = [2.6 2.7 2.8 2.9 3.0 3.1 3.2 3.3 3.4 3.5 3.6 3.7 3.8 3.9 4.0 4.1 4.2 4.3 4.4];
    ax_strain(3).XTick = [2.6 2.7 2.8 2.9 3.0 3.1 3.2 3.3 3.4 3.5 3.6 3.7 3.8 3.9 4.0 4.1 4.2 4.3 4.4];
    ax_strain(3).XTickLabel = {'2.6','','','2.9','','','3.2','','','3.5','','','3.8','','','4.1','','','4.4'};
end
end

% Plot echem, stress, and strain
if plot7 == 1
for i = 1:2:sweep_num+1

    % Allows last cycle to plot even if there's no cathodic sweep
    if i <= strain_sweep_num
       j = i + 1;
    else
          j = i;
    end
```

```
    figure; %echem
    set(gcf,'Position',[100 100 400 600])
    subplot(3,1,1);
    p = plot(echem_pot{i}, echem_cur{i}, echem_pot{j}, echem_cur{j});
    axis = gca;
%     xlabel(axis, 'Potential, E (V vs Li)');
    ylabel(axis, 'Current (\muA/cm^{2})');
    set(axis,'FontSize',10);
    legend('anodic', 'cathodic', 'Location', 'southeast');
    p(1).LineWidth = 2;
    p(2).LineWidth = 2;

    cycletitle = (['Cycle ' num2str(j/2) ' ' sweep]);
    title(cycletitle);


    subplot(3,1,2); %stress
    p = plot(stress_pot_even, stress_smooth{i}, stress_pot_even, stress_smooth{j});
    axis = gca;
%     xlabel(axis, 'Potential(V vs Li)');
    ylabel(axis, 'Stress (N/m)');
    set(axis,'FontSize',10);
    p(1).LineWidth = 2;
    p(2).LineWidth = 2;

    subplot(3,1,3); %strain
    p = plot(strain_pot_even, strain_smooth{i}, strain_pot_even, strain_smooth{j});
    axis = gca;
    xlabel(axis, 'Potential (V vs Li)');
    ylabel(axis, 'Strain (%)');
    set(axis,'FontSize',10);
    p(1).LineWidth = 2;
    p(2).LineWidth = 2;

end
end

% Plot echem, stress, and stress derivative
if plot8 == 1
for i = 1:2:sweep_num+1

    % Allows last cycle to plot even if there's no cathodic sweep
    if i <= sweep_num
        j = i + 1;
    else
```

```
        j = i;
    end

    figure; %echem
    set(gcf,'Position',[100 100 400 600])
    subplot(3,1,1);
    p = plot(echem_pot{i}, echem_cur{i}, echem_pot{j}, echem_cur{j});
    axis = gca;
%     xlabel(axis, 'Potential, E (V vs Li)');
    ylabel(axis, 'Current (\muA/cm^{2})');
    set(axis,'FontSize',10);
    legend('anodic', 'cathodic', 'Location', 'southeast');
    p(1).LineWidth = 2;
    p(2).LineWidth = 2;
    cycletitle = (['Stress - Cycle ' num2str(j/2) ' ' sweep]);
    title(cycletitle);

    subplot(3,1,2); %stress
    p = plot(stress_pot_even, stress_smooth{i}, stress_pot_even, stress_smooth{j});
    axis = gca;
%     xlabel(axis, 'Potential(V vs Li)');
    ylabel(axis, 'Stress (N/m)');
    set(axis,'FontSize',10);
    p(1).LineWidth = 2;
    p(2).LineWidth = 2;

    subplot(3,1,3); %strain
    p = plot(stress_pot_even, stress_deriv{i}, stress_pot_even, stress_deriv{j});
    axis = gca;
    xlabel(axis, 'Potential (V vs Li)');
    ylabel(axis, 'Stress derivative (N/m V)');
    set(axis,'FontSize',10);
    p(1).LineWidth = 2;
    p(2).LineWidth = 2;


end
end


% Plot echem, strain, and strain derivative
if plot9 == 1
for i = 1:2:sweep_num+1

    % Allows last cycle to plot even if there's no cathodic sweep
    if i <= strain_sweep_num
```

```
        j = i + 1;
    else
        j = i;
    end

    figure; %echem
    set(gcf,'Position',[100 100 400 600])
    subplot(3,1,1);
    p = plot(strain_echem_pot{i}, strain_echem_cur{i}, strain_echem_pot{j},
strain_echem_cur{j});
    axis = gca;
%     xlabel(axis, 'Potential, E (V vs Li)');
    ylabel(axis, 'Current (\muA/cm^{2})');
    set(axis,'FontSize',10);
    legend('anodic', 'cathodic', 'Location', 'southeast');
    p(1).LineWidth = 2;
    p(2).LineWidth = 2;
    cycletitle = (['Strain - Cycle ' num2str(j/2) ' ' sweep]);
    title(cycletitle);

    subplot(3,1,2); %stress
    p = plot(strain_pot_even, strain_smooth{i}, strain_pot_even, strain_smooth{j});
    axis = gca;
%     xlabel(axis, 'Potential(V vs Li)');
    ylabel(axis, 'Strain (%)');
    set(axis,'FontSize',10);
    p(1).LineWidth = 2;
    p(2).LineWidth = 2;

    subplot(3,1,3); %strain
    p = plot(strain_pot_even, strain_deriv{i}, strain_pot_even, strain_deriv{j});
    axis = gca;
    xlabel(axis, 'Potential (V vs Li)');
    ylabel(axis, 'Strain derivative (%/V)');
    set(axis,'FontSize',10);
    p(1).LineWidth = 2;
    p(2).LineWidth = 2;


end
end

%% Plot integrated current with stress or strain
if plot10 == 1
int = cell(1,sweep_num+1);
```

```
for i = 1:2:sweep

    temp_pot = strain_pot_even;
    temp_cur = strain_cur_interp{i};
    temp_pot(isnan(temp_cur)) = [];
    temp_cur(isnan(temp_cur)) = [];
    int{i} = cumtrapz(temp_cur);


    figure;
    plotyy(strain_pot_even, strain_smooth{i}, temp_pot, -1*int{i});
    legend('strain', 'charge')

    cycletitle = (['Cycle ' num2str(i) ' Anodic']);
    title(cycletitle);

    clear temp_pot temp_cur
end


for i = 2:2:sweep

    temp_pot = strain_pot_even;
    temp_cur = strain_cur_interp{i};
    temp_pot(isnan(temp_cur)) = [];
    temp_cur(isnan(temp_cur)) = [];
    int{i} = cumtrapz(temp_cur);


    figure;
    plotyy(strain_pot_even, strain_smooth{i}, temp_pot, int{i});
    legend('strain', 'charge')

    cycletitle = (['Cycle ' num2str(i) ' Cathodic']);
    title(cycletitle);

    clear temp_pot temp_cur
end
end


%%**************************************************************************
%**************************************************************************
% %% Calculate stiffness by taking derivative of stress wrt strain
% % This method was only ever used for graphite paper, not cathode papers
```

```
% % Pick your derivative method!
%
%
% % METHOD 1: Derivative of the smoothed stress
%
% stiffness = cell(1,sweep);
% % for i = 1:sweep_num+1
% %     stiffness{i} = diff(stress_smooth{i},strain_smooth{i});
% % end
%
% % METHOD 2: Elizabeth's alternative derivative method. n determines how large the
% % interval over which the derivative is taken. n is odd.
%
% for i = 1:sweep
%     stiffness{i} = gradient_mod(-1*stress_smooth{i}, strain_smooth{i}, 7);
% end
%
%
%
% % Plot stiffness
% for i = 1:sweep
%
%     stiff = figure('units','inch','position',[1.5,2,5,4], 'outerposition', [1,1,6,5.5]);
%     axi(1) = subplot('position',[0.16, 0.2, 0.69, 0.7]);
%
%
%     plot(stress_pot_even', stiffness{i});
%
%     hold on
% %     p1.Color = 'r';
% %     p2.Color = 'g';
% %     ax(1).YColor = 'r';
% %     ax(2).YColor = 'g';
%
%     ylabel('Electrochemical Stiffness');
%     xlabel('Potential, E (V vs Li)');
% %     set(ax,'FontSize',15);
% %     p(1).XLim = [3.5 4.5];
% %     p(1).XTick = [3.5 4.0 4.5];
%
%     r = rem(i,2);
%     if r == 0
%         j = i/2;
%         anod_cath = 'cathodic';
%    else
%         j = (i+1)/2;
```

```
%         anod_cath = 'anodic';
%     end
%
%     cycletitle = (['Cycle ' num2str(j) ' ' anod_cath]);
%     title(cycletitle);
%
% end
%
%  %Compare stiffness and echem
%
% for i = 1:sweep
%
%
%     stiff_echem = figure('units','inch','position',[1.5,2,5,4], 'outerposition', [1,1,6,5.5]);
%     axi(1) = subplot('position',[0.15, 0.2, 0.69, 0.7]);
%
%     [ax, p1, p2] = plotyy(stress_pot_even', stiffness{i}, stress_pot_even', cur_interp{i})
%     hold on
%     p1.Color = 'b';
%     p2.Color = 'r';
%     ax(1).YColor = 'b';
%     ax(2).YColor = 'r';
%
%     ylabel(ax(1), 'Stiffness')
%     ylabel(ax(2), 'Current, I ({\mu}A)');
%     xlabel(ax(1), 'Potential, E (V vs Li)');
%     set(ax(1),'FontSize',15);
%     set(ax(2),'FontSize',15);
%     ax(1).XLim = [3.5 4.5];
%     ax(2).XLim = [3.5 4.5];
%     ax(1).XTick = [3.5 4.0 4.5];
%
%      r = rem(i,2);
%     if r == 0
%         j = i/2;
%         anod_cath = 'cathodic';
%     else
%         j = (i+1)/2;
%         anod_cath = 'anodic';
%     end
%
%     cycletitle = (['Cycle ' num2str(j) ' ' anod_cath]);
%     title(cycletitle);
%
% end
%
```

```
%
% %% Plot stress wrt strain
%
%
% A = gt(sweep_num, strain_sweep_num); %determine if more stress or strain data
%
% if A == 1
%     sweep = strain_sweep_num;
% else
%     sweep = sweep_num;
% end
%
% for i = 1:2:sweep
%
%  strain_stress = figure('units','inch','position',[1,1,5,4]);
%  axis(1) = subplot('position',[0.16, 0.2, 0.69, 0.7]);
%  plot(strain_smooth{i}, stress_smooth{i}, 'o', strain_smooth{i+1}, stress_smooth{i+1}, 's');
%  set(axis(1), 'FontSize',15, 'Ydir', 'reverse');
%  ylabel('Stress')
%  xlabel('Strain');
%  hold on
%
%  j = (i+1)/2;
%
%  cycletitle = (['Cycle ' num2str(j)]);
%  title(cycletitle);
%  legend('anodic', 'cathodic', 'Location', 'southeast');
% end




% %% **********Uncomment to plot lots of stress and strain data separately
%    ************************************************************************
% %% Plot all stress data
%
% width = 0.8;
% height = 0.28;
% bot = 0.11;
% left = 0.16;
%
% % Plot echem
%  pechem = figure('units','inch','position',[1,1,5,4]);
%  plot(org_echem_pot, org_echem_cur*1E6)
%  xlabel('Potential, E (V vs Li)')
%  ylabel('Current, I ({\mu}A)')
```

```
%  set(gca,'FontSize',15)
%  ax = gca;
% %  ax.XLim = [3.5 4.5];
%  hold on
%
%  % Plot stress wrt time
%  tstress = figure('units','inch','position',[1,1,5,4]);
%  axis(1) = subplot('position',[left, 0.2, 0.69, 0.7]);
%  t = org_time(10:end-100, 1)/3600;
%  s = org_stress(10:end-100, 1);
%  c = org_cur(10:end-100, 1)*1E6;
%  [ax, a1, a2] = plotyy(t, s, t, c);
%  set(ax(1),'FontSize',15);
%  set(ax(2),'FontSize',15);
%  ylabel(ax(1), 'Stress, f (N m^{-1})')
%  ylabel(ax(2), 'Current, I ({\mu}A)');
%  xlabel(ax(1), 'Time (hr)');
%  hold on
%
% % Plot echem and derivative together
% for i = 1:sweep_num
%
%     astress = figure('units','inch','position',[1.5,2,5,4], 'outerposition', [1,1,6,5.5]);
%     axi(1) = subplot('position',[left, 0.2, 0.69, 0.7]);
%
%     [ax, p1, p2] = plotyy(echem_pot{i}, echem_cur{i}, stress_pot_even, stress_deriv{i});
%     hold on
%     p1.Color = 'r';
%     p2.Color = 'g';
%     ax(1).YColor = 'r';
%     ax(2).YColor = 'g';
%
%     ylabel(ax(1), 'Current, I ({\mu}A)')
%     ylabel(ax(2), '{\partial}{\sigma} / {\partial}E');
%     xlabel(ax(1), 'Potential, E (V vs Li)');
%     set(ax(1),'FontSize',15);
%     set(ax(2),'FontSize',15);
% %      ax(1).XLim = [3.5 4.5];
% %      ax(2).XLim = [3.5 4.5];
% %      ax(1).XTick = [3.5 4.0 4.5];
%
%     r = rem(i,2);
%     if r == 0
%         j = i/2;
%         sweep = 'cathodic';
%         ax(2).YDir = 'reverse';
```

```
%     else
%         j = (i+1)/2;
%         sweep = 'anodic';
%     end
%
%     cycletitle = (['Cycle ' num2str(j) ' ' sweep]);
%     title(cycletitle);
%
% end
%
% % Plot stress derivative
% for i = 1:2:sweep_num
%
%     % Allows last cycle to plot even if there's no cathodic sweep
%     if i < sweep_num
%         j = i + 1;
%     else
%             j = i;
%     end
%
%
%     % Stress figure
%     hstress = figure('units','inch','position',[1,0.5,5,6.3]);
%     ax_stress(1) = subplot('position',[left, bot, width, height]);
%     ax_stress(2) = subplot('position',[left, bot+height, width, height]);
%     ax_stress(3) = subplot('position',[left, bot+height*2, width, height]);
%
%
%     cycletitle = (['Cycle ' num2str((i+1)/2)]);
%
%     % Plot stress
%     plot(ax_stress(2), stress_pot_even, stress_interp{i}, 'linestyle', '-', 'Color', [.55 .51 .88]);
%     hold(ax_stress(2), 'on');
%     plot(ax_stress(2), stress_pot_even, stress_interp{j}, 'linestyle', '-', 'Color', [.4 .4 .4]);
%     hold(ax_stress(2), 'on');
%
%     % Plot echem
%     %plot(ax_stress(3), stress_pot_even, cur_interp{i}, '-b') %labview data
%     plot(ax_stress(3), echem_pot{i}, echem_cur{i}, '-b'); %potentiostat data
%     hold(ax_stress(3), 'on');
%     %plot(ax_stress(3), stress_pot_even, cur_interp{j}, '-k';) %labview data
%     plot(ax_stress(3), echem_pot{j}, echem_cur{j}, '-k'); %potentiostat data
%     hold(ax_stress(3), 'on');
%     title(cycletitle);
%     legend('anodic', 'cathodic', 'Location', 'northwest');
%
```

```
%     % Plot smoothed stress
%     plot(ax_stress(2), stress_pot_even, stress_smooth{i}, '-b');
%     hold(ax_stress(2), 'on');
%     plot(ax_stress(2), stress_pot_even, stress_smooth{j}, '-k');
%     hold(ax_stress(2), 'on');
%
%     % Plot stress derivative
%     plot(ax_stress(1), stress_pot_even, stress_deriv{i}, '-b');
%     hold(ax_stress(1), 'on');
%     plot(ax_stress(1), stress_pot_even, stress_deriv{j}, '-k');
%     hold(ax_stress(1), 'on');
%
%     % % Customize plot labels
%     xlabel(ax_stress(1), 'Potential, E (V vs Li)');
%     set (ax_stress(2), 'xtick', get(ax_stress(1),'xtick'), 'xticklabel', '');
%     set (ax_stress(3), 'xtick', get(ax_stress(1),'xtick'), 'xticklabel', '');
%
%     ylabel(ax_stress(2), 'Stress, f (N m^{-1})');
%     ylabel(ax_stress(3), 'Current, I ({\mu}A)');
%     ylabel(ax_stress(1), '{\partial}{\sigma} / {\partial}E');
%
%     set(ax_stress(1),'FontSize',15);
%     set(ax_stress(2),'FontSize',15);
%     set(ax_stress(3),'FontSize',15);
%
%
% %     ax_stress(1).XLim = [3.5 4.5];
% %     ax_stress(2).XLim = [3.5 4.5];
% %     ax_stress(3).XLim = [3.5 4.5];
% %     ax_stress(1).XTick = [3.5 4.0 4.5];
% %     ax_stress(2).XTick = [3.5 4.0 4.5];
% %     ax_stress(3).XTick = [3.5 4.0 4.5];
% end
%
%
%
% %% Plot all strain data
%
% width = 0.8;
% height = 0.28;
% bot = 0.11;
% left = 0.16;
%
% % Plot strain echem
%  strainechem = figure('units','inch','position',[1,1,5,4]);
%  plot(org_strain_echem_pot, org_strain_echem_cur)
```

```
%  xlabel('Potential, E (V vs Li)')
%  ylabel('Current, I ({\mu}A)')
%  set(gca,'FontSize',15)
%  ax = gca;
% %  ax.XLim = [3.5 4.5];
%  hold on
%
%  % Plot all strain
%  tstrain = figure('units','inch','position',[1,1,5,4]);
%  axis(1) = subplot('position',[left, 0.2, 0.69, 0.7]);
%  plot(org_strain_pot, org_strain);
%  ax = gca;
% %  ax.XLim = [3.5 4.5];
%  set(ax,'FontSize',15);
%  ylabel(ax, 'Strain')
%  xlabel(ax, 'Potential, E (V vs Li)');
%  hold on
%
% % Plot echem and derivative together
% for i = 1:strain_sweep_num+1
%
%     astrain = figure('units','inch','position',[1.5,2,5,4], 'outerposition', [1,1,6,5.5]);
%     axi(1) = subplot('position',[left, 0.2, 0.69, 0.7]);
%
%     [ax, p1, p2] = plotyy(strain_pot_interp{i}, strain_cur_interp{i},strain_pot_interp{i},
strain_deriv{i});
%     hold on
%     p1.Color = 'r';
%     p2.Color = 'g';
%     ax(1).YColor = 'r';
%     ax(2).YColor = 'g';
%
%     ylabel(ax(1), 'Current, I ({\mu}A)')
%     ylabel(ax(2), 'Strain Derivative');
%     xlabel(ax(1), 'Potential, E (V vs Li)');
%     set(ax(1),'FontSize',15);
%     set(ax(2),'FontSize',15);
% %      ax(1).XLim = [3.5 4.5];
% %      ax(2).XLim = [3.5 4.5];
% %      ax(1).XTick = [3.5 4.0 4.5];
%
%     r = rem(i,2);
%     if r == 0
%         j = i/2;
%         sweep = 'cathodic';
%    else
```

```
%        j = (i+1)/2;
%        sweep = 'anodic';
%        ax(2).YDir = 'reverse';
%    end
%
%    cycletitle = (['Cycle ' num2str(j) ' ' sweep]);
%    title(cycletitle);
%
% end
```

B.2 Function Called by Main Body of Code: gradient_mod, written by Elizabeth Jones, Sottos Group

```
%This function takes the gradient of a function by fitting a linear line to
%a portion of the data.  The size of the portion to be fitted is determined
%by the user.

%n should be odd!

function slope = gradient_mod(f,x,n)

R = rem(n,2); %Remainder of n/2
if R==0 %N is even
   n = n+1; %Make n odd
end

N_pts = length(f);

slope = zeros(N_pts,1);
for i = 1:N_pts

   %Get the section of f
   if i<(n-floor(n/2)) %Beginning of f (use only first n points of f)
      f_i = f(1:n);
      x_i = x(1:n);
   elseif i>(N_pts - floor(n/2)) %End of f (use only last n points of f)
      f_i = f((N_pts-n+1):end);
      x_i = x((N_pts-n+1):end);
   else %Middle of f - use points on either side of point i
      f_i = f((i-floor(n/2)):(i+floor(n/2)));
      x_i = x((i-floor(n/2)):(i+floor(n/2)));
   end

   %Remove NaN values:
   ind = isnan(f_i);
```

```
    x_i(ind) = [];
    f_i(ind) = [];
    ind = isnan(x_i);
    x_i(ind) = [];
    f_i(ind) = [];

    %Make sure both vectors are of the same orientation;
    %Polyfit won't work with a row vector and a column vector!
    [Nrow,Ncol] = size(x_i);
    if Ncol>1
        x_i = x_i';
    end
    [Nrow,Ncol] = size(f_i);
    if Ncol>1
        f_i = f_i';
    end

    %Fit a linear line to the section of f:
    if length(f_i)<2 %Not enough points to fit a line
        slope(i) = NaN;
    else
        pfit = polyfit(x_i,f_i,1);
        slope(i) = pfit(1);
    end

end

%To avoid a "constant" slope at beginning and end of f, delete slope points
%at start and at end
slope(1:(n-floor(n/2))) = NaN;
slope((N_pts-floor(n/2)):end) = NaN;
```

B.3 MATLAB Code for Processing Stress Data

```
% This script imports data from the original labview file, divides it up
% into individual anodic and cathodic sweeps for each cycle, smooths the
% data, takes the derivative, and plots the echem, stress, and dstress for
% all cycles.

% OPTIONS: There are two derivative options in this script. Comment out the
% one you don't want to use.

close all
clear all
```

```
%% ******The Options Section!******

% how to upload data
find_file = 1; % 0 = use windows explorer, 1 = use file paths below
   stress_path = 'C:\Users\Kimberly\Dropbox\Grad
school\LFP\LFP_Stress_Hanwha\180528_HanwhaLFP_OCP_25uVs_ClO4_PC';
   stress_echem_file = '2_echem_25uVs_180528_HanwhaLFP_OCP_25uVs_ClO4_PC.txt';
   stress_file = '2_stress_25uVs_180528_HanwhaLFP_OCP_25uVs_ClO4_PC';

% electrode area
area = 0.7;      % Currents at this time has units of ?A/cm^2
correction = 1E6;   % make current into microAmps etc.

% pick potential range which will be used throughout plotting and
% interpolation sections (this has not been implemented yet)
material = 4;  % 0 if LMO with range 3.5-4.5 V
            % 1 if LFP with range 2.6-4.2 V
            % 2 if PAQ with range 1.8-2.6 V
            % 3 if ITO with range 1.0-4.0 V
            % 4 if LFP with range 2.6-4.4 V

% how much smoothing of original stress data do you want?
stress_smooth_kernel = 11;

% how big of an interval should the derivative be performed over?
stress_deriv_kernel = 11;

% save data produced?
save_it = 0; % 0 = no, 1 = yes


%% Which plots to plot?

% plot comparison of interpolated echem CV and labview CV
interpCHI_labviewCV = 0; % 0 = no, 1 = yes

% plot anodic peak differences
anodic_diff = 0; % 0 = no, 1 = yes

% plot cathodic peak differences
cathodic_diff = 0; % 0 = no, 1 = yes

% plot CHI echem with color change
color_plot = 1; % 0 = no, 1 = yes
```

```
% plot CHI echem in one color
plot_echem = 0; % 0 = no, 1 = yes

% plot labview echem
plot_labview_echem = 0; % 0 = no, 1 = yes

% plot stress wrt time
plot_stress_time = 1; % 0 = no, 1 = yes

% plot echem and derivative together
plot_echem_deriv = 1; % 0 = no, 1 = yes

% plot all derivatives together
plot_all_derivs = 0; % 0 = no, 1 = yes

% plot triple panel
plot_triple_panel = 1; % 0 = no, 1 = yes

% plot stress magnitude change
plot_stress_mag = 0; % 0 = no, 1 = yes

% plot echem and stress together
plot_echem_stress = 0; % 0 = no, 1 = yes

% plot baselines for charge calculation
plot_chrg_baseline = 0; % 0 = no, 1 = yes

% plot charge calculated
plot_chrg = 0; % 0 = no, 1 = yes

% plot stress magnitude change
plot_stress_mag_chrg = 0; % 0 = no, 1 = yes



%% ******Import and chop up potentiostat data******

%import echem data
if find_file ==0
   [file,path] = uigetfile('*.txt');
   echem = importdata(fullfile(path,file));
else
   echem = importdata(fullfile(stress_path, stress_echem_file));
end
data = echem.data;
```

```
% Parse original echem data
% MAY NEED TO BE CHANGED depending on how individual potentiostat exports
% data
org_echem_pot = data(:,1);
org_echem_cur = data(:,2)*correction; % change to uA
org_echem_chrg = data(:,3);
org_echem_time = data(:,4);

org_echem_cur = org_echem_cur./area;
org_echem_chrg = org_echem_chrg./area;

num_data = numel(org_echem_pot); %total number of points in the data array

% Find line number for max and min of each cycle
[pot_max, maxind] = findpeaks(org_echem_pot, 'MinPeakProminence', 0.1); %used to be 0.4
DataInv = 1.01*max(org_echem_pot) - org_echem_pot;
[pot_min, minind] = findpeaks(DataInv, 'MinPeakProminence', 0.1); %used to be 0.4

% Combine max and min
maxmin = vertcat(maxind, minind);

% Sort max and min line numbers so each anodic/cathodic cycle can be
% accurately picked out
echem_cyclebounds =  sort(maxmin, 'ascend');
echem_sweep_num = numel(echem_cyclebounds);

% Chop up echem potential data into anodic and cathodic cycles
echem_pot = cell(1,echem_sweep_num);
i = 1;
x = 10;
y = echem_cyclebounds(i);
while echem_sweep_num - i +1 > 1
    echem_pot{i} = org_echem_pot(x + 1:y);
    x = echem_cyclebounds(i);
    i = i + 1;
    y = echem_cyclebounds(i);
end
echem_pot{i} = org_echem_pot(x:y); %gets the last bit of data
echem_pot{i+1} = org_echem_pot(y:num_data);

% Chop up echem current data into anodic and cathodic cycles
echem_cur = cell(1,echem_sweep_num);
i = 1;
x = 10;
y = echem_cyclebounds(i);
```

```
while echem_sweep_num - i + 1 > 1
    echem_cur{i} = org_echem_cur(x + 1:y);
    x = echem_cyclebounds(i);
    i = i + 1;
    y = echem_cyclebounds(i);
end
echem_cur{i} = org_echem_cur(x:y); %gets the last bit of data
echem_cur{i+1} = org_echem_cur(y:num_data);

% Chop up echem charge data into anodic and cathodic cycles
echem_chrg = cell(1,echem_sweep_num);
i = 1;
x = 10;
y = echem_cyclebounds(i);
while echem_sweep_num - i + 1 > 1
    echem_chrg{i} = org_echem_chrg(x + 1:y);
    x = echem_cyclebounds(i);
    i = i + 1;
    y = echem_cyclebounds(i);

end
echem_chrg{i} = org_echem_chrg(x:y); %gets the last bit of data
echem_chrg{i+1} = org_echem_chrg(y:num_data);
% plot(echem_pot{i}, echem_chrg{i}, echem_pot{i+1}, echem_chrg{i+1} )
%     hold on

%Chop up echem time data into anodic and cathodic cycles
echem_time = cell(1,echem_sweep_num);
i = 1;
x = 10;
y = echem_cyclebounds(i);
while echem_sweep_num - i + 1 > 1
    echem_time{i} = org_echem_time(x + 1:y);
    x = echem_cyclebounds(i);
    i = i + 1;
    y = echem_cyclebounds(i);
end
echem_time{i} = org_echem_time(x:y); %gets the last bit of data
echem_time{i+1} = org_echem_time(y:num_data);

%% ******Import and chop up labview data******

%import labview data
if find_file ==0
    [file,path] = uigetfile('*.');
    labview = importdata(fullfile(path,file));
```

```
else
   labview = importdata(fullfile(stress_path, stress_file));
end
data = labview.data;

% Parse original labview data
org_time = data(:,1);
org_pot = data(:,2);
org_cur = data(:,3)*correction; % change to uA
org_stress = data(:,4);
org_psd = data (:,5);

org_cur = org_cur./area;

%get rid of duplicate potential values and the other values associated
%with them
[pot, ind_unique,~] = unique(org_pot);
ind_unique = sort(ind_unique, 'ascend');
   org_pot = org_pot(ind_unique);
   org_time = org_time(ind_unique);
   org_cur = org_cur(ind_unique);
   org_stress = org_stress(ind_unique);
   org_psd = org_psd(ind_unique);

   num_data = numel(org_time); %total number of points in the data array

% Find line number for max and min of each cycle
[pot_max, maxind] = findpeaks(org_pot, 'MinPeakProminence', .1);
DataInv = 1.01*max(org_pot) - org_pot;
[pot_min, minind] = findpeaks(DataInv, 'MinPeakProminence', .1);

% Combine max and min
maxmin = vertcat(maxind, minind);

% Sort max and min line numbers so each anodic/cathodic cycle can be
% accurately picked out
cyclebounds =  sort(maxmin, 'ascend');
sweep_num = numel(cyclebounds);

% Chop up time data into anodic and cathodic cycles
stress_time = cell(1,sweep_num);
i = 1;
x = 10; %start 10 data points in to avoid weird values
y = cyclebounds(i);
while sweep_num - i + 1 > 1
   stress_time{i} = org_time(x + 1:y); %this variable will change throughout program
```

```
    org_cycle_time{i} = stress_time{i};
    x = cyclebounds(i);
    i = i + 1;
    y = cyclebounds(i);
end
stress_time{i} = org_time(x:y); %gets the last bit of data
stress_time{i+1} = org_time(y:num_data-10);

% Chop up potential data into anodic and cathodic cycles
stress_pot = cell(1,sweep_num);
i = 1;
x = 10;
y = cyclebounds(i);
while sweep_num - i + 1 > 1
    stress_pot{i} = org_pot(x + 1:y);
    org_cycle_pot{i} = stress_pot{i};
    x = cyclebounds(i);
    i = i + 1;
    y = cyclebounds(i);
end
stress_pot{i} = org_pot(x:y); %gets the last bit of data
stress_pot{i+1} = org_pot(y:num_data-10);

% Chop up current data into anodic and cathodic cycles
stress_cur = cell(1,sweep_num);
i = 1;
x = 10;
y = cyclebounds(i);
while sweep_num - i + 1 > 1
    stress_cur{i} = org_cur(x + 1:y);
    org_cycle_cur{i} = stress_cur{i};
    x = cyclebounds(i);
    i = i + 1;
    y = cyclebounds(i);
end
stress_cur{i} = org_cur(x:y); %gets the last bit of data
stress_cur{i+1} = org_cur(y:num_data-10);

% Chop up stress data into anodic and cathodic cycles
stress = cell(1,sweep_num);
i = 1;
x = 10;
y = cyclebounds(i);
while sweep_num - i + 1 > 1
    stress{i} = org_stress(x + 1:y);
    org_cycle_stress{i} = stress{i};
```

```
    x = cyclebounds(i);
    i = i + 1;
    y = cyclebounds(i);
end
stress{i} = org_stress(x:y); %gets the last bit of data
stress{i+1} = org_stress(y:num_data-10);

% NaN values
for i = 1:sweep_num+1
    stress_pot{i}(isnan(stress_pot{i})) = [];
%     echem_pot{i}(isnan(echem_pot{i})) = [];
    stress_cur{i}(isnan(stress_cur{i})) = [];
%     echem_cur{i}(isnan(echem_cur{i})) = [];
    stress{i}(isnan(stress{i})) = [];
end


%% ******Interpolate and smooth stress data******

% Resample stress and current data over an evenly spaced voltage vector
skip = 0.01; % pick the voltage difference between data points
if material == 0 % picks which interval to use
    stress_pot_even = 3.4:skip:4.6; % LMO
elseif material == 1
    stress_pot_even = 2.4:skip:4.3; % LFP
elseif material == 2
    stress_pot_even = 1.7:skip:2.7; % PAQ
elseif material == 3
    stress_pot_even = 1:skip:4;     % ITO
elseif material == 4
    stress_pot_even = 2.4:skip:4.5;     % LFP range up to 4.4 V
end
stress_pot_even = stress_pot_even';

stress_interp = cell(1,sweep_num+1);
cur_interp = cell(1,sweep_num+1);
for i = 1:sweep_num+1

    % Remove duplicate voltage values
    [stress_pot{i}, ind_unique,~] = unique(stress_pot{i});
    stress{i} = stress{i}(ind_unique);
    stress_cur{i} = stress_cur{i}(ind_unique);

    [echem_pot{i}, ind_unique,~] = unique(echem_pot{i});
    echem_cur{i} = echem_cur{i}(ind_unique);
    echem_chrg{i} = echem_chrg{i}(ind_unique);
```

```
    echem_time{i} = echem_time{i}(ind_unique);

    % Interpolate the stress over an evenly spaced voltage vector
    stress_interp{i} = interp1(stress_pot{i}, stress{i}, stress_pot_even);
    cur_interp{i} = interp1(stress_pot{i}, stress_cur{i}, stress_pot_even);
    pot_interp{i} = interp1(stress_pot{i}, stress_pot{i}, stress_pot_even);

    echem_cur_interp{i} = interp1(echem_pot{i}, echem_cur{i}, stress_pot_even);

    %Compare interpolated echem CV and labview CV
    if interpCHI_labviewCV == 0
    else
        pechem = figure('units','inch','position',[1,1,5,4]);
        plot(stress_pot_even, echem_cur_interp{i}, 'b', stress_pot_even, cur_interp{i}, 'r')
        xlabel('Potential (V vs Li/Li^{+})')
        ylabel('Current Density ({\mu}A cm^{-2})')
        set(gca,'FontSize',15)
        ax = gca;
        if material == 0 % pick which material
            ax.XLim = [3.5 4.5]; % LMO
        elseif material == 1
            ax.XLim = [2.6 4.2]; % LFP
        elseif material == 2
            ax.XLim = [1.8 2.6]; % PAQ
        elseif material == 3
            ax.XLim = [1.0 4.0];   % ITO
        elseif material == 4
            ax.XLim = [2.6 4.4]; % LFP with limit up to 4.4 V
        end
        hold on
    end
end



% Smooth stress data

stress_smooth = cell(1,sweep_num+1);
for i = 1:sweep_num+1

    % Smooth the stress
    stress_smooth{i} = smooth(stress_interp{i}, stress_smooth_kernel);
    cur_interp{i} = smooth(cur_interp{i}, stress_smooth_kernel);

    %Remove any stress values that were extropolated during smoothing
    ind_nan = isnan(stress_interp{i}); % assign indices to NaN values in
```

```
    %the vector that are outside of potential range
    stress_smooth{i}(ind_nan) = NaN; % get rid of extrapolated values
    cur_interp{i}(ind_nan) = NaN;
end

% Delta smoothed stress

delta_stress_smooth = cell(1,sweep_num+1);
for i = 1:2:sweep_num+1

    % Find first stress value during anodic scan
    notnan = ~isnan(stress_smooth{i}); % gives 0 for nan and 1 for any number
    delta = find(notnan); %extracts positions of 1s from previous query

    delta_stress_smooth{i} = stress_smooth{i} - stress_smooth{i}(delta(1)); % delta wrt
beginning of anodic cycle

    notnan = ~isnan(stress_smooth{i+1}); % gives 0 for nan and 1 for any number
    delta = find(notnan); %extracts positions of 1s from previous query

    delta_stress_smooth{i+1} = stress_smooth{i+1} - stress_smooth{i+1}(delta(end)); %delta wrt
beginning of cathodic cycle
end


%% ******Pick your derivative method!******


% METHOD 1: Derivative of the smoothed stress

stress_deriv = cell(1,sweep_num+1);
% for i = 1:sweep_num+1
%     stress_deriv{i} = gradient(stress_smooth{i},stress_pot_even);
% end

% METHOD 2: Elizabeth's alternative derivative method. n determines how large the
% interval over which the derivative is taken. n is odd.


for i = 1:sweep_num+1
    stress_deriv{i} = gradient_mod(stress_smooth{i}, stress_pot_even, stress_deriv_kernel);

    %Remove any stress values that were extropolated during smoothing
    ind_nan = isnan(stress_interp{i}); % assign indices to NaN values in
    %the vector that are outside of potential range
    stress_deriv{i}(ind_nan) = NaN; % get rid of extrapolated values
```

```
end

%% Separation between tallest echem and derivative peaks

for i = 1:2:sweep_num %cathodic and anodic
   [cur_anod, cur_anod_maxind] = max(echem_cur_interp{i});

  a = (i+1)/2;
  high = cur_anod_maxind+10; % checks +/- 0.1 V around the current peak
  low = cur_anod_maxind-10;
  [deriv_anod_postpeak, deriv_anod_postpeakind] = max(stress_deriv{i}(low: high));
  deriv_anod_postpeakind = cur_anod_maxind-11+deriv_anod_postpeakind;

  highind = 17;
  lowind = 35;
  high = cur_anod_maxind-highind; % echecks -0.35 to -.17 V relative to the current peak
  low = cur_anod_maxind-lowind;
  [deriv_anod_prepeak, deriv_anod_prepeakind] = max(stress_deriv{i}(low: high));
  deriv_anod_prepeakind = cur_anod_maxind-lowind+1+deriv_anod_prepeakind;

      max_prepeak_pot(a) = stress_pot_even(deriv_anod_prepeakind); % finds corresponding
potential for the second tallest peak
      max_deriv_anod(a) = stress_pot_even(deriv_anod_postpeakind); % finds potential for
tallest peak


   max_cur_anod(a) = stress_pot_even(cur_anod_maxind);

   j = i+1;

   [deriv_cath_max, deriv_cath_maxind] = max(stress_deriv{j}); %finds maximum current and
stress derivative values, cathodic
   DataInv = -1*echem_cur_interp{j}; %must invert echem so that peak is now a maximum
   [cur_cath_max, cur_cath_maxind] = max(DataInv);

   b = j/2;
   max_deriv_cath(b) = stress_pot_even(deriv_cath_maxind); %finds potentials related to the
maximums
   max_cur_cath(b) = stress_pot_even(cur_cath_maxind);
end

% for i = 1:2:sweep_num %cathodic and anodic
% %    [deriv_anod, deriv_anod_maxind] = max(stress_deriv{i}); %finds maximum current and
stress derivative values, anodic
%    [cur_anod, cur_anod_maxind] = max(echem_cur_interp{i});
%
```

```
%     a = (i+1)/2;
%     [deriv_max, derivmaxind] = findpeaks(stress_deriv{i}, 'MinPeakProminence', 0.9); %this
should find at least the two largest peaks, double check
%     [B,I] = sort(deriv_max, 'descend'); % this puts the peaks in order from greatest to least and
tells us their original index
%     peak_max1 = stress_pot_even(derivmaxind(I(1))); % find potentials of the two tallest peaks
%     peak_max2 = stress_pot_even(derivmaxind(I(2)));
%     if peak_max1 < peak_max2 % ensures that higher potenial stress derivative and prepeak
derivative are assigned correctly
%         max_prepeak_pot(a) = stress_pot_even(derivmaxind(I(1))); % finds corresponding
potential for the second tallest peak
%         max_deriv_anod(a) = stress_pot_even(derivmaxind(I(2))); % finds potential for tallest
peak
%     else
%         max_prepeak_pot(a) = stress_pot_even(derivmaxind(I(2)));
%         max_deriv_anod(a) = stress_pot_even(derivmaxind(I(1)));
%     end
%
%     max_cur_anod(a) = stress_pot_even(cur_anod_maxind);
%
%     j = i+1;
%
%     [deriv_cath_max, deriv_cath_maxind] = max(stress_deriv{j}); %finds maximum current
and stress derivative values, cathodic
%     DataInv = -1*echem_cur_interp{j}; %must invert echem so that peak is now a maximum
%     [cur_cath_max, cur_cath_maxind] = max(DataInv);
%
%     b = j/2;
%     max_deriv_cath(b) = stress_pot_even(deriv_cath_maxind); %finds potentials related to the
maximums
%     max_cur_cath(b) = stress_pot_even(cur_cath_maxind);
% end

delta_cur_deriv_cath = max_cur_cath - max_deriv_cath;
delta_cur_deriv_anod = max_cur_anod - max_deriv_anod;

delta_cur_deriv_cath = delta_cur_deriv_cath';
delta_cur_deriv_anod = delta_cur_deriv_anod';


%******Plot anodic differences
if anodic_diff == 0
else
 A = 1:(sweep_num+1)/2;
 A = A';
 delta_anodic = figure('units','inch','position',[1,1,5,4]);
```

```
 plot(A, delta_cur_deriv_anod)
 xlabel('Cycle number')
 ylabel('\DeltaE (current-derivative)')
 title('Anodic peak separation')
 set(gca,'FontSize',15)
 ax = gca;
 hold on
end

 %******Plot cathodic differences
 if cathodic_diff == 0
 else
 delta_cathodic = figure('units','inch','position',[1,1,5,4]);
 plot(A, delta_cur_deriv_cath)
 xlabel('Cycle number')
 ylabel('\DeltaE (current-derivative)')
 title('Cathodic peak separation')
 set(gca,'FontSize',15)
 ax = gca;
 hold on
 end

%  % Get splitting of pre-peak and echem
%
% delta_stressprepeak_current = (max_cur_anod - max_prepeak_pot)';
%
% % Plot anodic differences for both stress derivative peak wrt tallest
% % echem peak
%  delta_anodic = figure('units','inch','position',[1,1,5,4]);
%  plot(A, delta_stressprepeak_current, '*-', A, delta_cur_deriv_anod, 'o-')
%  xlabel('Cycle number')
%  ylabel('\DeltaE (current-derivative)')
%  title('Anodic peak separation')
%  set(gca,'FontSize',15)
%  legend('Prepeak', 'Later peak', 'Location', 'best');
%  ax = gca;
%  hold on

% for i = 1:2:sweep_num %anodic
%     a = (i+1)/2;
%     [deriv_max, derivmaxind] = findpeaks(stress_deriv{5}, 'MinPeakProminence', 2); %this
should find at least the two largest peaks, double check
%     max_prepeak_pot(a) = stress_pot_even(derivmaxind(1)); % finds corresponding potential
of the first of the two peaks
% end
%
```

```
% delta_stressprepeak_current = (max_cur_anod - max_prepeak_pot)';
%
% %******Plot anodic differences
%  A = 1:(sweep_num+1)/2;
%  A = A';
%  delta_anodic = figure('units','inch','position',[1,1,5,4]);
%  plot(A, delta_stressprepeak_current, '*-', A, delta_cur_deriv_anod, 'o-')
%  xlabel('Cycle number')
%  ylabel('\DeltaE (current-derivative)')
%  title('Anodic peak separation')
%  set(gca,'FontSize',15)
%  legend('Prepeak', 'Later peak', 'Location', 'best');
%  ax = gca;
%  hold on


%% Save things

if save_it == 0
else
save('alldata', 'stress_pot', 'echem_cur_interp', 'stress_time', 'stress_pot_even',...
   'org_cycle_cur', 'org_cycle_pot', 'stress_smooth', 'stress_deriv',...
   'echem_pot', 'echem_cur', 'stress_smooth_kernel', 'stress_deriv_kernel', 'area', 'skip');
end

%% **********Plot all stress data**********

width = 0.8;
height = 0.28;
bot = 0.11;
left = 0.16;

if color_plot == 0
else
% % Plot all CHI echem with **color change**
allcycles = figure('units','inch','position',[1,1,5,4]);
axis(1) = subplot('position',[0.2, 0.2, 0.69, 0.7]);
x = 1; %change x and y here and in brackets below to set where color change should start
y = 0;
d = 2/(echem_sweep_num+2);
for i = 1:2:echem_sweep_num
 p = plot(echem_pot{i}, echem_cur{i}, echem_pot{i+1}, echem_cur{i+1});
 p(1).Color = [x 0 y]; % [red green blue]
 p(2).Color = [x 0 y];
 p(1).LineWidth = 1.5;
 p(2).LineWidth = 1.5;
```

```
 hold on
 x = x - d; % set increment and direction of color change
 y = y + d;
end
set(axis(1), 'FontSize',15);
ylabel('Current (\muA cm^{-2})')
xlabel('Potential (V vs Li/Li^{+})');
title('all cycles');
end

if plot_echem == 0
else
%******Plot echem
 pechem = figure('units','inch','position',[1,1,5,4]);
 plot(org_echem_pot, org_echem_cur)
 xlabel('Potential (V vs Li/Li^{+})')
 ylabel('Current Density ({\mu}A cm^{-2})')
 set(gca,'FontSize',15)
 ax = gca;
 if material == 0 % pick which material
    ax.XLim = [3.5 4.5]; % LMO
    ax.XTick = [3.5 3.6 3.7 3.8 3.9 4.0 4.1 4.2 4.3 4.4 4.5];
    ax.XTickLabel = {'3.5','','','','4.0','','','','4.5'};
 elseif material == 1
    ax.XLim = [2.6 4.2]; % LFP
    ax.XTick = [2.6 2.7 2.8 2.9 3.0 3.1 3.2 3.3 3.4 3.5 3.6 3.7 3.8 3.9 4.0 4.1 4.2];
    ax.XTickLabel = {'2.6','','','','3.0','','','','3.4','','','','3.8','','','','4.2'};
 elseif material == 2
    ax.XLim = [1.8 2.6]; % PAQ
    ax.XTick = [1.8 1.9 2.0 2.1 2.2 2.3 2.4 2.5 2.6];
    ax.XTickLabel = {'1.8','','2.0','','2.2','','2.4','','2.6'};
 elseif material == 3
    ax.XLim = [1.0 4.0];   % ITO
    ax.XTick = [1.0 1.2 1.4 1.6 1.8 2.0 2.2 2.4 2.6 2.8 3.0 3.2 3.4 3.6 3.8 4.0];
    ax.XTickLabel = {'1.0', '', '', '', '', '2.0', '', '', '', '', '3.0', '', '', '', '', '4.0'};
 elseif material == 4
    ax.XLim = [2.6 4.4]; % LFP with limit up to 4.4 V
    ax.XTick = [2.6 2.7 2.8 2.9 3.0 3.1 3.2 3.3 3.4 3.5 3.6 3.7 3.8 3.9 4.0 4.1 4.2 4.3 4.4];
    ax.XTickLabel = {'2.6','','','2.9','','','3.2','','','3.5','','','3.8','','','4.1','','','4.4'};
 end
 hold on
end

if plot_labview_echem == 0
else
 % ******Plot echem from labview data
```

```
 pechem = figure('units','inch','position',[1,1,5,4]);
 plot(org_pot, org_cur)
 xlabel('Potential (V vs Li/Li^{+})')
 ylabel('Current Density ({\mu}A cm^{-2})')
 set(gca,'FontSize',15)
 ax = gca;
 if material == 0 % pick which material
 ax.XLim = [3.5 4.5]; % LMO
 elseif material == 1
 ax.XLim = [2.6 4.2]; % LFP
 elseif material == 2
 ax.XLim = [1.8 2.6]; % PAQ
 elseif material == 3
 ax.XLim = [1.0 4.0]; % ITO
elseif material == 4
    ax.XLim = [2.6 4.4]; %LFP with limit up to 4.4 V
 end
 hold on
end

if plot_stress_time == 0
else
 % ******Plot stress wrt time
 tstress = figure('units','inch','position',[1,1,5,4]);
 axis(1) = subplot('position',[left, 0.2, 0.69, 0.7]);
 t = org_time(10:end-100, 1)/3600;
 s = org_stress(10:end-100, 1);
 tt = org_echem_time/3600;
 c = org_echem_cur;
 [ax, a1, a2] = plotyy(tt, c, t, s);
 set(ax(1),'FontSize',15);
 set(ax(2),'FontSize',15);
 ylabel(ax(2), 'Stress (N m^{-1})')
 ylabel(ax(1), 'Current Density ({\mu}A cm^{-2})');
 xlabel(ax(1), 'Time (hr)');
 a2.Color = [0.8500 0.3250 0.0980]; %orange
 a1.Color = [ 0    0.4470    0.7410]; %blue
 ax(2).YColor = [0.8500 0.3250 0.0980];
 ax(1).YColor = [ 0    0.4470    0.7410];
 hold on
end

 if plot_echem_deriv == 0
 else
% ******Plot echem and derivative together
for i = 1:sweep_num+1
```

```
    astress = figure('units','inch','position',[1.5,2,5,4], 'outerposition', [1,1,6,5.5]);
    axi(1) = subplot('position',[0.16, 0.2, 0.69, 0.7]);

%     [ax, p1, p2] = plotyy(echem_pot{i}, echem_cur{i}, stress_pot_even,
%     stress_deriv{i}); % uses potentiostat echem
    [ax, p1, p2] = plotyy(stress_pot_even, echem_cur_interp{i}, stress_pot_even, stress_deriv{i});
% uses labview echem
    hold on
    p1.Color = [ 0    0.4470    0.7410]; %blue
    p2.Color = [0.4660    0.6740    0.1880]; %green
    ax(1).YColor = [ 0    0.4470    0.7410];
    ax(2).YColor = [0.4660    0.6740    0.1880];

    ylabel(ax(1), 'Current Density ({\mu}A cm^{-2})')
    ylabel(ax(2), '{\partial}{\sigma} / {\partial}E');
    xlabel(ax(1), 'Potential (V vs Li/Li^{+})');
    set(ax(1),'FontSize',15);
    set(ax(2),'FontSize',15);
    if material == 0 % pick which material
        ax(1).XLim = [3.5 4.5]; % LMO
        ax(2).XLim = [3.5 4.5];
        ax(1).XTick = [3.5 3.6 3.7 3.8 3.9 4.0 4.1 4.2 4.3 4.4 4.5];
        ax(1).XTickLabel = {'3.5','','','','4.0','','','','4.5'};
    elseif material == 1
        ax(1).XLim = [2.6 4.2]; % LFP
        ax(2).XLim = [2.6 4.2];
        ax(1).XTick = [2.6 2.7 2.8 2.9 3.0 3.1 3.2 3.3 3.4 3.5 3.6 3.7 3.8 3.9 4.0 4.1 4.2];
        ax(1).XTickLabel = {'2.6', '','','3.0','','','3.4', '','','3.8','','','4.2'};
        ax(2).XTick = [2.6 2.7 2.8 2.9 3.0 3.1 3.2 3.3 3.4 3.5 3.6 3.7 3.8 3.9 4.0 4.1 4.2];
    elseif material == 2
        ax(1).XLim = [1.8 2.6]; % PAQ
        ax(2).XLim = [1.8 2.6];
        ax(1).XTick = [1.8 1.9 2.0 2.1 2.2 2.3 2.4 2.5 2.6];
        ax(1).XTickLabel = {'1.8','','2.0','','2.2','','2.4','','2.6'};
        ax(2).XTick = [1.8 1.9 2.0 2.1 2.2 2.3 2.4 2.5 2.6];
    elseif material == 3
        ax(1).XLim = [1.0 4.0];   % ITO
        ax(2).XLim = [1.0 4.0];
        ax(1).XTick = [1.0 1.2 1.4 1.6 1.8 2.0 2.2 2.4 2.6 2.8 3.0 3.2 3.4 3.6 3.8 4.0];
        ax(1).XTickLabel = {'1.0', '', '', '', '', '2.0', '', '', '', '', '3.0', '', '', '', '', '4.0'};
        ax(2).XTick = [1.0 1.2 1.4 1.6 1.8 2.0 2.2 2.4 2.6 2.8 3.0 3.2 3.4 3.6 3.8 4.0];
    elseif material == 4
        ax(1).XLim = [2.6 4.4]; % LFP with limit up to 4.4 V
        ax(2).XLim = [2.6 4.4];
        ax(1).XTick = [2.6 2.7 2.8 2.9 3.0 3.1 3.2 3.3 3.4 3.5 3.6 3.7 3.8 3.9 4.0 4.1 4.2 4.3 4.4];
```

```
        ax(1).XTickLabel = {'2.6','','','2.9','','','3.2','','','3.5','','','3.8','','','4.1','','','4.4'};
        ax(2).XTick = [2.6 2.7 2.8 2.9 3.0 3.1 3.2 3.3 3.4 3.5 3.6 3.7 3.8 3.9 4.0 4.1 4.2 4.3 4.4];
    end


    r = rem(i,2);
    if r == 0
        j = i/2;
        sweep = 'cathodic';
        ax(2).YDir = 'reverse';

    else
        j = (i+1)/2;
        sweep = 'anodic';
%         ax(2).YDir = 'reverse';
    end

    cycletitle = (['Cycle ' num2str(j) ' ' sweep]);
    title(cycletitle);

end
 end

 if plot_all_derivs == 0
 else
% ******Plot all derivatives together
adstress = figure('units','inch','position',[1.5,2,5,4], 'outerposition', [1,1,6,5.5]);
axi(1) = subplot('position',[0.14, 0.2, 0.69, 0.7]);
for i = 1:2:sweep_num+1

    p = plot(stress_pot_even, stress_deriv{i});
    hold on
    ax = gca;
    x = i/(sweep_num + 15);
    p.Color = [0.3660+x    0.5740+x    0.1880+x]; %green
    p.LineWidth = 2;

    ylabel(ax, 'Stress Derivative (N m^{-1} V^{-1})')
    xlabel(ax, 'Potential (V vs Li/Li^{+})');
    set(ax,'FontSize',15);
    if material == 0 % pick which material
        ax.XLim = [3.5 4.5]; % LMO
        ax.XTick = [3.5 3.6 3.7 3.8 3.9 4.0 4.1 4.2 4.3 4.4 4.5];
        ax.XTickLabel = {'3.5','','','','','4.0','','','','','4.5'};
    elseif material == 1
        ax.XLim = [2.6 4.2]; % LFP
```

```
        ax.XTick = [2.6 2.7 2.8 2.9 3.0 3.1 3.2 3.3 3.4 3.5 3.6 3.7 3.8 3.9 4.0 4.1 4.2];
        ax.XTickLabel = {'2.6', ','.','3.0','.','.','3.4', '.','.','3.8','.','.','4.2'};
    elseif material == 2
        ax.XLim = [1.8 2.6]; % PAQ
        ax.XTick = [1.8 1.9 2.0 2.1 2.2 2.3 2.4 2.5 2.6];
        ax.XTickLabel = {'1.8','.','2.0','.','2.2','.','2.4','.','2.6'};
    elseif material == 3
        ax.XLim = [1.0 4.0];   % ITO
        ax.XTick = [1.0 1.2 1.4 1.6 1.8 2.0 2.2 2.4 2.6 2.8 3.0 3.2 3.4 3.6 3.8 4.0];
        ax.XTickLabel = {'1.0', '.', '.', '.', '.', '2.0', '.', '.', '.', '.', '3.0', '.', '.', '.', '.', '4.0'};
elseif material == 4
     ax.XLim = [2.6 4.4]; % LFP with limit up to 4.4 V
     ax.XTick = [2.6 2.7 2.8 2.9 3.0 3.1 3.2 3.3 3.4 3.5 3.6 3.7 3.8 3.9 4.0 4.1 4.2 4.3 4.4];
     ax.XTickLabel = {'2.6','.','.','2.9','.','.','3.2','.','.','3.5','.','.','3.8','.','.','4.1','.','.','4.4'};
    end

    cycletitle = ('Anodic Stress Derivatives');
    title(cycletitle);

end
 end


 if plot_triple_panel ==0
 else
% ******Plot echem, stress, and stress derivative
for i = 1:2:sweep_num+1

    % Allows last cycle to plot even if there's no cathodic sweep
    if i < sweep_num+1
        j = i + 1;
    else
            j = i;
    end


    % Stress figure
    hstress = figure('units','inch','position',[1,0.5,5,6.3]);
    ax_stress(1) = subplot('position',[left, bot, width, height]);
    ax_stress(2) = subplot('position',[left, bot+height, width, height]);
    ax_stress(3) = subplot('position',[left, bot+height*2, width, height]);


    cycletitle = (['Cycle ' num2str((i+1)/2)]);

    % Plot stress
```

```
plot(ax_stress(2), pot_interp{i}, stress_interp{i}, 'linestyle', '-', 'Color', [.55 .51 .88]);
hold(ax_stress(2), 'on');
plot(ax_stress(2), pot_interp{j}, stress_interp{j}, 'linestyle', '-', 'Color', [.4 .4 .4]);
hold(ax_stress(2), 'on');

% Plot echem
%plot(ax_stress(3), stress_pot_even, cur_interp{i}, '-b') %labview data
plot(ax_stress(3), echem_pot{i}, echem_cur{i}, '-b'); %potentiostat data
hold(ax_stress(3), 'on');
%plot(ax_stress(3), stress_pot_even, cur_interp{j}, '-k';) %labview data
plot(ax_stress(3), echem_pot{j}, echem_cur{j}, '-k'); %potentiostat data
hold(ax_stress(3), 'on');
title(cycletitle);
legend('anodic', 'cathodic', 'Location', 'northwest');

% Plot smoothed stress
plot(ax_stress(2), stress_pot_even, stress_smooth{i}, '-b');
hold(ax_stress(2), 'on');
plot(ax_stress(2), stress_pot_even, stress_smooth{j}, '-k');
hold(ax_stress(2), 'on');

% Plot stress derivative
plot(ax_stress(1), stress_pot_even, stress_deriv{i}, '-b');
hold(ax_stress(1), 'on');
plot(ax_stress(1), stress_pot_even, stress_deriv{j}, '-k');
hold(ax_stress(1), 'on');

% % Customize plot labels

ylabel(ax_stress(2), 'Stress (N m^{-1})');
ylabel(ax_stress(3), 'Current ({\mu}A cm^{-2})');
ylabel(ax_stress(1), '{\partial}{\sigma} / {\partial}E');

set(ax_stress(1),'FontSize',15);
set(ax_stress(2),'FontSize',15);
set(ax_stress(3),'FontSize',15);

if material == 0
    ax_stress(1).XLim = [3.5 4.5]; % LMO
    ax_stress(2).XLim = [3.5 4.5];
    ax_stress(3).XLim = [3.5 4.5];
    ax_stress(1).XTick = [3.5 3.6 3.7 3.8 3.9 4.0 4.1 4.2 4.3 4.4 4.5];
    ax_stress(1).XTickLabel = {'3.5','','','','4.0','','','','4.5'};
    ax_stress(2).XTick = [3.5 3.6 3.7 3.8 3.9 4.0 4.1 4.2 4.3 4.4 4.5];
    ax_stress(3).XTick = [3.5 3.6 3.7 3.8 3.9 4.0 4.1 4.2 4.3 4.4 4.5];
elseif material == 1
```

```
        ax_stress(1).XLim = [2.6 4.2]; % LFP
        ax_stress(2).XLim = [2.6 4.2];
        ax_stress(3).XLim = [2.6 4.2];
        ax_stress(1).XTick = [2.6 2.7 2.8 2.9 3.0 3.1 3.2 3.3 3.4 3.5 3.6 3.7 3.8 3.9 4.0 4.1 4.2];
        ax_stress(1).XTickLabel = {'2.6', ','',','3.0',','',','3.4', ','',','3.8',','',','4.2'};
        ax_stress(2).XTick = [2.6 2.7 2.8 2.9 3.0 3.1 3.2 3.3 3.4 3.5 3.6 3.7 3.8 3.9 4.0 4.1 4.2];
        ax_stress(3).XTick = [2.6 2.7 2.8 2.9 3.0 3.1 3.2 3.3 3.4 3.5 3.6 3.7 3.8 3.9 4.0 4.1 4.2];
    elseif material == 2
        ax_stress(1).XLim = [1.8 2.6]; % PAQ
        ax_stress(2).XLim = [1.8 2.6];
        ax_stress(3).XLim = [1.8 2.6];
        ax_stress(1).XTick = [1.8 1.9 2.0 2.1 2.2 2.3 2.4 2.5 2.6];
        ax_stress(1).XTickLabel = {'1.8',','2.0',','2.2',','2.4',','2.6'};
        ax_stress(2).XTick = [1.8 1.9 2.0 2.1 2.2 2.3 2.4 2.5 2.6];
        ax_stress(3).XTick = [1.8 1.9 2.0 2.1 2.2 2.3 2.4 2.5 2.6];
    elseif material == 3
        ax_stress(1).XLim = [1.0 4.0];   % ITO
        ax_stress(2).XLim = [1.0 4.0];
        ax_stress(3).XLim = [1.0 4.0];
        ax_stress(1).XTick = [1.0 1.2 1.4 1.6 1.8 2.0 2.2 2.4 2.6 2.8 3.0 3.2 3.4 3.6 3.8 4.0];
        ax_stress(1).XTickLabel = {'1.0', '', '', '', '', '2.0', '', '', '', '', '3.0', '', '', '', '', '4.0'};
        ax_stress(2).XTick = [1.0 1.2 1.4 1.6 1.8 2.0 2.2 2.4 2.6 2.8 3.0 3.2 3.4 3.6 3.8 4.0];
        ax_stress(3).XTick = [1.0 1.2 1.4 1.6 1.8 2.0 2.2 2.4 2.6 2.8 3.0 3.2 3.4 3.6 3.8 4.0];
    elseif material == 4
        ax_stress(1).XLim = [2.6 4.4]; % LFP with limit up to 4.4 V
        ax_stress(2).XLim = [2.6 4.4];
        ax_stress(3).XLim = [2.6 4.4];
        ax_stress(1).XTick = [2.6 2.7 2.8 2.9 3.0 3.1 3.2 3.3 3.4 3.5 3.6 3.7 3.8 3.9 4.0 4.1 4.2 4.3
4.4];
        ax_stress(1).XTickLabel = {'2.6',','',','2.9',','',','3.2',','',','3.5',','',','3.8',','',','4.1',','',','4.4'};
        ax_stress(2).XTick = [2.6 2.7 2.8 2.9 3.0 3.1 3.2 3.3 3.4 3.5 3.6 3.7 3.8 3.9 4.0 4.1 4.2 4.3
4.4];
        ax_stress(3).XTick = [2.6 2.7 2.8 2.9 3.0 3.1 3.2 3.3 3.4 3.5 3.6 3.7 3.8 3.9 4.0 4.1 4.2 4.3
4.4];
    end
    xlabel(ax_stress(1), 'Potential (V vs Li/Li^{+})');
    set (ax_stress(2), 'xtick', get(ax_stress(1),'xtick'), 'xticklabel', '');
    set (ax_stress(3), 'xtick', get(ax_stress(1),'xtick'), 'xticklabel', '');

end
 end

 if plot_stress_mag ==0
 else
% ******Plot change in stress magnitude *anodic!*
    stressmag = figure('units','inch','position',[1.5,2,5,4], 'outerposition', [1,1,6,5.5]);
```

```
    axis(1) = subplot('position',[0.14, 0.2, 0.69, 0.7]);
    x=1; %for the color change
    y=0;
    colorchange = 2/(sweep_num+1);
for i = 1:2:sweep_num+1

    p = plot(stress_pot_even, delta_stress_smooth{i});
    hold on
    p.Color = [x 0 y]; % [red green blue], currently starts red and ends green
    x = x - colorchange; % set increment and direction of color change
    y = y + colorchange;
    p.LineWidth = 2;
    ylabel('\DeltaStress (N m^{-1})')
    xlabel('Potential (V vs Li/Li^{+})');
    ax=gca;
    set(ax,'FontSize',15);

    if material == 0 % pick which material
        ax.XLim = [3.5 4.5]; % LMO
        ax.XTick = [3.5 3.6 3.7 3.8 3.9 4.0 4.1 4.2 4.3 4.4 4.5];
        ax.XTickLabel = {'3.5','','','','4.0','','','','4.5'};
    elseif material == 1
        ax.XLim = [2.6 4.2]; % LFP
        ax.XTick = [2.6 2.7 2.8 2.9 3.0 3.1 3.2 3.3 3.4 3.5 3.6 3.7 3.8 3.9 4.0 4.1 4.2];
        ax.XTickLabel = {'2.6', '','','3.0','','','3.4', '','','3.8','','','4.2'};
    elseif material == 2
       ax.XLim = [1.8 2.6]; % PAQ
       ax.XTick = [1.8 1.9 2.0 2.1 2.2 2.3 2.4 2.5 2.6];
       ax.XTickLabel = {'1.8','','2.0','','2.2','','2.4','','2.6'};
    elseif material == 3
        ax.XLim = [1.0 4.0];   % ITO
        ax.XTick = [1.0 1.2 1.4 1.6 1.8 2.0 2.2 2.4 2.6 2.8 3.0 3.2 3.4 3.6 3.8 4.0];
        ax.XTickLabel = {'1.0', '', '', '', '', '2.0', '', '', '', '', '3.0', '', '', '', '', '4.0'};
    elseif material == 4
        ax.XLim = [2.6 4.4]; % LFP with limit up to 4.4 V
        ax.XTick = [2.6 2.7 2.8 2.9 3.0 3.1 3.2 3.3 3.4 3.5 3.6 3.7 3.8 3.9 4.0 4.1 4.2 4.3 4.4];
        ax.XTickLabel = {'2.6','','','2.9','','','3.2','','','3.5','','','3.8','','','4.1','','','4.4'};
    end

    title('Anodic Stress Change');

end


% ******Plot change in stress magnitude *cathodic!*
    stressmag = figure('units','inch','position',[1.5,2,5,4], 'outerposition', [1,1,6,5.5]);
```

```
    axis(1) = subplot('position',[0.14, 0.2, 0.69, 0.7]);
    x=1; %for the color change
    y=0;
for i = 2:2:sweep_num+1

     p = plot(stress_pot_even, delta_stress_smooth{i});
    hold on
    p.Color = [x 0 y]; % [red green blue], currently starts red and ends green
    x = x - colorchange; % set increment and direction of color change
    y = y + colorchange;
    p.LineWidth = 2;
    ylabel('\DeltaStress (N m^{-1})')
    xlabel('Potential (V vs Li/Li^{+})');
    ax=gca;
    set(ax,'FontSize',15);

    if material == 0 % pick which material
        ax.XLim = [3.5 4.5]; % LMO
        ax.XTick = [3.5 3.6 3.7 3.8 3.9 4.0 4.1 4.2 4.3 4.4 4.5];
        ax.XTickLabel = {'3.5',",",",",",'4.0',",",",",",'4.5'};
    elseif material == 1
        ax.XLim = [2.6 4.2]; % LFP
        ax.XTick = [2.6 2.7 2.8 2.9 3.0 3.1 3.2 3.3 3.4 3.5 3.6 3.7 3.8 3.9 4.0 4.1 4.2];
        ax.XTickLabel = {'2.6', ",",",",'3.0',",",",",'3.4', ",",",",'3.8',",",",",'4.2'};
    elseif material == 2
       ax.XLim = [1.8 2.6]; % PAQ
       ax.XTick = [1.8 1.9 2.0 2.1 2.2 2.3 2.4 2.5 2.6];
       ax.XTickLabel = {'1.8',",",'2.0',",",'2.2',",",'2.4',",",'2.6'};
    elseif material == 3
        ax.XLim = [1.0 4.0];   % ITO
        ax.XTick = [1.0 1.2 1.4 1.6 1.8 2.0 2.2 2.4 2.6 2.8 3.0 3.2 3.4 3.6 3.8 4.0];
        ax.XTickLabel = {'1.0', ", ", ", ", ", '2.0', ", ", ", ", ", '3.0', ", ", ", ", ", '4.0'};
    elseif material == 4
        ax.XLim = [2.6 4.4]; % LFP with limit up to 4.4 V
        ax.XTick = [2.6 2.7 2.8 2.9 3.0 3.1 3.2 3.3 3.4 3.5 3.6 3.7 3.8 3.9 4.0 4.1 4.2 4.3 4.4];
        ax.XTickLabel = {'2.6',",",",'2.9',",",",'3.2',",",",'3.5',",",",'3.8',",",",'4.1',",",",'4.4'};
    end

    title('Cathodic Stress Change');

end
 end

 if plot_echem_stress ==0
 else
% ******Plot echem and stress together
```

```
for i = 1:sweep_num +1

    astress = figure('units','inch','position',[1.5,2,5,4], 'outerposition', [1,1,6,5.5]);
    axi(1) = subplot('position',[0.14, 0.2, 0.69, 0.7]);

    smoothed = stress_smooth{i}.';
    [ax, p1, p2] = plotyy(echem_pot{i}, echem_cur{i}, [stress_pot_even', stress_pot_even'],
[smoothed', stress_interp{i}']);
    hold on
    p1.Color = [ 0    0.4470    0.7410]; %blue
%     p2.Color = [0.4660    0.6740    0.1880]; %green
    ax(1).YColor = [ 0    0.4470    0.7410];
    ax(2).YColor = [0.8500 0.3250 0.0980]; %orange

    ylabel(ax(1), 'Current Dentsity ({\mu}A cm^{-2})')
    ylabel(ax(2), 'Stress (N m^{-1})');
    xlabel(ax(1), 'Potential (V vs Li/Li^{+})');
    set(ax(1),'FontSize',15);
    set(ax(2),'FontSize',15);
    if material == 0
        ax(1).XLim = [3.5 4.5]; % LMO
        ax(2).XLim = [3.5 4.5];
        ax(1).XTick = [3.5 3.6 3.7 3.8 3.9 4.0 4.1 4.2 4.3 4.4 4.5];
        ax(1).XTickLabel = {'3.5','','','','4.0','','','','4.5'};
    elseif material == 1
        ax(1).XLim = [2.6 4.2]; % LFP
        ax(2).XLim = [2.6 4.2]; % LFP
        ax(1).XTick = [2.6 2.7 2.8 2.9 3.0 3.1 3.2 3.3 3.4 3.5 3.6 3.7 3.8 3.9 4.0 4.1 4.2];
        ax(1).XTickLabel = {'2.6','','','3.0','','','3.4','','','3.8','','','4.2'};
    elseif material == 3
        ax(1).XLim = [1.0 4.0];   % ITO
        ax(2).XLim = [1.0 4.0];
        ax(1).XTick = [1.0 1.2 1.4 1.6 1.8 2.0 2.2 2.4 2.6 2.8 3.0 3.2 3.4 3.6 3.8 4.0];
        ax(1).XTickLabel = {'1.0', '', '', '', '', '2.0', '', '', '', '', '3.0', '', '', '', '', '4.0'};
    elseif material == 4
        ax(1).XLim = [2.6 4.4]; % LFP with limit up to 4.4 V
        ax(2).XLim = [2.6 4.4];
        ax(1).XTick = [2.6 2.7 2.8 2.9 3.0 3.1 3.2 3.3 3.4 3.5 3.6 3.7 3.8 3.9 4.0 4.1 4.2 4.3 4.4];
        ax(1).XTickLabel = {'2.6','','','2.9','','','3.2','','','3.5','','','3.8','','','4.1','','','4.4'};
        ax(2).XTick = [2.6 2.7 2.8 2.9 3.0 3.1 3.2 3.3 3.4 3.5 3.6 3.7 3.8 3.9 4.0 4.1 4.2 4.3 4.4];
    end

    r = rem(i,2);
    if r == 0
        j = i/2;
        sweep = 'cathodic';
```

```
    else
        j = (i+1)/2;
        sweep = 'anodic';
    end

    cycletitle = (['Cycle ' num2str(j) ' ' sweep]);
    title(cycletitle);

end
 end

%% ***************** Calculate charge by hand **********************

% First, normalize current. For anodic scan, find baseline with slope
% determined between 3.0 and 3.3 V. For cathodic scan , between 3.6 and 3.8

for i = 1:echem_sweep_num+1 % find indicies for certain potentials, indicies
     r = rem(i,2);
     if r == 0 % cathodic

         % assign potentials for cathodic baseline
         % p1 < p2, type as appears in CHI file

        if material == 0
            % LMO
        elseif material == 1
            % LFP
        elseif material == 3
            % ITO
        elseif material == 4
            val_1pot = 3.800;
            val_2pot = 4.000;
        end


         ind_1p = find(echem_pot{i} == val_1pot);
         ind_2p = find(echem_pot{i} == val_2pot);

         sweep = 'cathodic'; % for title
         j = i/2;

     else %anodic

         % assign potentials for anodic baseline
         % p1 < p2, type as appears in CHI file
```

```
        if material == 0
            % LMO
        elseif material == 1
            % LFP
        elseif material == 3
            % ITO
        elseif material == 4
           val_1pot = 2.8000;
           val_2pot = 3.0000;
        end


         ind_1p = find(echem_pot{i} == val_1pot);
         ind_2p = find(echem_pot{i} == val_2pot);

        sweep = 'anodic'; % for title
        j = (i+1)/2;
    end

    if i == 1
        val_1cur = echem_cur{1}(1); % force numberator of slope to be zero so no baseline
subracted
        val_2cur = echem_cur{1}(1);
    else
        val_1cur = echem_cur{i}(ind_1p);
        val_2cur = echem_cur{i}(ind_2p);
    end

    slope = (val_1cur-val_2cur)/(val_1pot-val_2pot);
    y_int = val_1cur - (slope*val_1pot);
    background = slope*echem_pot{i} + y_int;
    echem_cur_bkgrdsub{i} = echem_cur{i};%-background;

    if plot_chrg_baseline == 0
    else
    figure;
    plot( echem_pot{i}, echem_cur{i}, echem_pot{i}, background);
    title(['Original, Cycle ' num2str(j) ' ' sweep]);
    hold on
    figure;
    plot(echem_pot{i}, echem_cur_bkgrdsub{i});
    title(['Subracted, Cycle ' num2str(j) ' ' sweep]);
    hold on
    end

end
```

```
% Second, integrate background subtracted current with respect to time
% This is microAmps per cm squared integrated...
for i = 1:echem_sweep_num+1
        time = echem_time{i}-echem_time{i}(1);
        charge(i) = (trapz(time, echem_cur_bkgrdsub{i}))/correction;
end



% Plot charge
for i = 1:echem_sweep_num+1
    if rem(i,2) == 0
        j = i/2;
        cathodic_charge(j) = charge(i);
    else
        j = (i+1)/2;
        anodic_charge(j) = charge(i);
        cycle(j) = j;
    end
end


if plot_chrg == 0
else
% ******Plot change in charge *anodic!*
    anodchrg = figure('units','inch','position',[1.5,2,5,4], 'outerposition', [1,1,6,5.5]);
    axis(1) = subplot('position',[0.14, 0.2, 0.69, 0.7]);

    plot(cycle, anodic_charge, 'r*');
    hold on
    ylabel('Charge (C/cm^{2})')
    xlabel('Cycle');
    ax=gca;
    set(ax,'FontSize',15);
    title('C3 Anodic Charge');


% Plot change in charge *cathodic!*
    cathchrg = figure('units','inch','position',[1.5,2,5,4], 'outerposition', [1,1,6,5.5]);
    axis(1) = subplot('position',[0.14, 0.2, 0.69, 0.7]);

    plot(cycle, cathodic_charge, 'b*');
    hold on
    ylabel('Charge (C/cm^{2})')
    xlabel('Cycle');
```

```
    ax=gca;
    set(ax,'FontSize',15);
    title('C3 Cathodic Charge');
end

if plot_stress_mag_chrg ==0
 else
% ******Plot change in stress magnitude *anodic!*
    stressmag = figure('units','inch','position',[1.5,2,5,4], 'outerposition', [1,1,6,5.5]);
    axis(1) = subplot('position',[0.14, 0.2, 0.69, 0.7]);
    x=1; %for the color change
    y=0;
    colorchange = 2/(sweep_num+1);
for i = 1:2:sweep_num+1
    p = plot(stress_pot_even, delta_stress_smooth{i}./anodic_charge((i+1)/2));
    hold on
    p.Color = [x 0 y]; % [red green blue], currently starts red and ends green
    x = x - colorchange; % set increment and direction of color change
    y = y + colorchange;
    p.LineWidth = 2;
    ylabel('\DeltaStress (N m^{-1} C^{-1} cm^{-2})')
    xlabel('Potential (V vs Li/Li^{+})');
    ax=gca;
    set(ax,'FontSize',15);

    if material == 0 % pick which material
       ax.XLim = [3.5 4.5]; % LMO
       ax.XTick = [3.5 3.6 3.7 3.8 3.9 4.0 4.1 4.2 4.3 4.4 4.5];
       ax.XTickLabel = {'3.5','','','','','4.0','','','','','4.5'};
    elseif material == 1
       ax.XLim = [2.6 4.2]; % LFP
       ax.XTick = [2.6 2.7 2.8 2.9 3.0 3.1 3.2 3.3 3.4 3.5 3.6 3.7 3.8 3.9 4.0 4.1 4.2];
       ax.XTickLabel = {'2.6', '','','','3.0','','','','3.4', '','','','3.8','','','','4.2'};
    elseif material == 2
      ax.XLim = [1.8 2.6]; % PAQ
      ax.XTick = [1.8 1.9 2.0 2.1 2.2 2.3 2.4 2.5 2.6];
      ax.XTickLabel = {'1.8','','2.0','','2.2','','2.4','','2.6'};
    elseif material == 3
       ax.XLim = [1.0 4.0];   % ITO
       ax.XTick = [1.0 1.2 1.4 1.6 1.8 2.0 2.2 2.4 2.6 2.8 3.0 3.2 3.4 3.6 3.8 4.0];
       ax.XTickLabel = {'1.0', '', '', '', '', '2.0', '', '', '', '', '3.0', '', '', '', '', '4.0'};
    elseif material == 4
       ax.XLim = [2.6 4.4]; % LFP with limit up to 4.4 V
       ax.XTick = [2.6 2.7 2.8 2.9 3.0 3.1 3.2 3.3 3.4 3.5 3.6 3.7 3.8 3.9 4.0 4.1 4.2 4.3 4.4];
       ax.XTickLabel = {'2.6','','','2.9','','','3.2','','','3.5','','','3.8','','','4.1','','','4.4'};
    end
```

```
    title('Charge Normalized Anodic Stress Change');

end



% ******Plot change in stress magnitude *cathodic!*
    stressmag = figure('units','inch','position',[1.5,2,5,4], 'outerposition', [1,1,6,5.5]);
    axis(1) = subplot('position',[0.14, 0.2, 0.69, 0.7]);
    x=1; %for the color change
    y=0;
for i = 2:2:sweep_num+1

    p = plot(stress_pot_even, delta_stress_smooth{i}./cathodic_charge(i/2));
    hold on
    p.Color = [x 0 y]; % [red green blue], currently starts red and ends green
    x = x - colorchange; % set increment and direction of color change
    y = y + colorchange;
    p.LineWidth = 2;
    ylabel('\DeltaStress (N m^{-1} C^{-1} cm^{-2})')
    xlabel('Potential (V vs Li/Li^{+})');
    ax=gca;
    set(ax,'FontSize',15);

    if material == 0 % pick which material
        ax.XLim = [3.5 4.5]; % LMO
        ax.XTick = [3.5 3.6 3.7 3.8 3.9 4.0 4.1 4.2 4.3 4.4 4.5];
        ax.XTickLabel = {'3.5','','','','','4.0','','','','','4.5'};
    elseif material == 1
        ax.XLim = [2.6 4.2]; % LFP
        ax.XTick = [2.6 2.7 2.8 2.9 3.0 3.1 3.2 3.3 3.4 3.5 3.6 3.7 3.8 3.9 4.0 4.1 4.2];
        ax.XTickLabel = {'2.6', '','','','3.0','','','','3.4', '','','','3.8','','','','4.2'};
    elseif material == 2
       ax.XLim = [1.8 2.6]; % PAQ
       ax.XTick = [1.8 1.9 2.0 2.1 2.2 2.3 2.4 2.5 2.6];
       ax.XTickLabel = {'1.8','','2.0','','2.2','','2.4','','2.6'};
    elseif material == 3
        ax.XLim = [1.0 4.0];   % ITO
        ax.XTick = [1.0 1.2 1.4 1.6 1.8 2.0 2.2 2.4 2.6 2.8 3.0 3.2 3.4 3.6 3.8 4.0];
        ax.XTickLabel = {'1.0', '', '', '', '', '2.0', '', '', '', '', '3.0', '', '', '', '', '4.0'};
    elseif material == 4
        ax.XLim = [2.6 4.4]; % LFP with limit up to 4.4 V
        ax.XTick = [2.6 2.7 2.8 2.9 3.0 3.1 3.2 3.3 3.4 3.5 3.6 3.7 3.8 3.9 4.0 4.1 4.2 4.3 4.4];
        ax.XTickLabel = {'2.6','','','2.9','','','3.2','','','3.5','','','3.8','','','4.1','','','4.4'};
    end
```

```
    title('Charge Normalized Cathodic Stress Change');

end
 end

%%%%%%%%%%%%%%%%%%%%%%%%%%%%%%%%%%%%%%%%%%%%%%%%%%%%%%%%%%%%%%%%%%%%%%%%
% % Plot echem with stress, and stress derivatives cathodic and anodic
% for i = 1:2:sweep_num+1
%
%     % Allows last cycle to plot even if there's no cathodic sweep
%     if i < sweep_num+1
%         j = i + 1;
%     else
%             j = i;
%     end
%
%     % Stress figure
%     bstress = figure('units','inch','position',[1,0.5,5,6.3]);
%     ax_stress(1) = subplot('position',[left, bot, width, height]);
%     ax_stress(2) = subplot('position',[left, bot+height, width, height]);
%     ax_stress(3) = subplot('position',[left, bot+height*2, width, height]);
%
%
%     cycletitle = (['Cycle ' num2str((i+1)/2)]);
%
%     % Top plot - echem and stress
%     [aAx, aline1, aline2] = plotyy(ax_stress(3), echem_pot{i}, echem_cur{i}, pot_interp{i},
stress_interp{i});
%     hold(ax_stress(3), 'on');
%     plot(ax_stress(3), echem_pot{j}, echem_cur{j}, pot_interp{j}, stress_interp{j});
%     hold(ax_stress(3), 'on');
%     title(cycletitle);
%     %legend('anodic', 'cathodic', 'Location', 'northwest');
%     ylabel(aAx(1), 'Current');
%     ylabel(aAx(2), 'Stress');
%
%     % Middle plot - anodic stress derivative with current
%     [bAx, bline1, bline2] = plotyy(ax_stress(2), echem_pot{i}, echem_cur{i}, stress_pot_even,
stress_deriv{i});
%     hold(ax_stress(2), 'on');
%
% %     Plot smoothed stress
% %     plot(ax_stress(2), stress_pot_even, stress_smooth{i}, '-b');
% %     hold(ax_stress(2), 'on');
```

```
% %     plot(ax_stress(2), stress_pot_even, stress_smooth{j}, '-k');
% %     hold(ax_stress(2), 'on');
%
%     % Bottom plot - cathodic stress derivative with current
%     [cAx, cline1, cline2] = plotyy(ax_stress(1), echem_pot{j}, echem_cur{j}, stress_pot_even,
stress_deriv{j});
%     hold(ax_stress(1), 'on');
%
%     % % Customize plot labels
%     xlabel(ax_stress(1), 'Potential (V vs Li/Li^{+})');
%     set (ax_stress(2), 'xtick', get(ax_stress(1),'xtick'), 'xticklabel', '');
%     set (ax_stress(3), 'xtick', get(ax_stress(1),'xtick'), 'xticklabel', '');
%
%     ylabel(ax_stress(2), 'Stress (N m^{-1})');
%     ylabel(ax_stress(3), 'Current Density ({\mu}A cm^{-2})');
%     ylabel(ax_stress(1), '{\partial}{\sigma} / {\partial}E');
%
%     set(ax_stress(1),'FontSize',15);
%     set(ax_stress(2),'FontSize',15);
%     set(ax_stress(3),'FontSize',15);
%
%      if material == 0
%         ax_stress(1).XLim = [3.5 4.5]; % LMO
%         ax_stress(2).XLim = [3.5 4.5];
%         ax_stress(3).XLim = [3.5 4.5];
%         ax_stress(1).XTick = [3.5 3.6 3.7 3.8 3.9 4.0 4.1 4.2 4.3 4.4 4.5];
%         ax_stress(1).XTickLabel = {'3.5',",",",",'4.0',",",",",'4.5'};
%         ax_stress(2).XTick = [3.5 3.6 3.7 3.8 3.9 4.0 4.1 4.2 4.3 4.4 4.5];
%         ax_stress(3).XTick = [3.5 3.6 3.7 3.8 3.9 4.0 4.1 4.2 4.3 4.4 4.5];
%     elseif material == 1
%         ax_stress(1).XLim = [2.6 4.2]; % LFP
%         ax_stress(2).XLim = [2.6 4.2];
%         ax_stress(3).XLim = [2.6 4.2];
%         ax_stress(1).XTick = [2.6 2.7 2.8 2.9 3.0 3.1 3.2 3.3 3.4 3.5 3.6 3.7 3.8 3.9 4.0 4.1 4.2];
%         ax_stress(1).XTickLabel = {'2.6', ",",",'3.0',",",",'3.4', ",",",'3.8',",",",'4.2'};
%         ax_stress(2).XTick = [2.6 2.7 2.8 2.9 3.0 3.1 3.2 3.3 3.4 3.5 3.6 3.7 3.8 3.9 4.0 4.1 4.2];
%         ax_stress(3).XTick = [2.6 2.7 2.8 2.9 3.0 3.1 3.2 3.3 3.4 3.5 3.6 3.7 3.8 3.9 4.0 4.1 4.2];
%     elseif material == 3
%         ax_stress(1).XLim = [1.0 4.0];   % ITO
%         ax_stress(2).XLim = [1.0 4.0];
%         ax_stress(3).XLim = [1.0 4.0];
%         ax_stress(1).XTick = [1.0 1.2 1.4 1.6 1.8 2.0 2.2 2.4 2.6 2.8 3.0 3.2 3.4 3.6 3.8 4.0];
%         ax_stress(1).XTickLabel = {'1.0', ", ", ", ", '2.0', ", ", ", ", '3.0', ", ", ", ", '4.0'};
%         ax_stress(2).XTick = [1.0 1.2 1.4 1.6 1.8 2.0 2.2 2.4 2.6 2.8 3.0 3.2 3.4 3.6 3.8 4.0];
%         ax_stress(3).XTick = [1.0 1.2 1.4 1.6 1.8 2.0 2.2 2.4 2.6 2.8 3.0 3.2 3.4 3.6 3.8 4.0];
%     elseif material == 4
```

```
%         ax(1).XLim = [2.6 4.4]; % LFP with limit up to 4.4 V
%         ax(2).XLim = [2.6 4.4];
%         ax(3).XLim = [2.6 4.4];
%         ax(1).XTick = [2.6 2.7 2.8 2.9 3.0 3.1 3.2 3.3 3.4 3.5 3.6 3.7 3.8 3.9 4.0 4.1 4.2 4.3 4.4];
%         ax(1).XTickLabel = {'2.6',",",'2.9',",",'3.2',",",'3.5',",",'3.8',",",'4.1',",",'4.4'};
%         ax(2).XTick = [2.6 2.7 2.8 2.9 3.0 3.1 3.2 3.3 3.4 3.5 3.6 3.7 3.8 3.9 4.0 4.1 4.2 4.3 4.4];
%         ax(3).XTick = [2.6 2.7 2.8 2.9 3.0 3.1 3.2 3.3 3.4 3.5 3.6 3.7 3.8 3.9 4.0 4.1 4.2 4.3 4.4];
%     end
% end


% % Plot stress derivative wrt current
% for i = 1:sweep_num+1
%
%  dstress_cur = figure('units','inch','position',[1,1,5,4]);
%  axis(1) = subplot('position',[0.2, 0.2, 0.69, 0.7]);
%  plot(cur_interp{i}, stress_deriv{i});
%  set(axis(1), 'FontSize',15);
%  ylabel('Stress Derivative')
%  xlabel('Current Density, I ({\mu}A cm^{-2})');
%  hold on
%
%   r = rem(i,2);
%     if r == 0
%         j = i/2;
%         sweep = 'cathodic';
%    else
%         j = (i+1)/2;
%         sweep = 'anodic';
%    end
%
%     cycletitle = (['Cycle ' num2str(j) ' ' sweep]);
%     title(cycletitle);
% end

%
% % Plot stress wrt current
% for i = 1:sweep_num
%
%  stress_cur = figure('units','inch','position',[1,1,5,4]);
%  axis(1) = subplot('position',[0.2, 0.2, 0.69, 0.7]);
%  plot(cur_interp{i}, stress_smooth{i});
%  set(axis(1), 'FontSize',15);
%  ylabel('Stress')
%  xlabel('Current Density, I ({\mu}A cm^{-2})');
%  hold on
```

```
%
%   r = rem(i,2);
%    if r == 0
%        j = i/2;
%        sweep = 'cathodic';
%   else
%        j = (i+1)/2;
%        sweep = 'anodic';
%   end
%
%    cycletitle = (['Cycle ' num2str(j) ' ' sweep]);
%    title(cycletitle);
% end


% % Fourier transform of the stress and current definted in previous section
% % (stress wrt time)
%
% stress_fft = fft(s);
% stress_fft_mag = abs(stress_fft);
% cur_fft = fft (c);
% cur_fft_mag = abs(cur_fft);
% figure
% plot(stress_fft_mag, 'color', [ 0.8500 0.3250 0.0980]);
% hold on
% plot(cur_fft_mag, 'color', [ 0    0.4470    0.7410]);
% xlabel('Frequency Bins');
% legend('Stress', 'Current');
% ax = gca;
% set(ax, 'FontSize',15);
% hold on


% % Plot echem and derivative together with labview echem
% for i = 1:sweep_num +1
%
%    astress = figure('units','inch','position',[1.5,2,5,4], 'outerposition', [1,1,6,5.5]);
%    axi(1) = subplot('position',[0.14, 0.2, 0.69, 0.7]);
%
%    [ax, p1, p2] = plotyy(stress_pot{i}, stress_cur{i}, stress_pot_even, stress_deriv{i});
%    hold on
%    p1.Color = [ 0    0.4470    0.7410]; %blue
%    p2.Color = [0.4660    0.6740    0.1880]; %green
%    ax(1).YColor = [ 0    0.4470    0.7410];
%    ax(2).YColor = [0.4660    0.6740    0.1880];
%
```

```
%     ylabel(ax(1), 'Current Density ({\mu}A cm^{-2})')
%     ylabel(ax(2), '{\partial}{\sigma} / {\partial}E');
%     xlabel(ax(1), 'Potential (V vs Li/Li^{+})');
%     set(ax(1),'FontSize',15);
%     set(ax(2),'FontSize',15);
%     if material == 0
%         ax(1).XLim = [3.5 4.5]; % LMO
%         ax(2).XLim = [3.5 4.5];
%         ax(1).XTick = [3.5 3.6 3.7 3.8 3.9 4.0 4.1 4.2 4.3 4.4 4.5];
%         ax(1).XTickLabel = {'3.5',",",",",'4.0',",",",",'4.5'};
%     elseif material == 1
    %     ax(1).XLim = [2.6 4.2]; % LFP
    %     ax(2).XLim = [2.6 4.2]; % LFP
    %     ax(1).XTick = [2.6 2.7 2.8 2.9 3.0 3.1 3.2 3.3 3.4 3.5 3.6 3.7 3.8 3.9 4.0 4.1 4.2];
    %     ax(1).XTickLabel = {'2.6',",",",",'3.0',",",",",'3.4',",",",",'3.8',",",",",'4.2'};
%     elseif material == 3
%         ax(1).XLim = [1.0 4.0];   % ITO
%         ax(2).XLim = [1.0 4.0];
%         ax(1).XTick = [1.0 1.2 1.4 1.6 1.8 2.0 2.2 2.4 2.6 2.8 3.0 3.2 3.4 3.6 3.8 4.0];
%         ax(1).XTickLabel = {'1.0', '', '', '', '', '2.0', '', '', '', '', '3.0', '', '', '', '', '4.0'};
%     elseif material == 4
%         ax(1).XLim = [2.6 4.4]; % LFP with limit up to 4.4 V
%         ax(2).XLim = [2.6 4.4];
%         ax(1).XTick = [2.6 2.7 2.8 2.9 3.0 3.1 3.2 3.3 3.4 3.5 3.6 3.7 3.8 3.9 4.0 4.1 4.2 4.3 4.4];
%         ax(1).XTickLabel = {'2.6',",",'2.9',",",'3.2',",",'3.5',",",'3.8',",",'4.1',",",'4.4'};
%         ax(2).XTick = [2.6 2.7 2.8 2.9 3.0 3.1 3.2 3.3 3.4 3.5 3.6 3.7 3.8 3.9 4.0 4.1 4.2 4.3 4.4];
      %     end
%
%     r = rem(i,2);
%     if r == 0
%         j = i/2;
%         sweep = 'cathodic';
%         ax(2).YDir = 'reverse';
%
%     else
%         j = (i+1)/2;
%         sweep = 'anodic';
%
%     end
%
%     cycletitle = (['Cycle ' num2str(j) ' ' sweep]);
%     title(cycletitle);
%
% end
```

Appendix C: MATLAB Code for Processing Cyclic Voltammetry

C.1 Main Body of Code

```
%% Import and chop up potentiostat data

close all
clear all

area = 1;
correction = 1;%e6; % make current into microAmps etc.

%import echem data % use this or the next section to import data
% [file,path] = uigetfile('*.txt');
% echem = importdata(fullfile(path,file));
% data = echem.data;

echem_path = 'C:\Users\Kimberly\Dropbox\Grad
school\LFP\LFP_Stress_Hanwha\paper_170505_HanwhaLFP_OCP_25uVs_PF6_ECDMC';
echem_file = 'echem_170505_JapLFP_24hrOCP_25uVs.txt';
echem = importdata(fullfile(echem_path, echem_file));
data = echem.data;

% Parse original echem data
% MAY NEED TO BE CHANGED depending on how individual potentiostat exports
% data
org_echem_pot = data(:,1);
org_echem_cur = data(:,2)*correction/area; % change to uA
org_echem_chrg = data(:,3)/area;
org_echem_time = data(:,4);

num_data = numel(org_echem_pot); %total number of points in the data array

% Find line number for max and min of each cycle
[pot_max, maxind] = findpeaks(org_echem_pot, 'MinPeakProminence', 0.1);
DataInv = 1.01*max(org_echem_pot) - org_echem_pot;
[pot_min, minind] = findpeaks(DataInv, 'MinPeakProminence', 0.1);

% Combine max and min
maxmin = vertcat(maxind, minind);

% Sort max and min line numbers so each anodic/cathodic cycle can be
% accurately picked out
echem_cyclebounds =  sort(maxmin, 'ascend');
echem_sweep_num = numel(echem_cyclebounds);
```

```
% Chop up echem potential data into anodic and cathodic cycles
echem_pot = cell(1,echem_sweep_num);
i = 1;
x = 10;
y = echem_cyclebounds(i);
while echem_sweep_num - i + 1 > 1
   echem_pot{i} = org_echem_pot(x + 1:y);
   if rem(i,2) == 0
      echem_pot{i} = flip(echem_pot{i},1);
   end
   x = echem_cyclebounds(i);
   i = i + 1;
   y = echem_cyclebounds(i);
end
echem_pot{i} = org_echem_pot(x:y); %gets the last bit of data
echem_pot{i+1} = org_echem_pot(y:num_data);
echem_pot{i+1} = flip(echem_pot{i+1},1);

% Chop up echem current data into anodic and cathodic cycles
echem_cur = cell(1,echem_sweep_num);
i = 1;
x = 10;
y = echem_cyclebounds(i);
while echem_sweep_num - i + 1 > 1
   echem_cur{i} = org_echem_cur(x + 1:y);
   if rem(i,2) == 0
      echem_cur{i} = flip(echem_cur{i},1);
   end
   x = echem_cyclebounds(i);
   i = i + 1;
   y = echem_cyclebounds(i);
end
echem_cur{i} = org_echem_cur(x:y); %gets the last bit of data
echem_cur{i+1} = org_echem_cur(y:num_data);
echem_cur{i+1} = flip(echem_cur{i+1},1);

% Chop up echem charge data into anodic and cathodic cycles
echem_chrg = cell(1,echem_sweep_num);
i = 1;
x = 10;
y = echem_cyclebounds(i);
while echem_sweep_num - i + 1 > 1
   echem_chrg{i} = org_echem_chrg(x + 1:y);
   if rem(i,2) == 0
      echem_chrg{i} = flip(echem_chrg{i},1);
```

```
    end
    x = echem_cyclebounds(i);
    i = i + 1;
    y = echem_cyclebounds(i);
end
echem_chrg{i} = org_echem_chrg(x:y); %gets the last bit of data
echem_chrg{i+1} = org_echem_chrg(y:num_data);
echem_chrg{i+1} = flip(echem_chrg{i+1},1);

% Chop up echem time data into anodic and cathodic cycles
echem_time = cell(1,echem_sweep_num);
i = 1;
x = 10;
y = echem_cyclebounds(i);
while echem_sweep_num - i + 1 > 1
    echem_time{i} = org_echem_time(x + 1:y);
    if rem(i,2) == 0
        echem_time{i} = flip(echem_time{i},1);
    end
    x = echem_cyclebounds(i);
    i = i + 1;
    y = echem_cyclebounds(i);
end
echem_time{i} = org_echem_time(x:y); %gets the last bit of data
echem_time{i+1} = org_echem_time(y:num_data);
echem_time{i+1} = flip(echem_time{i+1},1);

%Option to chop off some data for integration. Enter potential of choice
% cutoff = 4.4; % high cutoff
%
% for i = 1:echem_sweep_num + 1
%     ind = find(echem_pot{i} == cutoff);
%     echem_pot{i} = echem_pot{i}(1:ind);
%     echem_cur{i} = echem_cur{i}(1:ind);
%     echem_chrg{i} = echem_chrg{i}(1:ind);
%     echem_time{i} = echem_time{i}(1:ind);
% end
%
% cutoff = 3.55; % low cutoff
%
% for i = 1:echem_sweep_num
%     ind = find(echem_pot{i} == cutoff);
%     echem_pot{i} = echem_pot{i}(ind:end);
%     echem_cur{i} = echem_cur{i}(ind:end);
%     echem_chrg{i} = echem_chrg{i}(ind:end);
%     echem_time{i} = echem_time{i}(ind:end);
```

```
% end
%% Write echem to excel file

% for i=1:echem_sweep_num+1
%
%     sheet = i;
%     X=[echem_pot{i}, echem_cur{i}];
%     xlswrite('echemexport.xls',X, sheet);
%
% end

%% Plot echem


% Plot all data

allCV = figure('units','inch','position',[1,1,5,4]);
axis(1) = subplot('position',[0.2, 0.2, 0.69, 0.7]);
plot(org_echem_pot, org_echem_cur);
set(axis(1), 'FontSize',15);
ylabel('Current (\muA cm^{-2})')
xlabel('Potential (V vs Li/Li^{+})');
title('all cycles');

% % Plot all data with **color change**
allcycles = figure('units','inch','position',[1,1,5,4]);
axis(1) = subplot('position',[0.2, 0.2, 0.69, 0.7]);
x = 1; %change x and y here and in brackets below to set where color change should start
y = 0;
d = 1/(echem_sweep_num/2);
for i = 1:2:echem_sweep_num
 p = plot(echem_pot{i}, echem_cur{i}, echem_pot{i+1}, echem_cur{i+1});
 if i == 1
    p(1).Color = [0 1 0]; % [red green blue]
    p(2).Color = [0 1 0];
 else
    p(1).Color = [x 0 y]; % [red green blue]
    p(2).Color = [x 0 y];
 end
 p(1).LineWidth = 1.5;
 p(2).LineWidth = 1.5;
 hold on
 if i > 1
    x = x - d; % set increment and direction of color change
    y = y + d;
 end
```

```
end
set(axis(1), 'FontSize',15);
ylabel('Current (A)')%('Current (\muA cm^{-2})')
xlabel('Potential (V vs Li/Li^{+})');
title('LPS 3');


% Plot CV by cycle
for i = 1:2:echem_sweep_num+1

 CV = figure('units','inch','position',[1,1,5,4]);
 axis(1) = subplot('position',[0.2, 0.2, 0.69, 0.7]);
 p = plot(echem_pot{i}, echem_cur{i}, 'b', echem_pot{i+1}, echem_cur{i+1}, 'r');
 set(axis(1), 'FontSize',15);
 p(1).LineWidth = 1;
 p(2).LineWidth = 1;
 ylabel('Current (A)')%('Current (\muA/cm^{2})')
 xlabel('Potential (V vs Li/Li^{+})');
%  legend('anodic', 'cathodic', 'Location', 'northwest');

 j = (i+1)/2;
 cycletitle = (['Cycle ' num2str(j)]);
 title(cycletitle);
 hold on
end

% Plot charge by cycle
for i = 1:2:echem_sweep_num

 chaaarge = figure('units','inch','position',[1,1,5,4]);
 axis(1) = subplot('position',[0.2, 0.2, 0.69, 0.7]);
 p = plot(echem_pot{i}, echem_chrg{i}, echem_pot{i+1}, echem_chrg{i+1});
 set(axis(1), 'FontSize',15);
 p(1).LineWidth = 2;
 p(2).LineWidth = 2;
 ylabel('Charge (?)')
 xlabel('Potential (V vs Li/Li^{+})');
%  legend('anodic', 'cathodic', 'Location', 'northwest');

 j = (i+1)/2;
 cycletitle = (['Cycle ' num2str(j)]);
 title(cycletitle);
 hold on
end
```

```
% Plot anodic and cathodic scans separately
for i = 1:echem_sweep_num

 scans = figure('units','inch','position',[1,1,5,4]);
 axis(1) = subplot('position',[0.2, 0.2, 0.69, 0.7]);
 p = plot(echem_pot{i}, echem_cur{i});
 set(axis(1), 'FontSize',15);
 ylabel('Current (A)')%('Current (\muA/cm^{2})')
 xlabel('Potential (V vs Li/Li^{+})');
 p(1).LineWidth = 2;

 hold on

  r = rem(i,2);
    if r == 0
        j = i/2;
        sweep = 'cathodic';
   else
        j = (i+1)/2;
        sweep = 'anodic';
   end

    cycletitle = (['Cycle ' num2str(j) ' ' sweep]);
    title(cycletitle);
end




%% ****************** Calculate total charge passed by hand ***********************

% First, normalize current. For anodic scan, find baseline with slope
% determined between 3.0 and 3.3 V. For cathodic scan , between 3.6 and 3.8

for i = 1:echem_sweep_num+1 % find indicies for certain potentials, indicies
     r = rem(i,2);
     if r == 0 % cathodic

         % assign potentials for cathodic baseline
         % p1 > p2

         val_1pot = 4.1;
         val_2pot = 4.0;

         ind_1pa = find(echem_pot{i} < val_1pot + 0.001);
```

```
        ind_2pa = find(echem_pot{i} < val_2pot + 0.001);

        ind_1pb = find(echem_pot{i} > val_1pot - 0.001);
        ind_2pb = find(echem_pot{i} > val_2pot - 0.001);

        ind_1p = intersect(ind_1pa, ind_1pb);
        ind_2p = intersect(ind_2pa, ind_2pb);
        ind_1p = ind_1p(1);
        ind_2p = ind_2p(1);

        sweep = 'cathodic'; % for title
        j = i/2;

    else %anodic

        % assign potentials for anodic baseline
        % p1 < p2
        if i == 1
            val_1pot = 3.5;
            val_2pot = 3.5;
        else
            val_1pot = 2.8;
            val_2pot = 2.9;
        end


        ind_1pa = find(echem_pot{i} < val_1pot + 0.001);
        ind_2pa = find(echem_pot{i} < val_2pot + 0.001);

        ind_1pb = find(echem_pot{i} > val_1pot - 0.001);
        ind_2pb = find(echem_pot{i} > val_2pot - 0.001);

        ind_1p = intersect(ind_1pa, ind_1pb);
        ind_2p = intersect(ind_2pa, ind_2pb);
        ind_1p = ind_1p(1);
        ind_2p = ind_2p(1);

       sweep = 'anodic'; % for title
       j = (i+1)/2;
    end

    if i == 1
        val_1cur = echem_cur{1}(1); % force numberator of slope to be zero so no baseline
subracted
        val_2cur = echem_cur{1}(1);
    else
```

```
        val_1cur = echem_cur{i}(ind_1p);
        val_2cur = echem_cur{i}(ind_2p);
    end

    slope = (val_1cur-val_2cur)/(val_1pot-val_2pot);
    y_int = val_1cur - (slope*val_1pot);
    background = slope*echem_pot{i} + y_int;
    echem_cur_bkgrdsub{i} = echem_cur{i}-background;


    figure;
    plot( echem_pot{i}, echem_cur{i}, echem_pot{i}, background);
    title(['Original, Cycle ' num2str(j) ' ' sweep]);
    hold on
    figure;
    plot(echem_pot{i}, echem_cur_bkgrdsub{i});
    title(['Subracted, Cycle ' num2str(j) ' ' sweep]);
    hold on

end

% Second, integrate background subtracted current with respect to time
% This is microAmps per cm squared integrated...
for i = 1:echem_sweep_num+1
%       time = echem_time{i}-echem_time{i}(1);
      charge(i) = (trapz(echem_pot{i}, echem_cur_bkgrdsub{i}));
end

% Plot charge

for i = 1:echem_sweep_num+1
   if rem(i,2) == 0
      j = i/2;
      cathodic_charge(j) = charge(i)*-1;
   else
      j = (i+1)/2;
      anodic_charge(j) = charge(i);
      cycle(j) = j;
   end
end



% ******Plot change in charge *anodic!*
   anodchrg = figure('units','inch','position',[1.5,2,5,4], 'outerposition', [1,1,6,5.5]);
   axis(1) = subplot('position',[0.14, 0.2, 0.69, 0.7]);
```

```
    plot(cycle, anodic_charge, 'r*');
    hold on
    ylabel('Charge (C/cm^{2})')
    xlabel('Cycle');
    ax=gca;
    set(ax,'FontSize',15);
    title('Bare LMO Anodic Charge');


% Plot change in charge *cathodic!*
    cathchrg = figure('units','inch','position',[1.5,2,5,4], 'outerposition', [1,1,6,5.5]);
    axis(1) = subplot('position',[0.14, 0.2, 0.69, 0.7]);

    plot(cycle, cathodic_charge, 'b*');
    hold on
    ylabel('Charge (C/cm^{2})')
    xlabel('Cycle');
    ax=gca;
    set(ax,'FontSize',15);
    title('Bare LMO Cathodic Charge');


%%
%Calculate Coulombic efficiency from charge. CE = discharge/charge aka
% lithiation/delithiation for cathodes
CE = cathodic_charge./anodic_charge*100;
figure;
plot(cycle, CE, 'k*')
ylabel('Coulombic efficiency (%)')
xlabel('Cycle');
ax=gca;
set(ax,'FontSize',15);


figure;
h(1) = subplot(3,1,1);
plot(cycle, anodic_charge, 'r*');
ylabel('Charge (C/cm^{2})')
xlabel('Cycle');
ax=gca;
set(ax,'FontSize',10);
title('Bare LMO Anodic Charge');

h(2) = subplot(3,1,2);
plot(cycle, cathodic_charge, 'b*');
```

```
ylabel('Charge (C/cm^{2})')
xlabel('Cycle');
ax=gca;
set(ax,'FontSize',10);
title('Bare LMO Cathodic Charge');

h(3) = subplot(3,1,3);
plot(cycle, CE, 'k*')
ylabel('CE (%)')
xlabel('Cycle');
ax=gca;
set(ax,'FontSize',10);
title('Coulombic Efficiency');

%% ****************** Integrate current *********************

for i = 1:echem_sweep_num
   int{i} = cumtrapz(echem_cur{i});

   figure;
   plotyy(echem_pot{i}, echem_cur{i}, echem_pot{i}, int{i});
   legend('current', 'charge')

   r = rem(i,2);
   if r == 0
      j = i/2;
      sweep = 'cathodic';
   else
      j = (i+1)/2;
      sweep = 'anodic';
   end

   cycletitle = (['Cycle ' num2str(j) ' ' sweep]);
   title(cycletitle);
end
```

Appendix D: MATLAB Code for Processing Integrated Powder Diffraction

D.1 MATLAB Code for Performing Different Types of Background Subtractions and Single Peak Fitting

```
close all
clear all

% Pick directory from which you want to import and export all of your files
datadirectory =
'F:\16Feb_AuLMO_Diffraction\diffraction_FisterFeb16\FreshAttempt_170512\C7_LMO50\allp
owder';
writedirectory =
'F:\16Feb_AuLMO_Diffraction\diffraction_FisterFeb16\Corrections\C4_Au25\background_subt
raction\alldata_bkgrdsub_nonormalization';
backgrounddirectory = 'F:\16Feb_AuLMO_Diffraction\diffraction_FisterFeb16\Corrections';

cd(datadirectory);

% Imports all files with .csv at the end from the directory above
csvFiles = dir('*.csv');
numfiles = length(csvFiles); % counts number of files uploaded
orgdata = cell(1, numfiles);  % creates cell to hold data

% Writes data into mydata cell
for k = 1:numfiles
  orgdata{k} = csvread(csvFiles(k).name, 1, 0);
end

% Chop off data before 2theta = 6
for j = 1:numfiles
   editdata{j} = orgdata{j}(401:end, :);
end

% Integrate data
for j = 1:numfiles
   integration(j) = trapz(editdata{j}(:,2));
end

% Divide by integration
for j = 1:numfiles
   editdata{j}(:,2) = editdata{j}(:,2)/integration(j);
end
```

```
%% Import background

% Pick directory from which you want to import the background
cd(backgrounddirectory);

% Imports all files with .csv at the end from the directory above
bkgdFile = dir('*.csv');
background = csvread(bkgdFile.name, 1, 0);

% Chop off data before 2theta = 6
background = background(401:end, :);

%% Simple Background subtraction
%  Fits background amorphouse peak maximum to the data's amorphous peak
%  maximum

% % Isolate amorphous peak and find maximum value
data_bkgdsub = editdata;
for j = 1:numfiles
   amorph{j} = editdata{j}(401:701, 2); % Isolate amorphous peak in data
   amorph_peak = max(amorph{j}); % Find peak maximum of amorphous peak
   bkgd_amorph = background(401:701, 2); % Isolate amorphous peak in background
   bkgd_amorph_peak = max(bkgd_amorph); % Find peak maximum of peak in background
   bkgd_correction = (amorph_peak/bkgd_amorph_peak); % Make scaling correction for
background
   bkgd = background(:,2)*bkgd_correction; % Apply correction
   data_bkgdsub{j}(:,2) = editdata{j}(:,2)-bkgd; % Subtraction scaled background from data
end

%% Complicated Background subtraction
%  Makes background amorphous peak same height as data amorphous peak. Then fits
background
%  to two points - the amorphous maximums and the very last data point at about
%  twotheta 45 - and then adjusts background baseline to fit the data. This is done
%  iteratively to achieve a background subtraction.

% Isolate amorphous peak and find maximum value
data_bkgdsub = editdata;
[length, width] = size(editdata{1});
for j = 1:numfiles
   amorph{j} = editdata{j}(401:701, 2); % Isolate amorphous peak in data
   [amorph_peak, amorph_ind] = max(amorph{j}); % Find peak maximum of amorphous peak
   data_slope = (amorph_peak-editdata{j}(length,2))/(editdata{j}(amorph_ind,1)-
editdata{j}(length,1));
```

```
    bkgd_amorph = background(401:701, 2); % Isolate amorphous peak in background
    [bkgd_amorph_peak, bkgd_ind] = max(bkgd_amorph); % Find peak maximum of peak in
background
    bkgd_correction = (amorph_peak/bkgd_amorph_peak); % Make scaling correction for
background
    bkgd = background;
    bkgd(:,2) = background(:,2)*bkgd_correction; % Apply correction
    bkgd_amorph = bkgd(401:701, 2);

    for i = 1:30
        [bkgd_amorph_peak, bkgd_ind] = max(bkgd_amorph); % Find peak maximum of peak in
background
        bkgd_slope = (bkgd_amorph_peak-bkgd(length,2))/(bkgd(bkgd_ind,1)-bkgd(length,1));
        slope_correction = data_slope - bkgd_slope;
        baseline_correction = background(:,1)*slope_correction;
        bkgd(:,2) = bkgd(:,2) + baseline_correction;
        bkgd_amorph = bkgd(401:701, 2);
       [bkgd_amorph_peak, bkgd_ind] = max(bkgd_amorph); % Find peak maximum of peak in
background
        bkgd_correction = (amorph_peak/bkgd_amorph_peak); % Make scaling correction for
background
        bkgd(:,2) = bkgd(:,2).*bkgd_correction; % Apply correction
        bkgd_amorph = bkgd(401:701, 2);
    end

    data_bkgdsub{j}(:,2) = editdata{j}(:,2)-bkgd(:,2); % Subtraction scaled background from data
end

%% Make tallest peak at least "10" units tall, so life is easier in GSAS II

peakmax = max(data_bkgdsub{1}(:,2));

for i = 1:numfiles
    data_bkgdsub{i}(:,2) = data_bkgdsub{i}(:,2)./peakmax.*10;
end


%% Writes intensity normalized data into csv file
%  for file numbering starting at a non-one number, you will have to adjust
%  the if and ifelse qualifiers statement
%   !!!Data is written into the chosen directory!!!
cd(writedirectory);
i = 1; % case a) i = 5; case b) i = 1
for j = 1:numfiles
    if j <= 9-4 % a) j<=9-4; b) j<= 9
        dlmwrite(['intnorm_C3_a_00' num2str(i) '.csv'], editdata{j}(:,:));
```

```
    elseif j <= 99-4 % a) j <= 99-4; b) j<= 99
        dlmwrite(['intnorm_C3_a_0' num2str(i) '.csv'], editdata{j}(:,:));
    else
        dlmwrite(['intnorm_C3_a_' num2str(i) '.csv'], editdata{j}(:,:));
    end
    i = i + 1;
end

%% Writes background subtracted data into csv file
%  for file numbering starting at a non-one number, you will have to adjust
%  the if and ifelse qualifiers statement
%   !!!Data is written into the chosen directory!!!
cd(writedirectory);
i = 1; % case a) i = 5; case b) i = 1
for j = 1:numfiles
    if j <= 9 % a) j<=9-4; b) j<= 9
        dlmwrite(['bkgsub_C4_b_00' num2str(i) '.csv'], data_bkgdsub{j}(:,:));
    elseif j <= 99 % a) j <= 99-4; b) j<= 99
        dlmwrite(['bkgsub_C4_b_0' num2str(i) '.csv'], data_bkgdsub{j}(:,:));
    else
        dlmwrite(['bkgsub_C4_b_' num2str(i) '.csv'], data_bkgdsub{j}(:,:));
    end
    i = i + 1;
end

%% Before normalization: Plot all data in a color map

for j = 1:numfiles
    org_data_truncate{j} = orgdata{j}(401:end, :);
end

twotheta = org_data_truncate{1}(:,1);
count = 1:numfiles;
% Concatonate Z/intensity values
intensity = horzcat(org_data_truncate{1}(:,2), org_data_truncate{2}(:,2));
for i = 3:numfiles
    intensity = horzcat(intensity, org_data_truncate{i}(:,2));
end
intensity = intensity'; % Transpose so graph has 2theta at front

    figure;
    map3D = mesh(twotheta, count, intensity);
    colormap(hsv);
    title('Original data');
    xlabel('2\theta');
    ylabel('Count');
```

```
    zlabel('Intensity (a.u.)');
    hold on

    figure;
    i = 1;
    for i = 1:numfiles
    plot(orgdata{i}(:,1), orgdata{i}(:,2));
    hold on
    end
    title('Original data');
    xlabel('2\theta');
    ylabel('Intensity (a.u.)');


%% After normaliztion: Plot all data in a color map

twotheta = editdata{1}(:,1);
count = 1:numfiles;

% Concatonate Z/intensity values
intensity = horzcat(editdata{1}(:,2), editdata{2}(:,2));
for i = 3:numfiles
    intensity = horzcat(intensity, editdata{i}(:,2));
end
intensity = intensity'; % Transpose so graph has 2theta at front

    figure;
    map3D = mesh(twotheta, count, intensity);
    colormap(hsv);
    title('After normalization by integration');
    xlabel('2\theta');
    ylabel('Count');
    zlabel('Intensity (a.u.)');
    hold on

    figure;
    i = 1;
    for i = 1:numfiles
    plot(editdata{i}(:,1), editdata{i}(:,2));
    hold on
    end
    title('After normalization by integration');
    xlabel('2\theta');
    ylabel('Intensity (a.u.)');

%
```

```
% %% Plot a specific spectra
%
%     figure;
%     plot(twotheta', intensity(100,:));

%% After background subtraction: Plot all data in a color map

twotheta = data_bkgdsub{1}(:,1);
count = 1:numfiles;

% Concatonate Z/intensity values
intensity = horzcat(data_bkgdsub{1}(:,2),data_bkgdsub{2}(:,2));
for i = 3:numfiles
   intensity = horzcat(intensity, data_bkgdsub{i}(:,2));
end
   intensity = intensity';% Transpose so graph has 2theta at front

   figure;
   map3D = mesh(twotheta, count, intensity);
   colormap(hsv);
   title('After background subtraction');
   xlabel('2\theta');
   ylabel('Count');
   zlabel('Intensity (a.u.)');
   hold on

   figure;
   for i = [1, 17, 47, 81]%:numfiles
      plot(data_bkgdsub{i}(:,1), data_bkgdsub{i}(:,2));
      hold on
   end
   title('After background subtraction');
   xlabel('2\theta');
   ylabel('Intensity (a.u.)');

   %% Fit 111 peak to get FWHM, peak height, etc.
   peakparam = zeros(numfiles,8);
   j = 1;
   k = 1;

   for i = 1:numfiles
      clear max max_ind
      [max,max_ind] = max(data_bkgdsub{i}(:,2)); % Find max peak, i.e. 111
      xmax = data_bkgdsub{1}(max_ind,1); % Find x value for max peak
%        for window = 0.05:0.04:0.25 % This commmented out bit is for
%        trying out different parameters and how they affect fits
```

```
        [FitResults, GOF] = peakfit(data_bkgdsub{i}(:,1:2), xmax, 0.15, 1, 1, 30); % Does the
peak fitting
%           width(j,k)= FitResults(4);
%           height(j,k)= FitResults(3);
%           Rsqu(j,k)=GOF(2);
%           paramind(j) = window;
%           j = j+1;
%       end
%       j = 1;
%       k = k + 1;
      peakparam(i,1) = i; % Column 1 is the data set number
      peakparam(i,2:6) = FitResults; %one row for each peak. Lists by column 2 Peak number, 3
Peak position, 4 Height, 5 Width, 6 Peak area
      peakparam(i,7:8) = GOF; % 7 rms and 8 R^2 of best trial
   end
   peakparamlabel = {'Data set' 'Peak number' 'Peak position', 'Height', 'Width', 'Peak area', 'rms
of best fit', ' R^2 of best fit'};
%    paramind = paramind';

   % Plot lots of parameters calculated by fit
   figure;
   ax1 = subplot(2,3,1)
   plot(peakparam(:,1), peakparam(:,3))
   title('peak position')
   ax2 = subplot(2,3,2)
   plot(peakparam(:,1), peakparam(:,4))
   title('height')
   ax3 = subplot(2,3,3)
   plot(peakparam(:,1), peakparam(:,5))
   title('width')
   ax4 = subplot(2,3,4)
   plot(peakparam(:,1), peakparam(:,6))
   title('area')
   ax5 = subplot(2,3,5)
   plot(peakparam(:,1), peakparam(:,7))
   title('RMS')
   ax6 = subplot(2,3,6)
   plot(peakparam(:,1), peakparam(:,8))
   title('R^{2}')
   linkaxes([ax1, ax2, ax3, ax4, ax5, ax6], 'x')

% This bit is for looking at different parameters and how they affect fits, turn on if you turn on
embedded for loop above
% [waste, ind] = size(width);

   figure;
```

```
for i = 1:ind
    plot(paramind,width(:,i))
    hold on
end
title('width')
legend(num2str(paramind), 'Location', 'Best')

figure;
for i = 1:ind
    plot(paramind,height(:,i))
    hold on
end
title('height')
legend(num2str(paramind), 'Location', 'Best')

figure;
for i = 1:ind
    plot(paramind,Rsqu(:,i))
    hold on
end
title('R^2')
legend(num2str(paramind), 'Location', 'Best')
```

D.2 MATLAB Code for Normalizing with Respect to the Incident Radiation Intensity

```
close all
clear all

% Pick directory from which you want to import all of your files
cd('F:\16Feb_AuLMO_Diffraction\diffraction_FisterFeb16\FreshAttempt_170512\C5_Au50\allpowder')

% Imports all files with .csv at the end from the directory above
csvFiles = dir('*.csv');
numfiles = length(csvFiles); % counts number of files uploaded
mydata = cell(1, numfiles);  % creates cell to hold data

% Writes data into mydata cell
for k = 1:numfiles
  mydata{k} = csvread(csvFiles(k).name, 1, 0);
end

% Import excel file with beam intensity values
% I make this file by extracting incoming beam intensity (i00) from FisterFeb16_expdata.xlsx
xlsFiles = dir('*.xls');
```

```
i0 = xlsread(xlsFiles.name);

% Some i0 values are anonamosly low. This replaces those values with an
% average value of the i0s to either side of it
i = 1;
while i <= numfiles
   if i0(i) < 10000
      i0(i) = (i0(i-1)+i0(i+1))/2;
   end
   i = i + 1;
end


% Divide powder data by imported beam intensities
editdata = mydata; % Create copy of data cell. Preserve original data and save edited data.
j = 1;
while j <= numfiles
   editdata{1,j}(:,2) = editdata{j}(:,2)/i0(j);
   j = j + 1;
end

% Writes data into csv file
% for file numbering starting at a non-one number, you will have to adjust
% the if and ifelse qualifiers
% statement
i = 1; % case a) i = 5; case b) i = 1
j = 1;
while j <= numfiles
   if j <= 9%-4 % a) j<=9-4; b) j<= 9
      dlmwrite(['i0norm_LMO25_C3_b_00' num2str(i) '.csv'], editdata{j}(:,:));
   elseif j <= 99%-4 % a) j<=99-4; b) j<= 99
      dlmwrite(['i0norm_LMO25_C3_b_0' num2str(i) '.csv'], editdata{j}(:,:));
   else
      dlmwrite(['i0norm_LMO25_C3_b_' num2str(i) '.csv'], editdata{j}(:,:));
   end
   i = i + 1;
   j = j + 1;
end

%% After normaliztion: Plot all data in a color map

twotheta = editdata{1}(:,1);
twotheta = twotheta(401:end,1);
count = 1:numfiles;

% Concatonate Z/intensity values
```

```
i = 3;
intensity = horzcat(editdata{1}(:,2), editdata{2}(:,2));
while i <= numfiles
    intensity = horzcat(intensity, editdata{i}(:,2));
    i = i + 1;
end
intensity = intensity(401:end, :);
intensity = intensity';

    figure;
    map3D = mesh(twotheta, count, intensity);
    colormap(hsv);
    hold on

    figure;
    map2D = contourf(twotheta, count, intensity);
    colormap(hsv);

    figure;
    map3D = mesh(twotheta, count, intensity);
    colormap(hsv);
    title('Data Normalized by I0');
    xlabel('2\theta');
    ylabel('Count');
    zlabel('Intensity (a.u.)');
    hold on


%% Before normalization: Plot all data in a color map

twotheta = mydata{1}(:,1);
twotheta = twotheta(401:end,1);
count = 1:numfiles;

% Concatonate Z/intensity values
i = 3;
intensity = horzcat(mydata{1}(:,2), mydata{2}(:,2));
while i <= numfiles
    intensity = horzcat(intensity, mydata{i}(:,2));
    i = i + 1;
end
intensity = intensity(401:end, :);
intensity = intensity';

    figure;
    map2D = contourf(twotheta, count, intensity);
```

```
colormap(hsv);


figure;
map3D = mesh(twotheta, count, intensity);
colormap(hsv);
title('Original');
xlabel('2\theta');
ylabel('Count');
zlabel('Intensity (a.u.)');
hold on
```

D.3 MATLAB Code for Subtracting Two Datasets from One Another for Comparison

```
close all
clear all


%%

% Pick directory from which you want to import and export all of your files
A_datadirectory =
'F:\16Feb_AuLMO_Diffraction\diffraction_FisterFeb16\FreshAttempt_170512\C5_Au50\allpow
der';
B_datadirectory =
'F:\16Feb_AuLMO_Diffraction\diffraction_FisterFeb16\FreshAttempt_170512\C7_LMO50\allp
owder';
writedirectory =
'F:\16Feb_AuLMO_Diffraction\diffraction_FisterFeb16\Corrections\C4_Au25\background_subt
raction\alldata_bkgrdsub_nonormalization';
backgrounddirectory = 'F:\16Feb_AuLMO_Diffraction\diffraction_FisterFeb16\Corrections';
LMO =
csvread('F:\16Feb_AuLMO_Diffraction\diffraction_FisterFeb16\IntensityOnlyMainPhases\LMO
.csv');
MnO2 =
csvread('F:\16Feb_AuLMO_Diffraction\diffraction_FisterFeb16\IntensityOnlyMainPhases\MnO
2.csv');
Au =
csvread('F:\16Feb_AuLMO_Diffraction\diffraction_FisterFeb16\IntensityOnlyMainPhases\Au.c
sv');


cd(A_datadirectory);

% Imports all files with .csv at the end from the directory above
csvFiles = dir('*.csv');
```

```
A_numfiles = length(csvFiles); % counts number of files uploaded
A_orgdata = cell(1, A_numfiles);  % creates cell to hold data

% Writes data into mydata cell
for k = 1:A_numfiles
  A_orgdata{k} = csvread(csvFiles(k).name, 1, 0);
end


for j = 1:A_numfiles-1 %% for C4+C3 need -1 here and orgdata{j+1} on next line. Remove -1
and +1 if C5+C7
    A_editdata{j} = A_orgdata{j+1}(401:end, :); % Chop off data before 2theta = 6
end

cd(B_datadirectory);

% Imports all files with .csv at the end from the directory above
csvFiles = dir('*.csv');
B_numfiles = length(csvFiles); % counts number of files uploaded
B_orgdata = cell(1, B_numfiles);  % creates cell to hold data

% Writes data into mydata cell
for k = 1:B_numfiles
  B_orgdata{k} = csvread(csvFiles(k).name, 1, 0);
end


for j = 1:B_numfiles
    B_editdata{j} = B_orgdata{j}(401:end, :); % Chop off data before 2theta = 6
    B_integration(j) = trapz(B_editdata{j}(:,2)); % Integrate data
    B_editdata{j}(:,2) = B_editdata{j}(:,2)/B_integration(j); % Divide by integration
end

numfiles = min(A_numfiles, B_numfiles)-1;

%% Normalize by amorphous peak
%  Fits background amorphous peak maximum to the data's amorphous peak
%  maximum

% Isolate amorphous peak and find maximum value, normalize by that value

for j = 1:numfiles
    A_amorph{j} = A_editdata{j}(401:601, 2); % Isolate amorphous peak in data
    A_amorph_peak = max(A_amorph{j}); % Find peak maximum of amorphous peak
    A_data_norm{j} = A_editdata{j}(:,2)/A_amorph_peak; % Divide by amorphous peak height
```

```
    B_amorph{j} = B_editdata{j}(401:601, 2); % Isolate amorphous peak in data
    B_amorph_peak = max(B_amorph{j}); % Find peak maximum of amorphous peak
    B_data_norm{j} = B_editdata{j}(:,2)/B_amorph_peak; % Divide by amorphous peak height
end

%% Subtract one spectra from another

% subtract = cell(numfiles);
for j=1:numfiles
%     subtract{j}=A_data_norm{j}./B_data_norm{j};
    subtract{j}=A_data_norm{j}-B_data_norm{j};
end


%% Structure phases for graphing

[LMO_row,column]=size(LMO);
[MnO2_row,column]=size(MnO2);
[Au_row,column]=size(Au);


%% After normaliztion: Plot all data in a color map

twotheta = A_editdata{1}(:,1);
count = 1:numfiles;

% Concatonate Z/intensity values
% intensity = horzcat(subtract{1}(:,1), subtract{2}(:,1)); %subtracted data
% intensity = horzcat(B_data_norm{1}(:,1), B_data_norm{2}(:,1)); %LMO data
% for i = 3:numfiles
% %     intensity = horzcat(intensity, subtract{i}(:,1)); %subtracted data
%     intensity = horzcat(intensity, B_data_norm{i}(:,1)); %LMO data
% end
% intensity = intensity'; % Transpose so graph has 2theta at front
%
%     figure;
%     map3D = mesh(twotheta, count, intensity);
%     colormap(hsv);
%     title('Au-Bare');
%     xlabel('2\theta');
%     ylabel('Count');
%     zlabel('Intensity (a.u.)');
%     hold on

    figure;
    j = 0;
```

```
   for i = [60 67 70 76] %1:2:numfiles %[1 46 97 162 229 295 362 412]%for C4/C3 [1 17 47 81
114 145 178 212 246 279 312 346 379 412] %for C5/C7
       %       figure;
       %figure('units','normalized','outerposition',[0 0 1 1]) %makes figure size of screen
       plot(A_editdata{i}(:,1), A_data_norm{i}(:,1)+j);
       hold on
       title(['Au-coated LMO']);
%        legend('Au', 'Bare', 'Subtract');
       xlabel('2\theta');
       ylabel('Intensity (a.u.)');
       j = j + 1.2;
   end

   %figure;
   j = 0;
   for i = [60 67 70 76] %1:2:numfiles %[1 46 97 162 229 295 362 412]%for C4/C3 [1 17 47 81
114 145 178 212 246 279 312 346 379 412] %for C5/C7
%       figure;
       %figure('units','normalized','outerposition',[0 0 1 1]) %makes figure size of screen
       plot(B_editdata{i}(:,1), B_data_norm{i}(:,1)+j, '--');
       hold on
       title(['LMO']);
%        legend('Au', 'Bare', 'Subtract');
       xlabel('2\theta');
       ylabel('Intensity (a.u.)');
       j = j + 1.2;
  end


%% Plot a specific spectra

   figure;
   plot(twotheta', intensity(100,:));
```

D.4 MATLAB Code for Subtracting One Dataset from Another, Two Sets at a Time

```
close all
clear all

%%
%Look at line 30 when switching between between data sets
%%

% Pick directory from which you want to import and export all of your files
```

```
Au25_datadirectory =
'F:\16Feb_AuLMO_Diffraction\diffraction_FisterFeb16\FreshAttempt_170512\C4_Au25\all_powder';
LMO25_datadirectory =
'F:\16Feb_AuLMO_Diffraction\diffraction_FisterFeb16\FreshAttempt_170512\C3_LMO25\all_powder';
Au50_datadirectory =
'F:\16Feb_AuLMO_Diffraction\diffraction_FisterFeb16\FreshAttempt_170512\C5_Au50\allpowder';
LMO50_datadirectory =
'F:\16Feb_AuLMO_Diffraction\diffraction_FisterFeb16\FreshAttempt_170512\C7_LMO50\allpowder';
writedirectory =
'F:\16Feb_AuLMO_Diffraction\diffraction_FisterFeb16\Corrections\C4_Au25\background_subtraction\alldata_bkgrdsub_nonormalization';
backgrounddirectory = 'F:\16Feb_AuLMO_Diffraction\diffraction_FisterFeb16\Corrections';
LMO =
csvread('F:\16Feb_AuLMO_Diffraction\diffraction_FisterFeb16\IntensityOnlyMainPhases\LMO.csv');
MnO2 =
csvread('F:\16Feb_AuLMO_Diffraction\diffraction_FisterFeb16\IntensityOnlyMainPhases\MnO2.csv');
Au =
csvread('F:\16Feb_AuLMO_Diffraction\diffraction_FisterFeb16\IntensityOnlyMainPhases\Au.csv');


cd(Au25_datadirectory);

% Imports all files with .csv at the end from the directory above
csvFiles = dir('*.csv');
Au25_numfiles = length(csvFiles); % counts number of files uploaded
Au25_orgdata = cell(1, Au25_numfiles);  % creates cell to hold data

% Writes data into mydata cell
for k = 1:Au25_numfiles
  Au25_orgdata{k} = csvread(csvFiles(k).name, 1, 0);
end


for j = 1:Au25_numfiles-1 %% for C4+C3 need -1 here and orgdata{j+1} on next line. Remove -1 and +1 if C5+C7
    Au25_editdata{j} = Au25_orgdata{j+1}(401:end, :); % Chop off data before 2theta = 6
end

cd(LMO25_datadirectory);
```

```
% Imports all files with .csv at the end from the directory above
csvFiles = dir('*.csv');
LMO25_numfiles = length(csvFiles); % counts number of files uploaded
LMO25_orgdata = cell(1, LMO25_numfiles);  % creates cell to hold data

% Writes data into mydata cell
for k = 1:LMO25_numfiles
  LMO25_orgdata{k} = csvread(csvFiles(k).name, 1, 0);
end


for j = 1:LMO25_numfiles
   LMO25_editdata{j} = LMO25_orgdata{j}(401:end, :); % Chop off data before 2theta = 6
%     B_integration(j) = trapz(B_editdata{j}(:,2)); % Integrate data
%     B_editdata{j}(:,2) = B_editdata{j}(:,2)/B_integration(j); % Divide by integration
end

cd(Au50_datadirectory);

% Imports all files with .csv at the end from the directory above
csvFiles = dir('*.csv');
Au50_numfiles = length(csvFiles); % counts number of files uploaded
Au50_orgdata = cell(1, Au50_numfiles);  % creates cell to hold data

% Writes data into mydata cell
for k = 1:Au50_numfiles
  Au50_orgdata{k} = csvread(csvFiles(k).name, 1, 0);
end


for j = 1:Au50_numfiles %% for C4+C3 need -1 here and orgdata{j+1} on next line. Remove -1
and +1 if C5+C7
   Au50_editdata{j} = Au50_orgdata{j}(401:end, :); % Chop off data before 2theta = 6
end

cd(LMO50_datadirectory);

% Imports all files with .csv at the end from the directory above
csvFiles = dir('*.csv');
LMO50_numfiles = length(csvFiles); % counts number of files uploaded
LMO50_orgdata = cell(1, LMO50_numfiles);  % creates cell to hold data

% Writes data into mydata cell
for k = 1:LMO50_numfiles
  LMO50_orgdata{k} = csvread(csvFiles(k).name, 1, 0);
```

```
end


for j = 1:LMO50_numfiles
   LMO50_editdata{j} = LMO50_orgdata{j}(401:end, :); % Chop off data before 2theta = 6
%     B_integration(j) = trapz(B_editdata{j}(:,2)); % Integrate data
%     B_editdata{j}(:,2) = B_editdata{j}(:,2)/B_integration(j); % Divide by integration
end

numfiles = min([Au25_numfiles LMO25_numfiles Au50_numfiles LMO50_numfiles]);

%% Normalize by amorphous peak
%  Fits background amorphous peak maximum to the data's amorphous peak
%  maximum

% Isolate amorphous peak and find maximum value, normalize by that value

for j = 1:numfiles
   Au25_amorph{j} = Au25_editdata{j}(401:601, 2); % Isolate amorphous peak in data
   Au25_amorph_peak = max(Au25_amorph{j}); % Find peak maximum of amorphous peak
   Au25_data_norm{j} = Au25_editdata{j}(:,2)/Au25_amorph_peak + 0.2; % Divide by
amorphous peak height

   LMO25_amorph{j} = LMO25_editdata{j}(401:601, 2); % Isolate amorphous peak in data
   LMO25_amorph_peak = max(LMO25_amorph{j}); % Find peak maximum of amorphous
peak
   LMO25_data_norm{j} = LMO25_editdata{j}(:,2)/LMO25_amorph_peak + 0.2; % Divide by
amorphous peak height

   Au50_amorph{j} = Au50_editdata{j}(401:601, 2); % Isolate amorphous peak in data
   Au50_amorph_peak = max(Au50_amorph{j}); % Find peak maximum of amorphous peak
   Au50_data_norm{j} = Au50_editdata{j}(:,2)/Au50_amorph_peak; % Divide by amorphous
peak height

   LMO50_amorph{j} = LMO50_editdata{j}(401:601, 2); % Isolate amorphous peak in data
   LMO50_amorph_peak = max(LMO50_amorph{j}); % Find peak maximum of amorphous
peak
   LMO50_data_norm{j} = LMO50_editdata{j}(:,2)/LMO50_amorph_peak; % Divide by
amorphous peak height
end

%% Subtract one spectra from another

% subtract = cell(numfiles);
for j=1:numfiles
%     subtract{j}=A_data_norm{j}./B_data_norm{j};
```

```
    subtract25{j}=Au25_data_norm{j}-LMO25_data_norm{j};
    subtract50{j}=Au25_data_norm{j}-LMO25_data_norm{j};
end


%% Structure phases for graphing

[LMO_row,column]=size(LMO);
[MnO2_row,column]=size(MnO2);
[Au_row,column]=size(Au);


%% After normaliztion: Plot all data in a color map

twotheta = Au25_editdata{1}(:,1);
count = 1:numfiles;

% Concatonate Z/intensity values
intensity = horzcat(subtract50{1}(:,1), subtract50{2}(:,1)); %subtracted data
% intensity = horzcat(LMO25_data_norm{1}(:,1), LMO25_data_norm{2}(:,1)); %LMO data
for i = 3:numfiles
    intensity = horzcat(intensity, subtract50{i}(:,1)); %subtracted data
%     intensity = horzcat(intensity, LMO25_data_norm{i}(:,1)); %LMO data
end
intensity = intensity'; % Transpose so graph has 2theta at front

    figure;
    map3D = mesh(twotheta, count, intensity);
    colormap(hsv);
    title('Au-Bare');
    xlabel('2\theta');
    ylabel('Count');
    zlabel('Intensity (a.u.)');
    hold on

%     index25 = [1 46 97 162 229 295 362 412];
%     index50 = [1 17 47 81 114 145 178 212 246 279 312 346 379 412];
    index25 = [1 46 97 162];
    index50 = [1 17 47 81];

    index = min(numel(index25), numel(index50));

    for i = 1:index
        figure('units','normalized','outerposition',[0 0 1 1]) %makes figure size of screen

        p = plot(Au25_editdata{index25(i)}(:,1), Au25_data_norm{index25(i)}(:,1),...
```

```
        LMO25_editdata{index25(i)}(:,1), LMO25_data_norm{index25(i)}(:,1), ...
        LMO25_editdata{index25(i)}(:,1), subtract25{index25(i)}, ...
        Au50_editdata{index50(i)}(:,1), Au50_data_norm{index50(i)}(:,1),...
        LMO50_editdata{index50(i)}(:,1), LMO50_data_norm{index50(i)}(:,1), ...
        LMO50_editdata{index50(i)}(:,1), subtract50{index50(i)});
    p(1).Color = 'r';
    p(2).Color = 'k';
    p(3).Color = 'm';
    p(4).Color = [1 0.5 0];
    p(5).Color = [0 0.4 0.8];
    p(6).Color = [0 0 0.8];
    p(1).LineWidth = 1.5;
    p(2).LineWidth = 1.5;
    p(3).LineWidth = 1.5;
    p(4).LineWidth = 1.5;
    p(5).LineWidth = 1.5;
    p(6).LineWidth = 1.5;

    hold on
    title(['After normalization - data set # ' num2str(i)]);
    legend('Au25', 'Bare25', 'Subtract25', 'Au50', 'Bare50', 'Subtract50');
    xlabel('2\theta');
    ylabel('Intensity (a.u.)');


    for j=1:2:LMO_row
        plot(LMO(j:j+1,1), LMO(j:j+1,2),'g', 'LineWidth', 1.5);
        plot(MnO2(j:j+1,1), MnO2(j:j+1,2),'k', 'LineWidth', 1.5);
    end
    for j=1:2:Au_row
        plot(Au(j:j+1,1), Au(j:j+1,2),'r', 'LineWidth', 1.5);
    end

    text(35.6, 0.15, 'LMO', 'Color', 'g');
    text(38.3, 0.11, 'Au', 'Color', 'r');
    text(39.9, 0.07, 'MnO2', 'Color', 'k');
end



%% Plot a specific spectra

    figure;
    plot(twotheta', intensity(100,:));
```